






Universitat Autònoma de Barcelona

ADVERTIMENT. L'accés als continguts d'aquesta tesi queda condicionat a l'acceptació de les condicions d'ús establertes per la següent llicència Creative Commons:  http://cat.creativecommons.org/?page_id=184

ADVERTENCIA. El acceso a los contenidos de esta tesis queda condicionado a la aceptación de las condiciones de uso establecidas por la siguiente licencia Creative Commons:  <http://es.creativecommons.org/blog/licencias/>

WARNING. The access to the contents of this doctoral thesis it is limited to the acceptance of the use conditions set by the following Creative Commons license:  <https://creativecommons.org/licenses/?lang=en>



**Universitat Autònoma
de Barcelona**

Obtaining value-added products from
agricultural wastes through pyrolysis and
torrefaction treatments

Cristina del Pozo Carvajal

Doctoral Thesis

Programa de Doctorat en Química

Esteve Fàbregas Martínez
Neus Puy Marimon

Chemistry Department
Science Faculty

2021

Doctoral thesis presented by Cristina del Pozo Carvajal for the Degree of Doctor of Philosophy with International European Mention inside the Chemistry Program at Universitat Autònoma de Barcelona.

The present thesis entitled “Obtaining value-added products from agricultural wastes through pyrolysis and torrefaction treatments” has been carried out in the Department of Chemistry at Universitat Autònoma de Barcelona (UAB) and in the Energy and Bioproducts Research Institute (EBRI) at Aston University, United Kingdom, as international internship, under the supervision of Dr. Esteve Fàbregas Martínez and Dr. Neus Puy Marimon.

Bellaterra, September 2021.



Esteve Fàbregas Martínez

Neus Puy Marimon

Table of contents

List of figures and tables.....	III
List of abbreviations	V
Acknowledgements	VII
Summary.....	XIX
Preface.....	XXI

Chapter I. Introduction

1.1 Introduction	3
1.1.1 Towards a circular bioeconomy	3
1.1.1.1 From linear economy to circular economy	3
1.1.1.2 Circular economy	4
1.1.1.3 Bioeconomy	8
1.1.1.4 Biorefinery of bio-based wastes	9
1.1.2 Thermochemical treatments: pyrolysis and torrefaction.....	12
1.1.2.1 Thermochemical degradation of biomass	12
1.1.2.2 Pyrolysis and torrefaction.....	16
1.1.2.3 Thermochemical products	18
1.1.2.4 Pyrolysis and torrefaction reactors	20
1.2 Motivations and objectives	27
1.2.1 Motivations	27
1.2.2 Objectives.....	28
1.3 References of Part I.....	29

Chapter II. Compendium of publications

2.1 Article I	39
Separation of value-added chemical groups from bio-oil of olive mill waste	39
2.2 Article II.....	49

Table of contents

	Production, identification, and quantification of antioxidants from torrefaction and pyrolysis of grape pomace	49
2.3	Article III	61
	Production of antioxidants and other value-added compounds from coffee silverskin via pyrolysis under a biorefinery approach	61
2.4	Article IV	73
	Converting coffee silverskin to value-added products by a slow pyrolysis-based biorefinery process	73

Chapter III. Submitted article

3.1	Article V (Submitted article)	89
	The effect of reactor scale on biochars and pyrolysis liquids from slow pyrolysis of coffee silverskin, grape pomace and olive mill waste, in auger reactors	89

Chapter IV. Discussion

4.1	Discussion of the results	119
4.2	References of Part IV	123

Chapter V. Conclusions

5.1	Conclusions	127
5.2	Future Prospects	131

Chapter VI. Annex

6.1	Contributions to congresses and seminars	135
------------	---	------------

List of figures and tables

Figures

Chaper I. Introduction

Figure 1. Linear economy vs circular economy..... 7

Figure 2. Biorefinery platforms and conversion processes (Ubando et al., 2020)..... 10

Figure 3. Main components of lignocellulosic biomass. 12

Figure 4. Thermochemical degradation of hemicellulose, cellulose and lignin. 13

Figure 5. Pyrolysis curves of hemicellulose, cellulose and lignin from thermogravimetric analysis..... 15

Figure 6. Pyrolysis and torrefaction products. 17

Figure 7. Biochar structure..... 19

Figure 8. Pilot plant from ENER-G-bas company. 21

Figure 9. Detailed scheme of the pilot scale reactor from ENER-G-bas company..... 23

Figure 10. Lab scale reactor from EBRI. 24

Figure 11. Detailed scheme of the lab scale reactor from EBRI..... 26

Chapter II. Compendium of publications

Figure 12. Graphical abstract of the article II. 49

Figure 13. Graphical abstract of the article III..... 61

Figure 14. Graphical abstract of the article IV..... 73

Chapter III. Submitted article

Fig. I. Schematic diagram of the lab auger pyrolysis system (A) at Aston University, and the pilot plant (B) at ENER-G-bas company. 95

Fig. II. Pyrolysis TGA curves of CSS (A), GP (B), OMW (C) and their respective biochars from the slow pyrolysis at different temperatures, performed at pilot and lab auger reactors. 97

List of figures and tables

Fig. III. CSS, GP and OMW feedstocks, and biochars from the slow pyrolysis of these compounds, performed at the lab and pilot auger reactors, at different temperatures.....	100
Fig. IV. FTIR spectra for CSS, GP and OMW feedstocks, and biochars from the slow pyrolysis of these compounds, performed at the lab and pilot auger reactors, at different temperatures.....	105
Fig. V. Pyrolysis liquids from the slow pyrolysis of CSS, GP and OMW feedstocks, performed at lab and pilot auger reactors, at different temperatures	107

Tables

Chaper I. Introduction

Table 1. Characteristics of pyrolysis and torrefaction process.....	17
--	----

Chapter III. Submitted article

Table I. Product yields from the slow pyrolysis of CSS, GP and OMW at the lab auger reactor.	99
Table II. Characterisation of CSS, GP, OMW and their respective biochars from slow pyrolysis at different temperatures.....	101
Table III. I. Most abundant compounds of the aqueous phase of the pyrolysis liquid obtained from the slow pyrolysis of CSS, GP and OMW at different temperatures, determined by GC–MS analysis.....	109
Table III. II. Most abundant compounds of the non-aqueous phase of the pyrolysis liquid obtained from the slow pyrolysis of CSS, GP and OMW at different temperatures, determined by GC–MS analysis.	111

List of abbreviations

OMW	Olive Mill Waste
GP	Grape Pomace
CSS	Coffee Silverskin
AP	Aqueous Phase of the pyrolysis liquid
NAP	Non-Aqueous Phase of the pyrolysis liquid
FC	Folin-Ciocalteu
DPPH	2,2-Diphenyl-1-picrylhydrazyl
GC	Gas Chromatography
GC-MS	Gas Chromatography – Mass Spectrometry
EEA	European Environment Agency
EBRI	Energy and Bioproducts Research Institute

Acknowledgements

This thesis has been performed thanks to the financial support of the Universitat Autònoma de Barcelona regarding the PIF and the stay abroad fellowships.

Particularly, I would like to thank my directors, Esteve Fàbregas and Neus Puy, for the opportunity, guidance, confidence, and patience they had during my PhD.

I would also like to thank the SAQ members (Alba Estaquio, Mari Berge and Oscar Palacios) for their help and advice with the analysis of the samples. Besides, I'm really grateful to all TFG students that have been part, in one way or another, of this thesis (Joan Casanova, Paula Martorell, Pau Redón, Paul Núñez, Sofia Taboada, Mireia Mora, David Sayós and Javi Orihuela); all my colleagues from Analytical Chemistry, with whom I have shared this experience (Raquel, Robert, Rodri, Fran, Sandra, Anna, Dioni, Marta, Mon, Montse, Eva, Toni, Mar); as well as, the administration members (Elena, Conxita) for their efficiency and solving all my doubts. I'm also especially grateful to Iris for the great time we spend together, mostly preparing NANO lessons, and for her predisposition to always help me; to Jose and Alba for the warm welcome; and Ale and Natalia, for the lovely chats, coffees and dinners we had.

Moreover, I'm really grateful to Tony Bridgwater and Yang Yang to let me be part of EBRI (Aston University) for some months. It has been an amazing experience where I learn a lot, and I could extend the research resulting in the thesis I'm presenting here. I would like to dedicate a special thanks to Filipe, which has been an incredible co-worker, introducing me to the world of augers and biochars, and for making nicer the time we spend at the lab; to Jorge, for his welcome, attention and being there always to help me; and Carmen, which I feel very lucky to have lived this wonderful experience with her.

I also want to thank Ivette, Rocio and Míriam for coming to lunch with me and make my days happier; to my parents-in-law for treating me like a daughter in all the long study nights; and to the "amics que són família", and my brothers-in-law, for the interest and understanding regarding the PhD, but above all, for all the moments we have lived together.

Acknowledgements

Finally, I want to especially thank my family: my father, who is my number one fan; my mother, who reads everything I write and is in everything I do; my brother-in-law for the time I have spent in his house, and for solving all my technical problems; my sister, for all the hours studying and being together, no matter where I am; and my future husband, for supporting me in everything I do.

Summary

Within the transition towards a circular bioeconomy, this study is focused on obtaining value-added products from agricultural wastes through pyrolysis and torrefaction treatments in a waste biorefinery context. Thus, in this work, the wastes are considered as by-products.

Specifically, it has been worked with olive mill waste (OMW), grape pomace (GP) and coffee silverskin (CSS), which are respectively the main solid wastes from olive oil, wine making and coffee roasting processes. The thermochemical treatments have been performed in an auger pilot plant (15 kg/h), with the collaboration of ENERGBAS company, that provided the products, and in a lab size auger reactor (0.3 kg/h), from EBRI institution (Aston University, U.K.), during a stay abroad. The resulting liquid and solid fractions have been studied to determine their potential applications.

Pyrolysis liquid from OMW (pilot plant, 400 °C) was composed of two phases, an aqueous phase (AP) containing acetic acid, monosaccharides and phenolic derivatives, and a non-aqueous phase (NAP) mainly composed of phenolic derivatives, fatty acids and their methyl esters. In order to separate the AP and NAP compounds in interesting chemical groups, a methodology based on acid-base extractions (performed with hexane at pH 12, followed by an ethyl acetate extraction at pH 6) was successfully developed.

Within these compounds, phenolics were the most interesting ones due to their antioxidant properties, so the suitability of two methods (Folin-Ciocalteu and DPPH) to quantify them in thermochemical liquids were studied using GP liquids (pilot plant, 225 °C and 400 °C). The results showed that phenolics from the 400 °C liquids (AP and NAP) can be successfully measured by these methods; however, in the 225 °C liquid, phenolics should be measured by DPPH assay since the high content of reducing sugars that the 225 °C liquid had, might interfere in the Folin-Ciocalteu measurement. Moreover, 400 °C was considered a suitable temperature to obtain phenolics, which come not only from the GP composition, but from lignin devolatilization reactions during the thermochemical process.

In addition, biochars from CSS (pilot plant, 280 °C, 400 °C and 500 °C) showed its potential use as energy source; on the other hand, CSS pyrolysis liquids were considered as a potential source of phenolics, mainly the 280 °C one. The research was extended studying the products from the lab size reactor, performed at the same temperatures and solid retention time. CSS biochars were studied as absorbent of organic pollutants in water, being potentially useful for

Summary

cationic and aromatic molecules; at the same time, CSS pyrolysis liquids were contemplated as a potential source of caffeine, among phenolics, with 400 °C AP phase having the highest concentration (14.3 g caffeine/L AP). Moreover, gas fraction was considered as a heat source for biomass drying before pyrolysis. Thus, it has showed that CSS could be completely valorised through thermochemical treatments, which would allow to achieve zero-waste in the coffee roasting industry, being CSS the only waste of the process.

Furthermore, OMW, GP and CSS thermochemical products from both reactors were compared, since using different size reactors could affect the properties and so, applications, of the resulting products. No major differences were observed between biochars, making the biorefinery of these wastes more feasible.; however, in the pyrolysis liquids, the ones from the pilot plant were richer in 2,6-dimethoxy-phenols and phenolics para-substituted by carbonyl groups.

Thus, this thesis has been focused on the valorisation of OMW, GP and CSS, through thermochemical treatments, within an integrated biorefinery context. Specifically, pyrolysis liquids have shown to be a potential source of chemicals, while biochars can be used as solid biofuel, among other potential high-valued applications.

Preface

This dissertation is presented as a compilation of peer-reviewed articles, following the guidelines of the Universitat Autònoma de Barcelona.

In addition, this thesis has been performed with the collaboration of ENERGBAS company, and Energy and Bioproducts Research Institute (EBRI), at Aston University (U.K.), the latter one during a stay abroad.

The contents of the present thesis have been organized in the following main chapters:

- I. Introduction
- II. Compendium of publications
- III. Submitted article
- IV. Discussion
- V. Conclusions
- VI. Annex

Chapter I provides an overview of circular bioeconomy, together with pyrolysis and torrefaction treatments as the context of this thesis, followed by the motivation and objectives of the dissertation.

Chapter II comprises the articles that are part of this thesis.

1. del Pozo, C., Bartrolí, J., Puy, N., Fàbregas, E., 2018. Separation of value-added chemical groups from bio-oil of olive mill waste. *Ind. Crops Prod.* 125. <https://doi.org/10.1016/j.indcrop.2018.08.062>
2. del Pozo, C., Bartrolí, J., Alier, S., Puy, N., Fàbregas, E., 2021a. Production, identification, and quantification of antioxidants from torrefaction and pyrolysis of grape pomace. *Fuel Process. Technol.* 211, 106602. <https://doi.org/10.1016/j.fuproc.2020.106602>
3. del Pozo, C., Bartrolí, J., Alier, S., Puy, N., Fàbregas, E., 2020. Production of antioxidants and other value-added compounds from coffee silverskin via pyrolysis under a biorefinery approach. *Waste Manag.* 109, 19–27.

4. del Pozo, C., Rego, F., Yang, Y., Puy, N., Bartrolí, J., Fàbregas, E., Bridgwater, A. V, 2021b. Converting coffee silverskin to value-added products by a slow pyrolysis-based biorefinery process. *Fuel Process. Technol.* 214.
<https://doi.org/10.1016/j.fuproc.2020.106708>

Chapter III contains a submitted article as also part of the work performed during this thesis.

Chapter IV consists in a general discussion of the results exposed in Chapters II and III.

Chapter V addresses the main conclusions of the thesis, as well as a brief description of the future perspectives.

Finally, Chapter VI presents the contributions to congress and seminars performed during this thesis.



I

Introduction

1.1 Introduction

1.1.1 Towards a circular bioeconomy

1.1.1.1 From linear economy to circular economy

Since the industrial revolution, economies have developed a ‘take-make-consume and dispose’ pattern of growth known as linear economy (Lieder and Rashid, 2016). However, it’s unsustainability makes it no longer an available model.

On one hand, linear economy is based on the assumption that natural resources are abundant, available, easy to source and cheap to dispose of, a fact that has brought to an unprecedented increase in natural resource use, exerting great pressure on the environment and even exceeding, in some cases, planetary boundaries (which include the biosphere's integrity, nitrogen and phosphorus cycles, climate change and land system changes) (EEA, 2016; European Commission, 2014; Steffen et al., 2015). This situation has led planet Earth to struggle to meet humanity's demands for land, food, and other natural resources, as well as, to absorb its wastes (Steffen et al., 2015). In fact, the demand for finite and sometimes scarce resources will continue to increase worldwide along with its growing population (European Commission, 2014), being global economic output projected to triple between 2020 and 2060 (OECD, 2021).

On the other hand, linear economic model also generates large number of wastes. Within the era of fashion and style, some of products are even provided with the explicit purpose of being discarded after use (planned obsolescence), stimulating throwaway-mindset which is today known as linear consumption behaviour (Lieder and Rashid, 2016). An important part of the wastes is, in addition, landfilled or incinerated. This generate harmful environmental impacts, apart from representing a loss of potential valuable products (present in some wastes), which also results in economic losses (European Commission, 2017a).

As problems of environmental pollution and landfill became severe, governments around the world have initiated more sustainable policies, based on waste reduction and recycling programs, with the aim to move away from the current linear economic model, and approach towards a green economy (Lieder and Rashid, 2016). This is the case of the 7th Environment

Action Programme, performed by the European Union, that set out 2050 vision of ‘living well within the limits of the planet’ (European Union, 2013).

From the past half-decade, circular economy has been gaining attention since it addresses the social, economic, and environmental concerns brought by the linear economic model (Ubando et al., 2020). Initially, the concept was formally accepted by the government of China as a new development strategy in 2002, and in January 2009, the first law ‘Circular Economy Promotion Law of the People's Republic of China’ took effect (Lieder and Rashid, 2016). At the end of 2015, European Commission also adopted the concept within the ‘EU Action Plan for the Circular Economy’ (European Commission, 2015a), being nowadays the current business model of Europe and China (Sharma et al., 2020).

1.1.1.2 Circular economy

The goal of circular economy has been to remodel the life cycle of a product, minimizing the resource consumption (both materials and energy) and waste generation, through maintaining the value of products, materials and resources in the economy for as long as possible, seeking to respect the ecological boundaries of our planet (European Commission, 2015a). Circular economy can be then represented as the core of a green economy perspective (EEA, 2016).

Benefits of a circular economy

By helping to decouple economic growth from resource use and its impacts, circular economy can offer the prospect of sustainable growth that will last, bringing resource, environmental, economic, and social benefits (European Commission, 2014).

a) Resource benefits

Circular economy seeks to increase the efficiency of primary resource consumption and so, reducing its demand (EEA, 2016). This would help to reduce countries high and increasing dependence on imports, making the procurement chains for many industrial sectors less subject to the price volatility of international commodity markets and supply uncertainty due to scarcity and/or geopolitical factors (EEA, 2016). As

more regions develop, international competition for resources increases and the dependence on imports become more vital. This is the case of Europe's economy, that depends on an uninterrupted flow of natural resources and materials (including water, crops, timber, metals, minerals and energy carriers) and where imports provide a substantial proportion of these materials, making this a source of vulnerability (EEA, 2016). Even if not scarce in absolute terms, many natural resources are unevenly distributed globally, exacerbating the potential for conflict (EEA, 2015). Moreover, uncertain and unstable prices can also disrupt the sectors that are dependent on these resources, forcing companies to lay people off, defer investment or stop providing goods and services (EEA, 2016). Therefore, circular economy could be the means by which companies and countries rise to the current and future challenges of global pressure on resources (EEA, 2016).

b) *Environmental benefits*

Reduction of resource demand also helps to enhance both ecosystem resilience and environmental impacts. The rapid increases in extraction and exploitation of natural resources are having a wide range of negative environmental impacts mainly due to using up resources at a rate that exceeds the Earth's capacity to renew them (EEA, 2014). This has led to air, water and soil pollution, acidification of ecosystems, biodiversity loss, climate change and waste generation, putting immediate, medium- and long-term economic and social well-being at risk. (EEA, 2016). A drawdown in extraction and imports also lead in parallel to a reduction in the emissions to the environment, caused in large part by the decrease of the transport involved in (EEA, 2016). In addition, circular economy seeks to reduce solid waste, landfill and greenhouse gases emissions through waste prevention, reuse, remanufacturing and/or recycling (Lieder and Rashid, 2016).

c) *Economic benefits*

The industry has recognised the strong business case for improving resource productivity (already discussed in the first point, a). In fact, it is estimated that resource efficiency improvements all along the value chains could reduce material inputs needs by 17%-24% by 2030 (Meyer, 2011). In this regard, circular economy pursues to create more economic value from fewer natural resources through innovative approaches,

such as technologies and business models, increasing opportunities for economic growth and innovation (EEA, 2016).

d) *Social benefits*

The implementation of a circular economy, and so, the creation of new business and market models (based on more efficient ways of producing and consuming), leads also to the creation of job opportunities, for instance, in the reuse and repairs sectors. Specifically, it is estimated that up to 178 000 new direct jobs (related to circular economy) could be create by 2030 (European Commission, 2015b).

The transition to a more circular economy would allow then to develop a sustainable, resource efficient, more resilient and competitive economy, creating new value chains and greener, more cost-effective industrial processes, while protecting biodiversity, reducing environmental pressures and delivering benefits in terms of job opportunities (EEA, 2016; European Commission, 2015a).

Implementation of a circular economy

Making the circular economy a reality requires however long-term involvement at all levels.

- i) In the first place, authorities (countries, regions, cities) should promote circular economic models through their policies. Economic measures, for instance, have proved instrumental in improving national waste management, in particular through landfill and incineration taxes. One example of this is ‘pay-as-you-throw’, where households (or whom it concerns) pay according to the amount of non-recyclable waste that they throw away (European Commission, 2014).
- ii) In the second place, circular economy has to be economically viable and present advantages (economic benefits) for the industry and business (Lieder and Rashid, 2016).
- iii) Finally, civil society is also a key factor in promoting products from a sustainable economy, such as the ones made with a certain level of recycled content, by means of a sufficient demand from consumers (European Commission, 2015a).

Moreover, the implementation of a circular economy also requires, as shown in Figure 1, changes throughout each step of the value chain (European Commission, 2015a).

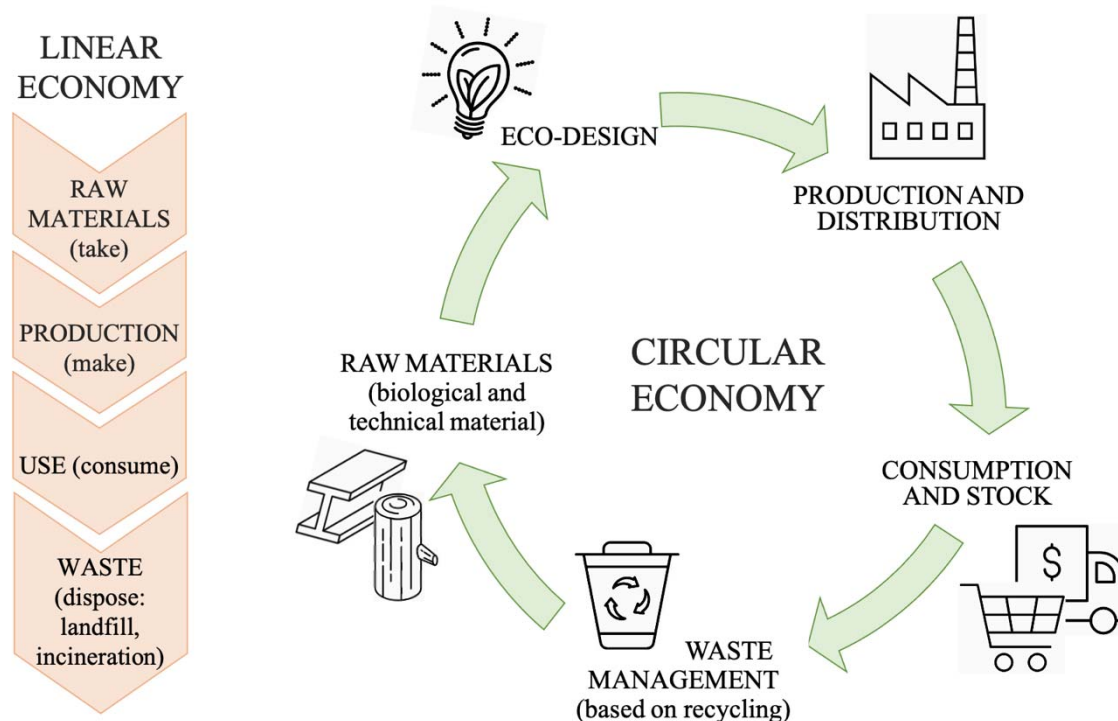


Figure 1. Linear economy vs circular economy.

Specifically, this thesis is focused on the waste management, which seeks to capture the value of the materials as far as possible, reducing losses and wastes (EEA, 2016). This step plays a central role in the circular economy, as it is based on transforming the wastes in value added products (or energy), feeding the products back into the economy as secondary materials. A reduction on products demand would also imply a reduction in emissions and environmental impacts, being most of natural resources extracted and imported (including the energy carriers) (EEA, 2016). Thus, actions to improve the waste management practices are crucial to promote the use of secondary materials, since they have a direct impact on the quantity and quality of these materials (European Commission, 2015a).

In this context, research and innovation play a key part in this systemic change, where new technologies, processes, services and business models are needed to rethink the way of producing and consuming, shaping the future of the economy and society.

Priority areas of a circular economy: biomass and bio-based products

The circular economy has been focused specifically on the following priority areas: plastics, food waste, critical raw materials, construction and demolition, and biomass and bio-based products (European Commission, 2015a), the latter one being the centre of this thesis.

Biomass and bio-based products are those coming from biological resources, such as wood, crops or fibres. These products can be used as raw materials in a wide range of areas, including construction, furniture, paper, food, textile, chemicals and plastics, or for energy purposes, such as biofuels (European Commission, 2015a). In particular, surfactants and cosmetics products already enjoy a large bio-based share; bio-based platform chemicals, on the other hand, are expected to grow rapidly in the coming years, while bio-based solvents are expected to grow much less (European Commission, 2018). Due to its biological origin, the biomass and bio-based products are also framed within the bioeconomy.

1.1.1.3 Bioeconomy

The bioeconomy is based on using renewable biological resources from land and sea, (like crops, forests, fish, animals and micro-organisms) in order to produce food, bio-based materials and bio-energy (European Commission, 2015a). Specifically, the European Union uses annually more than 1 billion tonnes of dry matter of biomass, 60% of which is used in the feed and food sector, followed by bioenergy (19.1%) and biomaterials (18.8%) (Camia et al., 2018).

The bioeconomy provides then alternatives to fossil-based energy and products, thus reducing dependence on non-renewable and unsustainable resources, apart from being potentially crucial to meet the increasing demand for food, jobs and income, caused by a rapidly growing world population, as well as, mitigate the effects of climate change (Camia et al., 2018; Ubando et al., 2020). Therefore, economic prosperity, society, resource and the health of the environment can be reinforced by each other through a sustainable circular bioeconomy, which adopts the circular economy framework, utilizing biomass as an integral component for the generation of biochemicals and bioenergy within a biorefinery (European Commission, 2018, 2017a; Ubando et al., 2020; Zabaniotou et al., 2018).

However, using biological resources also requires attention to their lifecycle environmental impacts and sustainable sourcing, since the multiple possibilities for their use can generate competition for them and create pressure on land-use. Hence, the natural/biological resources have to be managed in an efficient and sustainable way against the backdrop of an increasing demand for biomass (European Commission, 2018), avoiding negative impacts on biodiversity or ecosystem services (Camia et al., 2018).

The main sectors supplying biomass are specifically agriculture, forest-based sector and marine sector (fisheries, aquaculture and algae) (Camia et al., 2018). In the European Union, the agriculture sector occupied about half of the land area in 2015, generating 514 Mt of crop economic production and 442 Mt of residues¹ (Camia et al., 2018), agricultural wastes being therefore a potential source of sustainable biomass to be used in biorefineries (Cardoen et al., 2015; European Commission, 2018), and the focus of this thesis. In addition, the use of agricultural wastes can directly address the issue of environmental pollution, aside from avoiding pressure on land-use, and not necessarily adding the cost of producing feedstock as they are readily available (Ubando et al., 2020). Thus, the biorefinery of bio-based wastes should be considered as an integral part of the circular bioeconomy.

1.1.1.4 Biorefinery of bio-based wastes

A biorefinery is a facility wherein various conversion technologies are integrated to efficiently produce sustainable bio-based product streams, such as biochemicals or bioenergy, from biomass (Cherubini, 2010; Ubando et al., 2020). Therefore, biorefinery acts as a platform for biomass valorisation and so, as a strategic mechanism to achieve a circular bioeconomy, especially through the valorisation of bio-wastes (European Commission, 2017b; Ubando et al., 2020). Waste biorefineries allow then to convert bio-based wastes, which are considered renewable feedstock, into value-added products, maximizing the use of biomass and holistically integrating waste remediation and resource recovery (Mohan et al., 2016; Ubando et al., 2020). In the same way, the closed loop, which is one of the aims of the circular bioeconomy, is also a characteristic of the waste biorefinery, where the resulting biorefinery products are fed back into the economy (Mohan et al., 2016).

¹ EU-28 annual biomass production from land-based sectors, excluding pastures (10-year average 2006-2015, in megatons dry matter)

Furthermore, the concept of a circular economy has significantly changed the direction of waste management, now being moving towards the ultimate goal of a zero-waste economy (Mohan et al., 2016). This goal could be achieved through an integrated biorefinery, where all biomass could be transformed for different end-uses (del Pozo et al., 2021, 2020; Ubando et al., 2020). In addition, multi-product biorefineries can improve the efficiency of biomass utilisation by increasingly parallel exploitation of side flows (European Commission, 2018).

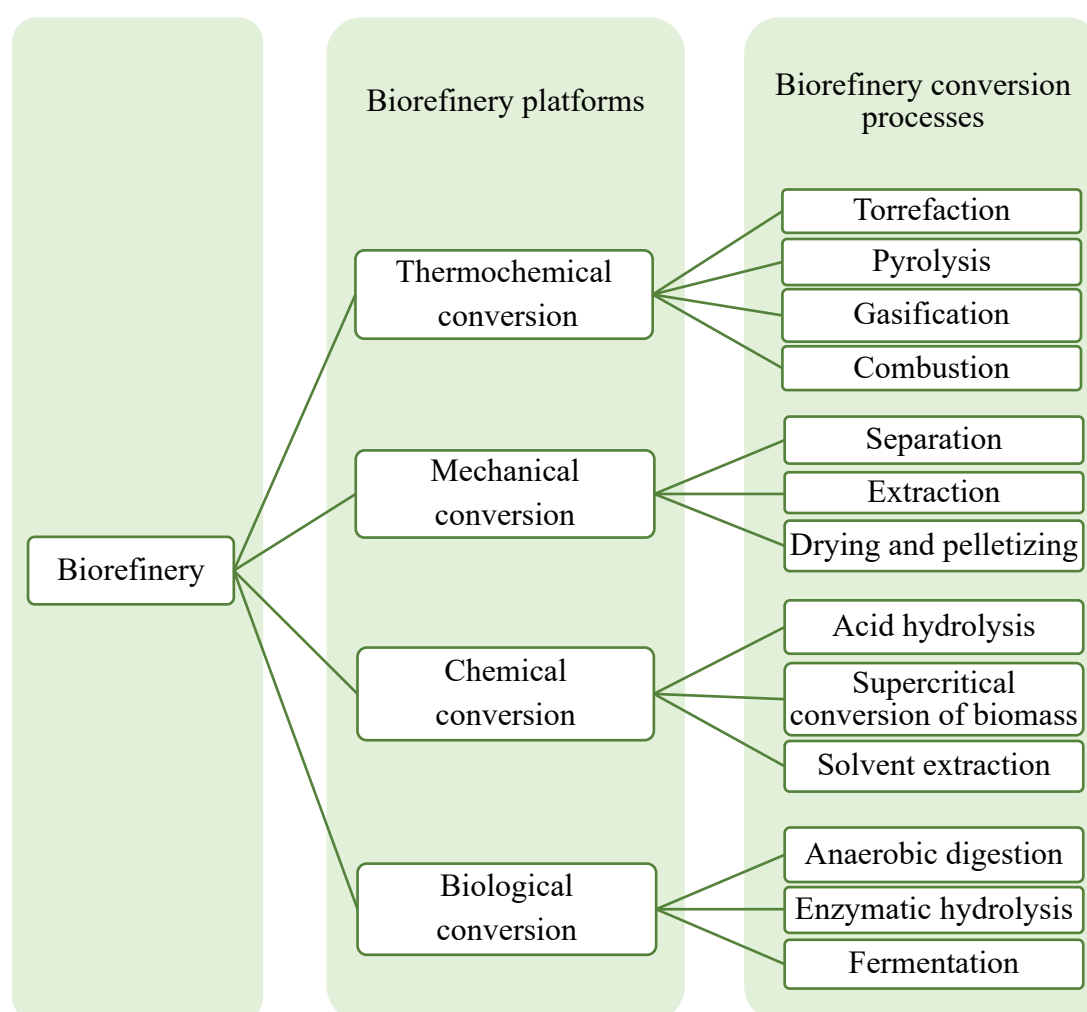


Figure 2. Biorefinery platforms and conversion processes (Ubando et al., 2020).

Different valorisation technologies have been investigated in order to carry out the biorefinery processes (see Figure 2), being pyrolysis and torrefaction (thermochemical conversion) the centre of this thesis. These thermochemical treatments consist in a thermal decomposition of biomass, performed at elevated temperatures under oxygen-limiting conditions, to give rise different value-added products. Pyrolysis is performed from around 300 °C to over 500 °C,

while torrefaction take place at 200–300 °C (Basu, 2018; Brassard et al., 2017; del Pozo et al., 2018).

One of the main advantages of these treatments is that many types of raw materials can be used, being able to address the seasonality of various feedstocks, including agricultural wastes, and therefore reducing the downtime period of biorefineries (Czajczyńska et al., 2017; EEA, 2020; Ubando et al., 2020). Another advantage is their potential to perform an integrated biorefinery, as each fraction resulting from the thermochemical process could have different applications, thus also contributing to zero-waste economy (del Pozo et al., 2021).

Therefore, the present thesis is focused on obtaining value-added products from agricultural wastes, that otherwise would be landfilled or incinerated, through thermochemical processes (pyrolysis and torrefaction), being framed within a waste biorefinery and a circular bioeconomy context.

1.1.2 Thermochemical treatments: pyrolysis and torrefaction

1.1.2.1 Thermochemical degradation of biomass

Biomass is mainly composed of three biopolymers, hemicellulose (20–35 wt.%), celluloses (35–50 wt.%) and lignin (10–25 wt.%) (Ma et al., 2019) (see Figure 3), that degraded during the thermochemical process, giving rise different value-added products (see Figure 4).

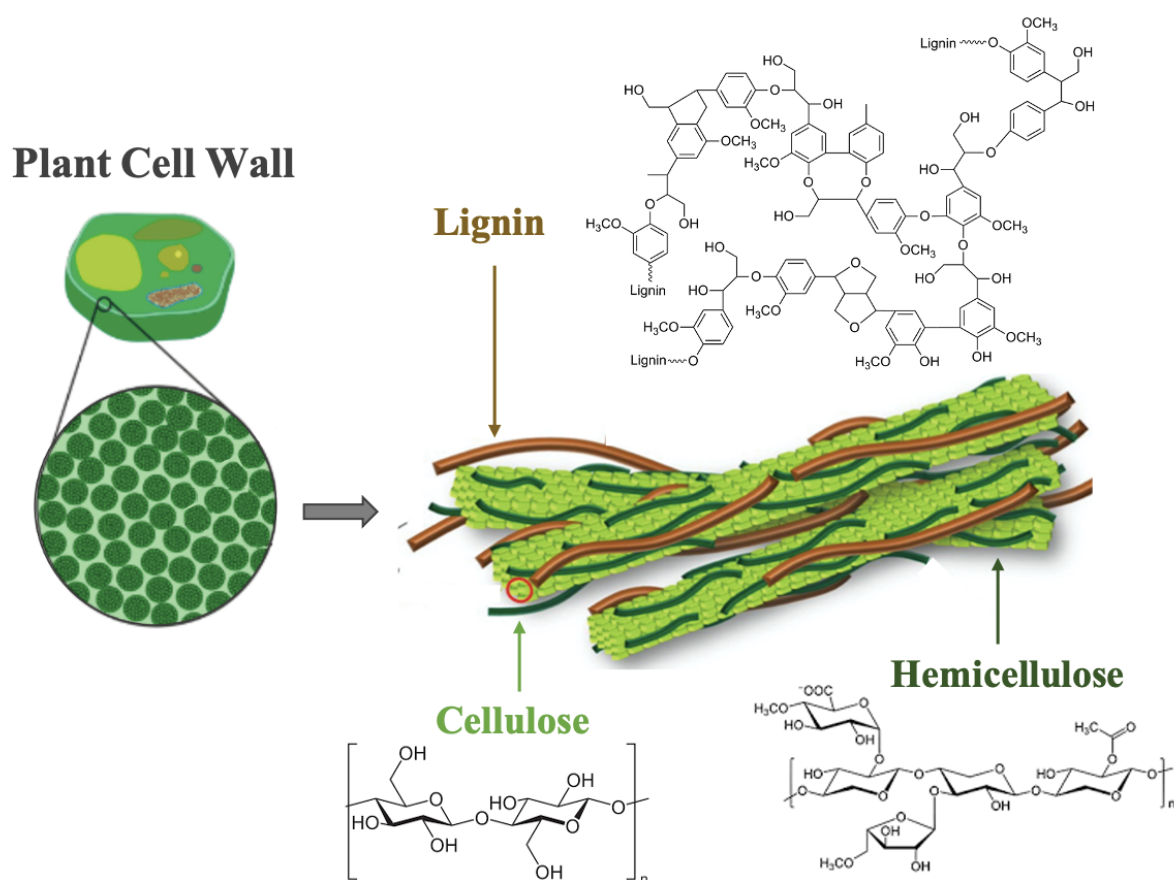


Figure 3. Main components of lignocellulosic biomass. Figure adapted from Jensen et al., (2017) and Hasanov et al., (2020).

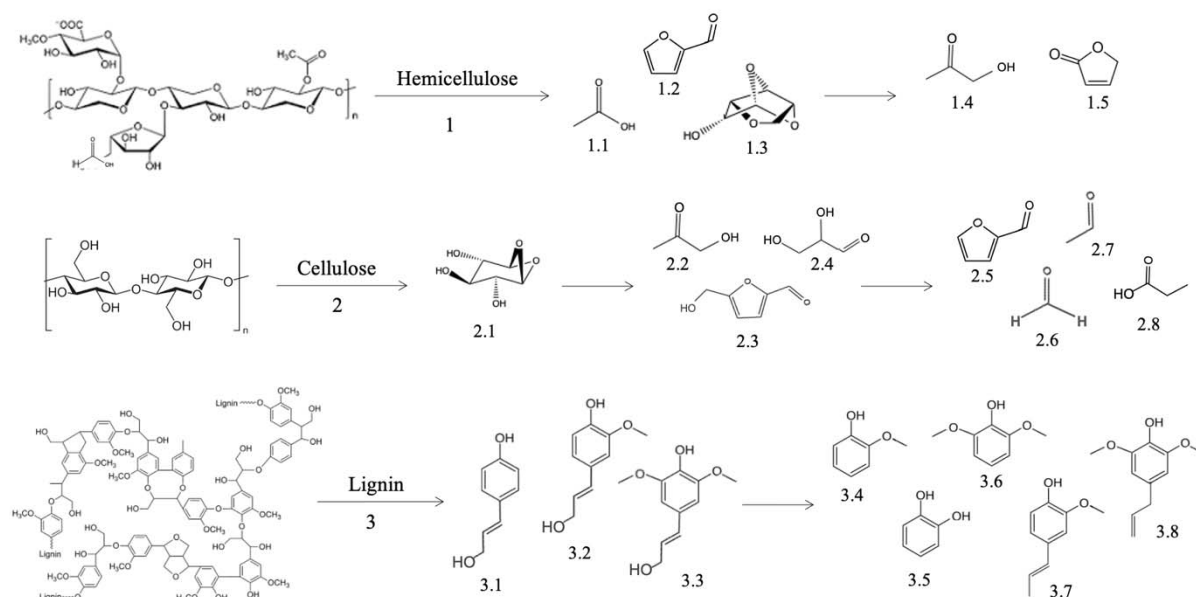


Figure 4. Thermochemical degradation of hemicellulose, cellulose and lignin.

1.1) Acetic Acid; 1.2) furfural; 1.3) 1,4;3,6-dianhydro- α -d-glucopyranose; 1.4) 1-hydroxy-2-propanone, 1.5) furanone; 2.1) levoglucosan; 2.2) 1-hydroxy-2-propanone; 2.3) 5-hydroxymethyl-furfural; 2.4) glyceraldehyde; 2.5) furfural; 2.6) formaldehyde; 2.7) acetaldehyde; 2.8) propanoic acid; 3.1) p-coumaryl alcohol; 3.2) coniferyl alcohol; 3.3) sinapyl alcohol; 3.4) 2-methoxyphenol; 3.5) catechol; 3.6) 2,6-dimethoxyphenol; 3.7) trans-isoeugenol; 3.8) 2,6-dimethoxy-4-(2-propenyl)-phenol.

Hemicellulose consists of a short-chain of heteropolysaccharides, mainly glucose and pentoses (xylose, galactose, rhamnose and arabinose), being xylose the most abundant monomer (Ma et al., 2019; Ubando et al., 2020). In addition, it is also composed of some uronic acids and acetyl groups (see Figure 3). Therefore, hemicellulose presents an amorphous and branched structure, that is easy to degrade at low temperatures due to weak chemical bonds (Zhao et al., 2017). Acids are one of the main products from the degradation of hemicellulose, especially acetic acid, which is formed by deacetylation reaction at the initial stage of the thermochemical process (see Figure 4, compound 1.1) (Mohan et al., 2006; Zhao et al., 2017). Other important products are furans (mainly furfural), ketones and anhydrosugars, the latter one being easily ring-opened and cracked, resulting in the formation of 1-hydroxy-2-propanone, furanone, and other small molecular compounds (see Figure 4) (Wang et al., 2017).

In contrast to hemicellulose, cellulose is composed of a long well-ordered linear polymer of glucose (D-glucose units connected with 1,4-glycosidic bond) with high structural stability,

requiring higher temperature to degrade it (Ma et al., 2019; Polidoro et al., 2018; Zhao et al., 2017). Initially, the thermal degradation of cellulose consists on a depolymerization that forms anhydrosugar derivatives, mainly levoglucosan (see Figure 4, compound 2.1) (Mohan et al., 2006; Shen and Gu, 2009). These dehydrated carbohydrates have low heat stability, so they easily degrade at higher temperatures (Zhao et al., 2017), resulting in 4-6 carbon atoms products, including the ones shown in Figure 4 (1-hydroxy-2-propanone (compound 2.2), 5-hydroxymethyl-furfural (compound 2.3) and glyceraldehyde (compound 2.4)) (Shen and Gu, 2009). At the same time, some of these compounds also degrade forming furfural (compound 2.5) from 5-hydroxymethyl-furfural, formaldehyde and acetaldehyde (compounds 2.6 and 2.7) from 1-hydroxy-2-propanone, and propanoic acid (compound 2.8) from glyceraldehyde, among others (see Figure 4) (Shen and Gu, 2009).

Lignin, on the other hand, is mainly composed of three aromatic basic units, p-coumaryl, coniferyl and sinapyl alcohols (see Figure 4, compounds 3.1, 3.2 and 3.3), that form an amorphous tridimensional structure difficult to degrade (Wang et al., 2017). Thus, and as shown in Figure 4, the thermal decomposition of lignin drives to the formation of phenolic derivatives from its principal units (Mohan et al., 2006). Specifically, the aliphatic hydroxyl groups can be easily removed through dehydration at low temperature leading to the formation of an unsaturated side chain structure; moreover, the methoxyl groups can also decompose to monophenols or catechols (Wang et al., 2017).

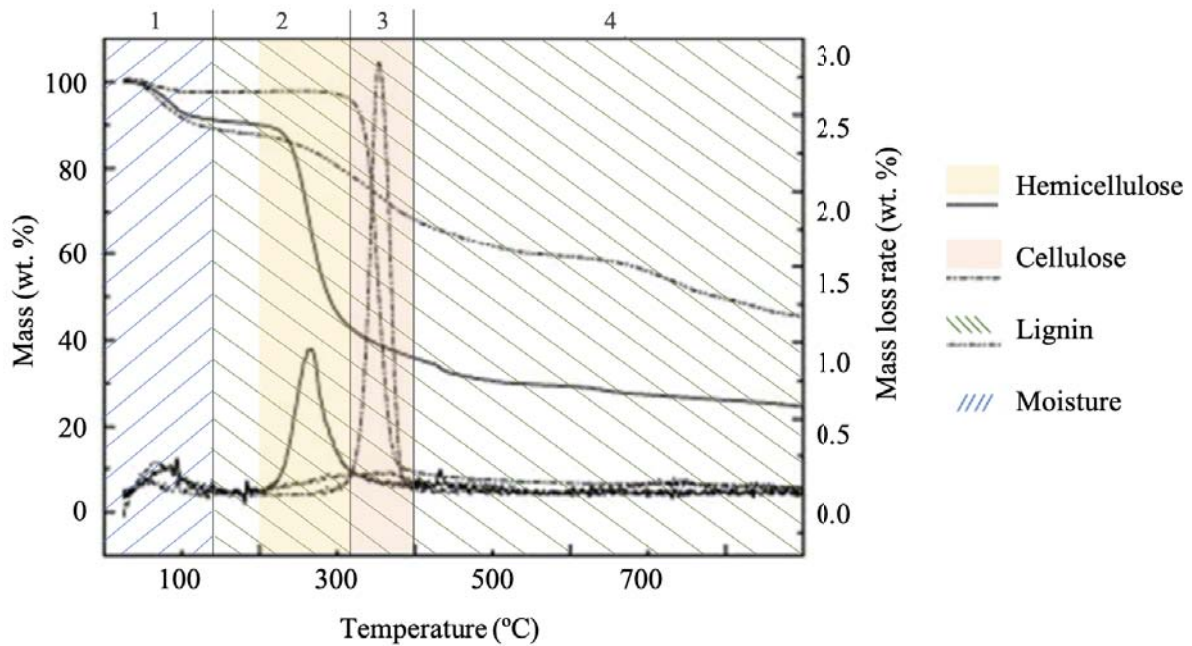


Figure 5. Pyrolysis curves of hemicellulose, cellulose and lignin from thermogravimetric analysis. Figure adapted from Yang et al., (2007).

Therefore, the thermal decomposition of biomass depends on the individual roles of its main components, hemicellulose, cellulose and lignin, which are thought to react independently and as such, they do not show synergetic effect (Chen and Kuo, 2011; Zhao et al., 2017). The degradation of biomass during the pyrolysis process can be studied through thermogravimetric analysis (Polidoro et al., 2018), and as shown in Figure 5, it involves 4 main stages:

- The first stage, that take place until approximately 130 °C, is where moisture elimination occurs; hence, the weight loss is attributed to water, and to a lesser extent, extractives removal (Polidoro et al., 2018).
- The second stage, with maximum loss weight rate around 250 °C, mainly refers to the degradation of hemicellulose, the first polymer to decompose (Polidoro et al., 2018).
- The third stage (from approximately 300 °C to 400 °C) is related to the decomposition of cellulose, that as hemicellulose, occurs quickly.
- Finally, the last stage represents the degradation of lignin, that take place in a wide range of temperatures since its branched structure is difficult to decompose (Polidoro et al., 2018; Yang et al., 2007). Moreover, after the pyrolysis process, a solid residue remains, consisting of mainly fixed carbon and inorganic materials (ash) from the starting material, which not decomposes (Polidoro et al., 2018).

The range of temperatures where biopolymers degrade may differ from one author to another. Mohan et al., (2006) reported that hemicellulose, cellulose and lignin decomposes when heated at 200-260 °C, 240-350 °C and 280-500 °C, respectively; Zhao et al., (2017) found that the thermal decomposition occurs at 203-386 °C for hemicellulose, 286-426 °C for cellulose and 215-585 °C for lignin; on the other hand, Yang et al., (2007) described it between 220–315 °C and 315–400 °C, in the case of hemicellulose and cellulose, and 160-900 °C for lignin; and Uzun et al., (2010) reported hemicellulose degradation at 150°C–350°C, cellulose at 275°C-350°C, and lignin, at 200°C–700°C.

From the decomposition of biomass, three main products (gas, liquid and solid) are always produced, but the yield and characteristics of each fraction varies over the thermochemical treatment used.

1.1.2.2 Pyrolysis and torrefaction

Pyrolysis and torrefaction, which are both thermochemical treatments performed at elevated temperatures under oxygen-limiting conditions, decompose biomass originating three different fractions: a solid fraction (biochar), non-condensable gases, and a liquid fraction mainly composed of condensable products from the degradation of hemicellulose, cellulose and lignin.

The type of thermochemical treatment is mainly defined by the temperature of the process and the residence time inside the reactor, since they both have a large impact on the properties and proportion of the resulting fractions (see Table 1 and Figure 6). It is observed that with the increase of the heating temperature, the yield of solid decreases, increasing the yield of liquid and gas fractions (see Table 1) (Yu et al., 2016). Regarding the retention time, it has been fixed at 10 min for the pyrolysis and torrefaction experiments of this thesis.

Table 1

Characteristics of pyrolysis and torrefaction process. Table adapted from Balat et al., (2009); Basu, (2018); Bridgwater, (2012); Jahirul et al., (2012); and Mohan et al., (2006).

	Operational conditions		Typical product weigh yield ¹		
	Temperature	Solid residence time	Solid	Liquid	Gas
Conventional pyrolysis	277 - 677 °C	5 - 30 min	25%	50% in 2 phases	25%
Torrefaction	200 - 300 °C	10 - 60 min	80%	0% ²	20%

¹ on dry basis

² unless condensed, then up to 5%

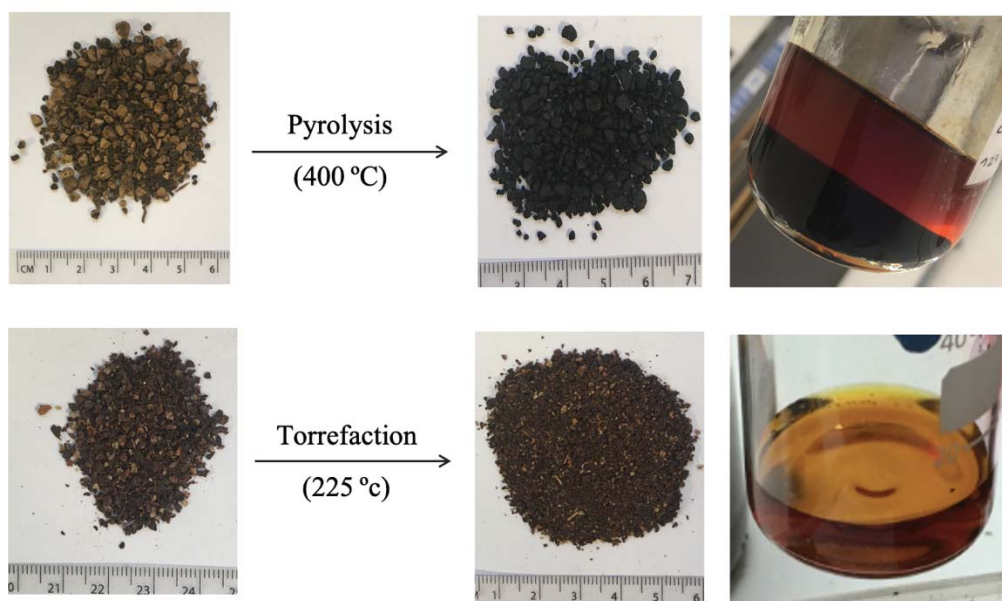


Figure 6. Pyrolysis and torrefaction products. Pyrolysis was performed on olive mill waste biomass, and torrefaction, on grape pomace biomass, which are respectively, the main solid wastes from olive oil and wine making process.

Conventional pyrolysis, also named slow, intermediate, or just pyrolysis in the present thesis, is characterised by the depolymerization of the main components of the biomass (hemicellulose, cellulose and lignin) due to the high temperature of the process, originating a principal liquid fraction, known as pyrolysis liquid or bio-oil (see Table 1). As shown in Figure

6, the liquid fraction usually comprises two phases since during the pyrolysis process high amount of reaction water is produced, driving to separate the hydrophilic and hydrophobic compounds in an aqueous and organic phase (del Pozo et al., 2018; Torri and Fabbri, 2014). The hydrophilic products are mainly related to the degradation of hemicellulose and cellulose, while the hydrophobic ones come mostly from lignin decomposition.

Torrefaction, on the other hand, takes place at a lower temperature (200–300 °C), giving rise to a main solid fraction and, to a lesser extent, a torrefaction liquid (see Table 1 and Figure 6). The liquid fraction is mostly composed of water from biomass moisture, and hemicellulose and lignin degradation products, as they are the first polymers to start to degrade (Basu, 2018; Bridgwater, 2012). In this case, liquid fraction only has one phase since at torrefaction temperatures lignin is not degraded enough to have enough hydrophobic compounds for the phase separation to take place.

Each of the resulting solid, liquid and gas fractions has potential to be used in different applications. Liquid and gas fractions have been reported as chemical and energy sources respectively, whereas the solid fraction can be considered as a value-added product itself due to the broad range of potential applications it has (del Pozo et al., 2021). Thus, this thesis is focused on pyrolysis and torrefaction treatments as the means to transform agricultural wastes into value-added products.

1.1.2.3 Thermochemical products

Pyrolysis and torrefaction processes always produce solid, liquid and gas fractions, with different potential uses.

The solid fraction, or biochar, consists in the solid product of the incomplete combustion of biomass under oxygen-limiting conditions. It is characterised by a stable and porous structure, large specific surface area and abundant surface functional groups (see Figure 7) (Chen et al., 2016). Biochar is also rich in ash and mineral content, such as N, P, K, and Ca, since inorganics from the original feedstock remains in this solid fraction. The main applications of biochars have been as soil amendment, thus returning to soils as fertilisers to increase crop yields (Rehrah et al., 2014; Tan et al., 2015; Wang and Liu, 2017), and as energy source for

combustion process, since they show better fuel qualities, and are better heat carriers, than raw biomass (Chen et al., 2016; Liu and Han, 2015; Ubando et al., 2020). However, both fertilizer and energy purposes imply a low valorisation of biochars (Ubando et al., 2020). Recently, they have increased attention due to their potential role in valued-added applications, including carbon sequestration and pollutants removal (Wang and Liu, 2017). Carbon sequestration are related to the reduction of greenhouse gas emissions (Brassard et al., 2016) and so, to the mitigation of global warming and climate change (Chen et al., 2016). On the other hand, several authors reported the role of biochars as adsorbents of organic and inorganic contaminants, such as heavy metals and pesticides, in soil and water mediums (Cabrera et al., 2014; Tan et al., 2015; Wang and Liu, 2018, 2017; Xie et al., 2015). Therefore, biochar shows high versatility in its applications, aside from environmental benefits (Dai et al., 2019).

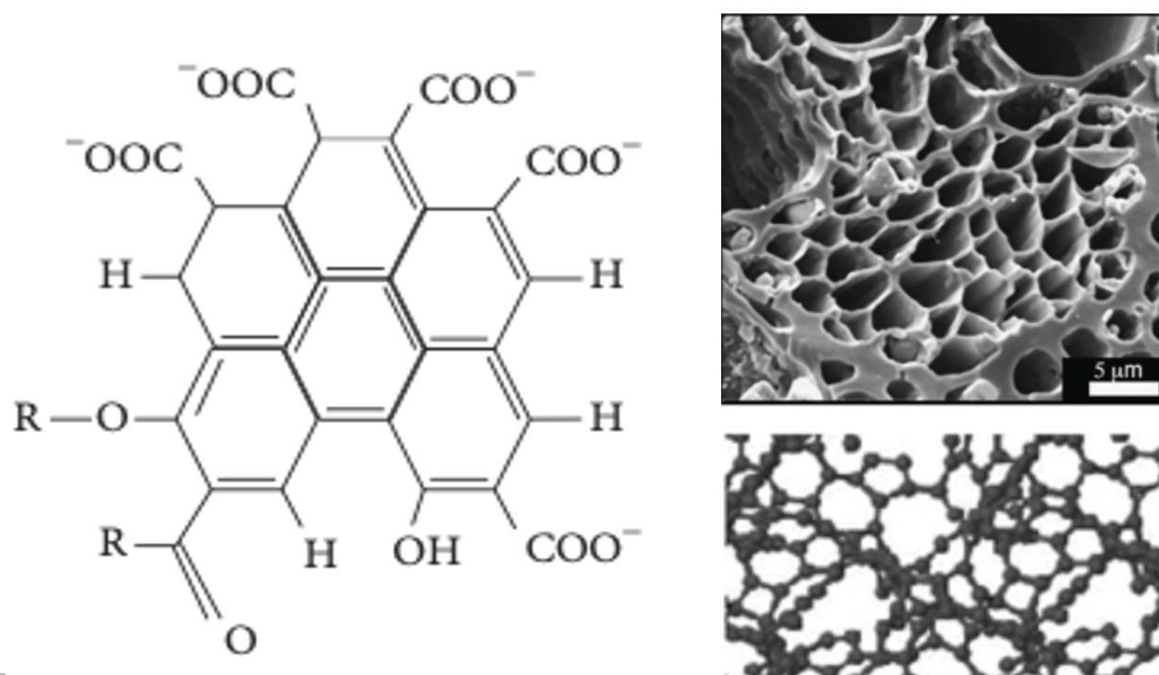


Figure 7. Biochar structure.

Figure adapted from Jouiad et al., (2015), Purwanto et al., (2018) and Tomczyk et al., (2020).

On the other hand, the liquid fraction is composed of the pyrolysis and torrefaction products from the degradation of the biomass that condense. These products consist in low molecular weight oxygenated compounds, such as carboxylic acids, esters, alcohols, ketones, aldehydes, phenols, 2-methoxy-phenols, 2,6-dimethoxy-phenols, alkenes, aromatics, nitrogen compounds, furans, sugars and other miscellaneous species (Goyal et al., 2008). As shown in

the previous section (Section 1.2.2), the hydrophilic products are concentrated in an aqueous solution, while the hydrophobic ones can be separated in an organic phase. Some of these compounds have industrial interest, thus liquid fraction can be considered as a potential source of value-added chemicals. Specifically, liquid fraction is usually rich in acetic acid, that is a chemical platform with high industrial demand (Zhao et al., 2017); sugars, that could be used in biogas/bioethanol production (del Pozo et al., 2018); and phenolics, which its antioxidant properties make them highly valued in nutraceutical and cosmetic industries (Kim, 2015). Moreover, liquid fraction has been also described as liquid fuel; however, its high water, oxygen and acid content makes necessary an upgrading (Brassard et al., 2017). In addition, Ubando et al., (2020) considers that its use as fuel are deemed to be of lowest valued product from an economic point of view.

Regarding the gas fraction, it is composed by the non-condensable gases released from the thermochemical process, consisting of carbon dioxide (CO₂), carbon monoxide (CO), hydrogen (H₂), methane (CH₄), ethane (C₂H₆), ethylene (C₂H₄), and small amounts of other gases, such as propane (C₃H₈), ammonia (NH₃), nitrogen oxides (NO_x), sulphur oxides (SO_x) and alcohols of low carbon numbers (Kan et al., 2016). Taking advantage of the hot temperature of the gas, one of the potential applications of this fraction could be its use as a heat source to dry biomass before the thermochemical process (del Pozo et al., 2021).

The properties, and so applications, of each fraction will be, however, highly influenced by the biomass feedstock, the operating parameters (mainly retention time and temperature) and the pyrolysis technology (reactor type) (Brassard et al., 2017; Wang and Liu, 2017).

1.1.2.4 Pyrolysis and torrefaction reactors

The pyrolysis and torrefaction products analysed in this thesis have been performed in two different auger reactors: a pilot plant (15 kg/h) and a lab size reactor (0.3 kg/h). Among the available pyrolysis units, auger reactor is a polyvalent and promising technology for producing both solid and liquid fractions (Brassard et al., 2017). Apart from that, auger reactors are simple to operate, can be mobile, require little or no carrier gas, and needs low energy to run (Brassard et al., 2017).

Pilot scale reactor

The thermochemical products from the pilot plan were provided by ENER-bas company, headquartered in Catalonia, Spain. This company designed and developed the technology of the reactor, registering in 2016, two European patents: EP3048161A1-Industrial plant for biomass thermochemical treatment and EP3470386B1-Method for treating the biomass of lignocellulosic agricultural waste and/or waste containing phenolic functional groups. As shown in Figure 8, this is a mobile plant that was designed to be moved close to harvests, as well as to be robust and flexible enough to be fed by different types of biomasses. The plant was therefore intended to address the seasonality of the feedstocks, thus reducing the downtime period of the biorefinery. Moreover, locating the reactor close to the primary production sites, it can be avoid the transportation of the biomass, that is bulky and so, expensive to move, together with bringing new added value generation into rural areas (European Commission, 2018).



Figure 8. Pilot plant from ENER-bas company.

The pilot scale reactor has a capacity of up to 100 kg/h of biomass, in a size range of 1–10 mm, and it is capable of operating at temperatures of up to 600 °C with low electricity consumption (10 kWh) (Recari et al., 2017). In this case, the working temperatures were settled between 225 and 500 °C, and the feeding rate was fixed at 15 kg/h. Moreover, the residence time of the experiments was 10 min, and they were carried out without a previous nitrogen purge.

Chapter I

The pilot plant comprises five main parts: the feeding system (1), a drying reactor (2), the torrefaction/pyrolysis reactor (3), a cooling screw, together with the vessel for solids collection (4), and the condensing system (5) (see Figure 9) (Recari et al., 2017).

After a natural drying and be crushed with a hammer crusher, biomass is introduced into the feeding system (1) and moved along the drying reactor (2). The drying reactor (electrical heating; internal diameter: 160 mm; length: 3000 mm) allows to dry the biomass, increasing the efficiency of the thermochemical process without the need for an oven, since it is already incorporated in the pilot plant, besides working continuously. Biomass is then driven to the torrefaction/pyrolysis reactor (3) (electrical heating, internal diameter: 160 mm; length: 4000 mm) where the thermochemical conversion take place. The temperature profiles along the different conveyors are measured and recorded by thermocouples (Recari et al., 2017). In this part (3), biomass decomposes in solid and gas fractions. The solid fraction is conducted into the cooling screw (4) (water jacket; internal diameter: 160 mm; length: 3000 mm), where it is cooled to avoid spontaneous combustion, and collected in the vessel. The gas fraction is led to the condensing system (5), which comprises a cyclone to remove particles, and a condenser, where the condensable gas is collected as the liquid fraction (Recari et al., 2017).

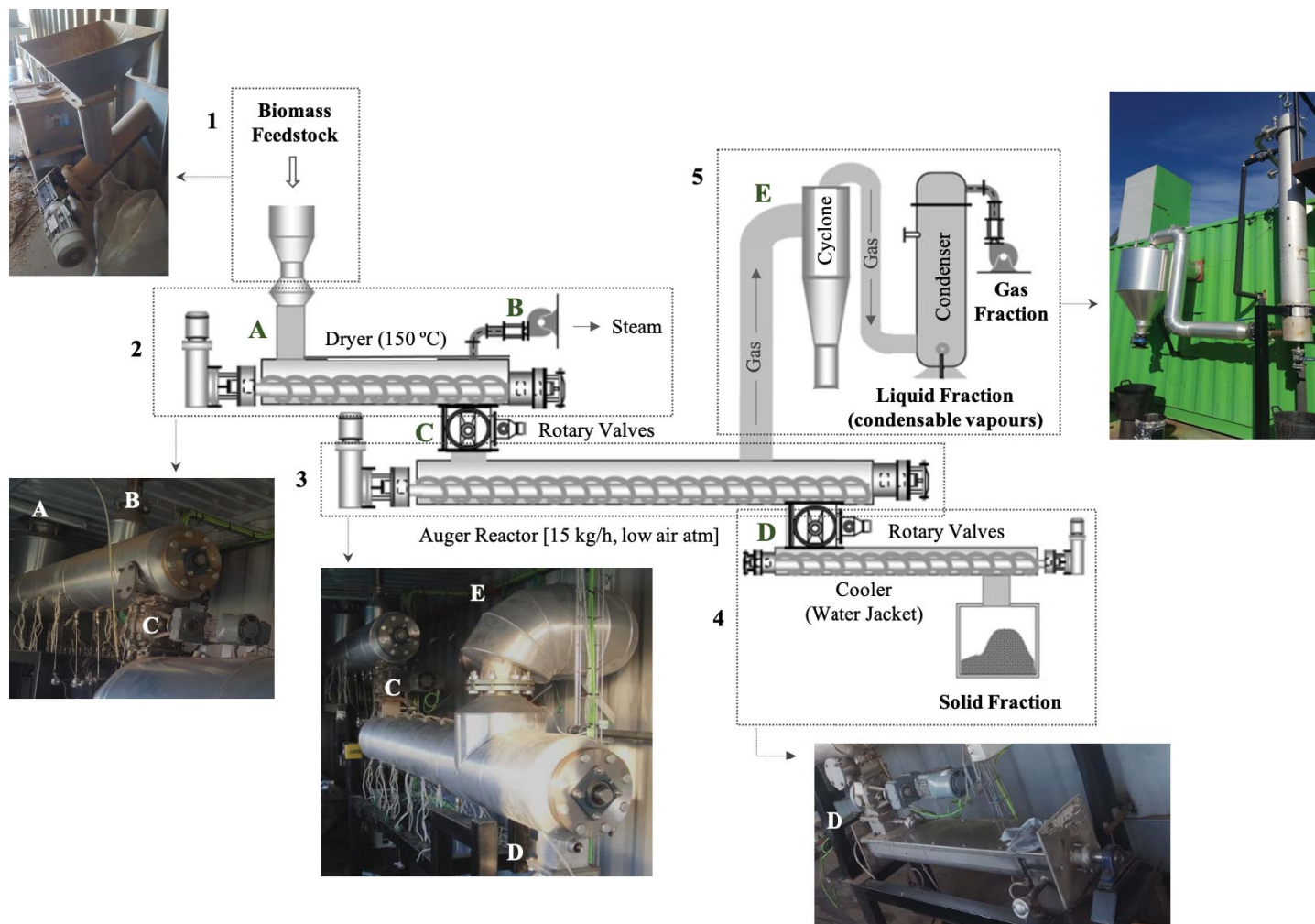


Figure 9. Detailed scheme of the pilot scale reactor from ENERG-bas company. Figure adapted from Recari et al., (2017).

Lab scale reactor

The lab scale reactor was designed and constructed at the Energy and Bioproducts Research Institute (EBRI), at Aston University, U.K. (see Figure 10).

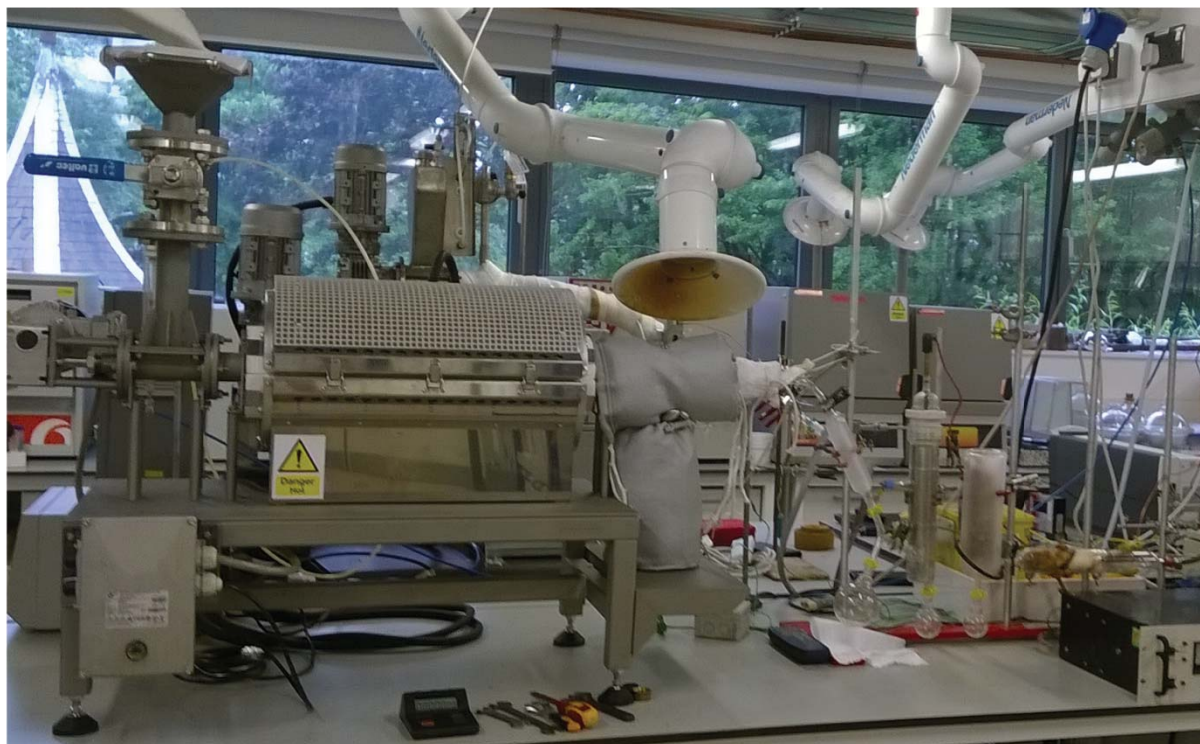


Figure 10. Lab scale reactor from EBRI.

The system consists in a compact stainless-steel bench-scale auger, that does not use a heat carrier, and operates continuously (Yu et al., 2016). The experiments were performed using a feeding rate of 0.3 kg/h and, as in the case of the pilot plan, the residence time was fixed at 10 min.

The lab scale reactor consists of the following main components: biomass feeding subsystem (1), auger reactor (2), solid (3) and liquid (4) collection subsystem and control subsystem, comprising a gas flow meter (5) and a micro-gas chromatography (MicroGC) (6) (see Figure 11) (Yu et al., 2016).

The main component of the biomass feeding subsystem (1) is a volumetric screw feeder, where biomass is fed manually through a vertical pipe (1.5", stainless steel) with a small feeding

hopper, a ball valve to allow isolation from outside air, and a gas inlet with a rotameter, to inject inert carrier gas into the system. The biomass feedstock should have a maximum moisture content of 10%, and a homogeneous particle size of about 1 cm. Moreover, before the thermochemical process, the system is purged with nitrogen to remove the inside air. The biomass from the feeding system is then passed to the auger reactor (2) (diameter: 26 mm; length: 500 mm), which is electrically heated by a Carbolite VST 12/400 2 kW furnace (Yu et al., 2016). The temperature is monitored using four K-type thermocouples placed at the beginning (T_1), at the middle (T_2) and at the end (T_3) of the reactor, and also closely to the gas outlet (next to the char pot) (T_4), and recorded with a data logger. The auger rotation moves the product along the axis until the end of the heating zone, decomposing the biomass. The gases and organic volatiles leave the reactor, and the biochar is collected by gravity in the char pot at the bottom (3). As shown in Figure 11, the char pot and gas outlet are also heated through electric heating tapes to avoid the condensation of gases inside this section. The char is collected once the reactor is cooled at room temperature. On the other hand, the condensable vapours are collected from the cooling and liquid collection system, comprised of a water-cooled condenser, fixed at 20 °C, and two ice-fingers filled with dry ice and acetone (4) (del Pozo et al., 2021). The non-condensable gases are filtered by a cotton filter to remove remaining particles and aerosols, and pass through a gas meter (5) that measures the volumetric flow. The gases are then directed to a vent, sending a small fraction to online MicroGC (6) (GC; VARIAN CP-4900, USA) (del Pozo et al., 2021).

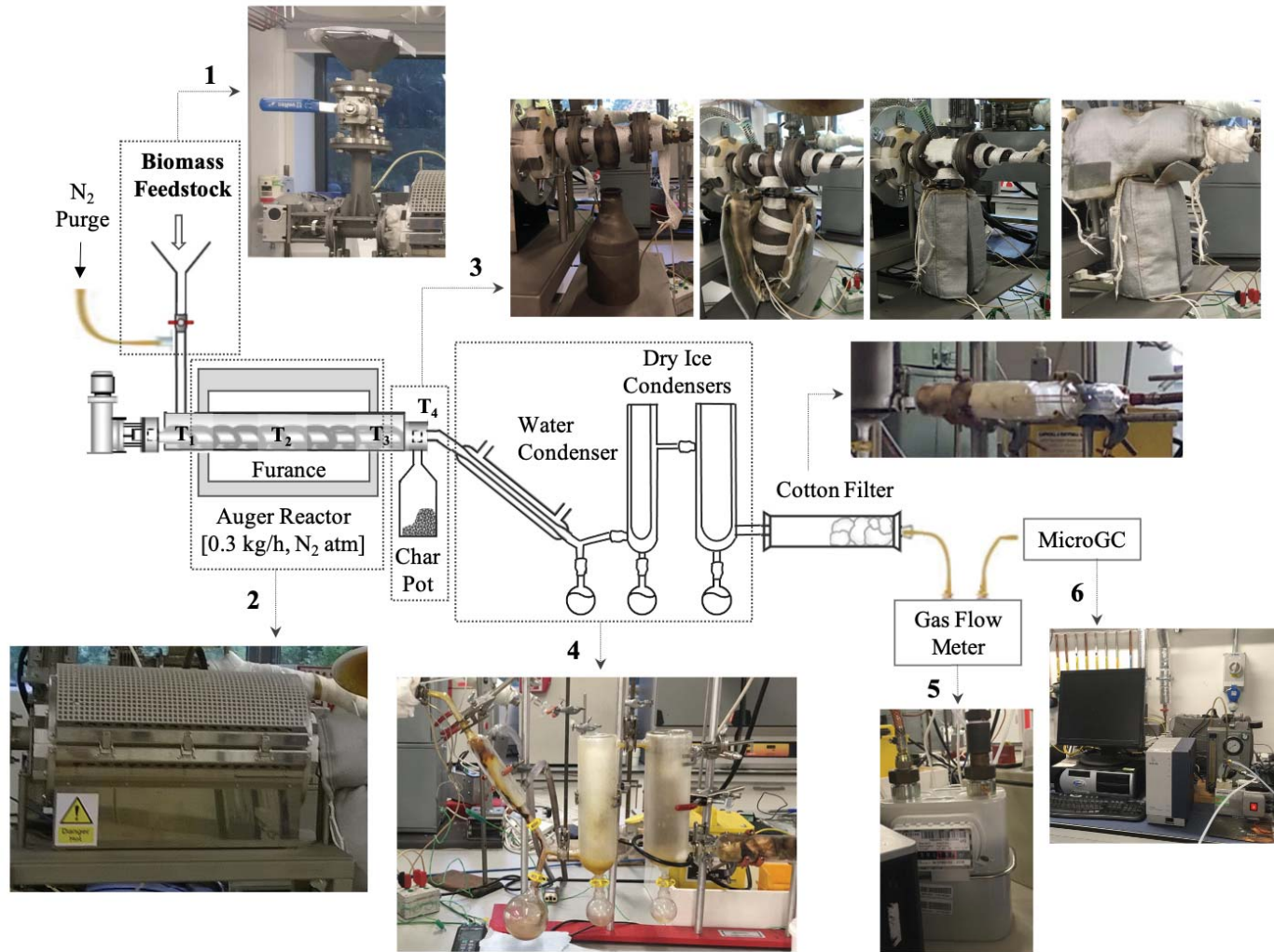


Figure 11. Detailed scheme of the lab scale reactor from EBRI. Figure adapted from Yu et al., (2016).

1.2 Motivations and objectives

1.2.1 Motivations

Within the transition towards a circular bioeconomy, this thesis is focused on obtaining value-added products from agricultural by-products, also known as wastes in this work, through pyrolysis and torrefaction treatments. The present work is then framed within a waste biorefinery context, holistically integrating waste remediation and resource recovery.

Specifically, this thesis has worked with olive mill waste (OMW), grape pomace (GP) and coffee silverskin (CSS), which are respectively the main solid wastes from the olive oil production, wine making and coffee roasting processes. Olive oil and wine production industries are important economic sectors of Mediterranean countries, thus amounting to large amounts of wastes. Regarding the coffee, it is one of the most commonly consumed beverages worldwide. Although coffee is cultivated in tropical areas, the roasting process is performed in the consuming countries, so CSS is also considered a local waste.

Most of these residues are disposed of as industrial waste, representing serious environmental problems due to their phytotoxicity, mainly caused by phenolic compounds (Polidoro et al., 2018; Volpe et al., 2015). At the same time, their rich content in phenolics makes them a potential source of value-added compounds, since phenolic antioxidant properties are highly valued in cosmetic and nutraceutical industries.

The present thesis has based on auger reactor technology to transform the agricultural wastes into a resource. This technology is used for producing both solid and liquid fractions (Brassard et al., 2017), both of them having different potential applications. Liquid fraction can be a potential source of not just phenolics, but also other value-added compounds as acetic acid, which has high demand. On the other hand, solid fraction can be used as solid biofuel, apart from having other potential higher value uses, such as pollutant adsorbent. The integrated biorefinery of the wastes permits therefore coming closer to the ultimate goal of a zero-waste economy.

1.2.2 Objectives

The aim of the present thesis is to study the products resulting from the pyrolysis and torrefaction of OMW, GP and CSS agricultural wastes, performed in auger reactors at different temperatures, in order to determine their potential applications within a waste biorefinery and circular bioeconomy context.

For this purpose, the following goals have been defined:

- To analyse the composition of the torrefaction and pyrolysis liquids.
- To develop a procedure to separate the compounds of pyrolysis liquid in value-added chemical groups.
- To study the suitability of Folin-Ciocalteu (FC) and 2,2-Diphenyl-1-picrylhydrazyl (DPPH) methods to quantify the phenolic compounds in torrefaction and pyrolysis liquids.
- To analyse the properties of biochar for energy purposes.
- To analyse the properties of CSS biochar as an absorbent of organic pollutants in aqueous media.
- To determine which temperatures are suitable to valorise each agricultural waste.
- To compare the thermochemical products obtained from different size auger reactors to understand the fundamental difference and create correlations on pyrolysis runs at different scale.

1.3 References of Part I

- Balat, Mustafa, Balat, Mehmet, Kirtay, E., Balat, H., 2009. Main routes for the thermo-conversion of biomass into fuels and chemicals. Part 1: Pyrolysis systems. *Energy Convers. Manag.* 50, 3147–3157. <https://doi.org/10.1016/j.enconman.2009.08.014>
- Basu, P., 2018. *Biomass Gasification, Pyrolysis and Torrefaction*, third. ed. Academic Press.
- Brassard, P., Godbout, S., Raghavan, V., 2017. Pyrolysis in auger reactors for biochar and bio-oil production: A review. *Biosyst. Eng.* 161, 80–92. <https://doi.org/10.1016/j.biosystemseng.2017.06.020>
- Brassard, P., Godbout, S., Raghavan, V., 2016. Soil biochar amendment as a climate change mitigation tool: Key parameters and mechanisms involved. *J. Environ. Manage.* 181, 484–497. <https://doi.org/10.1016/j.jenvman.2016.06.063>
- Bridgwater, A. V., 2012. Review of fast pyrolysis of biomass and product upgrading. *Biomass and Bioenergy* 38, 68–94. <https://doi.org/10.1016/j.biombioe.2011.01.048>
- Cabrera, A., Cox, L., Spokas, K., Hermosín, M.C., Cornejo, J., Koskinen, W.C., 2014. Influence of biochar amendments on the sorption-desorption of aminocyclopyrachlor, bentazone and pyraclostrobin pesticides to an agricultural soil. *Sci. Total Environ.* 470–471, 438–443. <https://doi.org/10.1016/j.scitotenv.2013.09.080>
- Camia, A., Rober, N., Jonsson, R., Pilli, R., Garcia-Condado, S., Lopez-Lozano, R., van der Velde, M., Ronzon, T., Gurria, P., M'Barek, R., Tamosiunas, S., Fiore, G., Araujo, R., Hoepffner, N., Marelli, L., Giuntoli, J., 2018. *Biomass production, supply, uses and flows in the European Union. First results from an integrated assessment*, ISBN978-92-79-77237-5. <https://doi.org/10.2760/181536>
- Cardoen, D., Joshi, P., Diels, L., Sarma, P.M., Pant, D., 2015. Agriculture biomass in India: Part 1. Estimation and characterization. *Resour. Conserv. Recycl.* 102, 39–48. <https://doi.org/10.1016/j.resconrec.2015.06.003>
- Chen, T., Liu, R., Scott, N.R., 2016. Characterization of energy carriers obtained from the pyrolysis of white ash, switchgrass and corn stover - Biochar, syngas and bio-oil. *Fuel Process. Technol.* 142, 124–134. <https://doi.org/10.1016/j.fuproc.2015.09.034>
- Chen, W.H., Kuo, P.C., 2011. Isothermal torrefaction kinetics of hemicellulose, cellulose, lignin and xylan using thermogravimetric analysis. *Energy* 36, 6451–6460.

<https://doi.org/10.1016/j.energy.2011.09.022>

Cherubini, F., 2010. The biorefinery concept: Using biomass instead of oil for producing energy and chemicals. *Energy Convers. Manag.* 51, 1412–1421. <https://doi.org/10.1016/j.enconman.2010.01.015>

Czajczyńska, D., Nannou, T., Anguilano, L., Krzyżyńska, R., Ghazal, H., Spencer, N., Jouhara, H., 2017. Potentials of pyrolysis processes in the waste management sector. *Energy Procedia* 123, 387–394. <https://doi.org/10.1016/j.egypro.2017.07.275>

Dai, Y., Zhang, N., Xing, C., Cui, Q., Sun, Q., 2019. The adsorption, regeneration and engineering applications of biochar for removal organic pollutants: A review. *Chemosphere* 223, 12–27. <https://doi.org/10.1016/j.chemosphere.2019.01.161>

del Pozo, C., Bartrolí, J., Alier, S., Puy, N., Fàbregas, E., 2020. Production of antioxidants and other value-added compounds from coffee silverskin via pyrolysis under a biorefinery approach. *Waste Manag.* 109, 19–27. <https://doi.org/10.1016/j.wasman.2020.04.044>

del Pozo, C., Bartrolí, J., Puy, N., Fàbregas, E., 2018. Separation of value-added chemical groups from bio-oil of olive mill waste. *Ind. Crops Prod.* 125. <https://doi.org/10.1016/j.indcrop.2018.08.062>

del Pozo, C., Rego, F., Yang, Y., Puy, N., Bartrolí, J., Fàbregas, E., Bridgwater, A. V, 2021. Converting coffee silverskin to value-added products by a slow pyrolysis-based biorefinery process. *Fuel Process. Technol.* 214. <https://doi.org/10.1016/j.fuproc.2020.106708>

EEA, 2020. Bio-waste in Europe — turning challenges into opportunities.

EEA, 2016. Circular economy in Europe - developing the knowledge base, European Environmental Agency.

EEA, 2015. Assessment of global megatrends — European Environment Agency [WWW Document]. URL <https://www.eea.europa.eu/soer/2015/global/action-download-pdf> (accessed 1.30.21).

EEA, 2014. Environmental indicator report 2014. Environmental impacts of production-consumption systems in Europe [WWW Document]. URL <https://www.eea.europa.eu/publications/environmental-indicator-report-2014> (accessed

1.30.21).

European Commission, 2018. A sustainable Bioeconomy for Europe: strengthening the connection between economy, society and the environment. <https://doi.org/10.2777/478385>

European Commission, 2017a. EU Waste Law [WWW Document]. URL https://www.era-comm.eu/EU_waste_law/index.html (accessed 1.23.21).

European Commission, 2017b. Expert Group Report: Review of the EU Bioeconomy Strategy and its Action Plan, European Commission.

European Commission, 2015a. Closing the loop - An EU action plan for the Circular Economy, Communication from the commission to the european parliament, the council, the European economic and social committee and the committee of the regions. Brussels.

European Commission, 2015b. Commission staff working document. Additional analysis to complement the impact assessment SWD (2014) 208 supporting the review of EU waste management targets. European Commission (EC) 21, 39.

European Commission, 2014. Towards a circular economy: A zero waste programme for Europe, Communication from the commission to the european parliament, the council, the European economic and social committee and the committee of the regions. Brussels,.

European Union, 2013. Decision No 1386/2013/EU of the European Parliament and of the Council of 20 November 2013 on a General Union Environment Action Programme to 2020 “Living well, within the limits of our planet.” Off. J. Eur. Union 171–200.

Goyal, H.B., Seal, D., Saxena, R.C., 2008. Bio-fuels from thermochemical conversion of renewable resources: A review. *Renew. Sustain. Energy Rev.* 12, 504–517. <https://doi.org/10.1016/j.rser.2006.07.014>

Hasanov, I., Raud, M., Kikas, T., 2020. The Role of Ionic Liquids in the Lignin Separation from Lignocellulosic Biomass. *Energies* 13. <https://doi.org/https://doi.org/10.3390/en13184864>

Jahirul, M.I., Rasul, M.G., Chowdhury, A.A., Ashwath, N., 2012. Biofuels Production through Biomass Pyrolysis—A Technological Review. *Energies* 5, 4952–5001. <https://doi.org/10.3390/en5124952>

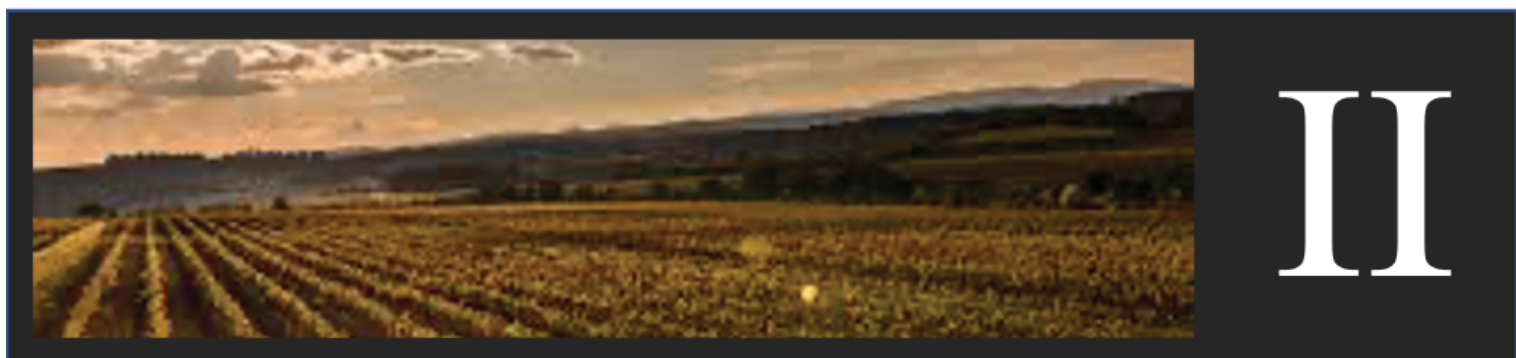
Jensen, C.U., Rodriguez Guerrero, J.K., Karatzos, S., Olofsson, G., Iversen, S.B., 2017.

- Fundamentals of HydrofactionTM: Renewable crude oil from woody biomass. *Biomass Convers. Biorefinery* 7, 495–509. <https://doi.org/10.1007/s13399-017-0248-8>
- Jouiad, M., Al-Nofeli, N., Khalifa, N., Benyettou, F., Yousef, L.F., 2015. Characteristics of slow pyrolysis biochars produced from rhodes grass and fronds of edible date palm. *J. Anal. Appl. Pyrolysis* 111, 183–190. <https://doi.org/10.1016/j.jaap.2014.10.024>
- Kan, T., Strezov, V., Evans, T.J., 2016. Lignocellulosic biomass pyrolysis: A review of product properties and effects of pyrolysis parameters. *Renew. Sustain. Energy Rev.* 57, 1126–1140. <https://doi.org/10.1016/j.rser.2015.12.185>
- Kim, J.S., 2015. Production, separation and applications of phenolic-rich bio-oil - A review. *Bioresour. Technol.* 178, 90–98. <https://doi.org/10.1016/j.biortech.2014.08.121>
- Lieder, M., Rashid, A., 2016. Towards circular economy implementation: A comprehensive review in context of manufacturing industry. *J. Clean. Prod.* 115, 36–51. <https://doi.org/10.1016/j.jclepro.2015.12.042>
- Liu, Z., Han, G., 2015. Production of solid fuel biochar from waste biomass by low temperature pyrolysis. *FUEL* 158, 159–165. <https://doi.org/10.1016/j.fuel.2015.05.032>
- Ma, J., Shi, S., Jia, X., Xia, F., Ma, H., Gao, J., Xu, J., 2019. Advances in catalytic conversion of lignocellulose to chemicals and liquid fuels. *J. Energy Chem.* 36, 74–86. <https://doi.org/10.1016/j.jechem.2019.04.026>
- Meyer, B., 2011. Macroeconomic modelling of sustainable development and the links between the economy and the environment. Osnabrück.
- Mohan, D., Pittman, C.U., Steele, P.H., 2006. Pyrolysis of wood/biomass for bio-oil: A critical review. *Energy and Fuels* 20, 848–889. <https://doi.org/10.1021/ef0502397>
- Mohan, S.V., Butti, S.K., Amulya, K., Dahiya, S., Modestra, J.A., 2016. Waste Biorefinery: A New Paradigm for a Sustainable Bioelectro Economy. *Trends Biotechnol.* 34, 852–855. <https://doi.org/10.1016/j.tibtech.2016.06.006>
- OECD, 2021. Long-term baseline projections, No. 103 [WWW Document]. <https://doi.org/https://doi.org/10.1787/68465614-en>
- Polidoro, A. dos S., Scapin, E., Lazzari, E., Silva, A.N., dos Santos, A.L., Caramao, E.B., Jacques, R.A., 2018. Valorization of coffee silverskin industrial waste by pyrolysis : From

- optimization of bio-oil production to chemical characterization by GC × GC / qMS. *J. Anal. Appl. Pyrolysis* 129, 43–52. <https://doi.org/10.1016/j.jaap.2017.12.005>
- Purwanto, H., Rozhan, A.N., Salleh, H.M., 2018. Innovative Process to Enrich Carbon Content of EFB-Derived Biochar as an Alternative Energy Source in Ironmaking. *Adv. Mater. Sci. Eng.* 2018. <https://doi.org/10.1155/2018/4067237>
- Recari, J., Berrueco, C., Puy, N., Alier, S., Bartrolí, J., Farriol, X., 2017. Torrefaction of a solid recovered fuel (SRF) to improve the fuel properties for gasification processes. *Appl. Energy* 203, 177–188. <https://doi.org/10.1016/j.apenergy.2017.06.014>
- Rehrah, D., Reddy, M.R., Novak, J.M., Bansode, R.R., Schimmel, K.A., Yu, J., Watts, D.W., Ahmedna, M., 2014. Production and characterization of biochars from agricultural by-products for use in soil quality enhancement. *J. Anal. Appl. Pyrolysis* 108, 301–309. <https://doi.org/10.1016/j.jaap.2014.03.008>
- Sharma, N.K., Govindan, K., Lai, K.K., Chen, W.K., Kumar, V., 2020. The transition from linear economy to circular economy for sustainability among SMEs: A study on prospects, impediments, and prerequisites. *Bus. Strateg. Environ.* 1–20. <https://doi.org/10.1002/bse.2717>
- Shen, D.K., Gu, S., 2009. The mechanism for thermal decomposition of cellulose and its main products. *Bioresour. Technol.* 100, 6496–6504. <https://doi.org/10.1016/j.biortech.2009.06.095>
- Steffen, W., Richardson, K., Rockström, J., Cornell, S.E., Fetzer, I., Bennett, E.M., Biggs, R., Carpenter, S.R., De Vries, W., De Wit, C.A., Folke, C., Gerten, D., Heinke, J., Mace, G.M., Persson, L.M., Ramanathan, V., Reyers, B., Sörlin, S., 2015. Planetary boundaries: Guiding human development on a changing planet. *Science* (80-.). 347. <https://doi.org/10.1126/science.1259855>
- Tan, X., Liu, Y., Zeng, G., Wang, X., Hu, X., Gu, Y., Yang, Z., 2015. Application of biochar for the removal of pollutants from aqueous solutions. *Chemosphere* 125, 70–85. <https://doi.org/10.1016/j.chemosphere.2014.12.058>
- Tomczyk, A., Sokołowska, Z., Boguta, P., 2020. Biochar physicochemical properties: pyrolysis temperature and feedstock kind effects. *Rev. Environ. Sci. Biotechnol.* 19, 191–215. <https://doi.org/10.1007/s11157-020-09523-3>
- Torri, C., Fabbri, D., 2014. Biochar enables anaerobic digestion of aqueous phase from

- intermediate pyrolysis of biomass. *Bioresour. Technol.* 172, 335–341. <https://doi.org/10.1016/j.biortech.2014.09.021>
- Ubando, A.T., Felix, C.B., Chen, W.H., 2020. Biorefineries in circular bioeconomy: A comprehensive review. *Bioresour. Technol.* 299. <https://doi.org/10.1016/j.biortech.2019.122585>
- Uzun, B.B., Apaydin-Varol, E., Ateş, F., Özbay, N., Pütün, A.E., 2010. Synthetic fuel production from tea waste: Characterisation of bio-oil and bio-char. *Fuel* 89, 176–184. <https://doi.org/10.1016/j.fuel.2009.08.040>
- Wang, S., Dai, G., Yang, H., Luo, Z., 2017. Lignocellulosic biomass pyrolysis mechanism: A state-of-the-art review. *Prog. Energy Combust. Sci.* 62, 33–86. <https://doi.org/10.1016/j.pecs.2017.05.004>
- Wang, Y., Liu, R., 2018. H₂O₂ treatment enhanced the heavy metals removal by manure biochar in aqueous solutions. *Sci. Total Environ.* 628–629, 1139–1148. <https://doi.org/10.1016/j.scitotenv.2018.02.137>
- Wang, Y., Liu, R., 2017. Comparison of characteristics of twenty-one types of biochar and their ability to remove multi-heavy metals and methylene blue in solution. *Fuel Process. Technol.* 160, 55–63. <https://doi.org/10.1016/j.fuproc.2017.02.019>
- Xie, T., Reddy, K.R., Wang, C., Yargicoglu, E., Spokas, K., 2015. Characteristics and applications of biochar for environmental remediation: A review. *Crit. Rev. Environ. Sci. Technol.* 45, 939–969. <https://doi.org/10.1080/10643389.2014.924180>
- Yang, H., Yan, R., Chen, H., Lee, D.H., Chuguang, Z., 2007. Characteristics of hemicellulose, cellulose and lignin pyrolysis. *Fuel* 86, 1781–1788.
- Yu, Y., Yang, Y., Cheng, Z., Blanco, P.H., Liu, R., Bridgwater, A. V., Cai, J., 2016. Pyrolysis of Rice Husk and Corn Stalk in Auger Reactor. 1. Characterization of Char and Gas at Various Temperatures. *Energy and Fuels* 30, 10568–10574. <https://doi.org/10.1021/acs.energyfuels.6b02276>
- Zabaniotou, A., Kamaterou, P., Pavlou, A., Panayiotou, C., 2018. Sustainable bioeconomy transitions: Targeting value capture by integrating pyrolysis in a winery waste biorefinery. *J. Clean. Prod.* 172, 3387–3397. <https://doi.org/10.1016/j.jclepro.2017.11.077>

Zhao, C., Jiang, E., Chen, A., 2017. Volatile production from pyrolysis of cellulose, hemicellulose and lignin. *J. Energy Inst.* 90, 902–913.
<https://doi.org/10.1016/j.joei.2016.08.004>



Compendium of publications

2.1 Article I

Separation of value-added chemical groups from bio-oil of olive mill waste

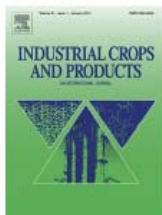
Cristina del Pozo^{1*}, Jordi Bartrolí¹, Neus Puy^{1,2}, Esteve Fàbregas¹

¹ *Department of Chemistry, Universitat Autònoma de Barcelona (UAB), Edifici Cn, Campus de la UAB, 08193 Cerdanyola del Vallès, Barcelona, Spain.*

² *Energies Tèrmiques Bàsiques SL. C/Maó 22, 2-1, 08022 Barcelona, Spain.*

* Corresponding author: Cristina.DelPozo@uab.cat

Journal: Ind. Crops Prod.
Volume 125, Pages 160-167
doi.org/10.1016/j.indcrop.2018.08.062
1 December 2018



Separation of value-added chemical groups from bio-oil of olive mill waste

Author: Cristina del Pozo, Jordi Bartrolí, Neus Puy, Esteve Fàbregas

Publication: Industrial Crops and Products

Publisher: Elsevier

Date: 1 December 2018

© 2018 Elsevier B.V. All rights reserved.

Journal Author Rights

Please note that, as the author of this Elsevier article, you retain the right to include it in a thesis or dissertation, provided it is not published commercially. Permission is not required, but please ensure that you reference the journal as the original source. For more information on this and on your other retained rights, please visit: <https://www.elsevier.com/about/our-business/policies/copyright#Author-rights>

BACK

CLOSE WINDOW



Contents lists available at ScienceDirect

Industrial Crops & Products

journal homepage: www.elsevier.com/locate/indcrop

Separation of value-added chemical groups from bio-oil of olive mill waste

Cristina del Pozo^{a,*}, Jordi Bartrolí^a, Neus Puy^{a,b}, Esteve Fàbregas^a^a Department of Chemistry, Universitat Autònoma de Barcelona (UAB), Edifici Cn, Campus de la UAB, 08193, Cerdanyola del Vallès, Barcelona, Spain^b Energies Tèrmiques Bàsiques SL, C/Maó 22, 2-1, 08022, Barcelona, Spain

ARTICLE INFO

Keywords:

Olive mill waste
 Pyrolysis
 Bio-oil
 Antioxidants
 Extraction methods
 Bioeconomy

ABSTRACT

The sector of olive oil (*Olea europaea*) produces a large quantity of waste per year which is usually dried and deoiled resulting in a by-product known as Olive Mill Wastes (OMW). This waste can be used as a source of energy; however, its composition also indicates a potential use as a source of chemicals. Intermediate pyrolysis of OMW resulted in a bio-oil composed of value-added products divided in two phases: an aqueous phase (AP) containing acetic acid, monosaccharides and phenolic derivatives, and a non-aqueous phase (NAP) composed of phenolic derivatives and fatty acids and their methyl esters. The main purpose of the study was to separate these compounds in interest chemical groups to increase the value of the residue inside biorefinery concept. Two liquid-liquid extraction methods, an extraction at original pH and an acid-base extraction, were studied. The results showed that acid-base extraction method, performed with hexane at pH 12 followed by an ethyl acetate extraction at pH 6, was the best method to extract value-added chemical groups in both AP and NAP bio-oil phases. Acetic acid used as chemical platform was found together with monosaccharides, that could be used to study its viability in biogas/bioethanol production, in AP aqueous phase. Phenolic derivatives, potentially useful in food, pharmaceutical and/or cosmetic industry, were found in both AP hexane and NAP ethyl acetate phases. Finally, methyl esters of fatty acids which could be directed to produce biodiesel were found in NAP hexane phase. As a result, this study allows the revaluation of OMW as a first step towards circular economy and bioeconomy.

1. Introduction

The global industry of olive oil (*Olea europaea*) has grown considerably over the past twenty-five years. In 2016/17 season, the olive oil sector produced over 2.5 Mt of olive oil. In Europe Union, olive oil production was accounted as 68.8% of the worldwide production (1.7 Mt). Concretely, in Spain, this production represented the 50.7% of the total world manufacturing (1.3 Mt) (International Olive Council, 2015).

The olive oil extraction process generates large amounts of by-products and wastes that require a specific management regarding minimisation, valorisation and mitigation of their environmental impact (Benavente and Fullana, 2015). As a result, at the end of 1991/92 season, a new olive oil extraction system, called two-phase centrifugation system (TPCS), was introduced in order to replace the three-phase old one, reducing by 75% the olive mill wastes (Roig et al., 2006) and specially, water and energy consumption. Nowadays, 90% of Spanish olive mills are using TPCS (Dermeche et al., 2013).

Despite the advantages, the new extraction system also generates huge quantities (800–950 kg/1 ton of olives) of a solid with doughy texture and high moisture content (65%) by-product called two phase olive mill waste (TPOMW) or *alperujo* in Spanish (Roig et al., 2006). TPOMW is a mixture of water, bone, pulp and skin of the olive rich in lignocellulosic matter (75 wt%), fatty remains (11 wt%), proteins (6 wt%) and hydrosoluble carbohydrates (7 wt%) and phenolic substances (1 wt%) (Alburquerque et al., 2004). However, composition and water content of TPOMW make it a high polluting waste difficult to treat. On one hand, moisture content cause low energy density hampering transport, management and disposal; on the other hand, phenol, organic and fatty acid content turns it into phytotoxic material complicating its use in current methods as composting (Volpe et al., 2015). Nowadays, TPOMW is usually revalorised by drying and extracting the fatty remains with hexane obtaining an extra yield of oil and a waste known as olive mill wastes (OMW) (Williams et al., 2017) or *orujo* in Spanish (Alburquerque et al., 2004).

The resulting dried and deoiled waste has a calorific value of

Abbreviations: OMW, olive mill waste; TPCS, two-phase centrifugation system; TPOMW, two phase olive mill waste; AP, aqueous phase of bio-oil; NAP, non-aqueous phase of bio-oil; EtAc, ethylacetate

* Corresponding author.

E-mail address: Cristina.DelPozo@uab.cat (C. del Pozo).

<https://doi.org/10.1016/j.indcrop.2018.08.062>

Received 27 April 2018; Received in revised form 17 July 2018; Accepted 22 August 2018

0926-6690/ © 2018 Elsevier B.V. All rights reserved.

approximately 3500 kcal/kg (Generalitat de Catalunya. Departament de Medi Ambient, 2002) and it is being used as a source of energy in combustion and gasification processes to generate electrical energy or cogeneration (simultaneous steam and electricity production) (Negro et al., 2017) and syngas (H_2 - CO) (Roig et al., 2006), respectively. However, composition of OMW (lignocellulosic biomass, fatty acids and methyl esters of the fatty acids) also indicates its potential use as a source of chemicals, which would allow increasing the value of the residue inside biorefinery concept.

This study uses pyrolysis as a thermochemical treatment to obtain the high-added value compounds from OMW. Pyrolysis is a thermal decomposition performed at elevated temperatures in absence of oxygen where the main compounds of biomass, hemicelluloses, cellulose (carbohydrate polymers) and lignin (aromatic polymer), depolymerize and fragment originating three different fractions: a solid fraction (biochar), non-condensable gases and a liquid fraction (bio-oil) that is a mixture of highly oxygenated organic compounds (Mohan et al., 2006) representing the richest fraction in high-added value products. The type of pyrolysis process, mainly temperature and residence time in the reactor, conditions the properties and proportion of the fractions.

Bio-oil, produced at temperatures around 500 °C (Bridgwater, 2012), is typically composed of acids, esters, alcohols, ketones, aldehydes, phenols, alkenes, aromatics, nitrogen compounds, furans, guaiacols (2-methoxy-phenols), syringols (2,6-dimethoxy-phenols), sugars and miscellaneous oxygenates (Goyal et al., 2008). Some of these compounds have industrial interest and could be directed to different applications in the chemical industry, bioethanol and biogas production, or as raw materials in food, pharmaceutical and/or cosmetic industry. Specifically, phenolic compounds could be of particular interest because of its antioxidant properties which make them highly valued products in the market (Kim, 2015).

The objective of the present work is to study a procedure to separate the interest fractions from OMW bio-oil as a first step in biorefinery process. Applying intermediate pyrolysis, a two-phase bio-oil is obtained, allowing more “efficiency” in the separation process. Chemical characterisation by GC-MS analysis was first performed in order to determine the composition of each phase of bio-oil; then, liquid-liquid extraction method was proposed as a suitable separation procedure to obtain the interest fractions. Considering the affinity of bio-oil compounds for the different solvents and its acid-basic character, two extraction procedures were studied; an extraction at original pH and an acid-base extraction.

2. Materials and methods

2.1. Materials

All chemicals were commercially available and were used without further purification.

Karl-Fischer reagents (Aquametric titrant 5 and Aquametric solvent for volumetric analysis) were purchased from Panreac; hexane ($\geq 95\%$), ethyl acetate (EtAc), sodium hydroxide pellets (NaOH) ($\geq 98\%$), trifluoroacetic acid (TFA) ($\geq 99.0\%$) and methanol (MeOH) (99.8%), from Sigma Aldrich.

2.2. Bio-oil production

The bio-oil used in the study is produced from the intermediate pyrolysis of OMW, the dried and deoiled by-product of TPCS in olive oil production. The mentioned organic waste was supplied by a co-operative from Catalonia, located in the north-east of Spain.

OMW were pyrolysed at 400 °C with a residence time of 10 min under low oxygen atmosphere in an auger reactor industrial plant by ENER-G-bas company described elsewhere (Recari et al., 2017).

The obtained bio-oil was composed of two phases: an aqueous phase

(AP) containing a wide variety of low molecular weight organo-oxygen compounds and a non-aqueous phase (NAP), tarry phase containing insoluble heavy organic species (Calonaci et al., 2010). Two-phase bio-oil is usually obtained in this type of pyrolysis where high amount of reaction water is produced and so, phase separation can occur (Torri and Fabbri, 2014).

2.3. Extraction method

Two different extraction methods were tested in order to separate the value-added chemical groups from bio-oil phases, AP and NAP. Extractions were performed using a rotary mixer Model LD 79 from Labinco, to shake the solvents, and a separating funnel, to separate the two immiscible phases. Hexane and EtAc were used as non-polar and polar organic solvents, respectively.

2.3.1. Extraction method at original pH (A)

NAP was dissolved in methanol (1:50) and the obtained solution was then dissolved in water (1:4). 20 mL of NAP and AP solution respectively were extracted with 5 mL of hexane for 30 min at 30 rpm. This step was repeated three times. The aqueous phase was then extracted with 10 mL of EtAc following the same extraction procedure. All phases were analyzed by GC-MS technique.

2.3.2. Acid-base extraction method (B)

Acid-base extractions were performed at pH 12 and 6 based on the pKa of the main bio-oil compounds. AP and NAP were basified to pH 12 with NaOH (4 M). At this pH, NAP was properly dissolved in the aqueous NaOH solution, so addition of MeOH was not required. 20 mL of the resulting solutions were then extracted with 15 mL of hexane for 1 h at 30 rpm. This step was repeated twice. After separating the two phases, pH of the AP and NAP aqueous phase was acidified to pH 6 with TFA ($\geq 99.0\%$). AP aqueous phase was then extracted with hexane as it is described above. Finally, AP and NAP aqueous phases at pH 6 were extracted with EtAc (20:15) following the same procedure. Hexane and EtAc phases were analyzed by GC-MS technique.

2.4. Analytical methods

2.4.1. Karl-Fischer titration

Water content of each phase was measured by triplicate by volumetric Karl Fischer titration (ASTM E 203) using 716 DMS Titrino (Metrohm) with Pt electrode.

2.4.2. pH determination

pH was determined using a solvotrode electrode with LiCl (2 mol/L) for non-aqueous media purchased by Metrohm. All measures were performed by triplicate.

2.4.3. GC-MS analysis

Two different chromatographic methods were performed in order to optimise the analysis time. The longest method was used in samples composed of fatty acids and their corresponding methyl esters (molecules with the highest retention time); the shortest one was applied for the rest of the samples. The methods were adapted from previous experience (Artigues et al., 2014; Martínez et al., 2014; Puy et al., 2011). GC-MS was performed with a HP 6890 Series II gas chromatograph coupled to a HP 5973 mass selective detector and equipped with a capillary DB-Petro column (100 m \times 0.25 mm inner diameter \times 0.50 μ m film thickness). Before injection, samples were filtered (0.45 μ m Millipore filter) to avoid obstruction of liner due to some ashes can rest after pyrolysis. A volume of 1 μ L was then injected, applying 1:7 split mode with the injection port at 300 °C and a syringe of 10 μ L. Helium was used as carrier gas with a flow of 2.3 L/min for 110 min. The oven temperature was as follows: 60 °C for 1 min, 1 °C/min to 55 °C, 2 °C/min to 175 °C, 5 °C/min to 300 °C and 300 °C for 20 and 0 min

depending on the method used. The total run time was 111 and 91 min respectively.

Compounds were identified by computer matching of mass spectra analysis of the peaks with the National Institute of Standards and Technology (NIST) library.

3. Results and discussion

Intermediate pyrolysis of OMW resulted in a bio-oil, with a pH of 3.2 ± 0.1 , composed of two phases, AP and NAP, easily separated by decantation. AP was a red wine colour solution with a water content of 67 ± 4 wt% and soluble in aqueous and polar organic solvents; NAP was a tarry phase with a low water content, 14 ± 3 wt%, which could be dissolved in water at $\text{pH} > 12$ and in polar organic solvents.

The data on pH, water content and solubility of OMW bio-oil did not show significant differences to the literature. In the first place, pH of bio-oil usually exhibits acidic values of 2.0–3.0 (Mohan et al., 2006); however, depending on the feedstock and pyrolysis conditions, pH can vary, as is the case for García-Pérez et al. (2002), which found a bio-oil pH range of 2.0–3.8 in its comparative study between bio-oils. In the second place, the water content values of AP and NAP were in agreement with those reported by Conrad et al. (2017) for barley/wheat straw fast pyrolysis bio-oil, where the aqueous phase had a water content of 72.3 wt% and the tarry phase of 19.6 wt%. Finally, Oasmaa and Peacocke (2001) reported as good solvents for bio-oil, alcohols and acetone, but not hydrocarbons. Moreover, Wang et al. (2014) described similar behaviour between the two phases of bio-oil with water.

3.1. Chemical characterisation of AP and NAP

Chemical characterisation of AP and NAP was performed by GC–MS to identify non-ionic compounds with boiling temperatures below 300 °C.

The OMW bio-oil derived from the pyrolysis of the dried and deoiled TPOMW, residue from olive oil production. TPOMW is mainly composed of lignocellulosic matter, lignin (34 wt%), hemicelluloses (26 wt%) and cellulose (15 wt%), and, to a lesser extent, of fats (11 wt%), proteins (6 wt%) and water-soluble carbohydrates and phenols (8 wt%) (Alburquerque et al., 2004), which determine the chemical composition of the OMW bio-oil.

Hence, OMW bio-oil was mainly composed of products from the decomposition of lignocellulosic matter, but also of compounds from bio-oil aged reactions and some fatty acids from the raw material. These compounds were distributed in the two phases of bio-oil, AP and NAP, according to its hydrophilicity and hydrophobicity, respectively, having AP a larger number of compounds than NAP due to the organic-matter fragmentation which derives in many different oxygenated low molecular weight aqueous-soluble compounds.

3.1.1. Chemical characterisation of AP

AP was mainly composed of the aqueous soluble organic species of bio-oil, being acetic acid the most abundant product and, therefore, the main responsible of the acid pH of bio-oil, which is usually attributed to the presence of low molecular weight carboxylic acids (Diebold, 2002; García-Pérez et al., 2002; Mohan et al., 2006).

Results of the GC–MS analysis, Fig. 1, indicate that AP was composed of a wide variety of oxygenated organic compounds with low molecular weight that can be divided into the following categories: miscellaneous oxygenated compounds, which includes acetone (1), methyl acetate (2), acetic acid (3), 1-hydroxy-2-propanone (4), propanoic acid (5), 1-hydroxy-2-butanone (6), butanoic acid (7), butyrolactone (8), 2-methyl-2-cyclopenten-1-one (9), 3-methyl-1,2-cyclopentanedione (11), 3-ethyl-2-hydroxy-2-cyclopenten-1-one (13) and levoglucosan (22); nitrogen compounds, referred to 3-ethyl-pyridine (10) as the most abundant in its category, and phenol derivatives as compounds 2-methoxy-phenol (12), Cresol (14), Catechol (15), 3-

methoxy-1,2-benzenediol (16), 4-ethyl-2-methoxy-phenol (17), 2,6-dimethoxy-phenol (18), 4-hydroxy-benzenoethanol (19), 2,6-dimethoxy-4-methylphenol (20), trans-isoeugenol (21), 1-(4-hydroxy-3-methoxyphenyl)-2-propanone (23), 5-tert-butylpyrogallol (24), E-2,6-dimethoxy-4-(prop-1-en-1-yl)-phenol (25), 1-(4-hydroxy-3,5-dimethoxyphenyl)-ethanone (26) and 1-(2,4,6-trihydroxyphenyl)-2-pentanone (27). Full information regarding the chromatograms are available in data in brief.

The presence of miscellaneous oxygenated compounds is related to decomposition of hemicelluloses and cellulose which give rise mostly to sugars and acetic acid, and anhydrocellulose and levoglucosan, respectively (Diebold, 2002). Moreover, Wu et al. (2009) also identified acetone (1), acetic acid (3), 1-hydroxy-2-propanone (4), 3-methyl-1,2-cyclopentanedione (11) and levoglucosan (22) in their study of main pyrolysis products from hemicelluloses and cellulose.

Esters of carboxylic acids were also present in the OMW bio-oil composition; however, these products could be derived from bio-oil aging reactions, specifically, from esterification between an acid with an alcohol as methanol or ethanol (Diebold, 2002; García-Pérez et al., 2002).

Nitrogen compounds of bio-oil could be related to the presence of proteins in raw material (Diebold, 2002), as is the case with OMW bio-oil.

Finally, phenol derivatives were mainly composed of 2-methoxyphenols (guaiacols) and 2,6-dimethoxy-phenols (syringols), mostly para-substituted by short aliphatic chain (C1–C3) or ketone substituent (C2–C3). The presence of these phenol compounds is related to the pyrolysis of lignin, which decomposes giving rise to phenol derivatives from its principal monomers: p-coumarly, coniferyl and sinapyl alcohols (see Fig. 2) (Mohan et al., 2006).

The potential use of AP compounds such as acetic acid, levoglucosan (monosaccharide) and phenol derivatives, as raw materials in chemical, bioethanol/biogas and food/pharmaceutical/cosmetic industries, respectively, allows to consider AP as a feedstock for the biorefinery and drives to study a method to obtain the value-added chemical groups from it.

3.1.2. Chemical characterisation of NAP

NAP mostly contained the non-aqueous soluble organic species of bio-oil. Specifically, data from GC–MS analysis (Fig. 3) shows that NAP was mainly composed of 2-methoxy-phenols and 2,6-dimethoxy-phenols, mostly para-substituted by short aliphatic chain (C1–C3), and, to a lesser extent, of acetic acid, ethyl acetate and fatty acids and their methyl esters. The complete information about NAP composition is shown in data in brief.

Phenol compounds and acetic acid are related to the pyrolysis of lignocellulosic matter; methyl and ethyl esters from carboxylic acids could be attributed to an aged bio-oil reaction, the esterification between the acids and alcohols, as mentioned above.

Although acetic acid shows a high affinity for aqueous solvents, its high abundance could be the reason of finding remains of the acid in NAP. In the same way, fatty acids were also identified as remains of raw material.

Composition of NAP in phenol derivatives, fatty acids and methyl esters of the fatty acids leads to study a method to separate them due to the possible use of these chemical groups in food / pharmaceutical / cosmetic industries and to produce biodiesel, respectively. This work proposed two liquid-liquid extraction methods: at original pH and an acid-base extraction.

3.2. Separation of the value-added chemical groups of AP and NAP

Intermediate pyrolysis of OMW resulted in a two-phase bio-oil, where each one of the phases, AP and NAP, were composed of high-added value products. Chemical characterisation of AP and NAP shows a partial separation, where the hydrophilic compounds were mostly

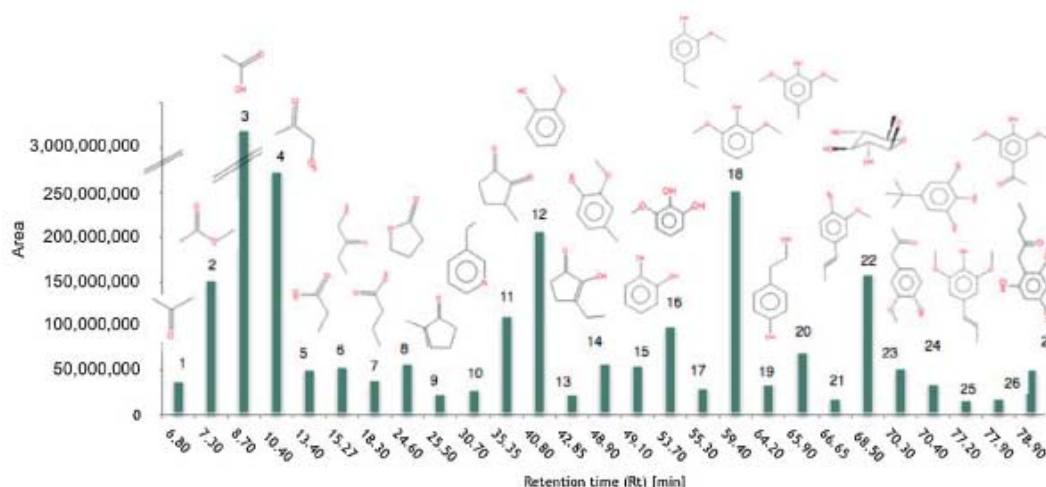


Fig. 1. Most abundant compounds of the aqueous phase (AP) of OMW bio-oil determined by GC-MS analysis. 1) acetone (Rt: 6.8); 2) methyl acetate (Rt: 7.3); 3) acetic acid (Rt: 8.7); 4) 1-hydroxy-2-propanone (Rt: 10.4); 5) propanoic acid (Rt: 13.4); 6) 1-hydroxy-2-butanone (Rt: 15.27); 7) butanoic acid (Rt: 18.3); 8) butyrolactone (Rt: 24.6); 9) 2-methyl-2-cyclopenten-1-one (Rt: 25.5); 10) 3-ethyl-pyridine (Rt: 30.7); 11) 3-methyl-1,2-cyclopentanedione (Rt: 35.35); 12) 2-methoxy-phenol (Rt: 40.8); 13) 3-ethyl-2-hydroxy-2-cyclopenten-1-one (Rt: 42.85); 14) Creosol (Rt: 48.9); 15) Catechol (Rt: 49.1); 16) 3-methoxy-1,2-benzenediol (Rt: 53.7); 17) 4-ethyl-2-methoxy-phenol (Rt: 55.3); 18) 2,6-dimethoxy-phenol (Rt: 59.4); 19) 4-hydroxy-benzeneethanol (Rt: 64.2); 20) 2,6-dimethoxy-4-methylphenol (Rt: 65.9); 21) trans-isoeugenol (Rt: 66.65); 22) levoglucosan (Rt: 68.5); 23) 1-(4-hydroxy-3-methoxyphenyl)-2-propanone (Rt: 70.3); 24) 5-*tert*-butylpyrogallol (Rt: 70.4); 25) E)-2,6-dimethoxy-4-(prop-1-en-1-yl)-phenol (Rt: 77.2); 26) 1-(4-hydroxy-3,5-dimethoxyphenyl)-ethanone (Rt: 77.9); 27) 1-(2,4,6-trihydroxyphenyl)-2-pentanone (Rt: 78.9).

placed in AP and hydrophobic ones to NAP. This fact represents an advantage in comparison to the usual one-phase bio-oil, facilitating the separation process.

The interest fractions of bio-oil were divided into four main groups: (i) acetic acid and (ii) monosaccharides, located in AP; (iii) phenolic compounds, that were present in both phases; and (iv) fatty acids and their methyl esters, placed in NAP. Acetic acid (i) is a low molecular weight carboxylic acid, with a pKa of 4.75 and soluble in aqueous and polar organic solvents. Monosaccharides (ii) do not have acid-base properties and are only soluble in water. The phenolic compounds (iii) have a pKa of 7.5–10.4 (Javor et al., 2000) and can be dissolved in

different types of solvents depending on the phenol substituent which influenced to the polarity of the molecule and so, to its affinity with solvents. Finally, fatty remains of olive oil (iv) were mostly composed of oleic acid, with a pKa of 5.02. The fatty acids and their methyl esters, without acid-base properties, were soluble in non-polar and polar organic solvents; however, fatty acids were also soluble in water at pH > 9 due to the possible formation of stable micelles (Small, 1992).

The affinity of compounds for the different solvents and its acid-base properties led to propose two liquid-liquid extraction methods as a way to obtain the interest chemical groups: an extraction at original pH (A) and an acid-base extraction (B). The extraction at original pH

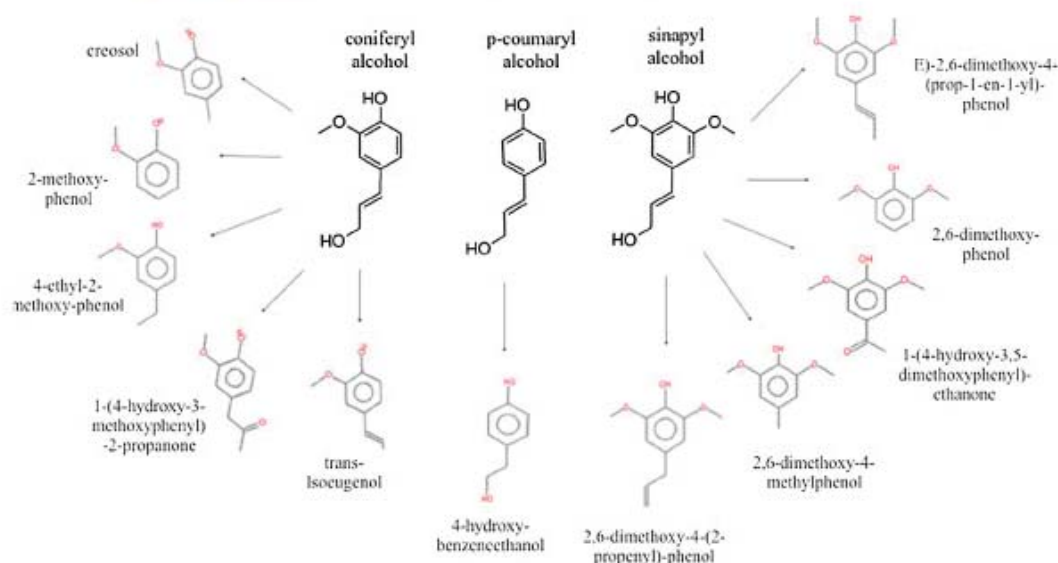


Fig. 2. Pyrolysis phenol derivatives from primary lignin monomers.

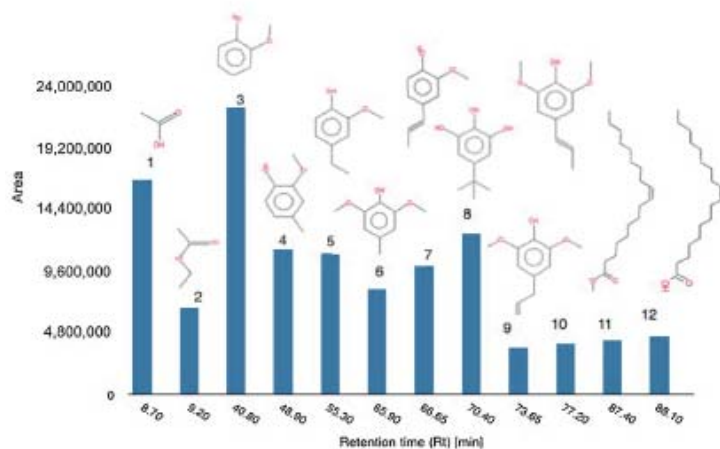


Fig. 3. Most abundant compounds of the non-aqueous phase (NAP) of OMW bio-oil determined by GC-MS analysis. 1) acetic acid (Rt: 8.7); 2) ethyl acetate (Rt: 9.2); 3) 2-methoxyphenol (Rt: 40.8); 4) Creosol (Rt: 48.9); 5) 4-ethyl-2-methoxyphenol (Rt: 55.3); 6) 2,6-dimethoxy-4-methylphenol (Rt: 65.9); 7) trans-Isoeugenol (Rt: 66.65); 8) 5-tert-butylpyrogallol (Rt: 70.4); 9) 2,6-dimethoxy-4-(2-propenyl)-phenol (Rt: 73.65); 10) E-2,6-dimethoxy-4-(prop-1-en-1-yl) phenol (Rt: 77.2); 11) oleic acid, methyl ester (Rt: 87.4); 12) oleic acid (Rt: 88.1).

(A) was based on extracting solvents, which separated the compounds according to its polarity. The solvents used in the separation process were hexane and EtAc. Other solvents as dichloromethane, pentane or diethyl ether were also used by different authors (García-Pérez et al., 2002; Murwanashyaka et al., 2001; Sipilä et al., 1998; Wang et al., 2014); however, the final purpose of phenolic extracts led to use solvents allowed for EU legislation in the production of foodstuffs and food ingredients (Directive 2009/32/EC), as in the case of hexane and EtAc. The acid-base extraction method (B) was based on both extracting solvents and pH of solution. The acid-base extractions intended to separate the acidic compounds deprotonating them and therefore, increasing its affinity with aqueous solvent. The pHs used at the extraction procedure were 12 and 6. At pH 12 all acidic compounds were in ionic state; at pH 6, phenolic compounds were in neutral state, but carboxylic acids were deprotonated. Hence, it seemed possible to induce the acidic species to one phase or another depending on the pH of the solution.

Composition of extraction phases were analyzed by GC-MS and the full results are available in data in brief.

3.2.1. Separation of the value-added chemical groups of AP

AP was composed of a wide variety of low molecular weight oxygenated compounds being acetic acid, monosaccharides (as levoglucosan) and phenolic compounds the most interesting ones due to their potential use in different industries.

In order to obtain the interest chemical groups, the extraction methods A and B were studied.

Extraction method A, performed at original pH of 3.2, was based on the affinity of AP compounds with solvents: hexane, EtAc and water. Hexane would separate the non-polar species from AP and EtAc, the polar organic ones, keeping the rest of compounds in aqueous phase. Results exposed in Fig. 4 show that hexane phase was mostly composed of 2-methoxyphenols and 2,6-dimethoxy-phenols para-substituted by short aliphatic chain (C1–C3) (compounds 14, 17, 20, 21 and 25), where 2-methoxyphenols and phenolic compounds para-substituted by more than one carbon chain showed a higher non-polarity than the other ones which were also found in EtAc phase. On the other hand, EtAc phase was composed of phenol derivatives (i) and miscellaneous oxygenated compounds (ii), being the phase with more species. Phenol derivatives (i) were mostly 2-methoxyphenol/2,6-dimethoxy-phenol para-substituted by ketones (C2–C3) (compounds 23 and 26) and polyphenols, understood as phenols with more than one alcohol in the aromatic ring (compounds 15, 16, 24 and 27). Miscellaneous species (ii) were composed of low molecular weight ketones (cyclic and alcohols ketones: 1, 4, 6, 9, 11 and 13), esters (2), acids (3, 5, 7) and lactones (8),

where some of that compounds, acetone (1), acetic acid (3), 1-hydroxy-2-propanone (4) and butyrolactone (8) were also found in water phase. Moreover, the aqueous phase was also composed of monosaccharides (22) and nitrogen compounds (10) which at acid pH (3.2) were protonated and so, soluble in water phase.

Extraction method B was carried out to study the effect of pH besides the solvents one. Firstly, AP was basified to pH 12 to ionize all acidic compounds, followed by a hexane extraction in order to separate the non-ionic species. Next, pH of solution was acidified to pH 6 and a second hexane extraction was performed to obtain the less polar phenol derivatives. Finally, EtAc extraction was carried out with the aim of separating the more polar phenolic compounds from aqueous phase which would be composed of deprotonated low molecular carboxylic acids and other water-soluble compounds. Results exposed in Fig. 5 show similar composition between hexane phase of extraction method A and B at pH 12, which was also composed of the less polar phenol compounds, 2-methoxyphenols and 2,6-dimethoxy-phenols para-substituted by aliphatic chain (14, 17, 20, 21 and 25) and, to a lesser extent, of 2-methyl-2-cyclopenten-1-one (9) and 5-tert-butylpyrogallol (24). Nitrogen compounds (10), which are in non-ionic form at pH 12, were also observed in this phase. On the other hand, pH 6 hexane extraction only separated 2-methoxyphenol (12), 2,6-dimethoxy-phenol (18) and its para-methyl derivate (20), which was identified in both pH 12 and 6 phases. Finally, EtAc phase was composed of ketones (cyclic and alcohols ketones: 4, 6, 11, 13), polyphenols (compounds 15, 16, 19, 27), and 2-methoxyphenols and 2,6-dimethoxy-phenols para-substituted by C2–C3 ketones (23, 26). Hence, part of the miscellaneous species found in EtAc phase of the previous extraction method A, low molecular carboxylic acids and lactones, seems to be in aqueous phase together with monosaccharides and the other water-soluble compounds.

The extraction methods studied to separate the interest chemical groups of AP showed similar results between hexane phases, which were composed of aliphatic chain para-substituted phenolic compounds. At the same time, significant differences between EtAc phases were observed; on one hand, EtAc phase from extraction method A was composed of a wide variety of miscellaneous oxygenated compounds and phenol derivatives; on the other hand, B was composed of phenol derivatives and ketones, being the rest of the miscellaneous compounds in water phase. Consequently, aqueous phase also presented important differences where extraction method A was mostly composed of monosaccharides, and B was also composed of low molecular carboxylic acids. These results led to consider acid-base extraction method as the best option.

Therefore, liquid-liquid extractions of AP allowed obtaining value-

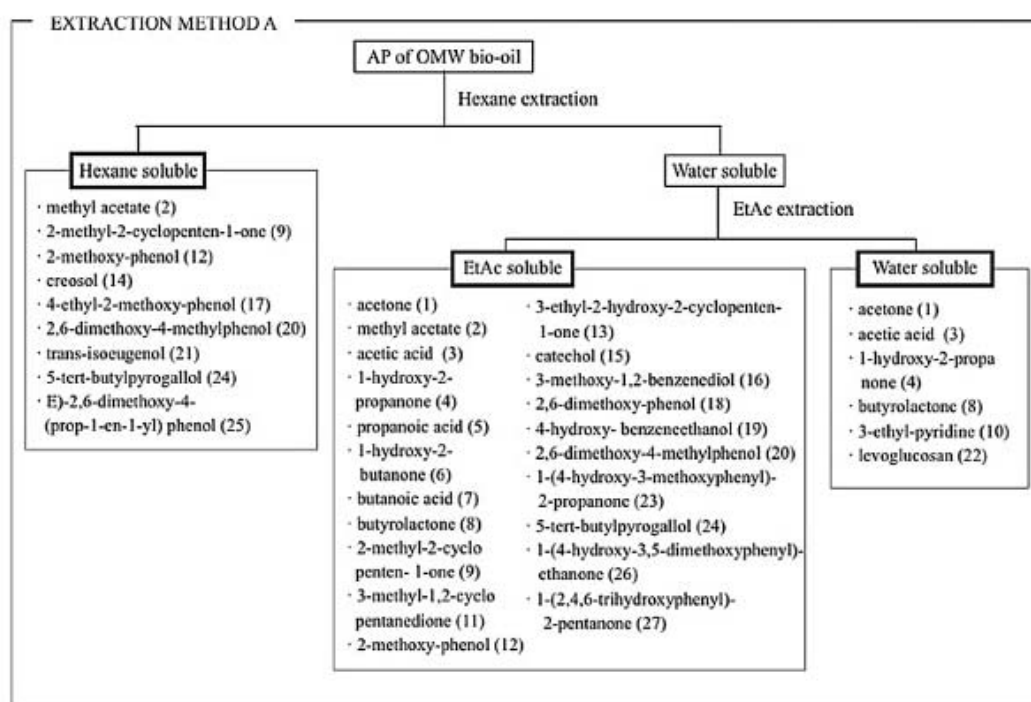


Fig. 4. Extraction method A (at original pH) of the value-added chemical groups of AP from OMW bio-oil and its most abundant compounds analyzed by GC–MS. The numbers in parentheses indicate the chronological order of compounds in the chromatogram.

added chemical groups as acetic acid and monosaccharides in water phase, and phenolic compounds in hexane and EtAc phases. The first one could be used to study its viability in biogas / bioethanol production due to the absence of phenols, a limiting factor which reduce yield

of the process (Roig et al., 2006); this phase could also be employed as a chemical platform because of acetic acid high abundance. The other phases, hexane and EtAc, were rich in phenolic compounds which are appreciated in food, pharmaceutical and cosmetic industry as

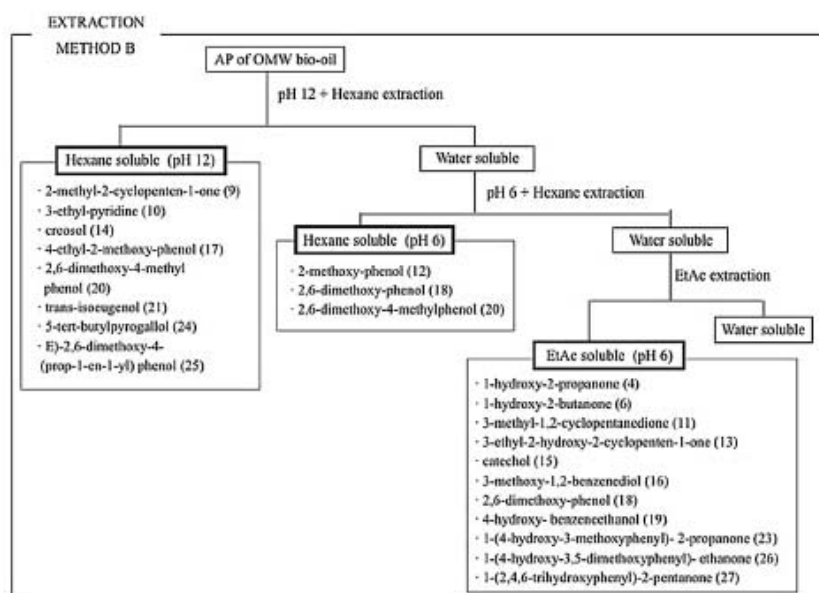


Fig. 5. Acid-base extraction method (B) of the value-added chemical groups of AP from OMW bio-oil and its most abundant compounds analyzed by GC–MS. The numbers in parentheses indicate the chronological order of compounds in the chromatogram.

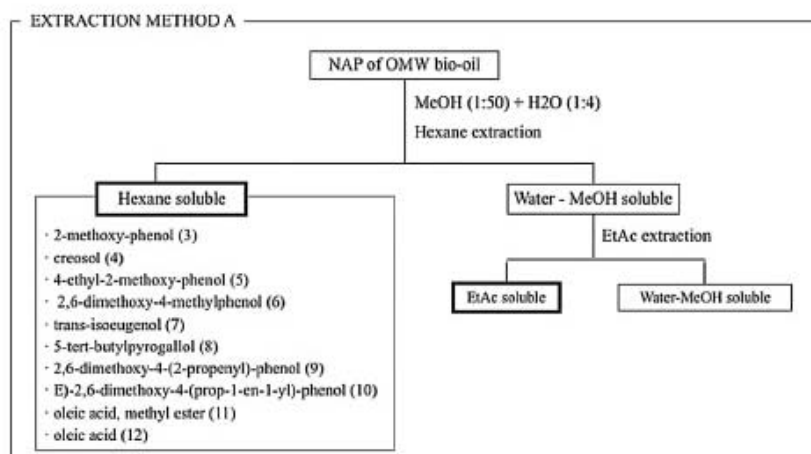


Fig. 6. Extraction method A (at original pH) of the value-added chemical groups of NAP from OMW bio-oil and its most abundant compounds analyzed by GC–MS. The numbers in parentheses indicate the chronological order of compounds in the chromatogram.

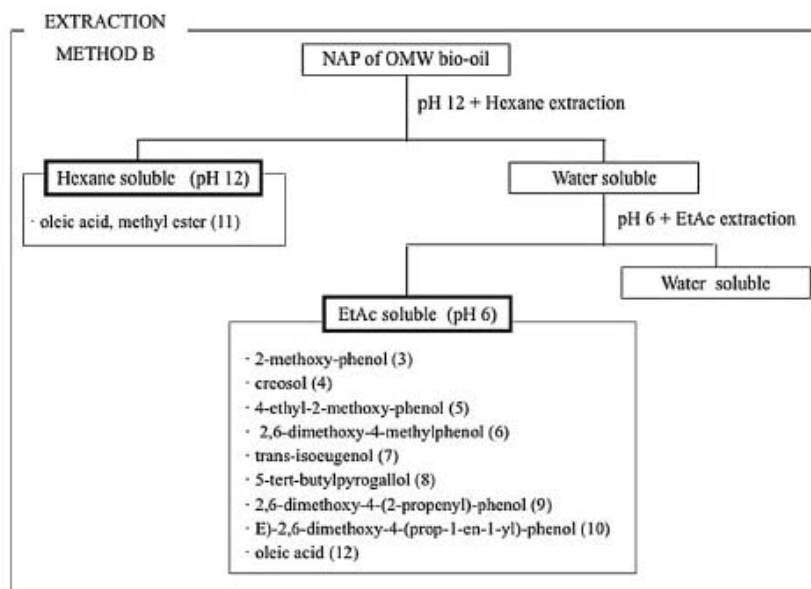


Fig. 7. Acid-base extraction method (B) of the value-added chemical groups of NAP from OMW bio-oil and its most abundant compounds analyzed by GC–MS. The numbers in parentheses indicate the chronological order of compounds in the chromatogram.

antioxidants. Hence, separation of value-added chemical groups from AP could revalorise OMW as a first step towards bioeconomy.

3.2.2. Separation of the value-added chemical groups of NAP

To separate the interest chemical groups of NAP, phenolic compounds, fatty acids and acetic acid, extraction procedures similar to AP ones were studied.

Extraction method A, performed at original pH of 3.2, intended to separate the NAP compounds based on its solubility with the different solvents: fats with hexane, phenol derivatives with EtAc and acetic acid with water. To carry out the extraction procedure, NAP was firstly dissolved in MeOH and then with water; after that, extraction method was developed in the same way as AP. Results summarised in Fig. 6 show that almost all compounds were extracted with hexane. These

results could be related to the acid pH of the solution (3.2) where phenolic compounds were in non-ionic state and so, had more affinity with hexane phase than aqueous one. This makes it necessary to study acid-base extractions (extraction method B).

Extraction method B intended to separate the NAP value-added chemical groups considering the acid-basic character of compounds. First, NAP was basified to pH 12 with NaOH solution which dissolved the tarry phase due to the basic pH. Then, hexane extraction was carried out to separate fats from ionic phenol compounds and finally, solution was acidified to pH 6 to return phenols to neutral state and then, extracted them with EtAc. Fig. 7 shows that methyl esters of fatty acids were separated with hexane: however, fatty acids and phenol compounds still remained in the same phase. Behaviour of fatty acids could be explained with the formation of stable micelles at pH > 9 (Small,

1992) which increase the solubility of fatty acids in water phase. Decreasing pH, stability of micelles also decreased, being extracted by EtAc as phenol compounds. On the other hand, acetic acid remained in the aqueous phase.

Extraction method B allowed to obtain three different interesting fractions from NAP: (1) one composed of methyl esters of fatty acids that would be direct to biodiesel; (2) other one rich in phenolic compounds, natural antioxidants highly appreciated in different industries; and (3) the last one, composed of acetic acid, a raw material in the chemical industry.

4. Conclusions

Two-phase bio-oil from intermediate pyrolysis of OMW was extracted by different methods: at original pH (A) and by an acid-base extraction (B). The acid-base extractions were determined as the best separation method to obtain the interest chemical groups in both AP and NAP bio-oil phases. This method, based on the polarity and acid-base properties of the extracted compounds, was performed by a first hexane extraction at pH 12 followed with EtAc extraction at pH 6, allowing to separate families of compounds in different solvents. AP hexane phase was mostly composed of phenolic derivatives (2-methoxy and 2,6-dimethoxy-phenols para-substituted by short aliphatic chain); EtAc phase was a mixture of phenolic derivatives with miscellaneous compounds as ketones; and the resulting aqueous phase was composed of acetic acid as the main compound, monosaccharides and other miscellaneous species such as low molecular weight carboxylic acids or lactones. Moreover, NAP hexane phase comprised methyl esters from fatty acids; EtAc phase, the phenol derivatives and, to a lesser extent, fatty acids; and aqueous phase, the acetic acid remains. The obtained fractions could be a first step towards biorefinery process due to its rich composition in high-added value compounds. Phenolic derivatives, found in AP hexane phase and NAP EtAc phase, present antioxidant properties which make them valued products in food, cosmetic and pharmaceutical industries. Acetic acid, a chemical platform, was highly abundant in AP aqueous phase, as well as monosaccharides, which could be used to produce biogas or bioethanol. Methyl esters of fatty acids, identified in NAP hexane phase, could be directed to biodiesel production.

As a result, this study allows an approach to olive oil waste management based on pyrolysis treatment which could revalorise OMW by obtaining rich value-added chemical groups from OMW bio-oil extractions as a first step towards circular economy and bioeconomy.

Declarations of interest

None.

Acknowledgements

This work was elaborated with the collaboration of ENER-bas company which provided the bio-oil. We also would like to thank the Montebre SCCL cooperative for the supply of the biomass. N. Puy is grateful for the funding from the Torres Quevedo subprogram from the Spanish Ministry of Economy and Competitiveness (PTQ-15-08063). C. del Pozo expresses her gratitude to the Universitat Autònoma de Barcelona for funding her PhD contract through PIF grant.

References

Albuquerque, J.A., González, J., García, D., Cegarra, J., 2004. Agrochemical characterization of "alperujo", a solid by-product of the two-phase centrifugation method for olive oil extraction. *Bioresour. Technol.* 91, 195–200. [https://doi.org/10.1016/S0960-8524\(03\)00177-9](https://doi.org/10.1016/S0960-8524(03)00177-9).

Artigues, A., Puy, N., Bartrolí, J., Fábregas, E., 2014. Comparative assessment of internal standards for quantitative analysis of bio-oil compounds by gas chromatography/mass spectrometry using statistical criteria. *Energy Fuels* 28, 3908–3915. <https://doi.org/10.1021/e500554s>.

Benavente, V., Fullana, A., 2015. Torrefaction of olive mill waste. *Biomass Bioenergy* 73, 186–194. <https://doi.org/10.1016/j.biombioe.2014.12.020>.

Bridgewater, A.V., 2012. Review of fast pyrolysis of biomass and product upgrading. *Biomass Bioenergy* 38, 68–94. <https://doi.org/10.1016/j.biombioe.2011.01.048>.

Calonaci, M., Grana, R., Barker Hemings, E., Bozzano, G., Dente, M., Ranzi, E., 2010. Comprehensive kinetic modeling study of bio-oil formation from fast pyrolysis of biomass. *Energy Fuels* 24, 5727–5734. <https://doi.org/10.1021/e1008902>.

Conrad, S., Blajin, C., Schube, T., 2017. Producing single phase fast pyrolysis oils from straw by staged condensation. 25th European Biomass Conference and Exhibition.

Dermeche, S., Nadour, M., Larroche, C., Moulit-Mati, F., Michaud, P., 2013. Olive mill wastes: biochemical characterizations and valorization strategies. *Process Biochem.* 48, 1532–1552. <https://doi.org/10.1016/j.procbio.2013.07.010>.

Diebold, J.P., 2002. A review of the chemical and physical mechanisms of the storage stability of fast pyrolysis bio-oils. In: Bridgewater, A.V. (Ed.), *Fast Pyrolysis of Biomass: A Handbook*. CPL Press, Newbury, UK p. 424.

García-Pérez, M., Chasla, A., Roy, C., 2002. Vacuum pyrolysis of sugarcane bagasse. *J. Anal. Appl. Pyrolysis* 65, 111–136. [https://doi.org/10.1016/S0165-2370\(01\)00184-X](https://doi.org/10.1016/S0165-2370(01)00184-X).

Generalitat de Catalunya. Departament de Medi Ambient, 2002. Prevenció de la contaminació en la producció d'oli d'oliva. *Manuals d'enginyeria*, pp. 8.

Goyal, H.B., Seal, D., Saxena, R.C., 2008. Bio-fuels from thermochemical conversion of renewable resources: a review. *Renew. Sustain. Energy Rev.* 12, 504–517. <https://doi.org/10.1016/j.rser.2006.07.014>.

International Olive Council, 2015. *The World Market in Figures*. (Accessed 9 April 2018). <http://www.internationaloliveoil.org/estaticos/view/131-world-olive-oil-figures>.

Javor, T., Buchberger, W., Tanács, I., 2000. Determination of low-molecular-mass phenolic and non-phenolic lignin degradation compounds in wood digestion solutions by capillary electrophoresis. *Mikrochim. Acta* 135, 45–53. <https://doi.org/10.1007/s006040070017>.

Kim, J.S., 2015. Production, separation and applications of phenolic-rich bio-oil—a review. *Bioresour. Technol.* 178, 90–98. <https://doi.org/10.1016/j.biortech.2014.08.121>.

Martínez, J.D., Vezes, A., Mastral, A.M., Murillo, R., Navarro, M.V., Puy, N., Artigues, A., Bartrolí, J., García, T., 2014. Co-pyrolysis of biomass with waste tyre: upgrading of liquid bio-fuel. *Fuel Process. Technol.* 119, 263–271. <https://doi.org/10.1016/j.fuproc.2013.11.015>.

Mohan, D., Pittman, C.U., Steele, P.H., 2006. Pyrolysis of wood/biomass for bio-oil: a critical review. *Energy Fuels* 20, 848–889. <https://doi.org/10.1021/e0502397>.

Murwanashyaka, J.N., Pakdel, H., Roy, C., 2001. Separation of syringol from birch wood-derived vacuum pyrolysis oil. *Sep. Purif. Technol.* 24, 155–165. [https://doi.org/10.1016/S1383-5866\(00\)00225-2](https://doi.org/10.1016/S1383-5866(00)00225-2).

Negro, M.J., Manzanares, P., Castro, E., Ballsteros, M., 2017. The biorefinery concept for the industrial valorization of residues from olive oil industry. In: Galanakis, C.M. (Ed.), *Olive Mill Waste. Recent Advances for Sustainable Management*. Academic Press. <https://doi.org/10.1016/B978-0-12-805314-0/00003-0>, pp. 57–79.

Oasmaa, A., Peacocke, C., 2001. A Guide to Physical Property Characterisation of Biomass-Derived Fast Pyrolysis Liquids. Technical Research Centre of Finland, Espoo.

Puy, N., Murillo, R., Navarro, M.V., López, J.M., Rieradevall, J., Fowler, G., Aranguren, I., García, T., Bartrolí, J., Mastral, A.M., 2011. Valorisation of forestry waste by pyrolysis in a super reactor. *Waste Manage.* 31, 1339–1349. <https://doi.org/10.1016/j.wasman.2011.01.020>.

Recari, J., Berruete, C., Puy, N., Alier, S., Bartrolí, J., Fariol, X., 2017. Torrefaction of a solid recovered fuel (SRF) to improve the fuel properties for gasification processes. *Appl. Energy* 203, 177–188. <https://doi.org/10.1016/j.apenergy.2017.06.014>.

Roig, A., Cayula, M.L., Sánchez-Monedero, M.A., 2006. An overview on olive mill wastes and their valorization methods. *Waste Manage.* 26, 960–969. <https://doi.org/10.1016/j.wasman.2005.07.024>.

Sipilä, K., Kuoppala, E., Ragemäs, L., Oasmaa, A., 1998. Characterization of biomass-based flash pyrolysis oils. *Biomass Bioenergy* 14, 103–113. [https://doi.org/10.1016/S0140-6701\(99\)92423-2](https://doi.org/10.1016/S0140-6701(99)92423-2).

Small, D.M., 1992. Physical properties of fatty acids and their extracellular and intracellular distribution. In: Bracco, U., Deckelbaum, R.J. (Eds.), *Polysaturated Fatty Acid in Human Nutrition*, pp. 25–39.

Torri, C., Fabbri, D., 2014. Biochar enables anaerobic digestion of aqueous phase from intermediate pyrolysis of biomass. *Bioresour. Technol.* 172, 335–341. <https://doi.org/10.1016/j.biortech.2014.09.021>.

Volpe, R., Messineo, A., Millan, M., Volpe, M., Kandiyoti, R., 2015. Assessment of olive wastes as energy source: pyrolysis, torrefaction and the key role of H loss in thermal breakdown. *Energy* 82, 119–127. <https://doi.org/10.1016/j.energy.2015.01.011>.

Wang, S., Wang, Y., Cai, Q., Wang, X., Jin, H., Luo, Z., 2014. Multi-step separation of monophenols and pyrolytic lignins from the water-insoluble phase of bio-oil. *Sep. Purif. Technol.* 122, 248–255. <https://doi.org/10.1016/j.seppur.2013.11.017>.

Williams, O., Eastwick, C., Kingman, S., Giddings, D., Lormor, S., Lester, E., 2017. Overcoming the caking phenomenon in olive mill wastes. *Ind. Crops Prod.* 101, 92–102. <https://doi.org/10.1016/j.indcrop.2017.02.036>.

Wu, Y., Zhao, Z., Li, H., He, F., 2009. Low temperature pyrolysis characteristics of major components of biomass. *J. Fuel Chem. Technol.* 37, 427–432. [https://doi.org/10.1016/S1872-5813\(10\)60002-3](https://doi.org/10.1016/S1872-5813(10)60002-3).

2.2 Article II

Production, identification, and quantification of antioxidants from torrefaction and pyrolysis of grape pomace

Cristina del Pozo ^{a*}, Jordi Bartrolí ^a, Santi Alier ^b, Neus Puy ^{a,c}, Esteve Fàbregas ^a

^a Department of Chemistry, Universitat Autònoma de Barcelona (UAB), Edifici Cn, Campus de la UAB, 08193 Cerdanyola del Vallès, Barcelona, Spain.

^b Energies Tèrmiques Bàsiques SL. C/Maó 22, 2-1, 08022 Barcelona, Spain.

^c Forest Science and Technology Centre of Catalonia (CTFC), Crta. Sant Llorenç de Morunys, km 2, 25280 Solsona, Lleida, Spain

* Corresponding author: Cristina.DelPozo@uab.cat; crisdelpozo19@gmail.com

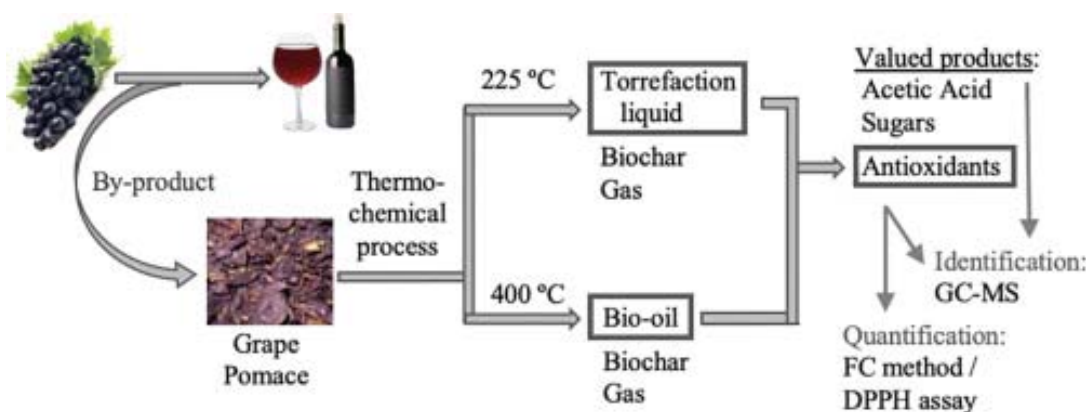


Figure 12. Graphical abstract of the article II.

Journal: Fuel Process. Technol.

Volume 211, 106602

<https://doi.org/10.1016/j.fuproc.2020.106602>

January 2021



Production, identification, and quantification of antioxidants from torrefaction and pyrolysis of grape pomace

Author: Cristina del Pozo, Jordi Bartrolí, Santi Alier, Neus Puy, Esteve Fàbregas

Publication: Fuel Processing Technology

Publisher: Elsevier

Date: January 2021

© 2020 Elsevier B.V. All rights reserved.

Journal Author Rights

Please note that, as the author of this Elsevier article, you retain the right to include it in a thesis or dissertation, provided it is not published commercially. Permission is not required, but please ensure that you reference the journal as the original source. For more information on this and on your other retained rights, please visit: <https://www.elsevier.com/about/our-business/policies/copyright#Author-rights>

BACK

CLOSE WINDOW



Production, identification, and quantification of antioxidants from torrefaction and pyrolysis of grape pomace

Cristina del Pozo^{a,*}, Jordi Bartrolí^a, Santi Alier^b, Neus Puy^{a,c}, Esteve Fàbregas^a

^a Department of Chemistry, Universitat Autònoma de Barcelona (UAB), Edifici Cn, Campus de la UAB, 08193 Cerdanyola del Vallès, Barcelona, Spain

^b Energies Tèrmiques Bàsiques SL, C/Maó 22, 2-1, 08022 Barcelona, Spain

^c Forest Science and Technology Centre of Catalonia (CTFC), Crta. Sant Llorenç de Morunys, km 2, 25280 Solsona, Lleida, Spain



ARTICLE INFO

Keywords:

Grape pomace
Pyrolysis
Torrefaction
Bio-oil
Antioxidants
Phenolic compounds

ABSTRACT

Wine production generates huge amounts of residues, with grape pomace (GP) being the main solid waste. This work attempted to determine whether the use of thermochemical treatments (pyrolysis (400 °C) and torrefaction (225 °C)) are suitable processes to transform GP to a value-added compounds source, paying special attention to phenolics. GP management through thermochemical treatments could then provide ecological and economic benefits. Composition of the liquid fractions was determined by GC-MS. Phenolic quantification was performed using Folin-Ciocalteu (FC) and DPPH assay. Firstly, the suitability of these methods was discussed: DPPH assay was used to quantify phenolics in all the samples; however, in FC method, reducing sugars could interfere in the measurement. The results showed that phenolics were mainly concentrated in the non-aqueous phase of bio-oil (pyrolysis process). It was also observed that these compounds not only came from the GP composition, but from lignin devolatilization during the thermochemical process. Apart from phenolics, bio-oil was also composed of other products, such as acetic acid or levoglucosan. Therefore, this study showed that intermediate pyrolysis is a suitable treatment to add value to GP within a biorefinery concept, turning the winemaking waste into a potential source of antioxidants, together with other value-added compounds.

1. Introduction

Wine is one of the most important alcoholic beverages worldwide. The global wine industry has increased over the last decades, and currently accounts for 29.2 billion liters. Although there is currently significant number of wine producer countries nowadays, the sector continues to be dominated by Italy, France, and Spain, representing 18.8%, 16.6%, and 15.2% of the global production, respectively [1].

The winemaking sector also generates huge amounts of waste that need to be treated to prevent contamination of the environment. The main solid waste from winemaking is grape pomace (GP), the residue left after the juice is extracted from the grapes (skin, seeds, residual pulp, and stalks) [2]. This residue is composed of phytotoxic chemicals [3] and represents approximately 20–30% of the original grape weight [4], reaching nearly 9 million tons per year [5]. In the last few years, most of the winemaking companies have tended to dispose of the waste in landfills or by incineration, with it being necessary to look for greener waste management alternatives [6,7]. In this regard, several studies have been performed based on recovering compounds of interest from GP as a way to reduce the waste and achieve a more

sustainable winemaking process [8,9]. GP is mostly composed of fiber (up to 40%), sugars (15%), phenolics (0.9%), and oils (16%) [4,9] from its principal components, seeds and skin, which represent 38–52% and 5–10% of GP, respectively, of dry winemaking residue [10]. The rich composition of GP means it can be used as a source of compounds that could be applied in many different fields, including functional foods (dietary fiber and polyphenols), food processing (biosurfactants), pharmaceutical and cosmetics (grape seed oil and phenolics) [2,4,11].

Within the GP value-added compounds, phenolics could be considered the most interesting ones due to their antioxidant properties. These antioxidant properties are able to protect living systems from oxidative damages and to prevent severe diseases, such as cardiovascular pathologies [8,12].

Most of phenolics, approximately 70%, remain in the GP after the winemaking process [4], so recovery of them would be of great interest. However, traditional extraction methods, such as mechanical agitation using aqueous-organic solvents, can be inefficient because some of the phenolic compounds remain linked to the dietary fiber matrix [10]. This is because the aromatic rings and hydroxyl groups of phenolics are able to bind to polysaccharides, protein, and cell walls through covalent

* Corresponding author.

E-mail addresses: Cristina.DelPozo@uab.cat, crisdelpozo19@gmail.com (C. del Pozo).

<https://doi.org/10.1016/j.fuproc.2020.106602>

Received 16 March 2020; Received in revised form 26 August 2020; Accepted 4 September 2020
0378-3820/ © 2020 Elsevier B.V. All rights reserved.

bonds (esters and ether), hydrogen bonding, and hydrophobic and hydrophilic interactions [13]. To separate the phenolic compounds, it is then necessary to break these bonds and interactions.

Thermochemical treatments, such as torrefaction or pyrolysis, could be potential methods to obtain some of the value-added products from GP. These treatments, performed at elevated temperatures in absence of oxygen, decompose biomass in solid (biochar), gas, and liquid fractions, with the latter being the richest fraction in high-added value products [14,15]. During the thermochemical treatments, bonds between phenolics and fiber break, concentrating some of the GP phenolics in this liquid fraction. The type of thermochemical process has a large impact on the properties and proportion of the fractions. Pyrolysis is performed at 300–500 °C, where the main components of biomass (hemicelluloses, cellulose and lignin) depolymerize, from which originates a principal liquid fraction, known as bio-oil [16]. On the other hand, torrefaction takes place at 200–300 °C, giving rise to a main solid fraction and, to a lesser extent, a torrefaction liquid (TL), mostly composed of hemicellulose degradation products [16,17].

Several authors have studied the pyrolysis of grape residues under different experimental conditions [18–20]. Their work has been focused on increasing the yields of the products in order to mainly use them as a source of energy. In this case, liquid and solid fractions from the torrefaction and intermediate pyrolysis of GP have been studied to determine the suitability of these processes to obtain value-added products from GP, paying particular attention to phenolic compounds. The thermochemical treatments, torrefaction (225 °C) and intermediate pyrolysis (400 °C), have been performed under low air atmosphere. This makes it a more economic process than conventional treatments, which commonly use nitrogen gas. Bio-oil is typically composed of phenolic derivatives, such as 2-methoxy-phenols and 2,6-dimethoxy-phenols, together with other low molecular weight compounds, such as acids, esters, alcohols, ketones, aldehydes, alkenes, aromatics, nitrogen compounds, furans, sugars, and miscellaneous oxygenates [21]. On the other hand, TL contains water, lipids and organics such as alcohols, furans and acetic acid [16]. This means that both bio-oil and TL may not only be composed of phenolics, but other interesting products such as acetic acid, which has a significant market demand [22]. Apart from liquid fractions, biochars also have potentially interesting applications. Casazza et al. [12] considered that GP biochar is a good source of graphitic carbon with higher calorific value with respect to the initial grape waste, and applicable for energy production. GP biochar has also been considered as a potential biofertilizer or for undergoing direct and efficient gasification [20,23]. Moreover, Brachi [24] has recently investigated the synthesis of fluorescent carbon-based quantum nanodots (CQDs) through GP slow pyrolysis in the presence of a catalysis, with successful results. Torrefaction and intermediate pyrolysis could then become promising processes to valorize GP inside a biorefinery concept, transforming GP into a value-added product source.

Chemical characterization of bio-oils is generally performed by gas chromatography–mass spectrometry (GC–MS). However, the complexity of bio-oil matrix hampers the quantification of its value-added products using GC–MS. This fact requires finding complementary methods that particularly focus on phenolic compounds. The Folin-Ciocalteu (FC) method is widely used in the wine industry to determine the total phenolic content of their products [25]. Rover and Brown [25] also reported that it could be used for quantifying total phenolic compounds in bio-oils poor in aromatic amines, proteins, and sulphur. This method is based on the ability of antioxidant molecules to reduce the FC reagent (a mixture of phosphomolybdic and phosphotungstic acid) to complexes that are detected spectrophotometrically [26]. Another method that could be used to quantify phenolics is the 2,2-diphenyl-1-picrylhydrazyl (DPPH) assay, which evaluates the radical scavenging ability of antioxidant substances towards DPPH· radical [27]. The FC method and DPPH assay measure then two properties that are closely related to antioxidant capacity of the samples, and that can be mainly attributed to the presence of phenolic compounds.

The aim of the present work is to study the potential use of GP bio-oil and TL as a source of value-added products, with a particular focus on phenolic derivatives, in order to transform the winemaking residue into a resource. Both GP and the resulting solid fraction from the thermochemical treatment have also been analyzed. The suitability of FC and DPPH methods to quantify the phenolic compounds of the samples were also studied.

2. Materials and methods

2.1. Materials

All chemicals were commercially available and were used without further purification.

Gallic acid; FC's phenol reagent (2 N), DPPH, trifluoroacetic acid ($\geq 99.0\%$), and methanol (99.8%) were purchased from Sigma Aldrich; acetone (99.0%), and sodium carbonate anhydrous (Na_2CO_3) (99.5%) from Alco. Furthermore, the GP was supplied by a wine company from Spain. The GP was air dried (10% (w/w) moisture) and ground with a hammer crusher to about 3 mm particle size before thermochemical treatments.

2.2. Thermochemical treatment

2.2.1. Thermogravimetric analysis (TGA)

TGA was performed using a Netzsch STA 449 F1 thermobalance. The sample (approximately 6 mg) was inserted into an alumina crucible and heated from room temperature to 1000 °C. The measurement was performed under inert atmosphere (nitrogen) with a heating rate of 10 °C/min.

2.2.2. Pyrolysis and torrefaction

Thermochemical treatment of GP was performed at 400 °C (pyrolysis) and 225 °C (torrefaction), obtaining the bio-oil, TL, and biochars of the study (see Fig. 1). The temperatures of the processes were chosen based on TGA data (see Section 3.1.1) to ensure a proper devolatilization of GP compounds. Pyrolysis and torrefaction experiments were performed in an auger reactor semi-industrial plant described elsewhere [28], continuously operated, and under a low air atmosphere. The mass flow rate was of 15 kg/h, with a biomass residence time of 10 min. Once the stationary state was achieved, solid and liquid samples were taken for analysis; TL and bio-oil were stored at 4 °C to avoid aging [29,30].

As shown in Fig. 1, torrefaction liquid was composed of a single aqueous phase, whereas the bio-oil consisted of two phases: an aqueous phase (AP), and a non-aqueous phase (NAP).

2.3. GP and biochars extraction

Phenolic derivatives, together with other organic molecules, were extracted from the GP and biochars in order to obtain a liquid fraction to be analyzed by GC–MS, FC, and DPPH methods.

Briefly, 1 g of solid sample was extracted with 20 mL of 80% acetone at pH 2, acidified with trifluoroacetic acid using a pH electrode (Solvotrode®) with LiCl (2 mol/L) for non-aqueous media, purchased from Metrohm. Extraction was performed at 30 rpm for 3 h using a rotary mixer. The solid was then filtered, and the resulting filtrate was added to a 25 mL volumetric flask and made up to the mark with 80% acetone. The extraction method was adapted from the described by Marina [27].

2.4. Analytical methods for liquid characterization

2.4.1. GC–MS analysis

GC–MS was performed with a HP 6890 Series II gas chromatograph coupled to a HP 5973 mass selective detector and equipped with a

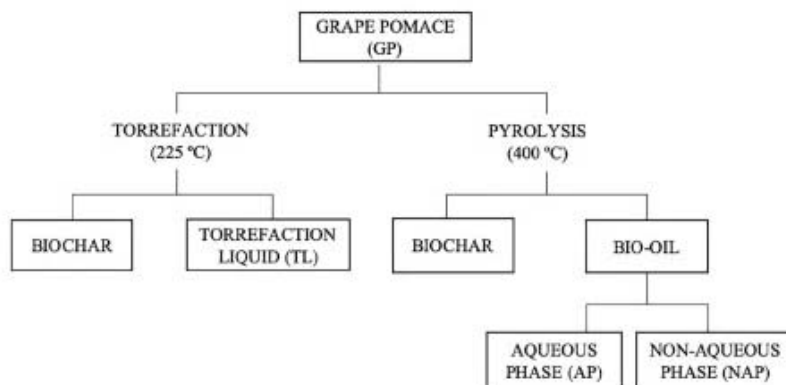


Fig. 1. Thermochemical treatment of GP and the products obtained from the process.

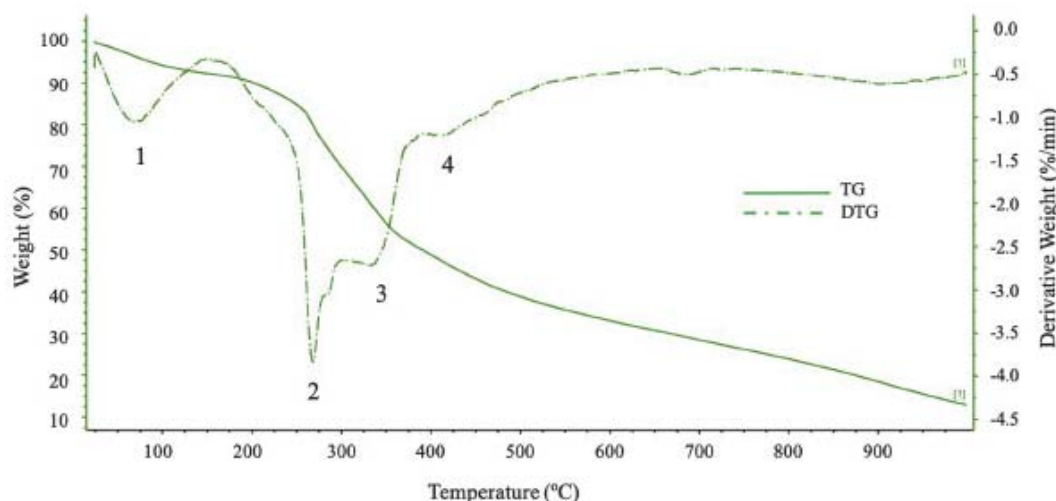


Fig. 2. Pyrolysis curves of GP from TGA. The numbers correspond to the weight loss mainly associated to water loss (1), hemicellulose decomposition (2), cellulose decomposition (3), and the end of lignin decomposition (4). (TG, thermogravimetry; DTG, derivative thermogravimetry).

capillary ZB-5 column (30 m × 0.25 mm inner diameter × 0.25 μm film thickness). TL, AP, and GP and biochar extracts were analyzed without diluting; NAP, on the other hand, had to be dissolved in methanol (1:50) due to its tarry condition. Before injection, samples were filtered (0.45 μm Millipore filter) to avoid obstruction of liner due to some ashes can remain after the thermochemical treatment. A volume of 1 μL of sample was injected into the GC-MS, using a 1:7 split mode and with the injection port at 300 °C. Helium was used as carrier gas with a flow of 0.9 mL/min. The oven temperature was as follows: 45 °C for 1 min, 8 °C/min to 200 °C, 15 °C/min to 310 °C, and 310 °C for 10 min. The total run time was 37.71 min. This method was adapted from that described by Artigues [31]. Compounds were identified from the chromatograms by computer matching of the mass spectra of the peaks with the NIST 17 mass spectral library.

2.4.2. FC method

Total phenolic content of the samples was determined using the FC method, adapted from that described by Ivanova [32]. This method, based on spectrophotometry, was performed using a Lambda 45 UV/Vis Spectrometer from Perkin Elmer. TL, AP and NAP were first diluted in 80% acetone (1:50, 1:30 and 1:500, respectively) in order to have a suitable concentration for the measurements; GP and biochar extracts were analyzed without further dilution. In brief, 0.5 mL of sample was

mixed with 2.5 mL of distilled water. Then, 0.25 mL of FC reagent was added, and the contents were mixed and allowed to react for 3 min. After this time, 1.75 mL of Na₂CO₃ (2 g/L) was added. The mixture was incubated at room temperature for 90 min and the absorbance was then measured at 765 nm using distilled water as blank. Total phenolics content was calculated from a calibration curve prepared with gallic acid (25–250 mg/L). The results were expressed as mg of gallic acid equivalents (GAE)/g of GP, biochar, TL, or bio-oil. All samples were prepared in triplicate.

2.4.3. DPPH assay

The radical scavenging ability of samples was analyzed according to the method described by Marina [27], with some modifications. As in the FC method, the samples were previously diluted in 80% acetone as follows: GP and biochar extracts (1:30), TL (1:278), AP (1:587), and NAP (1:3237). Briefly, 2.5 mL of sample was mixed with 2.5 mL of a freshly prepared DPPH solution (500 μM in 80% acetone). The mixture was then allowed to react away from light for 30 min at room temperature. After this time, absorbance was read at 520 nm against 80% acetone as the blank, using a Lambda 45 UV/Vis Spectrometer from Perkin Elmer. Results were expressed as mg of gallic acid equivalents (GAE)/g of GP, biochar, TL, or bio-oil by interpolation of the gallic acid standard curve (10–150 μM in 80% acetone). All samples were

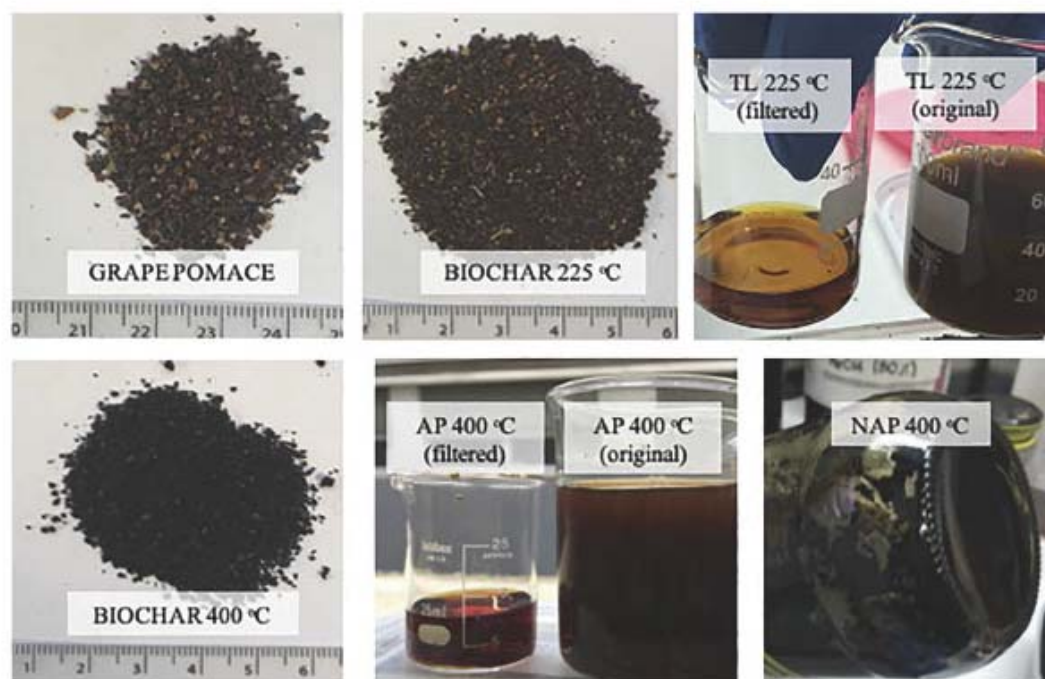


Fig. 3. Grape pomace and the products obtained from torrefaction (225 °C) and intermediate pyrolysis (400 °C): biochar 225 °C, TL 225 °C (filtered and original); biochar 400 °C; AP bio-oil 400 °C (filtered and original) and NAP bio-oil 400 °C. The unit of the ruler is in cm. (AP: aqueous phase of bio-oil; NAP: non-aqueous phase of bio-oil).

prepared in triplicate.

3. Results and discussion

3.1. Thermal decomposition of GP

3.1.1. TGA

Fig. 2 represents the GP degradation process, as the loss of weight of GP vs temperature. GP, as any type of biomass, consists of the main biopolymers, cellulose, hemicellulose, and lignin [33] that are thought to decompose independently, and as such they do not show a synergetic effect [22,34]. The mass loss of GP thus corresponds to the sum of the individual mass loss of the components that make it up [16]. However, as shown in Fig. 2, some weight loss could be mainly attributed to decomposition of a particular compound. The main GP loss of weight takes place between 150 °C and 550 °C, as also observed by Torres-García and Brachi [35]. Moreover, these data are similar to that reported by Zhao [22], who found that hemicellulose and cellulose achieved the maximum mass loss rate at 295 °C and 335 °C, respectively. In the case of lignin, it decomposes slower, over a broad range of temperatures, starting to degrade at 200 °C up to 500 °C (see Fig. 2). The derivative thermogravimetric (DTG) curve of lignin decomposition then shows a wide and flat peak with a gently sloping baseline, which differs from the sharper DTG peaks of cellulose and hemicellulose.

In this work, thermochemical treatment was performed at 225 °C (torrefaction) and 400 °C (pyrolysis) to study the early, and more advanced degradation of GP, as well as the products obtained from it. As seen in Fig. 2, GP torrefaction was mainly characterized by the decomposition of hemicellulose, and the partial decomposition of cellulose and lignin. In the pyrolysis process, on the other hand, both hemicellulose and cellulose were decomposed, while lignin was only partly degraded.

According to TGA data (see Fig. 2), it is expected to obtain about

88% (w/w) and 49% (w/w) of solid fraction at 225 °C and 400 °C, respectively.

3.1.2. Products obtained from the thermochemical treatments of GP

Torrefaction (225 °C) of GP resulted in brown biochar 225 °C and TL that, as shown in Fig. 3, consisted of an orange-brown aqueous phase with suspended solids. Intermediate pyrolysis (400 °C), on the other hand, resulted in black biochar 400 °C and a bio-oil composed of two phases: AP and NAP (see Fig. 3). This type of bio-oil is usually produced in the pyrolysis processes that generates a high amount of reaction water, favoring the phase separation to take place [14,37]. As shown in Fig. 3, AP was a red-brown aqueous phase, with suspended solids, composed of the hydrophilic species of bio-oil. NAP, on the other hand, was a tarry phase containing insoluble heavy organic species [38].

3.2. Chemical characterization of GP and its torrefaction and pyrolysis products

Chemical composition of GP extract, together with GP torrefaction and pyrolysis products, was analyzed by GC-MS. The obtained results are discussed and summarized in the following sections, although full information regarding the chromatograms and the compounds identified in them are available in supplementary material.

3.2.1. Chemical characterization of TL and bio-oil (AP and NAP)

During the thermochemical treatments, the main biopolymers of GP are degraded into a large number of low molecular weight oxygenated products that condense in a liquid fraction (TL and bio-oil). As described in the previous Section 3.1.1, torrefaction (225 °C) involves hemicellulose degradation and the very partial decomposition of cellulose and lignin. By contrast, GP pyrolysis process (400 °C) is characterized by the decomposition of hemicellulose and cellulose, and to a lesser extent, lignin. The resulting bio-oil is composed of two phases, AP

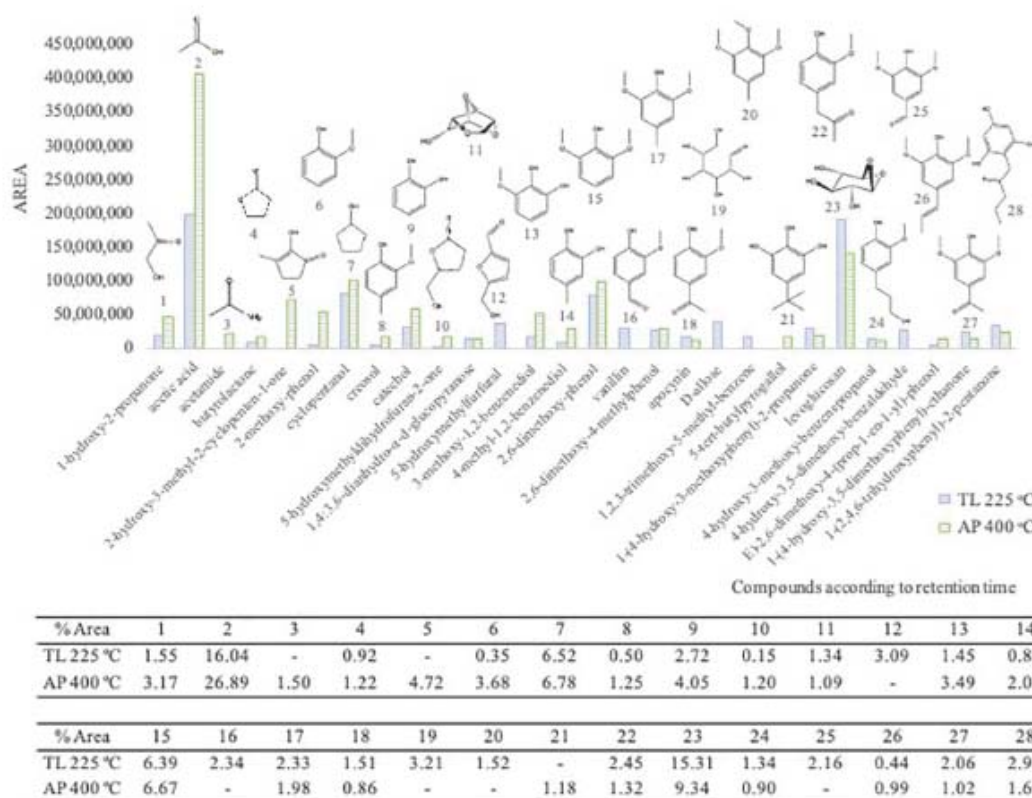


Fig. 4. Most abundant compounds of the torrefaction liquid (TL) and the aqueous phase (AP) of bio-oil from the thermochemical treatment of GP at 225 °C and 400 °C, respectively, determined by GC-MS analysis.

and NAP. AP and TL consisted of an aqueous fraction mostly made up of the hydrophilic thermochemical products, while NAP mainly contained the hydrophobic ones. The use of thermochemical treatments could also lead to breaking the bonds between phenolics and fiber, releasing the phenolics linked in it.

The results from GC-MS analysis showed that TL and AP were composed of similar products. This composition was also similar to that presented by bio-oil from classic forest bio-mass [39,40]. TL and AP mainly consisted of alcohols, ketones, ethers, carboxylic acids, esters, furans, 2(5H)-furanones, 2-cyclopenten-1-ones, pyridines, sugars, and phenols, with the most abundant ones being shown in Fig. 4. These products were divided into three main groups: acetic acid (i), sugars and other derivatives (ii), and phenolics (iii). As can be seen from Fig. 4, acetic acid (2) (i) was the major compound in both samples. Its presence is related to the decomposition of hemicellulose which gives rise to the acid as main product [41]. The higher abundance of the acid in AP compared to TL, could be attributed to an almost complete degradation of hemicellulose during the pyrolysis process (400 °C), which could not be fully accomplished in torrefaction (225 °C). Hemicellulose and cellulose degradation also resulted in sugars (ii), such as 1,4:3,6-dianhydro- α -D-glucopyranose (11), D-allose (19), and levoglucosan (23), the latter being the second most abundant product in both TL and AP (see Fig. 4). As can be observed, monosaccharides were more abundant in TL than AP, due to its low heat stability [22], that lead to the formation of compounds such as 1-hydroxy-2-propanone (1) [42] and water, the aqueous medium of TL and AP. Other cellulose derived compounds were 2-hydroxy-3-methyl-2-cyclopenten-1-one (5) and 5-hydroxymethylfurfural (12), the latter also being decomposed thermally [43], and thus was only found in TL. Phenolics (iii) was the major

group of products in both TL and AP fractions. This was related to the degradation of fiber in the pyrolysis process (400 °C), which released the phenolics linked in it. Moreover, the degradation of lignin also results in phenolic derivatives from its principal monomers: p-coumaryl, coniferyl, and sinapyl alcohols [41]. As shown in Fig. 4, this group was mainly composed of phenols, 2-methoxyphenols, and 2,6-dimethoxyphenols, most para-substituted by C1-C3 carbon atoms aliphatic chain (A) or carbonyl substituent (aldehydes or ketones) (B). Alkylated and non-substituted phenols (A) mostly consisted of 2-methoxy-phenol (6), creosol (8), catechol (9), 3-methoxy-1,2-benzenediol (13), 4-methyl-1,2-benzenediol (14), 2,6-dimethoxy-phenol (15), 2,6-dimethoxy-4-methylphenol (17), and (E)-2,6-dimethoxy-4-(prop-1-en-1-yl)-phenol (26). The major presence of alkylated and non-substituted phenols (A) in AP was related to the higher decomposition of lignin in the pyrolysis process (400 °C). These species (A) have some non-polar character, with them also being found in NAP (see Fig. 5), except for 3-methoxy-1,2-benzenediol (13) and 4-methyl-1,2-benzenediol (14), where their diol condition make them more hydrophilic. On the other hand, carbonyl phenols (B) mainly consisted of vanillin (16), apocynin (18), 1-(4-hydroxy-3-methoxyphenyl)-2-propanone (22), 4-hydroxy-3,5-dimethoxybenzaldehyde (25), and 1-(4-hydroxy-3,5-dimethoxyphenyl)-ethanone (27). In contrast to alkylated phenols (A), carbonyls (B) were only found in the AP fraction, due to its higher polarity and so, affinity for aqueous fraction. As seen from Fig. 4, TL was richer in carbonyl phenols (B) than AP. Zhao [22] described a similar behavior in their hemicellulose, cellulose and lignin bio-oils study, where ketones, such as 1-(4-hydroxy-3,5-dimethoxyphenyl)-ethanone (27), decreased as temperature increased. Moreover, most of the compounds (1, 2, 5, 6, 8, 9, 11, 13–15, 19, 23, and 27) were also identified by the author [22]. The

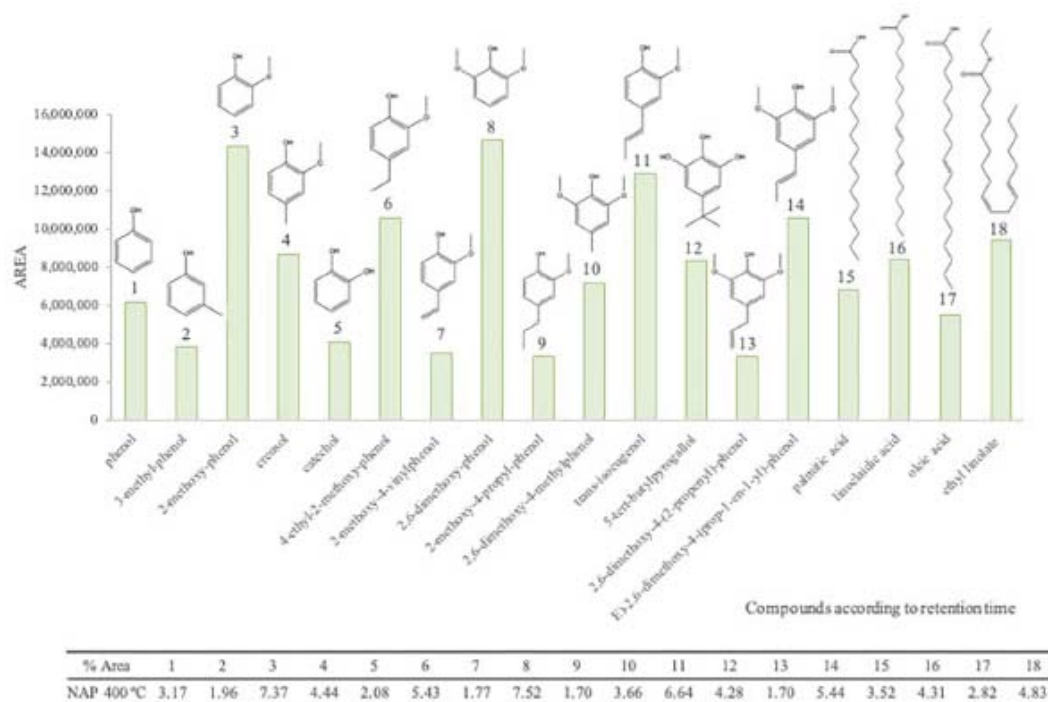


Fig. 5. Most abundant compounds of the non-aqueous phase (NAP) of bio-oil from the pyrolysis of GP at 400 °C, determined by GC-MS analysis.

described results are summarized in Fig. 6.

NAP, on the other hand, consisted of the GP bio-oil hydrophobic compounds, which were mainly obtained from the degradation of lignin during the thermochemical process. The decomposition of lignin increases at high temperatures, so the separation between hydrophilic and hydrophobic compounds only took place at pyrolysis process (400 °C), but not in torrefaction (225 °C), where lignin only degraded to some extent. Consequently, only bio-oil had two phases. As discussed earlier, lignin degradation mainly results in phenol, 2-methoxyphenol and 2,6-dimethoxy-phenol derivatives. This fact was reflected in NAP phenolic composition, which mainly consisted of phenol (1), 3-methylphenol (2), 2-methoxy-phenol (3), creosol (4), catechol (5), 4-ethyl-2-methoxy-phenol (6), 2-methoxy-4-vinylphenol (7), 2,6-dimethoxyphenol (8), 2-methoxy-4-propenyl-phenol (9), 2,6-dimethoxy-4-methylphenol (10), trans-isoegenol (11), 2,6-dimethoxy-4-(2-propenyl)-phenol (13), and E-2,6-dimethoxy-4-(prop-1-en-1-yl)-phenol (14) (see Fig. 5). As observed, most of the NAP phenolic compounds were para-substituted by aliphatic side chains that made them quite non-polar. Therefore, this type of phenolic was mainly concentrated in the hydrophobic NAP phase. The formation of an unsaturated chain in products such as 2-methoxy-4-vinylphenol (7), trans-isoegenol (11), 2,6-dimethoxy-4-(2-propenyl)-phenol (13), and E-2,6-dimethoxy-4-(prop-1-en-1-yl)-phenol (14) was related to dehydration of the aliphatic hydroxyl group from the main lignin monomers [42]. In the same way, the decomposition of methoxy groups led to the formation of monophenols (phenol (1), 3-methyl-phenol (2)), and catechol (5) [42]. The results obtained were similar to those described by Zhao [22] (compounds 1, 3, 4, 5, 6, 8 and 15), and Wang [42] (compounds 7, 11 and 14) in their respective lignin pyrolysis studies. Moreover, part of phenolics could also come from the GP phenolics released from the breakdown of fiber and phenolic bonds in the pyrolysis process (400 °C). Fatty acids and esters of fatty acids were also found in the NAP fraction. Zhao [22] reported on the formation of products such as palmitic acid [15] from the fracture of the ether bond and side chain in lignin samples.

However, most of these acids (palmitic acid (15), oleic acid (17), ethyl linolate? (18)), could also be associated with feedstock (see Fig. 7). The presented results are summarized in Fig. 6.

As seen in Fig. 6., chemical characterization of TL and bio-oil showed their composition in value-added products. Some of these compounds included acetic acid that can be used as chemical platform, and sugars that can be considered as potential feedstock to biogas / bioethanol production. Fatty acids and esters of fatty acids from NAP could also be applied in cosmetics and to produce biodiesel, respectively. From all these products, phenols were one of the most abundant chemicals, especially for NAP, and one of the most interesting ones due to their antioxidant properties that could be used for food, cosmetic, and pharmaceutical purposes. The application of some of the GP TL and bio-oil phenolic compounds are described below. Catechol (Fig. 4, compound 5 – Fig. 5, compound 5) is an important chemical intermediate, which can be used to manufacture rubber hardeners, a plating additive, skin antiseptics, fungicides, hair dyes, insecticides, and so on, and as well as, to make spices. Other interesting phenolics are creosol (Fig. 4, compound 8 – Fig. 5, compound 4), which is an intermediate for manufacturing pharmaceutical products; 2-methoxy-4-(1-propenyl)-phenol (Fig. 5, compound 11), which is applied to dental drugs; 4-ethyl-2-methoxy-phenol (Fig. 5, compound 6), which is used as food additive and fragrance bodies; 2-methoxy-4-vinylphenol (Fig. 5, compound 7), and 2,6-dimethoxy-phenol (Fig. 5, compound 8), which can be used in the food additive and spices industry; 4-methyl-2-benzenediol (Fig. 4, compound 14), which is used to make apple flavors, and 2-methoxyphenol (Fig. 4, compound 3 – Fig. 5, compound 3), which is also used in flavors such as coffee, vanilla, and tobacco, as well as in medicine to make calcium guaiacol sulfonate [44]. Apart from the individual applications of phenolics, García et al. [45] described the use of bio-oil phenolic set, extracted with acetate esters, as antioxidants (preservatives) in biodiesel.

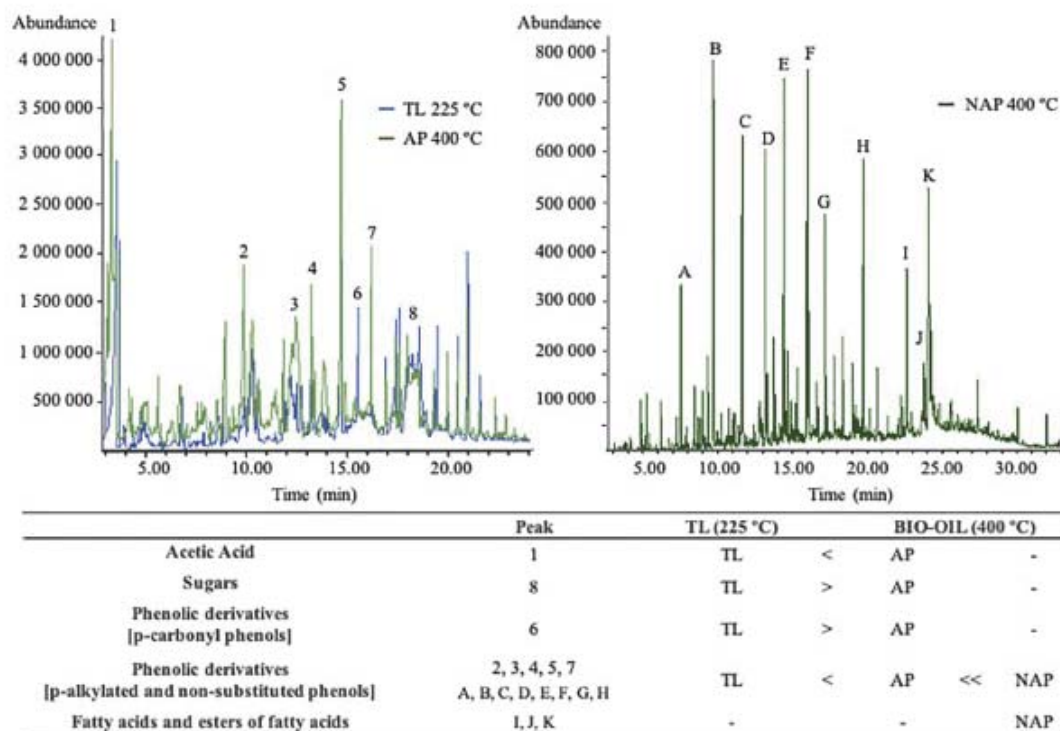


Fig. 6. GC-MS chromatograms of TL, AP and NAP and qualitative comparison of its major compounds. NAP sample was diluted in methanol (1:50) before the analysis (see Section 2.4.1). 1) acetic acid; 2) 2-methoxy-phenol; 3) catechol; 4) 3-methoxy-1,2-benzenediol; 5) 2,6-dimethoxy-phenol; 6) vanillin; 7) 2,6-dimethoxy-4-methylphenol; 8) levoglucosan; A) phenol; B) 2-methoxy-phenol; C) cresol; D) 4-ethyl-2-methoxy-phenol; E) 2,6-dimethoxy-phenol; F) trans-isoeugenol; G) 5-tert-butylpyrogallol; H) E)-2,6-dimethoxy-4-(prop-1-en-1-yl)-phenol; I) palmitic acid; J) linoleic acid; K) ethyl linoleate. (TL: torrefaction liquid; AP: aqueous phase of bio-oil; NAP: non-aqueous phase of bio-oil).

3.2.2. Chemical characterization of GP extract and biochars extracts

GP and the remaining solids fractions from the thermochemical treatments were also chemically characterized in order to identify their value-added products. Due to its solid condition, previous extractions of the interest compounds (phenols) were performed in order to obtain a liquid fraction that allowed them to be analyzed by GC-MS. Although phenolic compounds, together with other organic molecules, were separated from GP and biochars, part of them could still remain linked to the solid fiber [10].

The results from GC-MS analysis showed a quite similar composition between GP and torrefaction biochar (225 °C) extracts. However, almost no compound was detected in pyrolysis biochar (400 °C) sample, where most of the products degraded or remained in bio-oil (compounds 1, 4, 5, 7, 10, 12, and 13). As seen from Fig. 7, fatty acids and ethyl esters of fatty acids were the most abundant compounds in both GP and biochar 225 °C extracts. These acids were indeed part of the oil from grape seeds, one of the main components of GP [4,8,10]. Apart from fatty acids, GP extract was also composed of acetic acid (1), glycerin (3), and phenolics, such as catechol (4), 2,6-dimethoxy-phenol (5), and 1,2,3-benzenetriol (6). Some of these GP compounds (4, 5, and acetic acid) were also found in TL and AP liquid fractions. Therefore their presence was related to both the decomposition of lignocellulosic biomass and feedstock. As regards torrefaction compounds, part of the biochar hydrophilic products (acetic acid (1), catechol (4), and 2,6-dimethoxy-phenol (5), levoglucosan (7), and ethyl α -D-glucopyranoside (9)) were also found in TL. However, the hydrophobic ones (fatty acids and their esters) were only detected in biochar 225 °C due to the difficulty of separating them in the aqueous TL in the volatilization and condensation steps of torrefaction. This was not the case for pyrolysis,

where the higher temperatures of the process made it possible to volatilize and then separate these products by condensing them in NAP. Furthermore, as the torrefaction process partially degrades the biomass, composition of biochar 225 °C and GP feedstock was very similar (see Fig. 7).

Therefore, GP is composed of value-added compounds such as grape seed oils, acetic acid, or phenols. In the pyrolysis process (400 °C), these compounds were successfully separated in bio-oil, finding almost no products in biochar sample. As has been observed, intermediate pyrolysis not only enabled the separation of these compounds from GP, but also formed new ones by decomposing the lignocellulosic biomass, especially phenols. On the other hand, in the torrefaction process (225 °C), the biomass was also degraded, although to a lesser extent.

3.3. Measurement of phenolic content in GP extract and its torrefaction and pyrolysis products

As seen in the previous Section 3.2, phenols were one of the most abundant products from GP thermochemical treatments, especially in pyrolysis (400 °C) where its quantity increased through lignin degradation. Antioxidant properties and radical scavenging ability of phenols endowed them with potential health benefits [8], being highly valued products. Quantification of the phenolic content in the study samples could then provide information about the valorization of GP through these thermochemical treatments. Therefore, it is necessary to apply complementary methods to measure the phenolic compounds in a simpler way than GC-MS. To achieve this, a study was made of the suitability of FC and DPPH assays in these samples.

The values obtained from the analysis of GP pyrolysis products (AP,

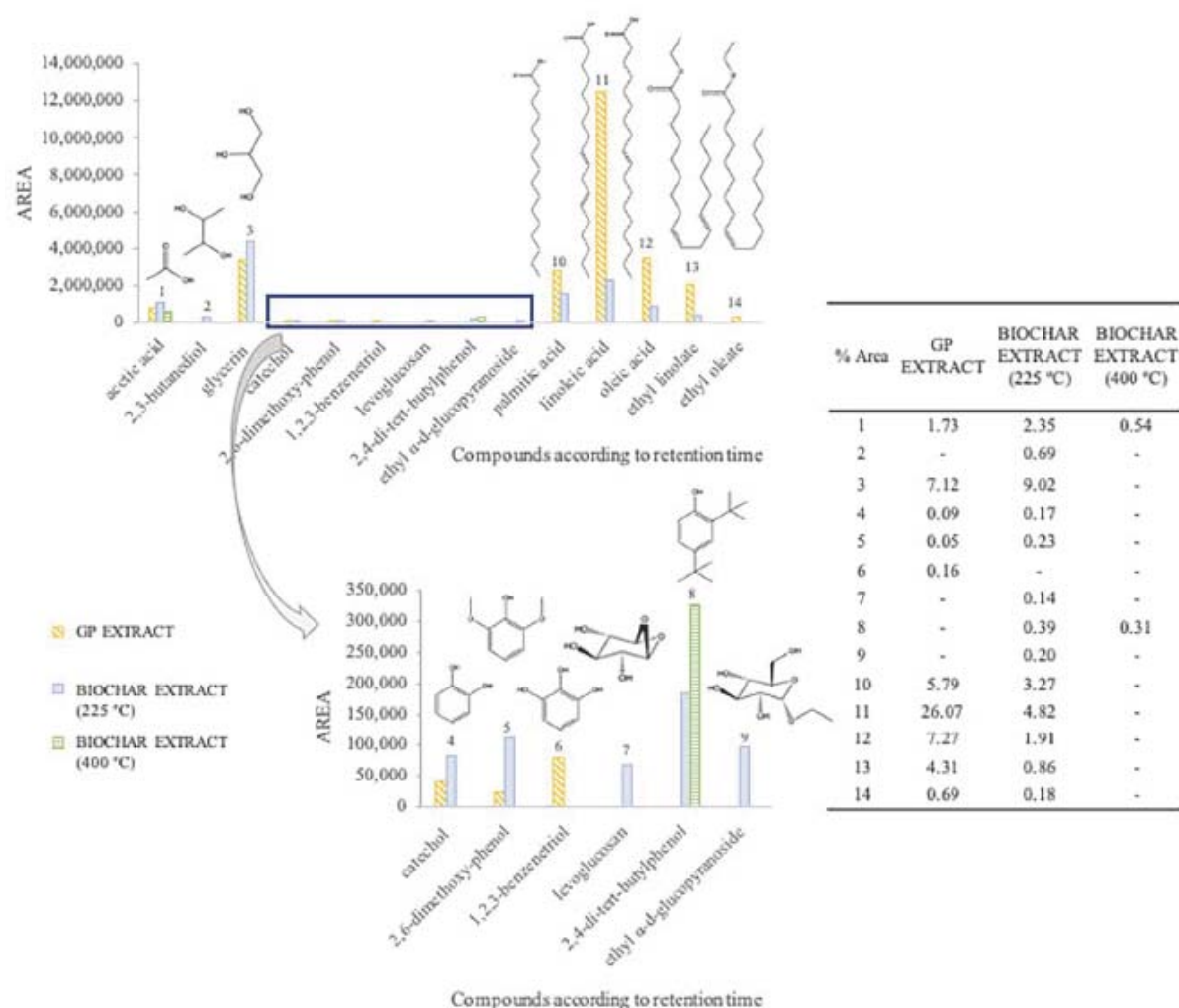


Fig. 7. Most abundant compounds of the extracts of GP and biochars from the thermochemical treatment of GP at 225 °C and 400 °C, determined by GC-MS analysis.

Table 1

Total phenolic content (TPC) and radical scavenging ability determined by FC method and DPPH assay, respectively, for GP and biochars (225 °C and 400 °C) extracts, TL, AP, and NAP from the thermochemical treatments of GP at 225 °C and 400 °C. Results were expressed as mg of gallic acid equivalents (GAE)/g of GP, biochar, TL, or bio-oil. The mean values and standard deviations are shown as \bar{x} and s , respectively.

	TPC (FC method)		DPPH	
	\bar{x}	s	\bar{x}	s
GP extract	3.04	0.18	7.26	0.66
Biochars extracts	225 °C	3.27	0.16	5.90
	400 °C	0.183	0.090	-
Liquid fraction	TL (225 °C)	7.30	0.25	3.23
	AP (400 °C)	5.21	0.09	5.09
	NAP (400 °C)	36.67	0.39	35.20
				0.39

NAP and biochar 400 °C), were in accordance with those observed in GC-MS chromatograms. As seen in Table 1, phenolic compounds were mainly found in NAP, although part of them were also identified in AP. As regards the solid fraction, almost no product was extracted from

biochar 400 °C (see Figs. 4, 5, and 6). As shown in Table 1, the results of GP pyrolysis products from both FC and DPPH methods were similar, so it could be assumed that these values were directly related to the presence of phenols. Moreover, values from GP extract were significantly lower than the pyrolysis products (see Table 1), demonstrating that intermediate pyrolysis (400 °C) can be considered as a suitable method to obtain phenolics from GP.

The results from GP and torrefaction biochar (225 °C) extracts were also in accordance with the information provided by GC-MS analysis, where both samples showed similar composition and trend. In reference to TL values, some discrepancies were noted, as results from DPPH assay and GC-MS chromatograms seemed to indicate that phenols were more abundant in AP than in TL. However, results from the FC method showed that the TL value was higher than AP. This could be explained by the fact that the FC method is non-specific and can be affected by other non-phenolic reducing molecules that do not have radical scavenging ability, with sugars being the most problematic ones [25,46]. Hence, the higher presence of monosaccharides in TL would act as interferences, increasing the value of the measurement, making it necessary to quantify the target TL compounds by DPPH assay. This was not the case for AP, where most of sugars thermally degraded [22,43].

Furthermore, data from DPPH assay indicates that, in the torrefaction process (225 °C), most of phenolics were not volatilized and remained in biochar.

Overall, the results showed that FC and DPPH assays were suitable methods to quantify antioxidants in GP bio-oil. In torrefaction products, the analysis should be performed by DPPH assay as the FC measurement could be affected by reducing sugars and other interferents. On the other hand, both FC and DPPH methods were able to confirm intermediate pyrolysis as a suitable process to separate and produce phenolic compounds. It was also clarified that phenolics were mainly in NAP.

4. Conclusions

Intermediate pyrolysis (400 °C) and torrefaction (225 °C) products of grape pomace (GP) were studied in order to evaluate these methods as potential processes to obtain value-added compounds from GP, with particular attention to phenolics. Data from GC-MS, Folin-Ciocalteu (FC), and DPPH assays showed that intermediate pyrolysis (400 °C) can be a good option to valorize GP inside a biorefinery. The resulting bio-oil was especially rich in phenolics that came from both GP feedstock and lignin decomposition. In particular, phenolics were mainly concentrated in the non-aqueous phase (NAP) of bio-oil. It was also shown that the number of phenolic compounds from pyrolysis process was significantly higher than that obtained from traditional solid-liquid extractions. Apart from phenolics, bio-oil also contained other value-added products, such as acetic acid, levoglucosan, and fatty acids and esters of fatty acids. In the torrefaction process (225 °C) on the other hand, most of phenolic compounds were not volatilized and remained in biochar.

This work also evaluated the use of Folin-Ciocalteu (FC) and DPPH methods for quantifying phenolics from GP intermediate pyrolysis (400 °C) and torrefaction (225 °C) products. The results showed that the DPPH assay was a successful method to quantify phenolic compounds in all the samples. The FC method was also used in GP bio-oil. However, in torrefaction products, the high content of reducing sugars interferes in the measurement.

Therefore, this study concludes that pyrolysis can be used to valorize the winemaking waste by turning it into a potential source of value-added products and so, taking a first step towards a circular economy and bioeconomy in the wine industry.

Declaration of competing interest

The authors declare that they have no known competing financial interests or personal relationships that could have appeared to influence the work reported in this paper.

Acknowledgements

C. del Pozo expresses her gratitude to the *Universitat Autònoma de Barcelona* for funding her PhD contract through a PIF grant. The authors are also thankful to Pau Redon, Paul Núñez, and Sofia Taboada for their collaboration in the presented study.

Appendix A. Supplementary data

Supplementary data to this article can be found online at <https://doi.org/10.1016/j.fuproc.2020.106602>.

References

- [1] International Organisation of Vine and Wine, 2019 Statistical Report on World Vitiviniculture, 2019 Stat. Rep. World Vitiviniculture, 23 (2019) doi:64/19/6825 [pii]10.1158/0008-5472.CAN-04-1678.
- [2] C. Beres, G.N.S. Costa, I. Cabezas, N.K. Silva-james, A.S.C. Teles, A.P.G. Cruz,

- C. Mellinger-silva, R.V. Tonon, L.M.C. Cabral, S.P. Freitas, Towards integral utilization of grape pomace from winemaking process: a review, *Waste Manag.* 68 (2017) 581–594, <https://doi.org/10.1016/j.wasman.2017.07.017>.
- [3] K.J. Olejar, C. Vandermeer, B. Fedrizzi, P.A. Kilmartin, A horticultural medium established from the rapid removal of phytotoxins from winery grape marc, *Horticulturae* 5 (2019), <https://doi.org/10.3390/horticulturae5040069>.
- [4] K. Dwyer, F. Hossainian, M. Rod, The Market Potential of Grape Waste Alternatives, 3, (2014), <https://doi.org/10.5539/jfr.v3n2p91>.
- [5] C.S.S. Coelho, M. Micheín, M.A. Cerqueira, C. Gonçalves, R.V. Tonon, L.M. Pastrana, O. Freitas-Silva, A.A. Vicente, L.M.C. Cabral, J.A. Teixeira, Cellulose nanocrystals from grape pomace: production, properties and cytotoxicity assessment, *Carbohydr. Polym.* 192 (2018) 327–336, <https://doi.org/10.1016/j.carbpol.2018.03.022>.
- [6] R. Devesa-Rey, X. Vecino, J.L. Varela-Alende, M.T. Barral, J.M. Cruz, A.B. Moldes, Valorization of winery waste vs. the costs of not recycling, *Waste Manag.* 31 (2011) 2327–2335, <https://doi.org/10.1016/j.wasman.2011.06.001>.
- [7] C. Kumanda, V. Mlambo, C.M. Mnisi, From landfills to the dinner table: red grape pomace waste as a nutraceutical for broiler chickens, *Sustainability* 11 (2019), <https://doi.org/10.3390/su11071931>.
- [8] I.S. Arvanitoyannis, D. Ladas, A. Mavromatis, Potential Uses and Applications of Treated Wine Waste: A Review, (2006), pp. 475–487, <https://doi.org/10.1111/j.1365-2621.2005.01111.x>.
- [9] M. Zacharof, Grape winery waste as feedstock for bioconversions: applying the biorefinery concept, *Waste and Biomass Valorization*. 8 (2017) 1011–1025, <https://doi.org/10.1007/s12649-016-9674-2>.
- [10] A. Brenes, A. Viveros, S. Chamorro, I. Ariza, Use of polyphenol-rich grape by-products in monogastric nutrition. a review, *Anim. Feed Sci. Technol.* (2015), <https://doi.org/10.1016/j.anifeedsci.2015.09.016>.
- [11] Y. Jiang, J. Simonsen, Y. Zhao, Compression-molded biocomposite boards from red and white wine grape pomaces, *J. Appl. Polym. Sci.* 119 (2010) 2834–2846, <https://doi.org/10.1002/app>.
- [12] A.A. Casazza, B. Aliakbarian, A. Lagazzo, G. Garbarino, M.M. Carnasciali, P. Perego, G. Busca, Pyrolysis of grape marc before and after the recovery of polyphenol fraction, *Fuel Process. Technol.* 153 (2016) 121–128, <https://doi.org/10.1016/j.fuproc.2016.07.014>.
- [13] F. Saura-Calixto, Concept and health-related properties of nonextractable polyphenols: the missing dietary polyphenols, *J. Agric. Food Chem.* 60 (2012) 11195–11200, <https://doi.org/10.1021/jf303758j>.
- [14] C. del Pozo, J. Bartrolí, N. Puy, E. Fábregas, Separation of value-added chemical groups from bio-oil of olive mill waste, *Ind. Crops Prod.* 125 (2018), <https://doi.org/10.1016/j.indcrop.2018.08.062>.
- [15] C. del Pozo, J. Bartrolí, S. Alier, N. Puy, E. Fábregas, Production of antioxidants and other value-added compounds from coffee silverskin via pyrolysis under a biorefinery approach, *Waste Manag.* 109 (2020) 19–27, <https://doi.org/10.1016/j.wasman.2020.04.044>.
- [16] P. Basu, *Biomass Gasification, Pyrolysis and Torrefaction*, third, Academic Press, 2018.
- [17] A.V. Bridgwater, Review of fast pyrolysis of biomass and product upgrading, *Biomass Bioenergy* 38 (2012) 68–94, <https://doi.org/10.1016/j.biombioe.2011.10.048>.
- [18] R. Xu, L. Ferrante, C. Briens, F. Berruti, Flash pyrolysis of grape residues into biofuel in a bubbling fluid bed, *J. Anal. Appl. Pyrolysis* 86 (2009) 58–65, <https://doi.org/10.1016/j.jaap.2009.04.005>.
- [19] I. Demiral, E.A. Ayan, Pyrolysis of grape bagasse: effect of pyrolysis conditions on the product yields and characterization of the liquid product, *Bioresour. Technol.* 102 (2011) 3946–3951, <https://doi.org/10.1016/j.biortech.2010.11.077>.
- [20] B. Khari, M. Jeguirim, Pyrolysis of grape marc from Tunisian wine industry: feedstock characterization, thermal degradation and kinetic analysis, *Energies* 11 (2018), <https://doi.org/10.3390/en11040730>.
- [21] H.B. Goyal, D. Seal, R.C. Saxena, Bio-fuels from thermochemical conversion of renewable resources: a review, *Renew. Sust. Energ. Rev.* 12 (2008) 504–517, <https://doi.org/10.1016/j.rser.2006.07.014>.
- [22] C. Zhao, E. Jiang, A. Chen, Volatile production from pyrolysis of cellulose, hemicellulose and lignin, *J. Energy Inst.* 90 (2017) 902–913, <https://doi.org/10.1016/j.joet.2016.08.004>.
- [23] A. Ibn Ferjani, M. Jeguirim, S. Jellali, L. Limousy, C. Courson, H. Alrouf, N. Thevenin, L. Ruidavets, A. Muller, S. Bennici, The use of exhausted grape marc to produce biofuels and biofertilizers: effect of pyrolysis temperatures on biochar properties, *Renew. Sust. Energ. Rev.* 107 (2019) 425–433, <https://doi.org/10.1016/j.rser.2019.03.034>.
- [24] P. Brachi, Synthesis of fluorescent carbon quantum dots (CQDs) through the mild thermal treatment of agro-industrial residues assisted by γ -alumina, *Biomass Convers. Biorefinery* (2019), <https://doi.org/10.1007/s12399-019-00503-4>.
- [25] M.R. Rover, R.C. Brown, Quantification of total phenols in bio-oil using the Folin-Ciocalteu method, *J. Anal. Appl. Pyrolysis* 104 (2013) 366–371, <https://doi.org/10.1016/j.jaap.2013.06.011>.
- [26] L.M. Magalhães, M.A. Segundo, S. Reis, J.L.F.C. Lima, Methodological aspects about in vitro evaluation of antioxidant properties, *Anal. Chim. Acta* 613 (2008) 1–19, <https://doi.org/10.1016/j.aca.2008.02.047>.
- [27] D. Marina, G. Avella, C. Alberto, O. García, A.M. Gáneros, Medición de fenoles y actividad antioxidante en malezas usadas para alimentación animal, *Simp. Metro.* (2008) 1–5 http://ceram.mx/simpocic2008/sm_2008/memorias/M2/SM2008-M220-1108.pdf.
- [28] J. Recari, C. Berruero, N. Puy, S. Alier, J. Bartrolí, X. Fariol, Torrefaction of a solid recovered fuel (SRF) to improve the fuel properties for gasification processes, *Appl. Energy* 203 (2017) 177–188, <https://doi.org/10.1016/j.apenergy.2017.06.014>.

- [29] J.P. Diebold, A review of the chemical and physical mechanisms of the storage stability of fast pyrolysis bio-oils, in: A.V. Bridgwater (Ed.), *Fast Pyrolysis Biomass A Handb*, CPL Press, Newbury, UK, 2002, p. 424 doi:NREL/SR-570-27612.
- [30] A. Oasmaa, C. Peacocke, *A Guide to Physical Property Characterisation of Biomass-Derived Fast Pyrolysis Liquids*, (2001).
- [31] A. Artigues, N. Puy, J. Bartrolí, E. Fábregas, Comparative assessment of internal standards for quantitative analysis of bio-oil compounds by gas chromatography/mass spectrometry using statistical criteria, *Energy Fuel* 28 (2014) 3908–3915, <https://doi.org/10.1021/e5005545>.
- [32] V. Ivanova, M. Stefova, F. Chinić, Determination of the polyphenol contents in Macedonian grapes and wines by standardized spectrophotometric methods, *J. Serbian Chem. Soc.* 75 (2010) 45–59, <https://doi.org/10.2298/JSC1001045I>.
- [33] C. Marculescu, S. Ciuta, Wine industry waste thermal processing for derived fuel properties improvement, *Renew. Energy* 57 (2013) 645–652, <https://doi.org/10.1016/j.renene.2013.02.028>.
- [34] W.H. Chen, P.C. Kuo, Isothermal torrefaction kinetics of hemicellulose, cellulose, lignin and xylan using thermogravimetric analysis, *Energy* 36 (2011) 6451–6460, <https://doi.org/10.1016/j.energy.2011.09.023>.
- [35] E. Torres-García, P. Brachi, Non-isothermal pyrolysis of grape marc: thermal behavior, kinetics and evolved gas analysis, *J. Therm. Anal. Calorim.* 139 (2020) 1463–1478, <https://doi.org/10.1007/s10973-019-08530-z>.
- [37] C. Torri, D. Fabbri, Biochar enables anaerobic digestion of aqueous phase from intermediate pyrolysis of biomass, *Bioresour. Technol.* 172 (2014) 325–341, <https://doi.org/10.1016/j.biortech.2014.09.021>.
- [38] M. Calonaci, R. Grana, E. Barker Hemings, G. Bozzano, M. Dente, E. Ranzi, Comprehensive kinetic modeling study of bio-oil formation from fast pyrolysis of biomass, *Energy and Fuels* 24 (2010) 5727–5734, <https://doi.org/10.1021/ef1008902>.
- [39] T. García, A. Vezes, J.M. López, B. Puértolas, J. Pérez-Ramírez, M.S. Callén, Determining bio-oil composition via chemometric tools based on infrared spectroscopy, *ACS Sustain. Chem. Eng.* (2017), <https://doi.org/10.1021/acscuschemeng.7b01483>.
- [40] N. Puy, R. Murillo, M.V. Navarro, J.M. López, J. Rieradevall, G. Fowler, I. Aranguren, T. García, J. Bartrolí, A.M. Mastral, Valorisation of forestry waste by pyrolysis in an auger reactor, *Waste Manag.* 31 (2011) 1339–1349, <https://doi.org/10.1016/j.wasman.2011.01.020>.
- [41] D. Mohan, C.U. Pittman, P.H. Steele, Pyrolysis of wood/biomass for bio-oil: a critical review, *Energy and Fuels* 20 (2006) 848–889, <https://doi.org/10.1021/ef0502397>.
- [42] S. Wang, G. Dai, H. Yang, Z. Luo, Lignocellulosic biomass pyrolysis mechanism: a state-of-the-art review, *Prog. Energy Combust. Sci.* 62 (2017) 33–86, <https://doi.org/10.1016/j.pecc.2017.05.004>.
- [43] D.K. Shen, S. Gu, The mechanism for thermal decomposition of cellulose and its main products, *Bioresour. Technol.* 100 (2009) 6496–6504, <https://doi.org/10.1016/j.biortech.2009.06.095>.
- [44] X. Liu, Y. Meng, Z. Zhang, Y. Wang, X. Geng, M. Li, Z. Li, D. Zhang, Functional nanocatalyzed pyrolyzates from branch of Cinnamomum camphora, *Saudi J. Biol. Sci.* 26 (2019) 1227–1246, <https://doi.org/10.1016/j.sjbs.2019.06.003>.
- [45] M. García, L. Botella, N. Gil-Lalaguna, J. Arauzo, A. Gonzalo, J.L. Sánchez, Antioxidants for biodiesel: Additives prepared from extracted fractions of bio-oil, *Fuel Process. Technol.* 156 (2017) 407–414, <https://doi.org/10.1016/j.fuproc.2016.10.001>.
- [46] Ó.A. Muñoz-Bernal, G.A. Torres-Aguirre, J.A. Núñez-Gastélum, L.A. de la Rosa, J. Rodrigo-García, J.F. Ayala-Zavala, E. Álvarez-Parrilla, Nuevo acercamiento a la interacción del reactivo de folín-ciocalteu con azúcares durante la cuantificación de polifenoles totales, *Tip.* 20 (2017) 23–28, <https://doi.org/10.1016/j.recqb.2017.04.003>.

2.3 Article III

Production of antioxidants and other value-added compounds from coffee silverskin via pyrolysis under a biorefinery approach

Cristina del Pozo ^{a*}, Jordi Bartrolí ^a, Santi Alier ^b, Neus Puy ^{a,c}, Esteve Fàbregas ^a

^a Department of Chemistry, Universitat Autònoma de Barcelona (UAB), Edifici Cn, Campus de la UAB, 08193 Cerdanyola del Vallès, Barcelona, Spain.

^b Energies Tèrmiques Bàsiques SL. C/Maó 22, 2-1, 08022 Barcelona, Spain.

^c Forest Science and Technology Centre of Catalonia (CTFC), Crta. Sant Llorenç de Morunys, km 2, 25280 Solsona, Lleida, Spain

* Corresponding author: Cristina.DelPozo@uab.cat; crisdelpozo19@gmail.com

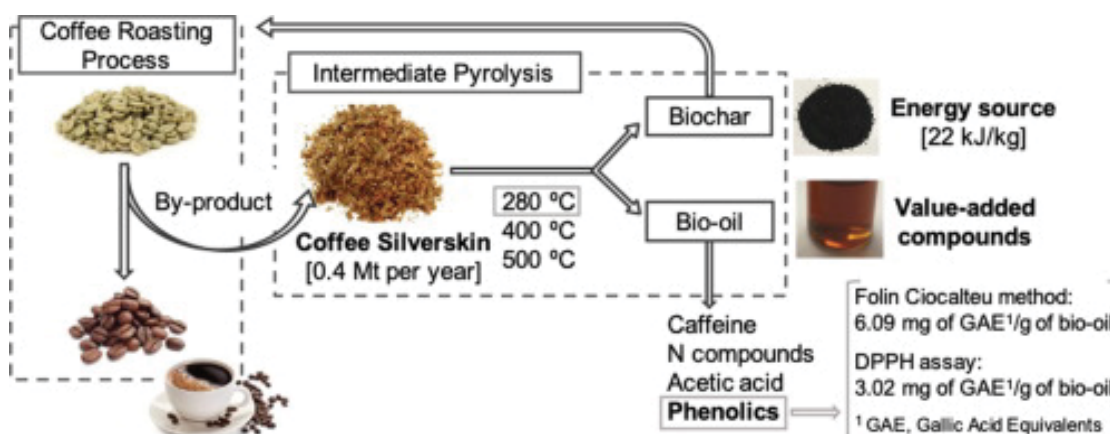


Figure 13. Graphical abstract of the article III.

Journal: Waste Manag.
Volume 109, Pages 19-27

<https://doi.org/10.1016/j.wasman.2020.04.044>

15 May 2020



Production of antioxidants and other value-added compounds from coffee silverskin via pyrolysis under a biorefinery approach

Author: Cristina del Pozo, Jordi Bartrolí, Santi Alier, Neus Puy, Esteve Fàbregas

Publication: Waste Management

Publisher: Elsevier

Date: 15 May 2020

© 2020 Elsevier Ltd. All rights reserved.

Journal Author Rights

Please note that, as the author of this Elsevier article, you retain the right to include it in a thesis or dissertation, provided it is not published commercially. Permission is not required, but please ensure that you reference the journal as the original source. For more information on this and on your other retained rights, please visit: <https://www.elsevier.com/about/our-business/policies/copyright#Author-rights>

BACK

CLOSE WINDOW



Contents lists available at ScienceDirect

Waste Management

journal homepage: www.elsevier.com/locate/wasman

Production of antioxidants and other value-added compounds from coffee silverskin via pyrolysis under a biorefinery approach



Cristina del Pozo^{a,*}, Jordi Bartrolí^a, Santi Alier^b, Neus Puy^{a,c}, Esteve Fàbregas^a

^aDepartment of Chemistry, Universitat Autònoma de Barcelona (UAB), Edifici Cn, Campus de la UAB, 08193 Cerdanyola del Vallès, Barcelona, Spain

^bEnergies Tèrmiques Bàsiques SL, C/Mod 22, 2-1, 08022 Barcelona, Spain

^cForest Science and Technology Centre of Catalonia (CTFC), Crta. Sant Llorenç de Morunys, km 2, 25280 Solsona, Lleida, Spain

ARTICLE INFO

Article history:

Received 19 November 2019

Revised 15 April 2020

Accepted 25 April 2020

Keywords:

Coffee silverskin

Pyrolysis

Biorefinery

Bio-oil

Value-added products

Antioxidants

ABSTRACT

The coffee roasting industry produces about 0.4 Mt of coffee silverskin (CSS) per year, the only residue generated from the roasting process that is mostly disposed as industrial waste. The aim of this study is to convert CSS into value-added products by intermediate pyrolysis, transforming the waste into a resource within an integrated biorefinery perspective. To this end, bio-oils and biochars from the intermediate pyrolysis of CSS at 280 °C, 400 °C and 500 °C have been studied. GC–MS analysis showed that bio-oils were composed of value-added products such as caffeine, acetic acid, pyridine and phenolics, the latter being the most interesting due to their antioxidant properties. Total phenolic content and antioxidant capacity of the samples were determined through Folin-Ciocalteu (FC) and DPPH methods, revealing an increase in phenolics in bio-oils compared to CSS extract directly from the feedstock. The bio-oil with the highest phenolic content and antioxidant properties was produced at 280 °C and contained 6.09 and 3.02 mg of gallic acid equivalents /g of bio-oil determined by FC and DPPH methods, respectively. This represents a global potential of up to 487 and 242 tones of gallic acid equivalents per year, considering the FC results and DPPH respectively. The resulting 280 °C biochar presented significant calorific values (22 MJ/kg), indicating its potential use as an energy source. Hence, CSS pyrolysis converts a waste into a by-product and a resource, increasing the environmental benefits and contributing to the circular economy and bioeconomy.

© 2020 Elsevier Ltd. All rights reserved.

1. Introduction

Coffee is one of the most commonly consumed beverages worldwide, approximately 168.1 million 60 kg bags being consumed in the 2018/19 season (International Coffee Organization, 2020). Such large coffee production also generates large amounts of residues, such as coffee silverskin (CSS), amounting to about 0.4 Mt per year (International Coffee Organization, 2020; Polidoro et al., 2018). This waste is the only by-product from the coffee roasting process, generated when the protective skin of beans is shed (Narita and Kuniyo, 2014). To this day, few studies have addressed the reuse of CSS, most of which is disposed of as industrial waste (Polidoro et al., 2018). This represents serious

environmental problems due to the phytotoxicity of CSS (Polidoro et al., 2018), and there is a need for greener waste management alternatives.

Within the wider Bioeconomy transition, solutions must be designed and implemented to ensure sustainable use of biomass (Zabaniotou et al., 2018), hence the biorefinery of unexploited solid wastes from industrial food and drink processes, including the coffee roasting sector, would enhance environmental, economic and sustainable management of waste (Zabaniotou et al., 2018).

Several studies indicate the potential use of CSS as a source of mainly dietary fibre and phenolics, the latter being functional compounds that could be used as natural antioxidant sources, nutraceuticals, and preservatives in food formulations (Borrelli et al., 2004; Bresciani et al., 2014; Murthy and Madhava Naidu, 2012; Narita and Kuniyo, 2014). Obtaining phenolics from CSS would therefore not only improve the revenue of the roasted coffee industry, but would also help the environment by reducing waste (Murthy and Madhava Naidu, 2012). However, some phenolics cannot be extracted by traditional methods because they are linked

Abbreviations: CSS, coffee silverskin; FC, Folin-Ciocalteu; DPPH, 2,2-diphenyl-1-picrylhydrazyl; ICP-MS, inductively coupled plasma - mass spectrometry; TGA, thermogravimetric analysis; LHV, Lower Heating Value; GC–MS, gas chromatography-mass spectrometry.

* Corresponding author.

E-mail address: Cristina.DelPozo@uab.cat (C. del Pozo).

<https://doi.org/10.1016/j.wasman.2020.04.044>

0956-053X/© 2020 Elsevier Ltd. All rights reserved.

to the dietary fibre matrix (Brenes et al., 2015) and these bonds must be broken in order to obtain them.

CSS could also be a potential energy source, as biomass has been used for energy purposes for time immemorial (Nisar et al., 2019). In contrast to fossil fuels, biomass is a readily available renewable resource that may be produced and consumed on a CO₂-neutral basis (Iakovou et al., 2010). Biofuels obtained from waste biomass also helps to avoid the economic, environmental and social impacts associated with the production and utilization of energy crops, such as sugar cane, corn and palm oil (Digman and Kim, 2008; Iakovou et al., 2010), whereby the residue from the coffee roasting process can be considered a resource to be used as solid biofuel or as a source of value-added products.

This study uses intermediate pyrolysis to valorise CSS under the integrated biorefinery concept. Through pyrolysis, CSS could be valorised via multi-product pathways instead of mono-product pathways, integrating pyrolysis in a cascade biorefinery.

Pyrolysis is a thermochemical treatment that is widely used to transform biomass into a chemical and energy source. This treatment, performed at high temperatures in absence of oxygen, decomposes the main polymers of biomass (hemicellulose, cellulose and lignin) in liquid (bio-oil), solid (biochar) and gas fractions, temperature being one of the main factors of the properties and proportion of the fractions. Apart from temperature, type of feedstock and global experimental conditions also affect the yield and composition of pyrolysis products (Nisar et al., 2016). Bio-oil is the richest fraction in value-added compounds and hence a potential source of chemicals (del Pozo et al., 2018). This fraction is typically composed of phenolic derivatives, acids, esters, alcohols, ketones, aldehydes, alkenes, aromatics, nitrogen compounds, furans, sugars and other low molecular weight oxygenate compounds (Goyal et al., 2008). Part of these compounds, such as phenolics and acetic acid, are of particular interest in industry. Biochar, on the other hand, can be used as a solid biofuel. The use of biochar instead of raw biomass in combustion processes helps to increase the thermal efficiency of the process (Santos et al., 2015).

In this study, pyrolysis has been performed at different temperatures under a limiting oxygen atmosphere, representing a more economic process than conventional pyrolysis. Pyrolysis of CSS could be used to obtain phenolic rich bio-oils by breaking the bonds between phenolics and fibre, which degrade in the thermochemical process. At the same time, CSS biochar could be a potential solid biofuel to be used in the roasting process itself (see Fig. 1).

The aim of this study is focused on studying and characterising CSS bio-oils and biochars in order to determine their potential applicability as a chemical and energy source. It is framed within a novel integrated coffee roasting waste valorisation pathway, based on intermediate pyrolysis (see Fig. 1), to bring about an increase in resource efficiency and environmental benefits. The study is therefore performed to transform CSS industrial waste into biorefinery feedstock.

2. Materials and methods

2.1. Materials

All chemicals were commercially available and were used without further purification. Gallic acid; Folin-Ciocalteu's (FC) phenol reagent (2 N), 2,2-diphenyl-1-picrylhydrazyl (DPPH), trifluoroacetic acid ($\geq 99.0\%$) and methanol (99.8%) were purchased from Sigma Aldrich (Spain); acetone (99.0%) and sodium carbonate anhydrous (Na₂CO₃) (99.5%), from Alco (Spain); and nitric acid (HNO₃), hydrochloric acid (HCl) and hydrofluoric acid (HF) from Merck (Spain). CSS was supplied by a roasted coffee company from Spain.

2.2. Thermochemical treatment.

CSS was first natural dried, until 5.5% (w/w) moisture, and crushed with a hammer crusher to 5 mm particle size. CSS was then pyrolysed at 280 °C, 400 °C and 500 °C, obtaining a bio-oil and biochar for each temperature. The thermochemical treatment was carried out under a limiting oxygen atmosphere, with a residence time of 10 min, in an auger reactor industrial plant by the ENER-bas company described elsewhere (Recari et al., 2017).

2.3. Analytical methods for CSS and biochar characterisation

2.3.1. Thermogravimetric analysis (TGA)

TGA analysis was performed using a thermobalance Netzsch STA 449 F1 (Germany). Approximately 4 mg of CSS was inserted in an alumina crucible and heated from room temperature to 1000 °C. The measurement was performed under inert atmosphere (nitrogen) with a heating rate of 10 °C/min.

2.3.2. Moisture content

CSS moisture was measured by heating the sample at 110 °C for 24 h in an oven. The moisture content corresponded to the weight loss. This method was adapted from the ASTM D4442-07 standard. The measurement was performed three times.

2.3.3. Ash content

Ash content of CSS was measured following a substantially similar procedure to the ASTM E1755-01 standard. Briefly, 1.5 g of CSS was heated in a muffle furnace at 600 °C for 24 h. After this time, CSS was cooled in a desiccator and weighed. This heating, cooling and weighing procedure was repeated until constant weight which is defined as less than ± 0.3 mg change in weight upon one hour of re-heating the sample (Sluiter et al., 2008). In this procedure, the same cool time must be maintained. The measurement was repeated five times.

2.3.4. Inductively coupled plasma - mass spectrometry (ICP-MS)

Inorganic composition of CSS and CSS ash was determined semi-quantitatively by ICP-MS. Briefly, 0.5 g of sample was digested in a mix of concentrated acids (HNO₃ + HCl + HF) using a Milestone microwave digester (Italy). Ultrawave model, with digestion blanks in parallel. The digestion solutions were then diluted in HNO₃ 1% (v/v). Inorganic element concentrations were semi-quantified by ICP-MS Agilent (USA), model 7500cs, from the molar response curve vs atomic weight.

2.3.5. Calorific value measurement

Lower Heating Value (LHV) of CSS and biochars were measured by weighing 0.4–1.0 g of samples and burning in an IKA 5000 bomb calorimeter (Germany). The measurements were performed twice.

2.3.6. Elemental analysis

Elemental analysis (C, H, N and S) of CSS and biochars was determined using a Thermo Fisher Scientific EA 1108 Elemental Analyzer (USA). Briefly, 1000 g of sample was weighed. The sample was then analysed using sulphanimide as patron. A mixture of vanadium pentoxide and tin powder was also used as additive to promote combustion. The measurements were performed twice.

2.4. CSS extraction

Phenolic derivatives and other organic molecules were extracted from CSS in order to obtain a liquid fraction to be analysed by Gas Chromatography-Mass Spectrometry (GC-MS), FC and DPPH methods. Briefly, 1 g of solid sample was extracted with 20 mL of acetone 80% at pH 2, acidified with trifluoroacetic acid.

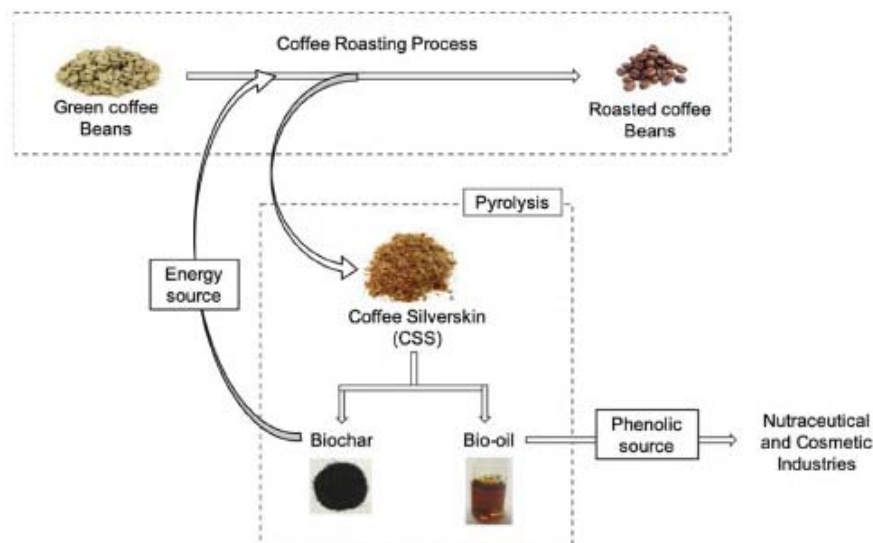


Fig. 1. Proposed integrated CSS biorefinery.

Extraction was performed at 30 rpm for 3 h using a rotary mixer. The solid was then filtered and the filtrate was added to a 25 mL volumetric flask and made up to the mark with acetone 80%. The extraction method was adapted from the one described by Marina et al., (2008).

2.5. Analytical methods for bio-oils and CSS extract characterisation

2.5.1. pH determination

pH of bio-oils was determined using a pH electrode (solventrode) with LiCl (2 mol/L) for non-aqueous media purchased from Metrohm (Switzerland).

2.5.2. GC–MS analysis

Chemical characterisation of bio-oils and CSS extract was performed by GC–MS analysis. GC–MS was carried out in a HP 6890 Series II gas chromatograph coupled to a HP 5973 mass selective detector from Agilent (USA) and equipped with a capillary ZB-5 column (30 m × 0.25 mm inner diameter × 0.25 μm film thickness) from Phenomenex (USA). Before injection, samples were filtered (0.45 μm Millipore filter) to avoid obstruction of liner due to some ash resting after pyrolysis. A volume of 1 μL was then injected, applying 1:7 split mode with the injection port at 300 °C and a syringe of 10 μL. Helium was used as carrier gas with a flow of 0.9 mL/min. The oven temperatures were as follows: 45 °C for 1 min, 8 °C/min to 200 °C, 15 °C/min to 310 °C and 310 °C for 10 min. The total run time was 37.71 min. This method was adapted from the one described by Artigues et al., (2014). Compounds were identified from the chromatograms by computer matching of mass spectra of the peaks with the National Institute of Standards and Technology (NIST) library.

2.5.3. Folin–Ciocalteu method

The FC method was used to determine the total phenolic content of bio-oils and CSS extract. This method, based on the antioxidant ability of phenolic molecules to reduce the FC reagent to spectrophotometrically detectable complexes (Magalhães et al., 2008), was performed using Lambda 45 UV/Vis Spectrometer from Perkin Elmer (USA). Bio-oils and CSS extract were filtrated and acidified to pH 4 with trifluoroacetic acid. Bio-oils were then

diluted in distilled water to obtain the following concentrations: 0.02 mg/mL for 280 °C bio-oil and 0.05 mg/mL for 400 °C and 500 °C bio-oils. CSS extracts were analysed without further dilution. In brief, 0.5 mL of sample was mixed with 2.5 mL of distilled water. Then, 0.25 mL of FC reagent was added, and the contents were mixed and left to react for 3 min. After this time, 1.75 mL of Na₂CO₃ (2 g/L) was added. The mixture was incubated at room temperature for 90 min and absorbance was then measured at 765 nm using distilled water as blank. Total phenolic content was calculated from a calibration curve prepared with gallic acid (25–300 mg/L; $r = 0.9996$). The results were expressed as mg of gallic acid equivalents /g of CSS or bio-oil. All samples were prepared three times. The FC method was adapted from the one described by Ivanova et al., (2010).

2.5.4. DPPH assay

DPPH assay evaluated the radical scavenging ability of antioxidant substances (phenolics) toward DPPH• radical (Marina et al., 2008). Bio-oils and CSS extract were analysed according to the method described by Marina et al., (2008) with some modifications. As in the FC method, the samples were previously filtrated and acidified to pH 4 with trifluoroacetic acid. They were then diluted in acetone 80% as follows: CSS extract (1:6); 280 °C bio-oil (1:500); and 400 °C and 500 °C bio-oils (1:300). Briefly, 2.5 mL of sample was mixed with 2.5 mL of a freshly prepared DPPH solution (500 μM in acetone 80%). The mixture was then left to react out of light for 30 min at room temperature. After this time, absorbance was read at 520 nm against acetone 80% as the blank, using a Lambda 45 UV/Vis Spectrometer from Perkin Elmer (USA). The results were expressed as mg of gallic acid equivalents/g of CSS or bio-oil by interpolation in gallic acid standard curve (10–150 μM in acetone 80%, $r = 0.9973$). All samples were prepared three times.

3. Results and discussion

3.1. Characterisation of CSS

CSS, the single residue from the coffee roasting process, was used as feedstock for the pyrolysis process. This waste is mainly

composed of cellulose (17.8%), hemicellulose (13.1%), proteins (18.6%) and, to a lesser extent, lignin (1%) (Murthy and Madhava Naidu, 2012). CSS has $30.13 \pm 1.2\%$ (w/w) moisture content and $7.78 \pm 0.12\%$ (w/w) ash content (mean of three measurements \pm standard deviation). The high moisture value implies that feedstock needs to be dried before the thermochemical process. Water removal also helps to preserve CSS from biological degradation.

Inorganic composition of CSS and CSS ash was analysed by ICP-MS, potassium being by far the most abundant inorganic element, with a concentration of 27 mg/g in CSS and 316 mg/g in CSS ashes. This means CSS ash could be used as fertilizer. The high content of this metal can be related to the fact that the main mineral in green coffee beans is potassium (Clarke and Walker, 1974). Other metals with a notable presence in CSS and CSS ash were calcium and magnesium. Specifically, CSS contains 7 mg/g of calcium and 3 mg/g of magnesium and CSS ashes, 85 mg/g of calcium and 26 mg/g of magnesium. The concentration of metals, which could be potentially dangerous in their combustion, are therefore low in CSS and CSS ash. Full ICP-MS results are available as supplementary information.

3.1.1. Thermogravimetric analysis (TGA)

Thermal decomposition of CSS was first studied by TGA to determine the operating temperature of the process.

As shown in Fig. 2, TGA analysis presented two main losses of weight. The first, around 260 °C (2), was mainly attributed to hemicellulose decomposition, and the second, around 310 °C (3), to cellulose degradation. These results are in line with those reported by Polidoro et al. (2018) in their study of CSS pyrolysis. The loss of weight mainly related to lignin decomposition (4) was very low due to the low lignin content of the sample (1%, w/w) (Murthy and Madhava Naidu, 2012). In order to study the degradation of the main components of CSS and the products obtained from it, the thermochemical treatment was performed at 280 °C, 400 °C and 500 °C. The first temperature corresponds to almost complete degradation of hemicellulose; 400 °C refers to practically total cellulose decomposition; and 500 °C is attributed to almost the end of CSS biomass degradation. The bio-oils and biochars resulting from the thermochemical treatment of CSS were studied focusing on their respective uses as chemical

and energy sources, with the aim of valorising CSS under an integrated biorefinery.

3.2. Characterisation of Bio-oils and CSS extract

Bio-oils from the intermediate pyrolysis of CSS have been studied and characterised in order to determine their potential use as a source of chemicals, mainly phenolic compounds. The pyrolysis treatment was performed at 280 °C, 400 °C and 500 °C, resulting in bio-oils composed of a single aqueous phase and, in the case of 400 °C and 500 °C bio-oils, suspended solids. In this type of pyrolysis, bio-oils usually separate in an aqueous phase and a non-aqueous phase due to the high amount of reaction water generated in the thermochemical process (Torri and Fabbri, 2014). The aqueous phase is mostly composed of hydrophilic products from hemicellulose and cellulose degradation, while the non-aqueous phase mainly contains hydrophobic compounds from lignin decomposition. In this case, the low lignin content of CSS (1%, w/w) (Murthy and Madhava Naidu, 2012) caused the phase separation not to take place.

3.2.1. pH

Bio-oils typically have acid pH (2.0 – 3.0) due to the presence of low molecular weight carboxylic acids, mainly acetic acid (Diebold, 2002; García-Pérez et al., 2002; Mohan et al., 2006). However, in 400 °C and 500 °C CSS bio-oils, pH was unusually basic (see Table 1). This could be related to the presence of caffeine and nitrogen compounds in the bio-oils. On one hand, caffeine (pKa = 14) could neutralise the acetic acid of bio-oils, increasing pH. On the other hand, 400 °C and 500 °C bio-oils are particularly rich in nitrogen compounds, which are generally basic and, consequently, increase even more the pH (see Fig. 3). Polidoro et al. (2018) also observed high content of nitrogen compounds in 560 °C CSS bio-oil.

3.2.2. Chemical characterisation of bio-oils and CSS extract

Chemical composition of bio-oils and CSS extract was determined through GC-MS.

This method was used to semi-quantitatively identify compounds with boiling temperatures below 300 °C. The obtained results are discussed and summarized in the following sections,

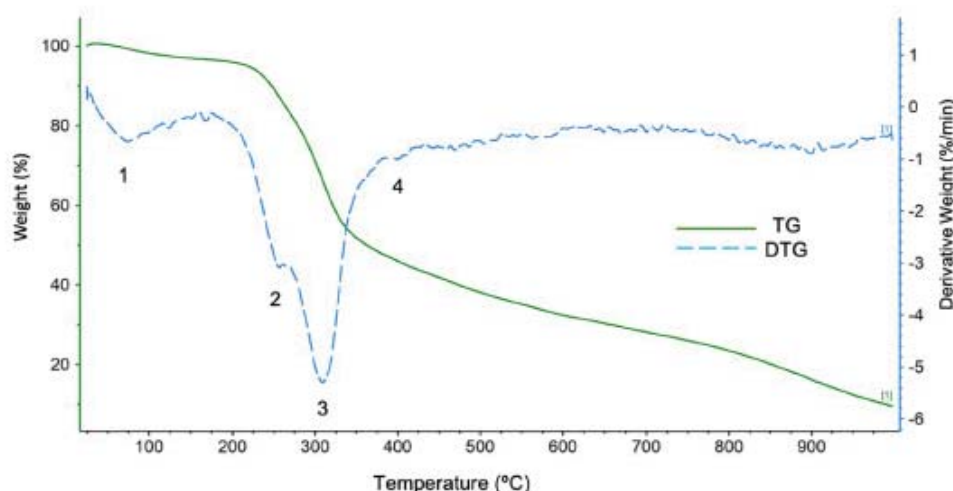


Fig. 2. Pyrolysis curves of CSS in TGA. The numbers correspond to the weight loss mainly associated to water loss (1), and to hemicellulose (2), cellulose (3) and lignin (4) decompositions, that took place around 260 °C, 310 °C and 400 °C, respectively. (TG, thermogravimetry; DTG, derivative thermogravimetry).

Table 1
pH data of bio-oils from the intermediate pyrolysis of CSS at 280 °C, 400 °C and 500 °C.

Bio-oil (AP)	pH
280 °C	4.3
400 °C	8.5
500 °C	8.1

although full information regarding the chromatograms and the compounds identified in them are available as supplementary information.

The results of GC–MS analysis showed that 280 °C, 400 °C and 500 °C bio-oils were mainly composed of caffeine, acetic acid and other low molecular weight oxygenated products, nitrogenated compounds and phenolic derivatives (see Fig. 3). Caffeine (23), the main product of CSS extract (see Fig. 4), was the major compound in all samples. Acetic acid (2) was the second most abundant product of bio-oils. Its presence is related to the decomposition of hemicellulose which gives rise to the acid as the main product (Mohan et al., 2006). The degradation of carbohydrates also resulted in compounds such as 1-hydroxy-2-propanone (1), 2-hydroxy-3-methyl-2-cyclopenten-1-one (12), 1,4:3,6-dianhydro- α -D-glucopyranose (17) and water, which was indeed the aqueous medium of bio-oils. Nitrogenated compounds derived mainly from the degradation of proteins, which takes place at around 400 °C (Russell et al., 1974). This group, which included pyridines (3), pyrroles (4) and amides (6, 11), was mostly present in 400 °C and 500 °C bio-oils, contributing to the basic pH of the samples (see Fig. 3 and Table 1). Phenolic derivatives were considered the most interesting compounds of bio-oils due to their antioxidant properties, making them highly value-added products. The results showed an increase of phenolics in bio-oils compared

to CSS extract (see Figs. 3 and 4). This was related to the degradation of fibre in the pyrolysis process, which released the phenolics linked in it. Specifically, 280 °C bio-oil presented the highest concentration in phenolic derivatives, such as 2-methoxyphenol (13), catechol (18), hydroquinone (19), 2,6-dimethoxyphenol (20) and 1-(4-hydroxy-3-methoxyphenyl)-2-propanone (22). This can be explained because, as temperature increases, part of the original phenolics can be degraded (Hamamat and Nawar, 1991). This behaviour differs to richer lignin samples, where at high temperatures, concentration of phenolics increases due to the degradation of lignin, which results in these antioxidant products (del Pozo et al., 2018). Phenolic compounds could be used in nutraceuticals and cosmetic industries as natural antioxidant sources (Murthy and Madhava Naidu, 2012). Caffeine, acetic acid and pyridine are also value-added products from CSS bio-oil. Caffeine is used in a wide array of beverages and pharmaceutical products for therapeutic purposes due to its stimulant effects on the nervous, muscular and cardiovascular systems (Cai et al., 2019; Cláudio et al., 2013; Rahimi et al., 2018); acetic acid is a chemical platform of high industrial demand (Zhao et al., 2017); and pyridine could be used as a precursor for many agrochemicals and pharmaceuticals (Parashar Pandey, 2018). It should be noted that these value-added products must be first separated and purified. A previous study by our research group showed that phenolic derivatives could be separated from bio-oil (del Pozo et al., 2018). This study consisted of an acid-base extraction with hexane at pH 12 followed by an ethyl acetate extraction at pH 6, where the phenolic derivatives were extracted in the ethyl acetate phase. If the extraction of antioxidants and other value-added compounds from bio-oil could not be performed at the time, bio-oil should be stored using stabilizers to avoid aging (Diebold, 2002; Oasmaa and Peacocke, 2001). On-going work on the separation of bio-oil compounds is being carried out and will be published in due course.

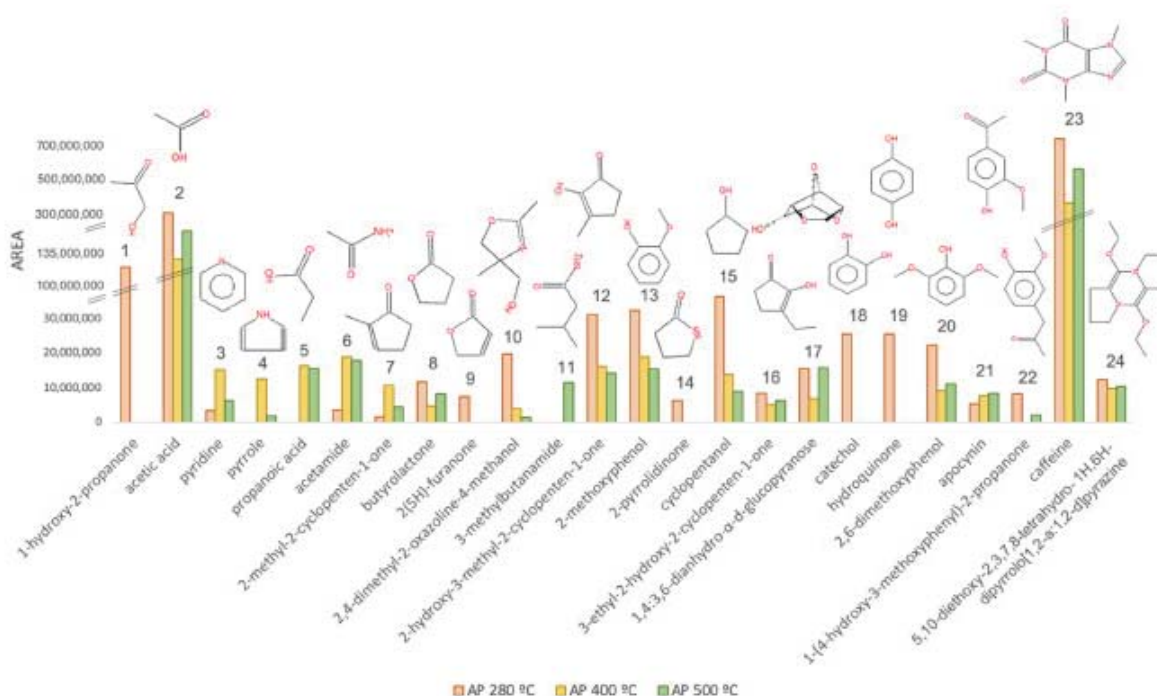


Fig. 3. Most abundant compounds of bio-oils from the intermediate pyrolysis of CSS at 280 °C, 400 °C and 500 °C, determined by GC–MS analysis.

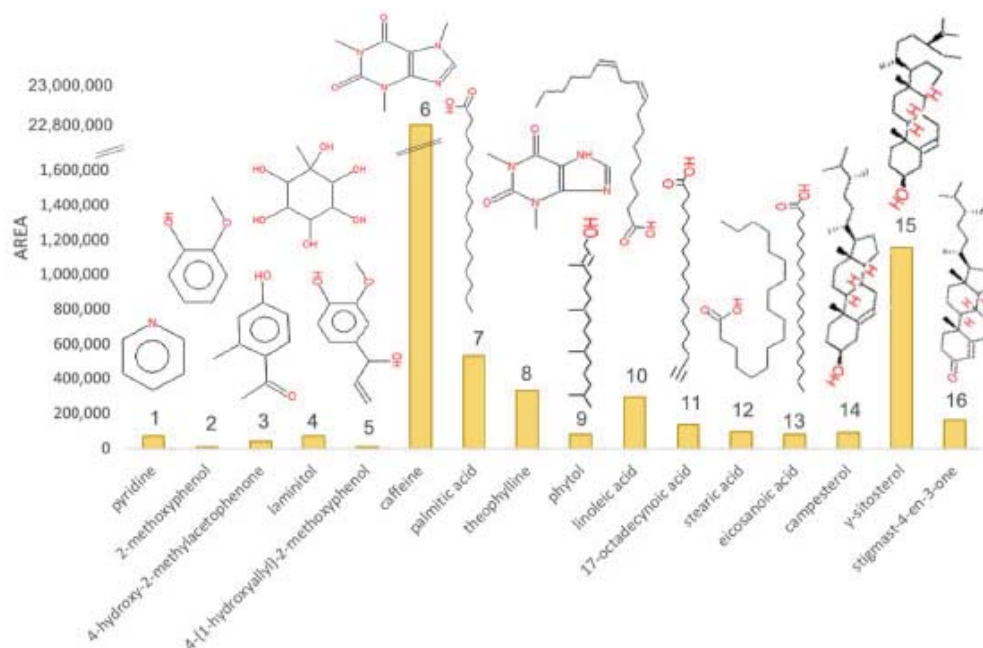


Fig. 4. Most abundant compounds of CSS extract determined by GC-MS analysis.

CSS extract was also analysed by GC-MS in order to compare its composition with that of the CSS bio-oils. As shown in Fig. 4, the main extracted products from CSS using acetone 80% at pH 2 were caffeine (6), fatty acids (7, 10, 11, 12, 13) and steroids (14, 15, 16). Phenolic compounds (2, 3, 5) were also extracted from CSS; however, part of them were linked to the CSS dietary fibre matrix through ester bonds, hindering their extraction (Brenes et al., 2015). The increase in phenolics in bio-oils compared to CSS extract (see Fig. 3) suggested that pyrolysis could be a suitable method for obtaining them by the degradation of fibre and hence the release of phenolics linked therein.

3.2.3. Measurement of phenolic content in CSS extract and bio-oils

Quantification of the phenolic content in CSS bio-oils is an essential step to evaluate bio-oils as a potential source of these antioxidant compounds. The measurement was performed by the FC method and DPPH assay, as complementary methods to the semi-quantitative information obtained from GC-MS analysis. The FC method measures the total phenolic content of the samples; and DPPH assay, its radical scavenging ability or antioxidant capacity, so these methods measure two properties that are closely related to the antioxidant capacity of bio-oils, which is mainly attributed to the presence of phenolic compounds (Borrelli et al., 2004).

The results obtained from the FC method and DPPH assay were in line with those observed in GC-MS analysis, revealing bio-oils to be a potential source of phenolic compounds (see Fig. 2). Moreover, these analyses corroborated that 280 °C was the best temperature tested to obtain a larger number of phenolic derivatives. As shown in Table 2, antioxidant capacity and total phenolic content decreased in 400 °C bio-oil and then remained quite constant at 500 °C bio-oil, due to the possible degradation of phenols at these temperatures (Hamamat and Nawar, 1991). It can also be observed that, in bio-oil samples, both FC and DPPH methods showed the same tendency, 400 °C and 500 °C bio-oils being at the same proportion between these methods, DPPH:FC (1.7:1).

Table 2

Analysis of the total phenolic content and antioxidant capacity of CSS extract and bio-oils from the intermediate pyrolysis of CSS at 280 °C, 400 °C and 500 °C by FC method and DPPH assay. Results were expressed as mg of gallic acid equivalents /g of CSS or bio-oil. The average values and standard deviations are shown as \bar{x} and s , respectively.

	FC method		DPPH assay	
	\bar{x}	s	\bar{x}	s
CSS (extract)	1.23	0.08	1.00	0.06
Bio-oil 280 °C	6.09	0.40	3.02	0.18
Bio-oil 400 °C	2.92	0.04	1.70	0.20
Bio-oil 500 °C	3.07	0.03	1.81	0.21

These results contrast with those obtained by Polidoro et al. (2018) in their study of the valorisation of CSS through pyrolysis. The researchers based their work on studying the best pyrolysis conditions to achieve the maximum yield of bio-oil, which was considered a potential source of phenolic compounds together with other chemical inputs. The study concluded that 560 °C was the optimal temperature to obtain the highest bio-oil yield; however, in the present study, it was observed that above 400 °C, part of the phenols degraded, 280 °C being the best temperature tested to obtain these value-added compounds. Bio-oils thus differ from richer lignin feedstocks, where phenolics also come from the degradation of lignin, which takes place at high temperatures (215–585 °C) (Zhao et al., 2017).

3.3. Biochars

The study and characterisation of CSS biochars was focused on their potential applicability as a source of energy. These solid fractions consisted of 280 °C, 400 °C and 500 °C biochars.

3.3.1. Elemental analysis and calorific value of CSS and CSS biochars.

Data obtained from the elemental analysis of CSS and biochars from the intermediate pyrolysis of CSS are shown in Table 3.

Table 3
Elemental analysis and calorific values of CSS and biochars from the intermediate pyrolysis of CSS at 280 °C, 400 °C and 500 °C. The average values and standard deviations are shown as \bar{x} and s , respectively. Elemental analysis is expressed as % (w/w) dry weight. (BC, biochar).

	CSS		BC 280 °C		BC 400 °C		BC 500 °C	
	\bar{x}	s	\bar{x}	s	\bar{x}	s	\bar{x}	s
%C	42.32	0.28	55.01	0.35	58.52	1.03	58.68	0.06
%H	5.69	0.20	4.76	0.16	2.80	0.04	2.39	0.06
%O*	48.87	0.53	36.63	0.49	35.71	1.06	36.12	0.02
%N	2.97	0.04	3.49	0.02	2.82	0.08	2.65	0.07
%S	0.17	0.02	0.13	0.01	0.16	0.01	0.17	0.08
LHV (MJ/kg)	16.73	0.03	21.96	0.96	23.08	0.16	21.09	0.50

*The oxygen content is calculated by difference.

Moreover, the calorific value of the samples was also measured to evaluate their potential use as solid biofuel.

Elemental analysis results showed an increase in carbon content and a decrease in oxygen content in biochars compared to CSS, indicating increased energy densities of biochars (Liu and Han, 2015). Table 3 also shows that the hydrogen content of biochars decreased when temperature is increased. This behaviour was related to dehydration reactions of mainly hemicellulose and cellulose during the pyrolysis process (Liu and Han, 2015). The rich hemicellulose-cellulose content of CSS could be corroborated by the polarity coefficient (O + N)/C, an important parameter inversely related with the aromatic character of the sample (Pujol et al., 2013). In this way, the polarity coefficient of CSS (0.93) was closer to the polarity range of cellulose (0.84–1.94) than to that of some commercial lignin (0.33–0.65) (Rodríguez-Cruz et al., 2007; Wang and Xing, 2007; Xing et al., 1994). Comparing biochars from different biomass, it is shown that carbon, oxygen and hydrogen content of 280 °C biochar is similar to biochar from orange peel at 250 °C – 350 °C (Santos et al., 2015), and similar to biochar from pine wood at 300 °C, regarding carbon and oxygen content (Liu and Han, 2015).

In reference to nitrogen content, CSS biochars presented higher %N values than biochars from coconut fibre, orange peel or pine wood (Liu and Han, 2015; Santos et al., 2015). The high amount of nitrogen (>2%) compared to other composting materials could promote the use of CSS biochars as compost (Preethu et al., 2007). It was also observed that nitrogen content decreased as temperature increased (see Table 3), a fact that was associated with the volatilisation of the nitrogenous compounds in the

thermochemical process, as already seen in pH and GC–MS analysis of bio-oils. In contrast, sulphur contents remained quite constant with an increase in temperatures (see Table 3). Although sulphur values were low, the combustion of biochars would produce sulphur oxide emissions, which would be similar to those of pine wood biochar (Liu and Han, 2015).

Calorific value analysis showed an increase of LHV in biochars compared to CSS where, as reported elsewhere, CSS can be used as solid biofuel (Borrelli et al., 2004) (see Table 3). Biochars also presented similar heating values in comparison with those of other fuels such as coal (14.6 – 26.7 MJ/kg) (Inguanzo et al., 2002; Sánchez et al., 2009), indicating the potential use of CSS biochars as solid biofuels. However, no significant differences were observed between CSS biochars. This can be attributed to the devolatilization of CSS biomass, which mainly takes place around 300 °C, due to it is mostly composed of hemicellulose and cellulose, having low lignin content that decomposes at higher temperatures (see Section 3.1.1.). In this way, pyrolysis of CSS could be performed at 280 °C, since working at higher temperatures to increase the LHV of biochars does not imply a significant improvement regarding the calorific value, which represents an energy saving in the pyrolysis process.

3.4. Integrated biorefinery of CSS

This study is focused on the integrated valorisation of CSS, the only by-product from the coffee roasting process, through pyrolysis-based biorefinery (see Fig 5).

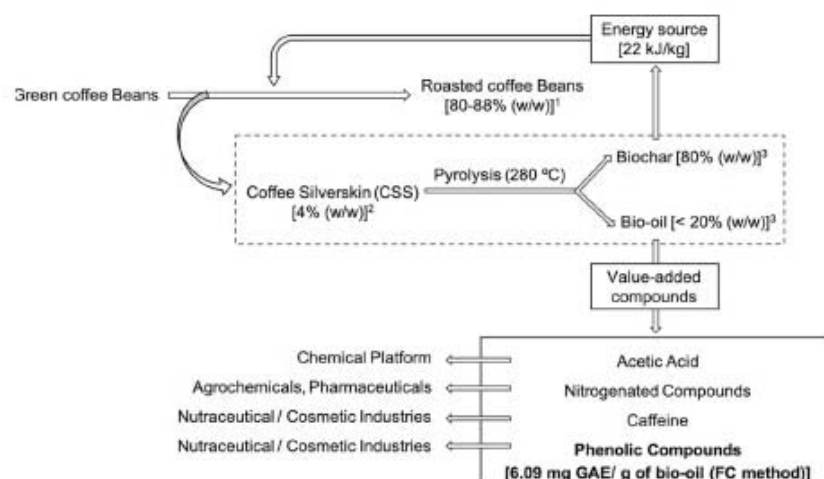


Fig. 5. Integrated biorefinery of CSS. (GAE, Gallic Acid Equivalents; FC, Folin-Ciocalteu). ¹ Pittia et al., *LWT - Food Sci. Technol.*, 2001, 34, 168–175. ² Polidoro et al., *J. Anal. Appl. Pyrolysis*, 2018, 129, 43–52. ³ Estimation from TGA data.

The coffee roasting process generates 80–88% (w/w) of roasted coffee beans and 4% (w/w) of CSS by-product (Pittia et al., 2001; Polidoro et al., 2018). Despite this small percentage, CSS production is approximately 0.4 Mt per year due to the high worldwide coffee consumption (International Coffee Organization, 2020; Polidoro et al., 2018). The remaining loss of weight is attributed to water and volatile removal during the roasting process (Pittia et al., 2001).

In the proposed integrated biorefinery (see Fig. 5), CSS is used as feedstock for the pyrolysis process, generating mainly biochar and bio-oil. The temperature of the process was determined to be 280 °C, based on the data obtained from bio-oil and biochar characterisation (Sections 3.2 and 3.3). At this temperature, about 80% (w/w) of biochar and < 20% (w/w) of bio-oil is expected (estimated values from TGA data).

As previously discussed (Section 3.3), biochar is a potential source of energy that could be used in the coffee roasting process itself (see Fig. 5). As shown in Section 3.3, biochar presented significant calorific values (up to 21 MJ/kg), as well as low sulphur content (0.13–0.17% w/w), which would lead to low sulphur oxide emissions in biochar combustion. Specifically, 280 °C biochar generates 22 MJ/kg of energy. Apart from solid biofuel, biochar could also be used as composting material or fertilizer due to its high amount of nitrogen (>2%) and potassium (316 mg/g in CSS ashes), respectively.

The resulting bio-oil is shown to be a potential source of chemicals, mainly phenolics (see Fig. 5). These compounds are highly valued in nutraceuticals and cosmetic industries as natural antioxidant sources (Murthy and Madhava Naidu, 2012), so their obtention is of great interest. As discussed in Section 3.2, 280 °C pyrolysis is a suitable method to obtain them by breaking the bonds that link phenolics to CSS fibre (Borrelli et al., 2004). Hence, this represents a more efficient method than traditional extractions, such as mechanical agitation using aqueous-organic solvents, which are not able to break these bonds (Brenes et al., 2015). Taking into account the global coffee production per year and the FC results, polyphenolics have the potential to represent up to 487 tones of gallic acid equivalents annually. Regarding the antioxidant capacity, it would represent 242 tones of gallic acid equivalents per year, calculated from the DPPH results. Caffeine, acetic acid and nitrogenated compounds are also value-added products from CSS bio-oil. As shown in Fig. 5, caffeine can be used in nutraceutical industries; acetic acid is a chemical platform; and nitrogenated compounds could be used in agrochemicals and pharmaceutical industries (Cai et al., 2019; Cláudio et al., 2013; Parashar Pandey, 2018; Rahimi et al., 2018). It should be noted that these compounds must be separated from the bio-oil prior to use (see Section 3.2.2).

The present proposal would therefore provide an integrated biorefinery perspective to the coffee roasting industry, coming closer to a zero waste concept, as well as contributing to the circular economy and bioeconomy. This strategy (see Fig. 5) represents greener waste management of CSS than waste disposal, and also significant energy savings by revalorising CSS in the coffee roasting industry itself.

4. Conclusions

This study shows intermediate pyrolysis to be a potential process for the integrated valorisation of CSS under a biorefinery approach. The best pyrolysis temperature tested was 280 °C to obtain greater value-added products. On the one hand, the resulting bio-oil (<20% (w/w)) has been shown to be a potential source of chemicals. This fraction is composed of value-added products such as acetic acid, nitrogenated compounds, caffeine and phenolics.

Phenolics are of special interest due to their antioxidant properties and, consequently, their high-added value. Considering the global coffee production per year and the FC results, polyphenolics have the potential to represent up to 487 tones of gallic acid equivalents annually. Additionally, the antioxidant capacity would represent 242 tones of gallic acid equivalents per year, calculated from the DPPH results. On the other hand, biochar (80% (w/w)) represents a potential energy source that can be used in the coffee roasting process itself, thus contributing to the circular economy. Biochar presents significant calorific values (up to 21 MJ/kg), together with low metal and sulphur content (0.13% w/w), involving low environmental emissions from its combustion. This study deals with the use of CSS, a waste produced by the coffee roasting industry, which can be transformed and reused through a biorefinery approach. It therefore converts a waste into a by-product and a resource, which increases the environmental benefits and contributes to the circular economy and the bioeconomy. Future projects include further work on the separation and purification of bio-oil compounds and other potential uses of biochar from CSS.

Declaration of Competing Interest

The authors declare that they have no known competing financial interests or personal relationships that could have appeared to influence the work reported in this paper.

Acknowledgements

This study was produced with support from the ENER-G-bas company, which provided the bio-oils and biochars. N. Puy is grateful for funding from the Torres Quevedo subprogram of the Spanish Ministry of Economy and Competitiveness (PTQ-15-08063). C. del Pozo expresses her gratitude to the Universitat Autònoma de Barcelona for funding her PhD contract through a PIF grant, as well as the financial support from the MINECO-FEDER through project CTQ2017-85011-R. The authors are also grateful to Mireia Mora for her collaboration with the presented study.

Appendix A. Supplementary data

Supplementary data to this article can be found online at <https://doi.org/10.1016/j.wasman.2020.04.044>.

References

- Artigues, A., Puy, N., Bartró, J., Fàbregas, E., 2014. Comparative Assessment of Internal Standards for Quantitative Analysis of Bio-oil Compounds by Gas Chromatography / Mass Spectrometry Using Statistical Criteria. *Energy Fuels* 28, 3908–3915. <https://doi.org/10.1021/ef500554s>.
- Borrelli, R.C., Esposito, F., Napolitano, A., Ridenti, A., Fogliano, V., 2004. Characterization of a New Potential Functional Ingredient: Coffee Silverskin. *J. Agric. Food Chem.* 52, 1338–1343. <https://doi.org/10.1021/jf034974x>.
- Brenes, A., Viveros, A., Chamorro, S., Arija, I., 2015. Use of polyphenol-rich grape by-products in monogastric nutrition: A review. *Anim. Feed Sci. Technol.* <https://doi.org/10.1016/j.anifeeds.2015.09.016>.
- Bresciani, L., Calani, L., Bruni, R., Brighenti, F., Del Rio, D., 2014. Phenolic composition, caffeine content and antioxidant capacity of coffee silverskin. *Food Res. Int.* 61, 196–201. <https://doi.org/10.1016/j.foodres.2013.10.047>.
- Cai, C., Li, F., Liu, L., Tan, Z., 2019. Deep eutectic solvents used as the green media for the efficient extraction of caffeine from Chinese dark tea. *Sep. Purif. Technol.* 227. <https://doi.org/10.1016/j.seppur.2019.115723>.
- Clarke, R.J., Walker, L.J., 1974. Potassium and Other Mineral Contents of Green, Roasted and Instant Coffees. *J. Sci. Food Agric.* 25, 1389–1404. <https://doi.org/10.1002/jsfa.2740251107>.
- Cláudio, A.F.M., Ferreira, A.M., Freire, M.G., Coutinho, J.A.P., 2013. Enhanced extraction of caffeine from guaraná seeds using aqueous solutions of ionic liquids. *Green Chem.* 15, 2002–2010. <https://doi.org/10.1039/c3gc40437d>.
- del Pozo, C., Bartró, J., Puy, N., Fàbregas, E., 2018. Separation of value-added chemical groups from bio-oil of olive mill waste. *Ind. Crops Prod.* 125. <https://doi.org/10.1016/j.indcrop.2018.08.062>.

- Diebold, J.P., 2002. A Review of the chemical and physical mechanisms of the storage stability of fast pyrolysis bio-oils. In: Bridgewater, A.V. (Ed.), *Fast Pyrolysis of Biomass: A Handbook*. CPL Press, Newbury, UK, p. 424.
- Digman, B., Kim, D.-S., 2008. Review: Alternative Energy from Food Processing Wastes. *Environ. Prog.* 27, 524–537. <https://doi.org/10.1002/ep>.
- García-Pérez, M., Chaala, A., Roy, C., 2002. Vacuum pyrolysis of sugarcane bagasse. *J. Anal. Appl. Pyrolysis* 65, 111–136. [https://doi.org/10.1016/S0165-2370\(01\)00184-X](https://doi.org/10.1016/S0165-2370(01)00184-X).
- Goyal, H.B., Seal, D., Saxena, R.C., 2008. Bio-fuels from thermochemical conversion of renewable resources: A review. *Renew. Sustain. Energy Rev.* 12, 504–517. <https://doi.org/10.1016/j.rser.2006.07.014>.
- Hamamat, A.A., Nawar, W.W., 1991. Thermal Decomposition of Some Phenolic Antioxidants. *J. Agric. Food Chem.* 39, 1063–1069.
- Iakovou, E., Karagiannidis, A., Vlachos, D., Toka, A., Malamakis, A., 2010. Waste biomass-to-energy supply chain management: A critical synthesis. *Waste Manag.* 30, 1860–1870. <https://doi.org/10.1016/j.wasman.2010.02.030>.
- Inguanzo, M., Domínguez, A., Menéndez, J.A., Blanco, C.G., Pis, J.J., 2002. On the pyrolysis of sewage sludge: The influence of pyrolysis temperature on biochar, liquid and gas fractions. *J. Anal. Appl. Pyrolysis* 63, 209–222. <https://doi.org/10.4028/www.scientific.net/AMR518-523.3412>.
- International Coffee Organization, 2020. World coffee consumption [WWW Document]. URL <http://www.icao.org/prices/new-consumption-table.pdf> (accessed 3.15.20).
- Ivanova, V., Stefova, M., Chinnici, F., 2010. Determination of the polyphenol contents in Macedonian grapes and wines by standardized spectrophotometric methods. *J. Serbian Chem. Soc.* 75, 45–59. <https://doi.org/10.2298/JSC1001045I>.
- Liu, Z., Han, G., 2015. Production of solid fuel biochar from waste biomass by low temperature pyrolysis. *FUEL* 158, 159–165. <https://doi.org/10.1016/j.fuel.2015.05.032>.
- Magalhães, L.M., Segundo, M.A., Reis, S., Lima, J.L.F.C., 2008. Methodological aspects about in vitro evaluation of antioxidant properties. *Anal. Chim. Acta* 613, 1–19. <https://doi.org/10.1016/j.aca.2008.02.047>.
- Marina, D., Avela, G., Alberto, C., García, O., Cisneros, A.M., 2008. Medición de Fenoles y Actividad Antioxidante en Malezas Usadas para Alimentación Animal. *Simp. Metrol.*, 1–5.
- Mohan, D., Pittman, C.U., Steele, P.H., 2006. Pyrolysis of wood/biomass for bio-oil: A critical review. *Energy and Fuels* 20, 848–889. <https://doi.org/10.1021/ef0502397>.
- Murthy, P.S., Madhava Naidu, M., 2012. Sustainable management of coffee industry by-products and value addition - A review. *Resour. Conserv. Recycl.* 66, 45–58. <https://doi.org/10.1016/j.resconrec.2012.06.005>.
- Narita, Y., Kuniyo, I., 2014. Review on utilization and composition of coffee silverskin. *Food Res. Int.* 61, 16–22. <https://doi.org/10.1016/j.foodres.2014.01.023>.
- Nisar, J., Ali, F., Malana, M.A., Ali, G., Iqbal, M., Shah, A., Bhatti, I.A., Khan, T.A., Rashid, U., 2019. Kinetics of the pyrolysis of cobalt-impregnated sesame stalk biomass. *Biomass Convers. Biorefinery*. <https://doi.org/10.1007/s13399-019-00477-3>.
- Nisar, J., Ullah, N., Awan, I.A., Iqbal, M., Khan, T.A., 2016. Pyrolysis-Gas Chromatography of Sugar Beet Bagasse. *Waste and Biomass Valorization* 7, 79–85. <https://doi.org/10.1007/s12649-015-9438-4>.
- Oasmaa, A., Peacocke, C., 2001. A guide to physical property characterisation of biomass-derived fast pyrolysis liquids. Technical Research Centre of Finland, Espoo.
- Parashar Pandey, P., Parashar Pandey, 2018. PyridinePyridine. In: *Pyridine*. IntechOpen, London, p. 3.
- Pittia, P., Dalla Rosa, M., Lerici, C.R., 2001. Textural Changes of Coffee Beans as Affected by Roasting Conditions. *LWT - Food Sci. Technol.* 34, 168–175. <https://doi.org/10.1006/food.2000.0749>.
- dos Polidoro, A., Scapin, S., Lazzari, E., Silva, A.N., dos Santos, A.L., Caramao, E.B., Jacques, R.A., 2018. Valorization of coffee silverskin industrial waste by pyrolysis: From optimization of bio-oil production to chemical characterization by GC × GC / qMS. *J. Anal. Appl. Pyrolysis* 129, 43–52. <https://doi.org/10.1016/j.jaap.2017.12.005>.
- Preethu, D.C., Prakash, B.N.U.H.B., Srinivasamurthy, C.A., Vasanthi, B.G., 2007. Maturity Indices as an Index to Evaluate the Quality of Compost of Coffee Waste Blended with Other Organic Wastes. *Proc. Int. Conference Sustain. Solid Waste Manag. Sept. 5–7, Chennai, India*, 270–275.
- Pujol, D., Liu, C., Gominho, J., Olivella, M.A., Fiol, N., Villalascusa, I., Pereira, H., 2013. The chemical composition of exhausted coffee waste. *Ind. Crop. Prod.* 50, 423–429. <https://doi.org/10.1016/j.indcrop.2013.07.056>.
- Rahimi, A., Zanjanchi, M.A., Bakhtiari, S., Dehsaraei, M., 2018. Selective determination of caffeine in foods with 3D-graphene based ultrasound-assisted magnetic solid phase extraction. *Food Chem.* 262, 206–214. <https://doi.org/10.1016/j.foodchem.2018.04.035>.
- Recari, J., Berruoco, C., Puy, N., Alier, S., Bartroli, J., Farriol, X., 2017. Torrefaction of a solid recovered fuel (SRF) to improve the fuel properties for gasification processes. *Appl. Energy* 203, 177–188. <https://doi.org/10.1016/j.apenergy.2017.06.014>.
- Rodríguez-Cruz, S., Andrades, M.S., Sánchez-Camazano, M., Sánchez-Martín, M.J., 2007. Relationship between The Adsorption Capacity of Pesticides by Wood Residues and The Properties of Woods and Pesticides. *Environ. Sci. Technol.* 41, 3613–3619. <https://doi.org/10.1021/es062616f>.
- Russell, J.D., Fraser, A.R., Watson, J.R., Parsons, J.W., 1974. Thermal decomposition of protein in soil organic matter. *Geoderma* 11, 63–65.
- Sánchez, M.E., Lindao, E., Margaleff, D., Martínez, O., Morán, A., 2009. Pyrolysis of agricultural residues from rape and sunflowers: Production and characterization of bio-fuels and biochar soil management. *J. Anal. Appl. Pyrolysis* 85, 142–144. <https://doi.org/10.1016/j.jaap.2008.11.001>.
- Santos, C.M., Dweck, J., Viotto, R.S., Rosa, A.H., de Moraes, L.C., 2015. Application of orange peel waste in the production of solid biofuels and biosorbents. *Bioresour. Technol.* 196, 469–479. <https://doi.org/10.1016/j.biortech.2015.07.114>.
- Sluiter, A., Hames, B., Ruiz, R., Scarlata, C., Skuter, J., Templeton, D., 2008. Determination of ash in biomass. NREL Laboratory Analytical Procedure (LAP). *Natl. Renew. Energy Lab.* 18.
- Torri, C., Fabbri, D., 2014. Biochar enables anaerobic digestion of aqueous phase from intermediate pyrolysis of biomass. *Bioresour. Technol.* 172, 335–341. <https://doi.org/10.1016/j.biortech.2014.09.021>.
- Wang, X., Xing, B., 2007. Importance of structural makeup of biopolymers for organic contaminant sorption. *Environ. Sci. Technol.* 41, 3559–3565. <https://doi.org/10.1021/es062589t>.
- Xing, B., McGill, W.B., Dudas, M.J., 1994. Cross-Correlation of Polarity Curves To Predict Partition Coefficients of Nonionic Organic Contaminants. *Environ. Sci. Technol.* 28, 1929–1933. <https://doi.org/10.1021/es00060a025>.
- Zabanitou, A., Kamaterou, P., Pavlou, A., Panayiotou, C., 2018. Sustainable bioeconomy transitions: Targeting value capture by integrating pyrolysis in a winery waste biorefinery. *J. Clean. Prod.* 172, 3387–3397. <https://doi.org/10.1016/j.jclepro.2017.11.077>.
- Zhao, C., Jiang, E., Chen, A., 2017. Volatile production from pyrolysis of cellulose, hemicellulose and lignin. *J. Energy Inst.* 90, 902–913. <https://doi.org/10.1016/j.joei.2016.08.004>.

2.4 Article IV

Converting coffee silverskin to value-added products by a slow pyrolysis-based biorefinery process

Cristina del Pozo ^{a,*}, Filipe Rego ^c, Yang Yang ^{c,*}, Neus Puy ^{a,b}, Jordi Bartrolí ^a, Esteve Fàbregas ^a, Anthony V. Bridgwater ^c

^a Department of Chemistry, Universitat Autònoma de Barcelona (UAB), Edifici Cn, Campus de la UAB, 08193 Cerdanyola del Vallès, Barcelona, Spain.

^b Forest Science and Technology Centre of Catalonia (CTFC), Crta. Sant Llorenç de Morunys, km 2, 25280 Solsona, Lleida, Spain

^c Bioenergy Research Group, EBRI, Aston University, Birmingham B4 7ET, United Kingdom

* Corresponding author: Cristina.DelPozo@uab.cat (C. del Pozo), y.yang6@aston.ac.uk (Y. Yang).

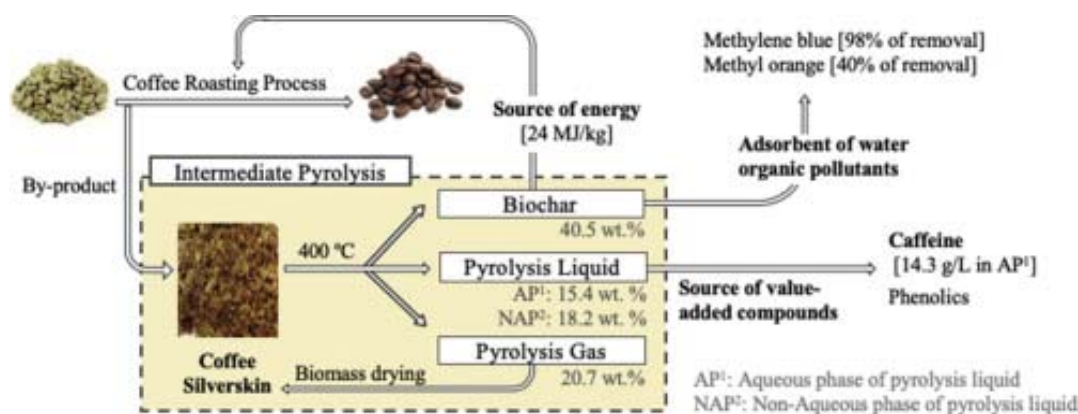


Figure 14. Graphical abstract of the article IV.

Journal: Fuel Process. Technol.

Volume 214, 106708

<https://doi.org/10.1016/j.fuproc.2020.106708>

April 2021



Converting coffee silverskin to value-added products by a slow pyrolysis-based biorefinery process

Author:

Cristina del Pozo, Filipe Rego, Yang Yang, Neus Puy, Jordi Bartrolí, Esteve Fàbregas, Anthony V. Bridgwater

Publication: Fuel Processing Technology

Publisher: Elsevier

Date: April 2021

© 2020 Elsevier B.V. All rights reserved.

Journal Author Rights

Please note that, as the author of this Elsevier article, you retain the right to include it in a thesis or dissertation, provided it is not published commercially. Permission is not required, but please ensure that you reference the journal as the original source. For more information on this and on your other retained rights, please visit: <https://www.elsevier.com/about/our-business/policies/copyright#Author-rights>

BACK

CLOSE WINDOW



Contents lists available at ScienceDirect

Fuel Processing Technology

journal homepage: www.elsevier.com/locate/fuproc

Research article

Converting coffee silverskin to value-added products by a slow pyrolysis-based biorefinery process

Cristina del Pozo^{a,*}, Filipe Rego^c, Yang Yang^{c,*}, Neus Puy^{a,b}, Jordi Bartrolí^a, Esteve Fàbregas^a, Anthony V. Bridgwater^c

^a Department of Chemistry, Universitat Autònoma de Barcelona (UAB), Edifici Cn, Campus de la UAB, 08193 Cerdanyola del Vallès, Barcelona, Spain

^b Forest Science and Technology Centre of Catalonia (CTFC), Crta. Sant Llorenç de Morunys, km 2, 25280 Solsona, Lleida, Spain

^c Bioenergy Research Group, EBRI, Aston University, Birmingham B4 7ET, United Kingdom



ARTICLE INFO

Keywords:

Coffee silverskin
Slow pyrolysis
Pyrolysis liquid
Biochar
Adsorption
Caffeine

ABSTRACT

This work aims to transform coffee silverskin (CSS), the only waste from the coffee roasting process, that worldwide amounts to about 76 million kg/year, into value-added products within an integrated slow pyrolysis process. The study, performed at 280 °C, 400 °C and 500 °C, determined the potential applications of the resulting fractions. Biochar has been studied as an adsorbent of organic pollutants in water, using methylene blue (MB) and methyl orange (MO), which are respectively cationic and anionic aromatic dyes, as model compounds, and with 400 °C biochar giving the highest removal values, at 98% with MB and 40% with MO. Moreover, CSS biochar could be used to obtain renewable energy from its combustion, with 22.6–24.2 MJ/kg calorific values. The liquid fraction could be a potential source of caffeine, among phenolics, with 400 °C aqueous phase presenting the highest concentration of caffeine (14.3 g/L). Concerning the gas fraction, it could be used to obtain heat for biomass drying before pyrolysis. Hence, use of the pyrolysis products as described would allow zero-waste to be achieved in the coffee roasting industry, thus promoting the green and circular economy and production of green chemicals and materials in a biorefinery context.

1. Introduction

Coffee is one of the most commonly consumed beverages worldwide [1]. The roasted coffee beans are produced in the coffee consuming countries from the roasting process of green coffee beans [2], which are cultivated and imported from tropical areas. Specifically, the most coffee consuming regions are EU, USA and Brazil, with around 2.8, 1.6 and 1.3 billion kg consumed in 2018/19 season respectively. From the roasting process, it is obtained 84 wt% of roasted coffee and around 0.75 wt% of coffee silverskin (CSS), which is the protective skin of beans that shed during the process [1,3]. CSS is the only by-product from the coffee roasting process, but it is generated on a large scale [4], amounting to about 76 million kg per year since at least 2016 [1,5]. CSS is composed by a high amount of dietary fibre (56–62%); it contains cellulose (18%), hemicellulose (13%) and it is also rich in protein (19%) and minerals (8% ash) [6]. Nowadays, most CSS is discarded and often used as fire-lighters or dispatched to landfills [1,7], representing a serious environmental problem due to the phytotoxicity of this waste as a result of its

high content of caffeine, polyphenols, and tannins [8]. Therefore, it is necessary to look for greener waste management alternatives, by converting the residue to a resource and complying with green solutions and circular economy (zero waste approach).

Pyrolysis is a widely used treatment to transform biomass into value-added products. This treatment, performed at elevated temperatures in the absence (or limited concentration) of oxygen, decomposes the main polymers of biomass (hemicellulose, cellulose and lignin) into liquid, gas and solid fractions [9]. The pyrolysis liquid and gas fractions could be used as chemical and energy sources respectively, whereas the solid fraction (biochar) could be considered as a value-added product itself due to the broad range of applications it has. Hence, this work uses pyrolysis to completely valorise CSS, aiming to reach zero-waste in the coffee roasting industry. Specifically, the treatment performed was slow pyrolysis in a lab-scale reactor with a capacity of 0.3 kg/h at 280 °C, 400 °C and 500 °C, with temperature being one of the main factors influencing the properties and proportion of the products.

However, and to the best of our knowledge, only a few papers have

* Corresponding authors.

E-mail addresses: Cristina.DelPozo@uab.cat (C. del Pozo), y.yang6@aston.ac.uk (Y. Yang).

<https://doi.org/10.1016/j.fuproc.2020.106708>

Received 17 September 2020; Received in revised form 12 November 2020; Accepted 9 December 2020

Available online 6 January 2021

0378-3820/© 2020 Elsevier B.V. All rights reserved.

been addressed on the pyrolysis of CSS and the valorisation of the resulting products. Polidoro et al. [8] optimised the pyrolysis process (slow pyrolysis) focusing on the pyrolysis liquid yield and its use as source of chemicals. On the other hand, a previous study from our research group [10] regarded the valorisation of CSS by slow pyrolysis in a pilot plant with a capacity of 15 kg/h, based mainly on pyrolysis liquid as a source of phenolics, and biochar as a solid fuel. There is not yet a detailed study of all CSS pyrolysis products, information that would allow to determine their potential applications.

In this sense, biochar has been attracting increasing attention due to its versatility and environmental benefits [11], with large number of studies highlighting its use in terms of mitigating global warming by means of carbon sequestration [12], and as a soil amendment to enhance crop yields [13–15]. Several studies also reported that biochar showed excellent ability to remove contaminants such as heavy metals and organic pollutants from water [13,15,16], since it can present large specific surface area, porous structure, abundant surface functional groups and mineral components, which suggests its use as a contaminant adsorbent [11,15,17]. The continuous development of industry and agriculture in recent years has increased the level of pollutants in the environment, seriously threatening ecology and human health [11,18]. Of the many ways to remove dissolved water contaminants, adsorption is widely considered to be superior to other processing technologies in terms of cost, viability and effectiveness [11,19,20]. Hence, the role of biochar as an adsorbent has gained attention mainly due to its low-cost, high-efficiency and renewable characteristics [11]. A large number of researchers also showed that biochar can have good adsorption of polycyclic aromatic hydrocarbons [21], herbicides [22], pesticides [17], antibiotics [23] and dyes [24], recently becoming a research hotspot in the environmental science field [11].

Based on the above, this work has studied the properties of CSS biochar as an adsorbent of organic pollutants in aqueous media. The study has been carried out using methylene blue (MB) and methyl orange (MO) as model compounds [25] in order to assess the adsorption performance of CSS biochar. MB and MO are respectively cationic and anionic aromatic dyes that may present same adsorption mechanisms on CSS biochar as other contaminants with similar structures. Some of these mechanisms can include electrostatic and aromatic π - π interactions, hydrogen bonds, and pore-filling [13]. Apart from their function as model adsorbates, MB and MO are also extensively used in fabric staining [20,26]. With the rapid development of the textile industry, dye effluents account for a large proportion of industrial wastewater, and have become a significant source of pollution [11], organic dyes being well known as toxic and carcinogenic substances [20]. Hence, the evaluation of the removal efficiency of MB and MO by CSS biochar is in itself of great interest. The use of CSS biochar as an adsorbent could protect the environment by both removing pollutants from water and improving the waste management of CSS. In order to increase the efficiency of biochars as adsorbents, they are usually activated with KOH, steam or carbon dioxide, increasing its surface area and functional groups. The activation process can be however prohibitively expensive at a large scale [16], so in this work, the study has been performed with the original biochar as it was produced.

Regarding CSS pyrolysis liquid, it has been described as a source of phenolics and caffeine, among other value-added compounds [8,10]. Phenolics, which have been quantified in our previous study by Folin-Ciocalteu and DPPH methods [10], are highly valued in nutraceuticals and cosmetic industries [9,10] due to their antioxidant properties. Caffeine, on the other hand, presents stimulant effects on the nervous, muscular and cardiovascular systems, being used in a wide array of beverages and pharmaceutical products [27–29], and so, making its quantification interesting. Hence, CSS pyrolysis liquid could be studied as a potential source of value-added compounds, which may differ from the previous work [10] due to the reactor used in that case (pilot plant) was different from the one used in the present study (lab-scale reactor).

In reference to gas fraction, it can be composed of CO, H₂ and CH₄,

which are combustible gases, and so, a potential energy source [12].

The objective of the present work is to study and characterise the solid, liquid and gas products resulting from the slow pyrolysis of CSS in a lab-scale reactor at 280 °C, 400 °C and 500 °C, in order to determine the potential applications of each pyrolysis fraction within an integrated CSS biorefinery context. In this way, and for the first time, biochar from CSS has been studied as an adsorbent of organic pollutants in aqueous media; CSS pyrolysis liquids have been considered as a source for caffeine production with quantitative analysis; and the gas fraction has been valued as an energy source. The valorisation of the CSS pyrolysis products would allow to achieve zero-waste in the coffee roasting industry and contribute to circular economy and bioeconomy, promoting the production of green chemicals and materials and representing a potential improvement for the economy and the environment.

2. Materials and methods

2.1. Feedstock

CSS was supplied by a roasting coffee company from Spain in briquette format. The CSS briquette was crushed and sieved to homogeneous particle size of 1 mm, before pyrolysis. The moisture of CSS (1 mm) was 10.1 wt% (data obtained from the loss of weight from heating 1.5 g of CSS at 105 °C overnight; 0.15 of standard deviation; measurement performed in triplicate and averaged).

2.2. Reactor system

Slow pyrolysis of CSS was performed at 280 °C, 400 °C and 500 °C in a bench-scale auger reactor described elsewhere [30]. Nitrogen gas was used to purge and remove oxygen from the system. The solid residence time was fixed at 10 min and the feeding rate at 300 g/h. The solid product was collected from the char collection vessel, after cooling to room temperature, and placed in a sealed plastic bag for further physicochemical analysis. The condensable vapours were collected from a cooling and liquid collection system, comprised of a water-cooled condenser fixed at 20 °C (flask 1) and two ice-fingers filled with dry ice and acetone (flasks 2 and 3), placed in sealed brown glass containers and stored at 4 °C for further analysis. The non-condensable gases were filtered using a cotton filter, passed through a gas meter and analysed every 3 min by an online MicroGC in order to analyse the gas distribution (GC; VARIAN CP-4900, USA).

2.3. Product yields

Yields of solid, liquid and gas fractions, from each pyrolysis experiment, were calculated by dividing the mass of the resulting pyrolysis products by the mass of the feedstock used in the experiment. Data was expressed as wt% on dry feedstock basis.

Biochar was weighed after cooling and collected from the char collection vessel. Liquid product weight was obtained from the difference between the mass of the glassware for liquid collection after the pyrolysis experiment and before. The 280 °C pyrolysis liquid only presented one phase. Two-phase pyrolysis liquid was obtained from the 400 °C and 500 °C pyrolysis experiments; these two phases were separated by decantation and weighed. The weight of gas product was obtained from the volume of the gas, measured by the gas meter, and its density (ρ), calculated from the MicroGC data according to Eq. (1).

$$\rho_{\text{gas}} = \frac{\sum \text{vol}_i\% \cdot \rho_i}{100} \quad (1)$$

where vol_i% was the volume percentage obtained from MicroGC, and ρ_i was the density, of each pyrolysis gas product. Losses of the pyrolysis experiment were calculated by difference.

2.4. Analysis of feedstock and biochars

2.4.1. Feedstock and biochars characterisation

The bulk density of CSS and biochar was measured by weighing 5 mL of sample using a graduated cylinder. The measurement was performed in triplicate.

The ash content was determined following ASTM standards E1755 and D1762 (for biomass and char, respectively), where about 0.5 g of dried sample (105 °C, overnight) was heated for 30 min at 250 °C, and then for 6 h at 750 °C for biochars and 575 °C for feedstock. The measurement was performed in triplicate and the results were expressed as wt% on dry basis.

For subsequent analysis (pH, TGA, FTIR, porosimetry, elemental), CSS and biochars were ground with a mortar and pestle and then sieved to a particle size under 425 µm using a mesh sieve. Before the analyses, the samples were dried at 105 °C, overnight.

The pH of CSS and biochars was determined in 1:100 wt. sample / distillate water suspension using a pH meter (Sartorius PB-11). The suspension was stirred overnight at 600 rpm before measurement. pH analysis was performed 5 times for each sample and the results averaged.

Thermogravimetric analysis (TGA) of feedstock and biochars was carried out with a Perkin Elmer Pyris 1 TGA, with each sample analysed in duplicate. The analysis was performed by heating the sample from 60 °C to 900 °C with a heating rate of 10 °C /min.

Proximate analyses (ash and volatile matter contents) were performed in accordance with the ASTM standards D1762–84 and E1131. The fixed carbon content was calculated by difference.

Surface functional groups of CSS and biochars were characterised by Fourier-transform infrared spectroscopy (FTIR, PIKE Technologies GladiATR and Spectrum software). The scanned wavelengths were 4000 to 400 cm⁻¹, with a resolution of 4 cm⁻¹ and using 16 scans. The measurement was performed in duplicate.

Nitrogen porosimetry was measured with a Quantasorb Nova 4000e. The analysis was performed only for the 400 °C and 500 °C biochars due to biochars produced at low temperatures are expected to have low surface areas [31]. The samples, weighing between 0.20 and 0.35 g, were outgassed under vacuum at 200 °C overnight and then, placed into the evacuated sample chamber of the analyser. BET surface area and pore size distribution output was obtained through the Novawin 11.0 software.

Elemental composition (CHNS) of CSS and biochars was determined in duplicate using a Thermo Fisher Scientific Flash 2000 Organic Elemental Analyzer. Oxygen content (on dry basis) was calculated by difference.

Higher Heating Value (HHV) was calculated by the following formula from Channiwalla and Parikh [32]:

$$\text{HHV} = 0.3491C + 1.1783H + 0.1005S - 0.1034O - 0.0151N - 0.0211\text{Ash} \quad (\text{MJ/kg}) \quad (2)$$

C, H, O, N, S and Ash were expressed in mass percentage on dry basis.

2.4.2. Adsorption tests

Methylene blue (MB) (≥82%) and methyl orange (MO) (≥85%), supplied by Sigma-Aldrich, were the dyes chosen to perform the adsorption tests. These tests were conducted in batch, equally for MB and MO, using 25 mg of adsorbent (CSS and biochars, with a particle size under 425 µm) and 10 mL of dye solution (100 mg/L) in a centrifuge tube. The mixture was placed in a sonicator for 3 h at 50 °C, and then, it was centrifuged at 3000 rpm for 2 h. The concentration of dye in the solution was analysed in triplicate using UV-Vis spectrophotometer (Thermo Scientific Evolution 220), on the basis of a linear calibration curve (20–100 mg/L). The results, expressed as percentage of dye removal (%R), were calculated by the following formula [19]:

$$\%R = \frac{100(C_0 - C_t)}{C_0} \quad (3)$$

C₀ (mg/L) was the initial concentration of dye (100 mg/L), and C_t (mg/L) was the concentration of dye after centrifugation step. In order to avoid deviations to the Beer-Lambert Law due to high values (> 2) of absorbance, mixtures were diluted 1:10 with distillate water. The measurements were performed by scanning from 800 nm to 600 nm in the case of MB (maximum wavelength around 670 nm) [19], and from 550 to 350 nm for MO (maximum wavelength of 464 nm) [20].

2.5. Analysis of pyrolysis liquid

CSS pyrolysis liquid was chemically characterised by gas chromatography – mass spectroscopy (GC–MS). The analysed samples were the ones collected in the first flask, after the water-cooled condenser (see Section 2.2). The analysis was carried out in a Shimadzu GCMS QP2010 SE system equipped with a capillary (Rtx-5MS) column (30 m × 0.25 mm inner diameter × 0.25 µm film thickness). Before injection, samples were diluted in HPLC grade acetone (≥ 99.9%, purchased from Sigma Aldrich), and then filtered (0.45 µg Millipore filter) to avoid obstruction of liner due to suspended ashes/solids after pyrolysis process. A volume of 1 µL was then injected, applying split mode, with the injection port at 300 °C. Helium was used as carrier gas with a flow of 2 mL/min. The oven temperature was as follows: 55 °C for 9 min, 20 °C/ min to 125 °C, 5 °C/min to 325 °C and 325 °C for 10 min. The total run time was 64.50 min. Compounds were identified from the chromatograms by computer matching of mass spectra of the peaks with the National Institute of Standards and Technology (NIST) library; the semi-quantification was performed relating the total area of the compounds, as shown in previous publications [9,10,33].

Caffeine from CSS pyrolysis liquids (aqueous fraction) was quantified by high-performance liquid chromatography system coupled to an ultraviolet-visible detector (HPLC-UV/Vis) (Series 1100, Agilent Technologies). The HPLC-UV/Vis was equipped with a binary pump, a DAD detector and ZORBAX SB-C18 analytical column (4.6 × 100 mm, 1.8 µm particle size) from Agilent Technologies. Water: methanol (60:40, v/v) was used as mobile phase, at a flow rate of 0.4 mL/min at room temperature (25 °C). 4 µL of sample was injected and caffeine was determined at the wavelength of maximum absorbance (λ = 273 nm), using an external standard calibration curve with a concentration range of 100–1000 ppm. Caffeine content was expressed as g caffeine/L of aqueous phase from the pyrolysis liquid.

2.6. Analysis of gas fraction

Data collected from the MicroGC was processed by the software provided by the manufacturer of the online gas chromatograph (GC; VARIAN CP-4900, USA). The MicroGC used 5 Å Molsieve and Porat-PLOT columns, and Helium as carrier gas. The chemical composition of gas was obtained by the average of the data corresponding to the pyrolysis process and expressed as vol%.

The heating value of gas was calculated using the following formula [30]:

$$\text{HHV}_{\text{gas}} = \sum (\text{vol}_i\%/100) \cdot \text{HHV}_i \quad (\text{MJ/m}^3) \quad (4)$$

where vol_i% and HHV_i were the volume percentage and the heating value, respectively, for each gas species present in the pyrolysis gaseous product.

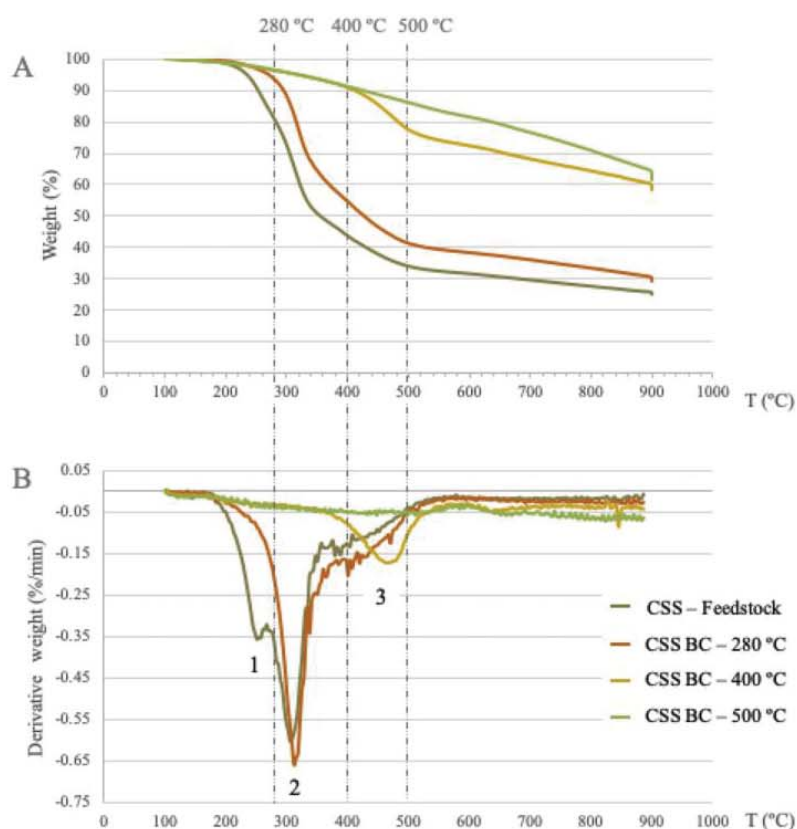


Fig. 1. Pyrolysis curves of CSS and biochars from the slow pyrolysis of CSS, at 280 °C, 400 °C and 500 °C. Graph A shows the weight loss, and graph B, the rate of weight loss, on dry basis. The numbers correspond to the weight loss mainly associated to hemicellulose (1), cellulose (2) and lignin (3) decomposition. (CSS, coffee silverskin; BC, biochar; T, temperature).

3. Results and discussion

3.1. Slow pyrolysis

3.1.1. Thermal degradation of CSS and biochars

TGA of CSS and biochars resulting from the slow pyrolysis of CSS at 280 °C, 400 °C and 500 °C were carried out in order to study the thermal degradation of CSS during the pyrolysis process. TGA, performed under nitrogen atmosphere, gave information on how the different polymers of biomass (hemicellulose, cellulose, and lignin) degrade in function of the temperature (see Fig. 1).

CSS TGA showed two main losses of weight around 255 °C (1) and 300 °C (2), attributed to hemicellulose and cellulose decomposition respectively, and a smaller weight loss around 400 °C (3), associated with lignin degradation (see Fig. 1). This data is consistent with the one obtained in a previous study carried out by our research group [10]. As expected from CSS TGA (see Fig. 1), pyrolysis at 280 °C resulted in the degradation of hemicellulose. This was reflected in 280 °C CSS biochar TGA, where only cellulose (2) and lignin (3) decomposition peaks were observed. In the same way, pyrolysis at 400 °C degraded hemicellulose and cellulose, resulting in a lignin-based biochar. Lignin decomposition peaks (3) shown in Fig. 1-B were very low due to the low lignin content of CSS (1 wt%) [34]. It is also shown that lignin from CSS and 280 °C CSS biochar degraded at around 250 °C to 500 °C, presenting small and wide peaks with a maximum at 400 °C; however, in 400 °C CSS biochar, part of lignin had already degraded and the peak (3) narrowed from 400 °C to 500 °C, changing its maximum to 470 °C. This could be due to structural

Table 1

Product yields from the slow pyrolysis of CSS at the following temperatures.

T (°C)	Solid (wt%)	Liquid		Gas (wt%)	Losses (wt%)
		AP (wt%)	NAP (wt%)		
280	80.5	4.1	–	10.3	5.1
400	40.5	15.4	18.2	20.7	5.2
500	31.5	15.7	22.5	22.4	7.9

Data is expressed as wt% on dry feedstock basis. (T, temperature; AP, aqueous phase of the pyrolysis liquid; NAP, non-aqueous phase of the pyrolysis liquid).

modifications of lignin at elevated temperatures [14]. Concerning the pyrolysis at 500 °C, all three polymers were decomposed since 500 °C corresponded to approximately the end of CSS biomass thermal degradation; this is evidenced in CSS and 500 °C CSS biochar TGA (see Fig. 1). As the resulting CSS biochars presented different hemicellulose, cellulose and lignin compositions, they are expected to have distinct properties from each other, which would be reflected in different potential applications.

3.1.2. Product yields

Slow pyrolysis of CSS, at 280 °C, 400 °C and 500 °C, resulted in the yields shown in Table 1, information that contributes to determine the best CSS pyrolysis temperature in function of the desired products.

Product distribution trends of CSS, shown in Table 1, are in accordance with the common thermal degradation of biomass: biochar yield

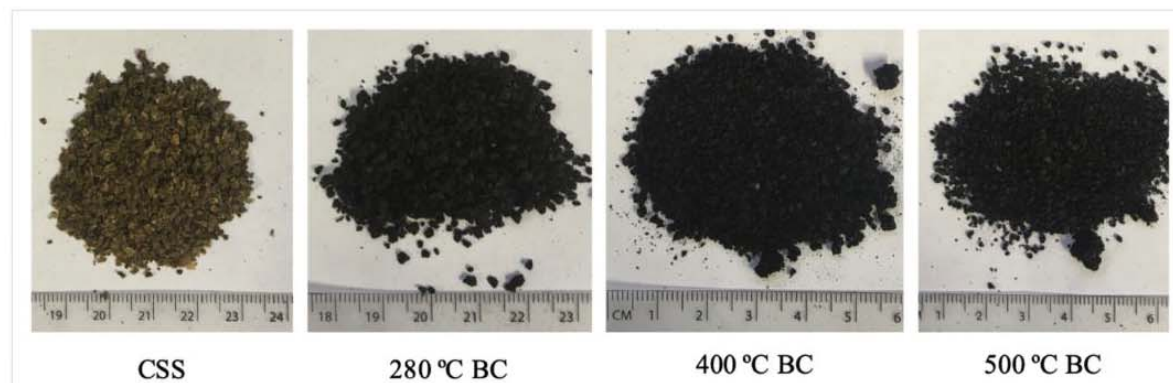


Fig. 2. CSS and biochars from the slow pyrolysis of CSS at 280 °C, 400 °C and 500 °C. The unit of the ruler is in cm. (CSS, coffee silverskin; BC, biochar).

Table 2

Characterisation of CSS and biochars from the slow pyrolysis of CSS at 280 °C, 400 °C and 500 °C.

	CSS	280 °C BC	400 °C BC	BC 500 °C
Ash (% large oven)	8.34 (0.11)	8.01 (0.14)	16.51 (0.36)	21.81 (0.11)
Density (g/mL)	0.31 (0.01)	0.26 (0.00)	0.20 (0.00)	0.19 (0.01)
pH	5.35 (0.03)	6.66 (0.04)	8.9 (0.00)	10.05 (0.05)
Proximate Analysis				
VM (%)	76.41 (0.05)	70.43 (0.67)	41.80 (0.16)	38.53 (1.74)
FC (%) ^a	16.07 (0.18)	20.95 (1.22)	41.90 (0.37)	40.74 (0.66)
Ash (%)	7.52 (0.13)	8.62 (0.55)	16.29 (0.53)	20.72 (1.08)
Ultimate Analysis				
N (%)	3.50 (0.07)	3.37 (0.09)	3.10 (0.02)	2.90 (0.05)
C (%)	47.69 (0.02)	54.23 (0.39)	60.10 (0.61)	60.78 (0.72)
H (%)	5.61 (0.00)	5.87 (0.02)	4.44 (0.07)	2.59 (0.05)
S (%)	0.24 (0.02)	0.11 (0.01)	0.04 (0.06)	0.15 (0.02)
O (%) ^a	34.66 (0.02)	28.42 (0.49)	15.92 (0.62)	11.78 (0.84)
Molar H/C	1.40 (0.00)	1.29 (0.00)	0.88 (0.02)	0.51 (0.00)
Molar O/C	0.55 (0.00)	0.39 (0.01)	0.20 (0.01)	0.15 (0.01)
Molar (O + N)/C	0.61 (0.00)	0.45 (0.01)	0.24 (0.01)	0.19 (0.01)
HHV (MJ/kg) ^b	19.47 (0.01)	22.70 (0.21)	24.18 (0.21)	22.56 (0.39)
N ₂ Porosimeter				
BET (m ² /g)	–	–	3.6	2.3
Pore size (nm)	–	–	39.6	88.8

Data is expressed as mean (standard deviation). Ash, proximate and ultimate analysis are expressed as wt% on dry basis. (CSS, coffee silverskin; BC, biochar; VM, volatile matter; FC, fixed carbon; HHV, higher heating value; BET surface area).

^a Fixed carbon and oxygen content are calculated by difference.

^b HHV is calculated mathematically from Chaniwala and Parikh [32] formula.

(% solid) decreased with temperature, while liquid (% AP, % NAP) and gas fractions increased. Biochar yields were also consistent with CSS TGA, that showed 80.7%, 43.6% and 33.7% of solid weight at 280 °C, 400 °C and 500 °C, respectively (see Table 1 and Fig. 1). The slight differences between TGA data and biochar yields are mainly related to the differences between heat transfer of the processes. Regarding the liquid fraction, and based on TGA data (Section 3.1.1), the aqueous phase (AP) was mainly composed of the hydrophilic products from hemicellulose decomposition in the 280 °C case, and hemicellulose and cellulose degradation in the 400 °C and 500 °C pyrolysis liquids. On the other hand, non-aqueous phase (NAP) mainly consisted of hydrophobic products from partial (400 °C) and total (500 °C) decomposition of lignin [10]. According to the hydrophilicity and hydrophobicity of pyrolysis liquid compounds, they usually separate in two phases, AP and NAP, as in the present case [9,35]. The pyrolysis process resulted in a mass loss of about 5.0–7.9% (see Table 1), which is mainly associated with the fact that some solid pyrolysis products could have remained

inside the reactor. The obtained losses values are nevertheless acceptable for the scale of the reactor.

3.2. Feedstock and biochars

3.2.1. Solid product characterisation

Raw CSS and biochars from the slow pyrolysis of CSS (see Fig. 2) were studied and characterised in order to determine their potential uses, paying particular attention to their role as adsorbents in aqueous media.

The analyses performed on CSS and CSS biochars are summarised in Table 2 and Fig. 3. Proximate analysis shows, as expected, a relative increase of ash content and fixed carbon with temperature, at the expense of volatile matter (see Table 2) [15]. This has also been observed in the previous section (3.1.1), where the number of volatile compounds removed from CSS increased with increasing the temperature of the pyrolysis process (see Fig. 1). In the same way, density decreased with increasing temperature due to the removal of volatile compounds. Ash data, which were obtained by different methods (oven and proximate analysis), presented similar results, with the highest difference between the values being 1%, for the 500 °C biochar (see Table 2). This biochar also presented the highest ash value (21%) as a result of the concentration of inorganic compounds with the temperature.

Regarding pH, it increased substantially at higher temperatures due to the increased relative concentration of basic surface oxides of alkali and alkaline earth metals [14,36] (see Table 2). The main metals present in the CSS are, specifically, potassium (27 mg/g), calcium (7 mg/g) and magnesium (3 mg/g) [10]. During pyrolysis, the mineral content of feedstock is largely retained and concentrated in biochars [37], justifying the basic pH of CSS biochars.

In reference to ultimate analysis, pyrolysis performed at high temperatures led to high degrees of carbonisation (see Table 2), that resulted in the formation of aromatic and graphitic structures on the biochar [31]. This fact is supported by increasing %C, and %H and %O decreasing, with increasing pyrolysis temperature. Molar ratios of the elements have been used to estimate the aromaticity (H:C), polarity (O:C) and oxygen functionality ((O + N)/C) of chars [38], information that can be related to their behaviour as adsorbents. The reduction of these values indicates the removal of polar surface functional groups and the formation of aromatic structures through a higher degree of carbonisation [31]. Specifically, the molar H/C ratio of ≤ 0.3 suggests highly condensed aromatic ring systems, and the lower molar O/C ratio, produced at higher temperature, indicated the arrangement of aromatic rings, originating stable crystal graphite-like structures [15]. In this way, with increasing temperature, biomass underwent dehydration and

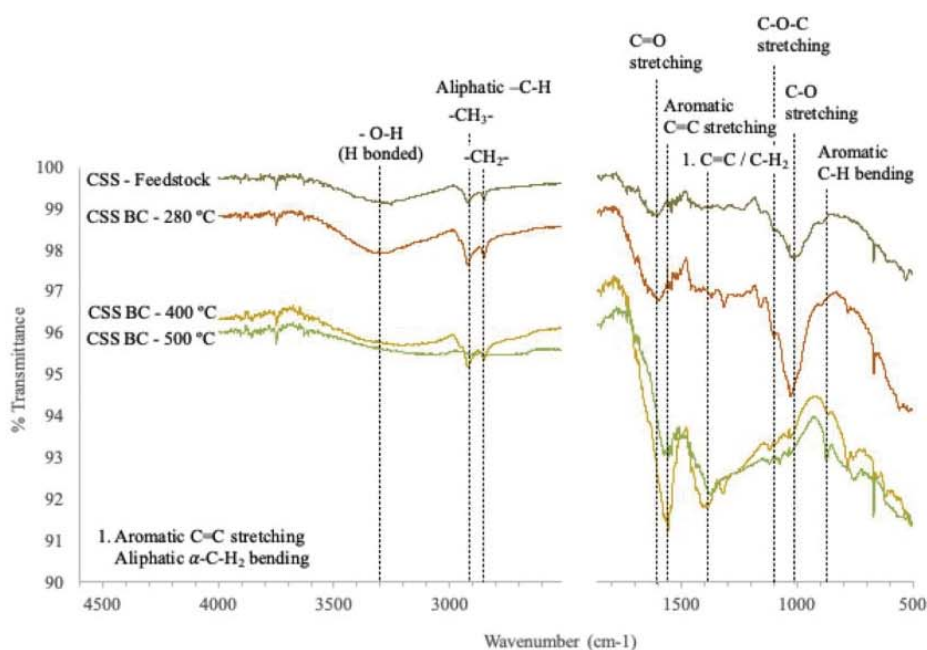


Fig. 3. FTIR spectra for CSS feedstock and CSS biochars from slow pyrolysis at 280 °C, 400 °C and 500 °C. (CSS, coffee silverskin; BC, biochar).

decarboxylation reactions, forming volatile dissociation products of lignin, cellulose and hemicelluloses, and condensation reactions, forming the graphitic structures [39,40]. Hence, as shown in Table 2, the more aromatic and less polar biochar was the one produced at 500 °C. Ultimate analysis also suggests the potential use of CSS biochars as compost due to their high amount of nitrogen (>2%) compared to other composting materials, such as cow dung (1.87%N) [41]. On the other hand, the carbon content of biochars, which was higher than 50% of the dry mass, complies with the European Biochar Certificate (EBC) requirements [42]. This indicates that the biochars produced from CSS can be potentially used in soil applications, although limited by a relatively high ash content.

Calorific values (HHV) also indicate the use of CSS biochars for combustion purposes, as already observed in a previous study by our research group [10] (see Table 2). The heating values of biochars, with no significant differences between them, were similar to other fuels such as coal (14.6–26.7 kJ/kg) [43,44], representing an ideal alternative to renewable energy [11]. The increase of the biochar energy value compared to CSS feedstock is related to the increase of %C and the decrease of %O in biochars [40]. The low sulphur content of biochars (0.04–0.15 wt%) can also favour their use as energy source due to the low sulphur oxides emissions that would be released in the combustion of biochars (see Table 2).

Concerning the role of CSS biochars as adsorbents, porosimetry and FTIR analysis, shown in Table 2 and Fig. 3, give information about properties associated to the adsorption capacity of biochars. Nitrogen porosimetry informs about the surface area (BET) and pore size distribution, which are related to the amount of active adsorption sites and the size of potential adsorbates, respectively. The analysis was carried out on the 400 °C and 500 °C biochars since appreciable surface area values are only expected for the highest pyrolytic temperatures [31]. This is because surface areas typically increase with increasing pyrolytic temperature due to the escape of volatile substances and the formation of channel/pore structures [45]. Nevertheless, the obtained surface areas were extremely low (< 4 m²/g) (see Table 2). This fact can be

explained due to the relatively low pyrolysis temperature, and the lack of an activation treatment, which are widely used to increase the surface area of biochars during the pyrolysis process [46]. Apart from that, porosity is also related to the lignin content of feedstock. Lignin-rich biomass, together with high pyrolysis temperature, typically results in high surface areas because of structural modifications of lignin at elevated temperature, after the release of volatiles [14]. The role that lignin plays in porosimetry is not only as a precursor but also as a porosity controller [47]. Hence, the low lignin content of CSS (1 wt%) [34] contributed as well to the low porosity of biochars. Furthermore, biochar pores could be plugged by inorganic compounds from ash, tars (condensed volatiles), and other amorphous decomposition products which are known to partially block the micropores [14]. In this case, blocking of the pores could be favoured due to the relatively long vapour residence time in the reactor during the slow pyrolysis, putting the vapour in contact with the solid product for longer time.

FTIR, on the other hand, indicated the functional groups located on the surface of CSS feedstock and CSS biochars, which affects their potential interactions with adsorbates [15]. As observed in Fig. 3, and in agreement with the ultimate analysis from Table 2, polar functional groups were removed, and aromatic structures were formed with increasing pyrolysis temperature. A broad peak around 3300 cm⁻¹, corresponding to O–H stretching for alcohols and phenols, and a 2800–3000 cm⁻¹ peak, attributable to aliphatic C–H stretching, were present in CSS, 280 °C and 400 °C biochars, but not in 500 °C biochar [31,38]. Similar results were seen by Uchimiya et al. [31] in a study of cottonseed hulls biochars. Reduction of C=O (around 1600 cm⁻¹), related to carboxylate group, and C–O (1078 cm⁻¹ for COC and 1000 cm⁻¹ for acidic CO) were also observed in 400 °C and 500 °C biochars [30,31]. By contrast, aromatic peaks from C=C stretching (1566 cm⁻¹), as well as C–H bending (874 cm⁻¹) increased in 400 °C and 500 °C biochars [13,31,38]. The reduction of the polar functional groups, from dehydration and depolymerisation reactions during the pyrolysis process, led to the growth of aromatic and graphitic structures [38], which can interact with aromatic species. Hence, although the porosity of CSS

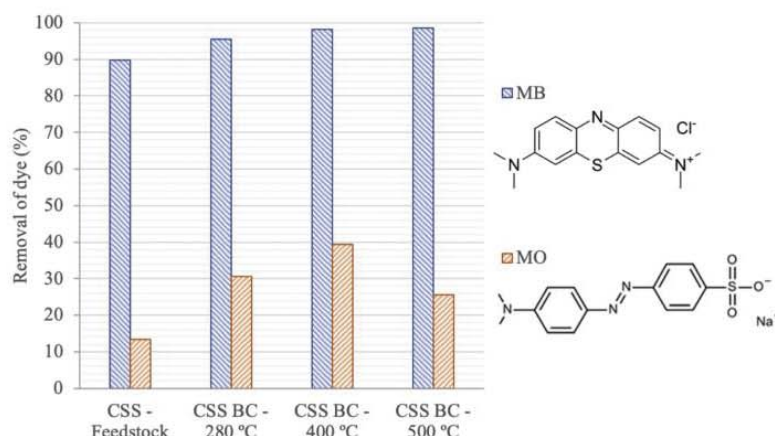


Fig. 4. Removal (%) of MB and MO from an aqueous solution using CSS feedstock and CSS biochars. (CSS, coffee silverskin; MB, methylene blue; MO, methyl orange; BC, biochar). (For interpretation of the references to colour in this figure legend, the reader is referred to the web version of this article.)

biochars was low, their surface chemical characteristics indicated that they could be used as potential adsorbents of aromatic organic pollutants.

3.2.2. Adsorption of MB and MO from aqueous solution

This section is focused on studying the adsorbent properties of CSS biochars in aqueous media. This would demonstrate their potential use to remove contaminants from water, increasing the value of the biochar and promoting a CSS pyrolysis-based biorefinery by using the resulting solid, liquid and gas pyrolysis products for different purposes.

The study was carried out using MB and MO as model compounds (see Fig. 4) which allowed to evaluate the potential removal efficiency of aromatic ionic pollutants by CSS biochar.

As shown in Fig. 4, CSS biochars were efficient in removing MB and, to a lesser extent, MO, with 400 °C CSS biochar being the best one in both cases, reaching respectively 98% and 40% removal. CSS feedstock also showed high MB removal values; however, with the production of biochar, it is also obtained liquid and solid products, which could be used as chemical and energy sources respectively, making pyrolysis a potential treatment for CSS. The affinity of biochars with MB and MO can be explained by π - π dispersion interaction between the aromatic rings of dyes and the aromatic structure of biochars (see Section 3.2.1, ultimate analysis) [26,48]. The functional groups present on the biochar

surface (see Section 3.2.1, FTIR analysis) can also play a major role in MB and MO adsorption, especially by means of electrostatic interactions, electron donor-acceptor and hydrogen bonding mechanisms [26]. Electrostatic interactions may take place between the negatively charged carboxylate of biochars and the charged groups of the dyes (See Fig. 4). In the MB case, there can be an electrostatic attraction between the nitrogen positive charge of MB and the biochars [26], whereas concerning MO, there can be a repulsion force between the negatively charged sulphonic group of MO and carboxylate anions of biochars, leading to lower levels of removal of MO compared to MB. The differences between MB and MO were reflected in Fig. 4, where MB removal values were substantially higher than the MO ones. Electron donor-acceptor interactions, on the other hand, could take place between carbonyl oxygens in the biochar, that would act as an electron donor, and the aromatic ring of MB and MO, that would be the electron acceptor [26]. In terms of hydrogen bonds, they could be formed between hydroxyl groups of biochars and nitrogen from MB and MO [26]. As CSS presents low lignin content [34], most of the hydroxyl groups originated from hemicellulose and cellulose. The restrictive effect of the hydrogen-bond network of cellulose molecules leads to hydroxyl groups having low accessibility on the biomass surface [19]. In this regard, the main contribution in MB and MO adsorption would be π - π dispersion and electrostatic interactions.

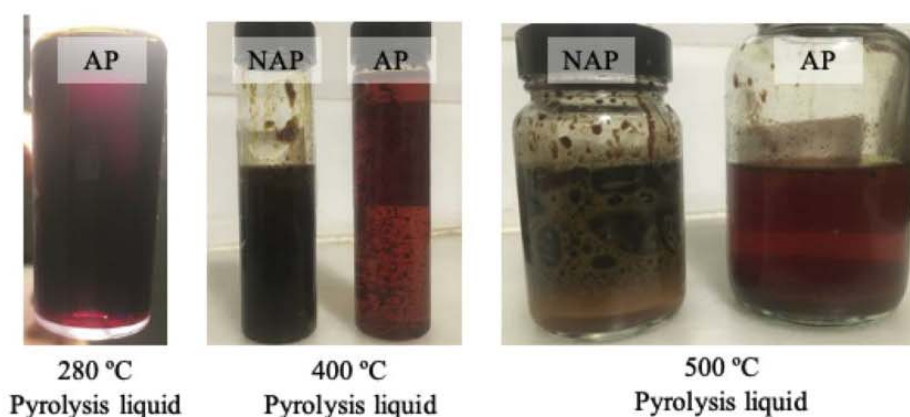


Fig. 5. Pyrolysis liquids from the slow pyrolysis of CSS at 280 °C, 400 °C and 500 °C. (CSS, coffee silverskin; AP, aqueous phase of the pyrolysis liquid; NAP, non-aqueous phase of the pyrolysis liquid).

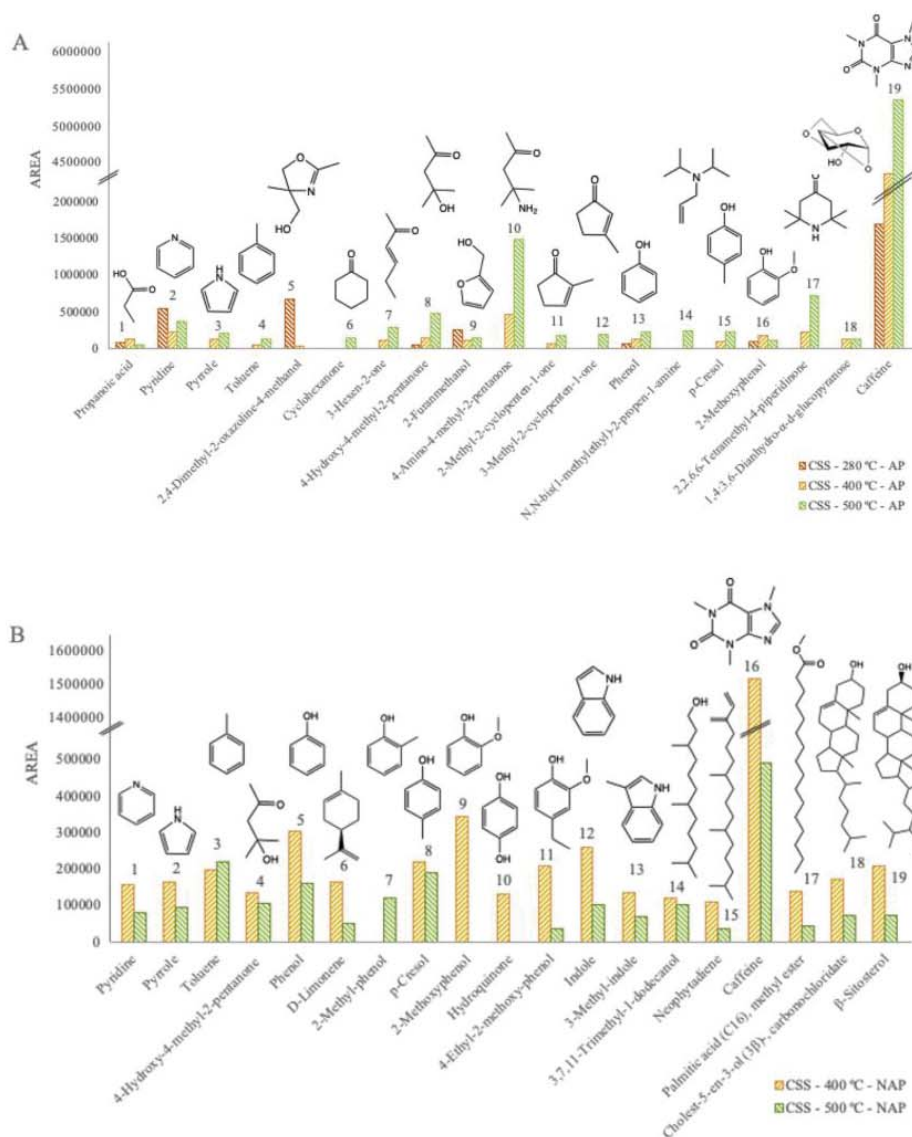


Fig. 6. Most abundant compounds of AP (A) and NAP (B) phases of CSS pyrolysis liquids determined by GC-MS analysis. (CSS, coffee silverskin; AP, aqueous phase of the pyrolysis liquid; NAP, non-aqueous phase of the pyrolysis liquid).

Based on the MB and MO main mechanisms, CSS biochar could be used to remove compounds with aromatic rings in their structure from water, and especially compounds with positive charge. Examples of this could be aromatic antiepileptic drugs (AED), sulphonamides (synthetic bacteriostatic antibiotics), thiacloprid pesticide, estrogens, ibuprofen and paracetamol derivatives, apart from the MB and MO dyes themselves [13,17,48]. Particularly in MB case, CSS biochars, which were performed without any activation treatment, presented similar removal values as a commercial activated carbon (Norit) ($\geq 99\%$ removal) shown in a previous work [49], with removal rates of 95.5% with 280 °C biochar (38.1 mg MB/g biochar), 98.2% with 400 °C biochar (39.3 mg MB/g biochar) and 98.5% with 500 °C biochar (39.4 mg MB/g biochar) (See Fig. 4). Commercial activated carbons are known to have the highest

removal efficiency since their large surface area and presence of surface functional groups facilitate interactions with various compounds [26]; however, their resource- and energy-intensive production process also makes them expensive products [13]. In this way, CSS biochars could be a potential sustainable and more affordable alternative to activated carbon for the adsorption of cationic aromatic compounds, as they present a similar structure to MB. Apart from organic pollutants, CSS biochars could be also effective in the removal of cationic heavy metals by means of electrostatic attraction [13] or complexation with carbonyl groups of biochar [16], considering that the contamination of water by toxic metals has become a pervasive problem throughout the world [13]. Biochars have also significant potential to address not just the pollutants in water, but also in soil and gaseous media [11].

Table 3

Content of caffeine in aqueous phase of pyrolysis liquid from the slow pyrolysis of CSS at 280 °C, 400 °C and 500 °C (CSS, Coffee Silverskin; AP, Aqueous Phase of the pyrolysis liquid).

Caffeine concentration	280 °C AP	400 °C AP	500 °C AP
In aqueous phase (g caffeine/L AP)	11.5	14.3	10.4
From feedstock (mg caffeine AP/g CSS)	1.75	3.81	2.81

3.3. Pyrolysis liquid

3.3.1. Pyrolysis liquid description

Slow pyrolysis of CSS at 280 °C, 400 °C and 500 °C also resulted in the pyrolysis liquid shown in Fig. 5. As shown, 280 °C pyrolysis liquid consisted of a single aqueous phase; on the other hand, 400 °C and 500 °C pyrolysis liquids were composed of two phases, an aqueous phase and a non-aqueous phase. This is because this type of pyrolysis generates high amounts of reaction water, separating the hydrophilic and hydrophobic compounds of pyrolysis liquid in two phases [9,35]. As hydrophobic compounds are mainly from lignin degradation [9,33], the phase separation only took place at 400 °C and 500 °C, at which a higher amount of lignin has been decomposed (see Section 3.1.1). On the contrary, hydrophilic compounds are mostly from hemicellulose, cellulose and part of lignin decomposition [9,33,50].

3.3.2. Pyrolysis liquid composition

The chemical composition of the CSS pyrolysis liquids was analysed by GC–MS (see Fig. 6), showing caffeine as the most abundant compound in all samples. In contrast with pyrolysis liquid from classical forest biomass [51,52] or other agricultural wastes, such as grape pomace [33] or olive mill waste [9], CSS pyrolysis liquids showed low phenolic content. This is due to most of the phenolics originating from the degradation of lignin, which is low in CSS (1 wt%) [34]. It is also observed that CSS pyrolysis liquids were particularly rich in nitrogen compounds, since the amount of nitrogen present in CSS was high (3 wt %) (see Section 3.2.1, ultimate analysis). This characteristic was detected as well by Polidoro et al. [8] and in the previous study performed by our research group [10].

As shown in Fig. 6, 400 °C and 500 °C pyrolysis liquids presented similar compositions, which were much higher than the one at 280 °C, as expected from TGA data that showed lower devolatilisation at 280 °C (see Section 3.1.1). AP (Graphic A) was mainly composed of caffeine (compound 19) and to a lesser extent, pyridine (2), phenolics (13, 15, 16) and other low molecular weight oxygenated products (1, 5, 7, 8, 9, 11, 12). NAP (Graphic B), on the other hand, mostly contained caffeine (16), phenolics (5, 7, 8, 9, 10, 11), nitrogenated compounds (1,2,12,13), hydrocarbon chains (14, 15, 17) and sterols (18, 19). Hence, CSS pyrolysis liquids seem to be a potential source of caffeine (see Fig. 6), which is a value-added compound widely used in food and pharmaceutical industry [27–29].

In this regard, caffeine concentration from AP samples was quantified by HPLC-UV/Vis (see Table 3), with AP 400 °C showing the highest amount of caffeine (14.3 g caffeine /L AP; 3.81 mg caffeine AP/ g CSS). Specifically, from each tonne of CSS, it was obtained 154 kg of AP (400 °C), which contained 2 kg of caffeine. It is reported that the total content of caffeine in CSS feedstock is around 4.4–10.0 mg caffeine /g CSS by Bresciani et al. [53], 8.3–13.7 mg caffeine /g CSS by Napolitano et al. [54], and 7.7–10.3 mg caffeine /g CSS by Toschi et al. [55], the difference between these values being attributed to the different methods used for its measurement [55]. In view of this data, it is assumed that just part of CSS caffeine was concentrated in the AP liquid fractions, while the rest should be in the NAP pyrolysis liquids (see Fig. 6, graphic B). Still, CSS AP pyrolysis liquids, mainly the 400 °C sample, contained an appreciable concentration of caffeine.

Apart from caffeine, CSS pyrolysis liquids were also composed of other value-added products, such as phenolics and β-sitosterol (19,

Table 4

HHVs and composition of gas fractions from the slow pyrolysis of CSS at 280 °C, 400 °C and 500 °C.

	Gas fraction		
	280 °C	400 °C	500 °C
HHV (MJ/m ³)	1.88	3.79	10.25
Gas composition (vol%)			
CO ₂	84.21	74.48	54.42
CO	15.44	23.07	26.23
CH ₄	0.07	1.41	9.47
H ₂	0.21	0.18	5.16
C ₂ H ₆	0.02	0.45	2.98
C ₂ H ₄	0.05	0.25	0.97
C ₃ H ₈	0.00	0.16	0.77

Data of gas composition is expressed as vol%, obtained from GC analysis. (HHV, higher heating value; CCS, coffee silverskin).

Fig. 6B). Phenolics are known for their antioxidant properties, which are highly valued in nutraceuticals and cosmetic industries [9,10]. Specifically, our previous study determined the total phenolic content and the antioxidant capacity of 280 °C, 400 °C and 500 °C CSS pyrolysis liquids, showing them as potential source of phenolics [10]. On the other hand, β-sitosterol is usually used in medicine for heart disease, hypercholesterolemia, modulating the immune system, prevention of cancer, as well as for rheumatoid arthritis, tuberculosis, cervical cancer, hair loss and benign prostatic hyperplasia [56]. In this way, CSS pyrolysis liquids could be considered as potential sources of value-added products, in particular caffeine, which amount between 10.4 and 14.3 g/L in the AP. It should be noted that these products need to be first separated and purified.

3.4. Gas fraction

CSS pyrolysis gases mainly consisted of CO₂, CO, CH₄, and, to a lesser extent, H₂, C₂H₆, C₂H₄ and C₃H₈ (see Table 4). From all gases, CO₂ was the most abundant compound, followed by CO. CO₂ and CO are related to the pyrolysis of hemicellulose and cellulose [57], the first polymers to be thermally degraded (see Section 3.1.1). CO₂ is mainly released from the cracking and reforming of carboxyl (C=O) and carboxylic acid (COOH), mostly present in hemicellulose, whereas CO is mainly obtained from carbonyl (COC) and carboxyl (C=O) decomposition, mostly concentrated in cellulose [57]. On the contrary, H₂ gave low percentages, being almost negligible at low pyrolysis temperatures (see Table 4). Similar results were obtained by Yu et al. [30] in the pyrolysis of rice husk and corn stalk, performed in the same auger reactor as the present study, where H₂ percentage was not significant till pyrolysis temperatures were above 500–550 °C [30,57]. Regarding CH₄ and the other light hydrocarbons, they are attributed to the reforming and cracking of methoxyl groups, mainly present in lignin, and heavier hydrocarbons [30,57].

Moreover, Table 4 shows that as the temperature of the pyrolysis process was increased, the proportion of CO₂ decreased, and the proportions of the other gas compounds increased, as also observed by Yu et al. [30]. This fact is reflected in the gas calorific values, which increased with the increase in CH₄ and light hydrocarbons [58]. In this way, 500 °C gas gave the highest calorific value (10.25 MJ/m³). The heat of combustion of the pyrolysis gases could be used for biomass drying before thermochemical treatment, since the feedstock should have low moisture content (typically no more than 10 wt% of moisture). Specifically, the resulting flue gas could be used as a drying medium in a direct rotary drums and belt conventional dryers, where biomass could be heated by the hot flue gas directly using the thermal energy in the hot gas [59]. Hence, the integration of biomass drying to pyrolysis process could improve the overall efficiency of the process, apart from contributing to the circular economy and the bioeconomy.

4. Conclusions

The present work deals with the management of CSS, which is the only by-product from the coffee roasting process. By employing slow pyrolysis, it allows closer biorefinery integration of CSS by exploring the potential uses of the resulting fractions, demonstrating biochar as an adsorbent of mainly cationic and aromatic organic pollutants from water; pyrolysis liquid as caffeine source; and gas fraction as a heat source for biomass drying before pyrolysis treatments. Specifically, pyrolysis of one tonne of CSS at 400 °C would generate 405 kg of biochar and could result in up to 2 kg of caffeine to be extracted from the aqueous pyrolysis liquid fraction. This study promotes the sustainability, circular economy and zero-waste in the coffee roasting industry.

Declaration of Competing Interest

The authors declare that they have no known competing financial interest or personal relationships that could have appeared to influence the work reported in this paper.

Acknowledgements

C. del Pozo expresses her gratitude to the Universitat Autònoma de Barcelona for funding her PhD contract through a PIF grant, as well as an Erasmus+ grant to support her exchange stay at Aston University (EBRI).

References

- R.C. Alves, F. Rodrigues, M. Antónia Nunes, A.F. Vinha, M.B.P.P. Oliveira, State of the Art in Coffee Processing by-Products, Elsevier Inc., 2017, <https://doi.org/10.1016/B978-0-12-811290-8.00001-3>.
- R.C. Borrelli, F. Esposito, A. Napolitano, A. Ritieni, V. Fogliano, Characterization of a New potential Functional Ingredient: Coffee Silverskin, *J. Agric. Food Chem.* 52 (2004) 1338–1343, <https://doi.org/10.1021/jf034974x>.
- The Coffee Guide, n.d. <http://www.thecoffeeguide.org/coffee-guide/world-coffee-trade/conversions-and-statistics/>. (Accessed 27 August 2020).
- Y. Narita, I. Kuniyo, Review on utilization and composition of coffee silverskin, *Food Res. Int.* 61 (2014) 16–22, <https://doi.org/10.1016/j.foodres.2014.01.023>.
- International Coffee Organization, World Coffee Consumption. <http://www.ico.org/prices/new-consumption-table.pdf>, 2020. (Accessed 15 March 2020).
- S.M.F. Bessada, R.C. Alves, M.B.P.P. Oliveira, Coffee silverskin: A review on potential cosmetic applications, *Cosmetics* 5 (2018), <https://doi.org/10.3390/cosmetics5010005>.
- A.S.G. Costa, R.C. Alves, A.F. Vinha, S.V.P. Barreira, M.A. Nunes, L.M. Cunha, M.B. P.P. Oliveira, Optimization of antioxidants extraction from coffee silverskin, a roasting by-product, having in view a sustainable process, *Ind. Crop. Prod.* 53 (2014) 350–357, <https://doi.org/10.1016/j.indcrop.2014.01.006>.
- A.S. dos Polidoro, E. Scapin, E. Lazzari, A.N. Silva, A.L. dos Santos, E.B. Caramao, R.A. Jacques, Valorization of coffee silverskin industrial waste by pyrolysis: From optimization of bio-oil production to chemical characterization by GC × GC / qMS, *J. Anal. Appl. Pyrolysis* 129 (2018) 43–52, <https://doi.org/10.1016/j.jaap.2017.12.005>.
- C. del Pozo, J. Bartroli, N. Puy, E. Fàbregas, Separation of value-added chemical groups from bio-oil of olive mill waste, *Ind. Crop. Prod.* 125 (2018), <https://doi.org/10.1016/j.indcrop.2018.08.062>.
- C. del Pozo, J. Bartroli, S. Alier, N. Puy, E. Fàbregas, Production of antioxidants and other value-added compounds from coffee silverskin via pyrolysis under a biorefinery approach, *Waste Manag.* 109 (2020) 19–27, <https://doi.org/10.1016/j.wasman.2020.04.044>.
- Y. Dai, N. Zhang, C. Xing, Q. Cui, Q. Sun, The adsorption, regeneration and engineering applications of biochar for removal organic pollutants: a review, *Chemosphere*. 223 (2019) 12–27, <https://doi.org/10.1016/j.chemosphere.2019.01.161>.
- T. Chen, R. Liu, N.R. Scott, Characterization of energy carriers obtained from the pyrolysis of white ash, switchgrass and corn Stover - Biochar, syngas and bio-oil, *Fuel Process. Technol.* 142 (2016) 124–134, <https://doi.org/10.1016/j.fuproc.2015.09.034>.
- X. Tan, Y. Liu, G. Zeng, X. Wang, X. Hu, Y. Gu, Z. Yang, Application of biochar for the removal of pollutants from aqueous solutions, *Chemosphere*. 125 (2015) 70–85, <https://doi.org/10.1016/j.chemosphere.2014.12.058>.
- D. Rehrah, M.R. Reddy, J.M. Novak, R.R. Bansode, K.A. Schimmel, J. Yu, D. W. Watts, M. Ahmedna, Production and characterization of biochars from agricultural by-products for use in soil quality enhancement, *J. Anal. Appl. Pyrolysis* 108 (2014) 301–309, <https://doi.org/10.1016/j.jaap.2014.03.008>.
- Y. Wang, R. Liu, Comparison of characteristics of twenty-one types of biochar and their ability to remove multi-heavy metals and methylene blue in solution, *Fuel Process. Technol.* 160 (2017) 55–63, <https://doi.org/10.1016/j.fuproc.2017.02.019>.
- Y. Wang, R. Liu, H₂O₂ treatment enhanced the heavy metals removal by manure biochar in aqueous solutions, *Sci. Total Environ.* 628–629 (2018) 1139–1148, <https://doi.org/10.1016/j.scitotenv.2018.02.137>.
- P. Zhang, H. Sun, L. Min, C. Ren, Biochars change the sorption and degradation of thiadoprid in soil: Insights into chemical and biological mechanisms, *Environ. Pollut.* 236 (2018) 158–167, <https://doi.org/10.1016/j.envpol.2018.01.030>.
- A. Jiang, Z. Cheng, Z. Shen, W. Guo, QSAR study on the removal efficiency of organic pollutants in supercritical water based on degradation temperature, *Chem. Cent. J.* 12 (2018) 1–8, <https://doi.org/10.1186/s13065-018-0380-y>.
- Y. Zhu, B. Yi, Q. Yuan, Y. Wu, M. Wang, S. Yan, Removal of methylene blue from aqueous solution by cattle manure-derived low temperature biochar, *RSC Adv.* 8 (2018) 19917–19929, <https://doi.org/10.1039/c8ra03018a>.
- J. Yu, X. Zhang, D. Wang, P. Li, Adsorption of methyl orange dye onto biochar adsorbent prepared from chicken manure, *Water Sci. Technol.* 77 (2018) 1303–1312, <https://doi.org/10.2166/wst.2018.003>.
- Y. Song, Y. Bian, F. Wang, M. Xu, N. Ni, X. Yang, C. Gu, X. Jiang, Dynamic effects of biochar on the bacterial community structure in soil contaminated with polycyclic aromatic hydrocarbons, *J. Agric. Food Chem.* 65 (2017) 6789–6796, <https://doi.org/10.1021/acs.jafc.7b02887>.
- A. Zhelezova, H. Cederlund, J. Stenström, Effect of biochar amendment and ageing on adsorption and degradation of two herbicides, *Water Air Soil Pollut.* 228 (2017), <https://doi.org/10.1007/s11270-017-3392-7>.
- H. Liu, Y. Wei, J. Luo, T. Li, D. Wang, S. Luo, J.C. Crittenden, 3D hierarchical porous-structured biochar aerogel for rapid and efficient phenicol antibiotics removal from water, *Chem. Eng. J.* 368 (2019) 639–648, <https://doi.org/10.1016/j.cej.2019.03.007>.
- L. Li, M. Yang, Q. Lu, W. Zhu, H. Ma, L. Dai, Oxygen-rich biochar from torrefaction: a versatile adsorbent for water pollution control, *Bioreour. Technol.* 294 (2019) 122142, <https://doi.org/10.1016/j.biortech.2019.122142>.
- B.H. Hameed, A.T.M. Din, A.L. Ahmad, Adsorption of methylene blue onto bamboo-based activated carbon: Kinetics and equilibrium studies, *J. Hazard. Mater.* 141 (2007) 819–825, <https://doi.org/10.1016/j.jhazmat.2006.07.049>.
- A.M.M. Vargas, A.L. Cazetta, M.H. Kunita, T.L. Silva, V.C. Almeida, Adsorption of methylene blue on activated carbon produced from flamboyant pods (*Delonix regia*): Study of adsorption isotherms and kinetic models, *Chem. Eng. J.* 168 (2011) 722–730, <https://doi.org/10.1016/j.cej.2011.01.067>.
- A.F.M. Cláudio, A.M. Ferreira, M.G. Freire, J.A.P. Coutinho, Enhanced extraction of caffeine from guaraná seeds using aqueous solutions of ionic liquids, *Green Chem.* 15 (2013) 2002–2010, <https://doi.org/10.1039/c3gc40437d>.
- A. Rahimi, M.A. Zanjanchi, S. Bakhtiari, M. Dehsaraei, Selective determination of caffeine in foods with 3D-graphene based ultrasound-assisted magnetic solid phase extraction, *Food Chem.* 262 (2018) 206–214, <https://doi.org/10.1016/j.foodchem.2018.04.035>.
- C. Cai, F. Li, L. Liu, Z. Tan, Deep eutectic solvents used as the green media for the efficient extraction of caffeine from Chinese dark tea, *Sep. Purif. Technol.* 227 (2019) 115723, <https://doi.org/10.1016/j.seppur.2019.115723>.
- Y. Yu, Y. Yang, Z. Cheng, P.H. Blanco, R. Liu, A.V. Bridgwater, J. Cai, Pyrolysis of rice husk and corn stalk in auger reactor. 1. Characterization of char and gas at various temperatures, *Energy Fuel* 30 (2016) 10568–10574, <https://doi.org/10.1021/acs.energyfuels.6b02276>.
- M. Uchimiya, L.H. Wartelle, K.T. Klasson, C.A. Fortier, I.M. Lima, Influence of pyrolysis temperature on biochar property and function as a heavy metal sorbent in soil, *J. Agric. Food Chem.* 59 (2011) 2501–2510, <https://doi.org/10.1021/jf104206c>.
- S.A. Channiwala, P.P. Parikh, A unified correlation for estimating HHV of solid, liquid and gaseous fuels, *Fuel* 81 (2002) 1051–1063, [https://doi.org/10.1016/S0016-2361\(01\)00131-4](https://doi.org/10.1016/S0016-2361(01)00131-4).
- C. del Pozo, J. Bartroli, S. Alier, N. Puy, E. Fàbregas, Production, identification, and quantification of antioxidants from torrefaction and pyrolysis of grape pomace, *Fuel Process. Technol.* 211 (2021) 106602, <https://doi.org/10.1016/j.fuproc.2020.106602>.
- P.S. Murthy, M. Madhava Naidu, Sustainable management of coffee industry by-products and value addition – a review, *Resour. Conserv. Recycl.* 66 (2012) 45–58, <https://doi.org/10.1016/j.resconrec.2012.06.005>.
- C. Torri, D. Fabbri, Biochar enables anaerobic digestion of aqueous phase from intermediate pyrolysis of biomass, *Bioreour. Technol.* 172 (2014) 335–341, <https://doi.org/10.1016/j.biortech.2014.09.021>.
- J.M. Novak, I.M. Lima, B. Xing, J.W. Gaskin, C. Steiner, K.C. Das, M. Ahmedna, D. Rehrah, D.W. Watts, W.J. Busscher, H. Schomberg, Characterization of designer biochar produced at different temperatures and their effects on a loamy sand, *Ann. Environ. Sci.* 5 (2009) 195–206.
- K. Raveendran, A. Ganesh, K. Khilar, Influence of mineral matter on biomass pyrolysis characteristic, *Fuel*. 74 (1995) 1812–1822.
- K. Lou, A.U. Rajapaksha, Y.S. Ok, S.X. Chang, Pyrolysis temperature and steam activation effects on sorption of phosphate on pine sawdust biochars in aqueous solutions, *Chem. Speciat. Bioavailab.* 28 (2016) 42–50, <https://doi.org/10.1080/09542299.2016.1165080>.
- M. Keilweit, P.S. Nico, M.G. Johnson, M. KLEBER, Dynamic molecular structure of Plant biomass-derived Black Carbon(Biochar)- supporting information, *Environ. Sci. Technol.* 44 (2010) 1247–1253, <https://doi.org/10.1021/es9031419>.
- Z. Liu, G. Han, Production of solid fuel biochar from waste biomass by low temperature pyrolysis, *FUEL*. 158 (2015) 159–165, <https://doi.org/10.1016/j.fuel.2015.05.032>.

- [41] D.C. Preethu, B.N.U.H.B. Prakash, C.A. Srinivasamurthy, B.G. Vasanthi, Maturity Indices as an Index to Evaluate the Quality of Compost of Coffee Waste Blended with Other Organic Wastes, *Proc. Int. Confer- Ence Sustain. Solid Waste Manag.* Sept. 5-7, Chennai, India, 2007, pp. 270-275.
- [42] EBC, European Biochar Certificate - Guidelines for a Sustainable Production of Biochar, Eur. Biochar Found. (EBC), Arbaz, Switzerland. Version 6.1 19th June, 2012, 2015, pp. 1-22, <https://doi.org/10.13140/RG.2.1.4658.7043>.
- [43] M. Inguanzo, A. Domínguez, J.A. Menéndez, C.G. Blanco, J.J. Pis, On the pyrolysis of sewage sludge: the influence of pyrolysis temperature on biochar, liquid and gas fractions, *J. Anal. Appl. Pyrolysis* 63 (2002) 209-222, <https://doi.org/10.4028/www.scientific.net/AMR.518-523.3412>.
- [44] M.E. Sánchez, E. Lindao, D. Margaleff, O. Martínez, A. Morán, Pyrolysis of agricultural residues from rape and sunflowers: production and characterization of bio-fuels and biochar soil management, *J. Anal. Appl. Pyrolysis* 85 (2009) 142-144, <https://doi.org/10.1016/j.jaap.2008.11.001>.
- [45] M. Ahmad, S.S. Lee, X. Dou, D. Mohan, J.K. Sung, J.E. Yang, Y.S. Ok, Effects of pyrolysis temperature on soybean Stover- and peanut shell-derived biochar properties and TCE adsorption in water, *Bioresour. Technol.* 118 (2012) 536-544, <https://doi.org/10.1016/j.biortech.2012.05.042>.
- [46] A.U. Rajapaksha, M. Vithanage, M. Zhang, M. Ahmad, D. Mohan, S.X. Chang, Y. S. Ok, Pyrolysis condition affected sulfamethazine sorption by tea waste biochars, *Bioresour. Technol.* 166 (2014) 303-308, <https://doi.org/10.1016/j.biortech.2014.05.029>.
- [47] Z.K. Huang, Q.F. Li, Q. Lin, X. Cheng, Microstructure, Properties and Lignin-based Modification of Wood-Ceramics from Rice Husk and Coal Tar Pitch, *J. Inorg. Organomet. Polym. Mater.* 22 (2012) 1113-1121, <https://doi.org/10.1007/s10904-012-9708-6>.
- [48] H.N. Tran, F. Tomul, N. Thi Hoang Ha, D.T. Nguyen, E.C. Lima, G.T. Le, C. T. Chang, V. Masindi, S.H. Woo, Innovative spherical biochar for pharmaceutical removal from water: Insight into adsorption mechanism, *J. Hazard. Mater.* 394 (2020) 122255, <https://doi.org/10.1016/j.jhazmat.2020.122255>.
- [49] F. Rego, J. Wang, Y. Yang, A.V. Bridgwater, Development of an integrated and continuous slow pyrolysis and activation process for the production of activated carbon from waste biomass, *Eur. Biomass Conf. Exhib. Proc.* (2019) 1076-1079.
- [50] J.P. Diebold, A Review of the chemical and physical mechanisms of the storage stability of fast pyrolysis bio-oils, in: A.V. Bridgwater (Ed.), *Fast Pyrolysis Biomass A Handb*, CPL Press, Newbury, UK, 2002, p. 424 (doi:NREL/SR-570-27613).
- [51] N. Puy, R. Murillo, M.V. Navarro, J.M. López, J. Rieradevall, G. Fowler, I. Aranguren, T. García, J. Bartroli, A.M. Mastral, Valorisation of forestry waste by pyrolysis in an auger reactor, *Waste Manag.* 31 (2011) 1339-1349, <https://doi.org/10.1016/j.wasman.2011.01.020>.
- [52] A. Artigues, N. Puy, J. Bartroli, E. Fàbregas, Comparative Assessment of Internal Standards for Quantitative Analysis of Bio-oil Compounds by Gas Chromatography / Mass Spectrometry using Statistical Criteria, *Energy Fuel* 28 (2014) 3908-3915, <https://doi.org/10.1021/ef5005545>.
- [53] L. Bresciani, L. Calani, R. Bruni, F. Brighenti, D. Del Rio, Phenolic composition, caffeine content and antioxidant capacity of coffee silverskin, *Food Res. Int.* 61 (2014) 196-201, <https://doi.org/10.1016/j.foodres.2013.10.047>.
- [54] A. Napolitano, V. Fogliano, A. Tafuri, A. Ritieni, Natural occurrence of ochratoxin a and antioxidant activities of green and roasted coffees and corresponding byproducts, *J. Agric. Food Chem.* 55 (2007) 10499-10504, <https://doi.org/10.1021/jf071959+>.
- [55] T.G. Toschi, V. Cardenia, G. Bonaga, M. Mandrioli, M.T. Rodríguez-Estrada, Coffee silverskin: Characterization, possible uses, and safety aspects, *J. Agric. Food Chem.* 62 (2014) 10836-10844, <https://doi.org/10.1021/jf503200z>.
- [56] S. Saednia, A. Manayi, A.R. Gohari, M. Abdollahi, The story of beta-sitosterol - a review, *Eur. J. Med. Plants.* 4 (2014) 590-609, <https://doi.org/10.9734/ejmp/2014/7764>.
- [57] T. Qu, W. Guo, L. Shen, J. Xiao, K. Zhao, Experimental study of biomass pyrolysis based on three major components: hemicellulose, cellulose, and lignin, *Ind. Eng. Chem. Res.* 50 (2011) 10424-10433, <https://doi.org/10.1021/ie1025453>.
- [58] A.V. Bridgwater, Renewable fuels and chemicals by thermal processing of biomass, *Chem. Eng. J.* 91 (2003) 87-102, [https://doi.org/10.1016/S1385-8947\(02\)00142-0](https://doi.org/10.1016/S1385-8947(02)00142-0).
- [59] J. Yi, X. Li, J. He, X. Duan, Drying efficiency and product quality of biomass drying: a review, *Dry. Technol.* 0 (2019) 1-16, <https://doi.org/10.1080/07373937.2019.1628772>.



III

Submitted article

3.1 Article V (Submitted article)

The effect of reactor scale on biochars and pyrolysis liquids from slow pyrolysis of coffee silverskin, grape pomace and olive mill waste, in auger reactors

Cristina del Pozo ^{a, *}, Filipe Rego ^c, Yang Yang ^{c, *}, Neus Puy ^{a, b}, Jordi Bartrolí ^a, Esteve Fàbregas ^a, Anthony V. Bridgwater ^c

^a *Department of Chemistry, Universitat Autònoma de Barcelona (UAB), Edifici Cn, Campus de la UAB, 08193 Cerdanyola del Vallès, Barcelona, Spain.*

^b *Forest Science and Technology Centre of Catalonia (CTFC), Crta. Sant Llorenç de Morunys, km 2, 25280 Solsona, Lleida, Spain*

^c *Bioenergy Research Group, EBRI, Aston University, Birmingham B4 7ET, United Kingdom*

* Corresponding authors: crisdelpozo19@gmail.com (C. del Pozo), y.yang6@aston.ac.uk (Y. Yang).

The effect of reactor scale on biochars and pyrolysis liquids from slow pyrolysis of coffee silverskin, grape pomace and olive mill waste, in auger reactors

Cristina del Pozo ^{a,*}, Filipe Rego ^c, Yang Yang ^{c,*}, Neus Puy ^{a,b}, Jordi Bartrolí ^a, Esteve Fàbregas ^a, Anthony V. Bridgwater ^c

^a *Department of Chemistry, Universitat Autònoma de Barcelona (UAB), Edifici Cn, Campus de la UAB, 08193 Cerdanyola del Vallès, Barcelona, Spain.*

^b *Forest Science and Technology Centre of Catalonia (CTFC), Crta. Sant Llorenç de Morunys, km 2, 25280 Solsona, Lleida, Spain*

^c *Bioenergy Research Group, EBRI, Aston University, Birmingham B4 7ET, United Kingdom*

* Corresponding authors: crisdelpozo19@gmail.com (C. del Pozo), y.yang6@aston.ac.uk (Y. Yang).

Abstract

Several studies have addressed the potential biorefinery, through pyrolysis, of coffee silverskin (CSS), grape pomace (GP) and olive mill waste (OMW), which are respectively the main solid residues from coffee roasting, wine making and olive oil production processes. However, not using the same reactor, especially if they have different sizes, may affect the properties and so, applications, of the resulting products, hampering the transferability of existing research. The aim of this study is then to perform pilot scale experiments to compare and verify the results of analytical study (TGA) and bench scale reactor runs, in order to understand the fundamental differences and create correlations on pyrolysis runs at different scale. To this end, pyrolysis liquids and biochars from the slow pyrolysis of CSS, GP and OMW, performed using same temperatures and solid retention time (10 min), but different scale reactors (15 kg/h and 0.3 kg/h), have been analysed (TGA, pH, density, proximate and ultimate analyses, HHV, FTIR, GCMS) and compared. The results showed no major differences in biochars; however, in pyrolysis liquids, the ones from pilot plant were richer in 2,6-dimethoxy-phenols and phenolics para-substituted by carbonyl groups, than lab reactor liquids. Moreover, GP 400 °C biochars showed the best properties for combustion; CSS biochars were especially rich in nitrogen, and

Abbreviations: CSS, Coffee Silverskin; GP, Grape Pomace; OMW, Olive Mill Waste; NAP, Non-Aqueous Phase of the pyrolysis liquid; AP, Aqueous Phase of the pyrolysis liquid

400 °C GP and OMW pyrolysis liquids showed the highest number of phenolics. Hence, this study addressed the transferability of CSS, GP and OMW pyrolysis-based biorefinery research, in a way towards a circular bioeconomy.

Keywords

Biochar; pyrolysis liquid; agricultural wastes; pyrolysis auger reactor; scale-up

1. Introduction

From the past half-decade, circular economy has been gaining attention due to its implication on sustainability, addressing the social, economic, and environmental concerns brought by the linear economic model (Ubando et al., 2020). The goal of circular economy has been to remodel the life cycle of a product, minimizing the resource consumption and waste generation, for instance, by industrial symbiosis, which consists of reusing the industrial by-products within the industrial network (Chertow, 2007). Biorefinery, employed to generate bio-products, biochemicals, and bioenergy from different types of biomass, also acts as a strategic mechanism for the realisation of a circular bioeconomy, which is based on the use of bioproducts (European Commission, 2017). The utilisation of agricultural wastes in biorefinery can additionally address the issue of environmental pollution, managing the mention wastes in a sustainable way by converting them in a resource (Ubando et al., 2020). Different technologies have been investigated in order to carry out the biorefinery process, including pyrolysis.

Pyrolysis consists of a thermochemical degradation, carried out at elevated temperatures under oxygen-limiting conditions, where the principal polymers of biomass (hemicellulose, cellulose and lignin) decompose into solid, liquid and gas fractions (Brassard et al., 2017; del Pozo et al., 2018). The resulting solid fraction (biochar) has been used in a broad range of applications, including soil amendment to increase crop yields (Rehrah et al., 2014; Tan et al., 2015; Wang and Liu, 2017), adsorbent of both organic and inorganic contaminants, heavy metals and pesticides in soil and water mediums (Cabrera et al., 2014; Tan et al., 2015; Wang and Liu, 2018, 2017; Xie et al., 2015), and as a negative emission technology (NET) to sequester carbon in soil (Smith, 2016) and to reduce greenhouse gas emissions (Brassard et al., 2016), thus mitigating global warming. Regarding the pyrolysis liquid, it usually contains a multitude of value-added chemicals, such as phenolics, levoglucosan and organic acids, that can be

extracted and valorised (del Pozo et al., 2018; Ren et al., 2017). Gas fraction, on the other hand, is often used to provide heat to the pyrolysis process, which can make the technology independent of external energy sources (Brassard et al., 2017). The properties, and so applications, of the resulting pyrolysis products are nevertheless highly influenced by the biomass feedstock, pyrolysis technology and operating parameters (mainly retention time and temperature), determining the proportions and characteristics of each product (Brassard et al., 2017).

The present work analyses the biochars and pyrolysis liquids from slow pyrolysis, performed in two auger reactors (a pilot plant of 15 kg/h, and a lab size reactor of 0.3 kg/h), at several temperatures and with a solid residence time of 10 min, of coffee silverskin (CSS), grape pomace (GP) and olive mill waste (OMW), which are respectively the main solid residues from the coffee roasting, wine making and olive oil production processes. Previous studies have shown the potentialities of CSS biochars as adsorbents of organic pollutants in water, apart from as a renewable energy source from its combustion (del Pozo et al., 2021b, 2020). Regarding GP and OMW biochars, Jin et al., (2020) evaluated the Pb adsorption from water by using GP biochars; Hmid et al., (2014) considered OMW biochar as a possible fuel candidate, as well as, suitable for amendment in agricultural soils and for long term carbon sequestration; besides, Hanandeh et al., (2016) indicated that OMW biochar can be also a good adsorbent for treatment of water contaminated with Hg^{2+} . On the other hand, CSS pyrolysis liquid can be considered as a potential source of mainly caffeine and phenolics, the latter being highly valued in cosmetic and nutraceuticals industries due to their antioxidant properties (del Pozo et al., 2021b, 2020). In the same way, GP and OMW pyrolysis liquids have also shown to be particularly rich in phenolics (del Pozo et al., 2021a, 2018). Hence, the mentioned studies show promising results for potential biorefinery of CSS, GP and OMW through slow pyrolysis. Nevertheless, most of the research has been performed in a lab scale, so it is necessary a scale-up study to implement the research in an industrial level, being reactor capacity, together with temperature and retention time, the parameters that usually most influence on the properties of the resulting products (Brassard et al., 2017).

Thus, the aim of this work is to study and compare the biochars and pyrolysis liquids from the slow pyrolysis of CSS, GP and OMW, performed at same temperatures and solid retention time, but using different size auger reactors (0.3 kg/h and 15 kg/h), in order to understand the fundamental difference and create correlations on pyrolysis runs at different scale. This will give information about the robustness of the pyrolysis process, which would allow to implement the existing research in different auger reactors, thus making the biorefinery of the

discussed agricultural by-products more feasible. Moreover, the potentialities of the pyrolysis products were also justified within a biorefinery perspective.

2. Materials and methods

2.1. Feedstock

CSS, GP and OMW were supplied respectively by a roasting coffee company, wine company and olive oil cooperative from Catalonia, located in the north-east of Spain.

The pre-treatment performed on the feedstocks before slow pyrolysis consisted of natural drying and then crushing with a hammer crusher, as described in the following previous publications: CSS (del Pozo et al., 2020), GP (del Pozo et al., 2021) and OMW (del Pozo et al., 2018).

2.2 Reactor systems

CSS was processed in a lab scale auger pyrolysis reactor (Fig. I) at heating temperature of 280 °C, 400 °C and 500 °C, GP at 225 °C and 400 °C, and OMW at 400 °C. In order to compare the resulting products with the ones obtained from a pilot plant (B) (del Pozo et al., 2021a, 2020, 2018), the solid residence time was fixed at 10 min for both reactors.

The detailed operating information of the lab scale reactor shown in Fig. I (A) has been described elsewhere (Yu et al., 2016). The system was first purged with nitrogen gas to remove the oxygen, and the feeding rate was fixed at 0.3 kg/h.

On the other hand, the pyrolysis products from the pilot scale reactor were produced and provided by Energ-bas company, using a pilot plant described elsewhere (Recari et al., 2017). The pyrolysis process in the pilot plant was carried out without a previous purge, using a feeding rate of 15 kg/h (see Fig. I, B).

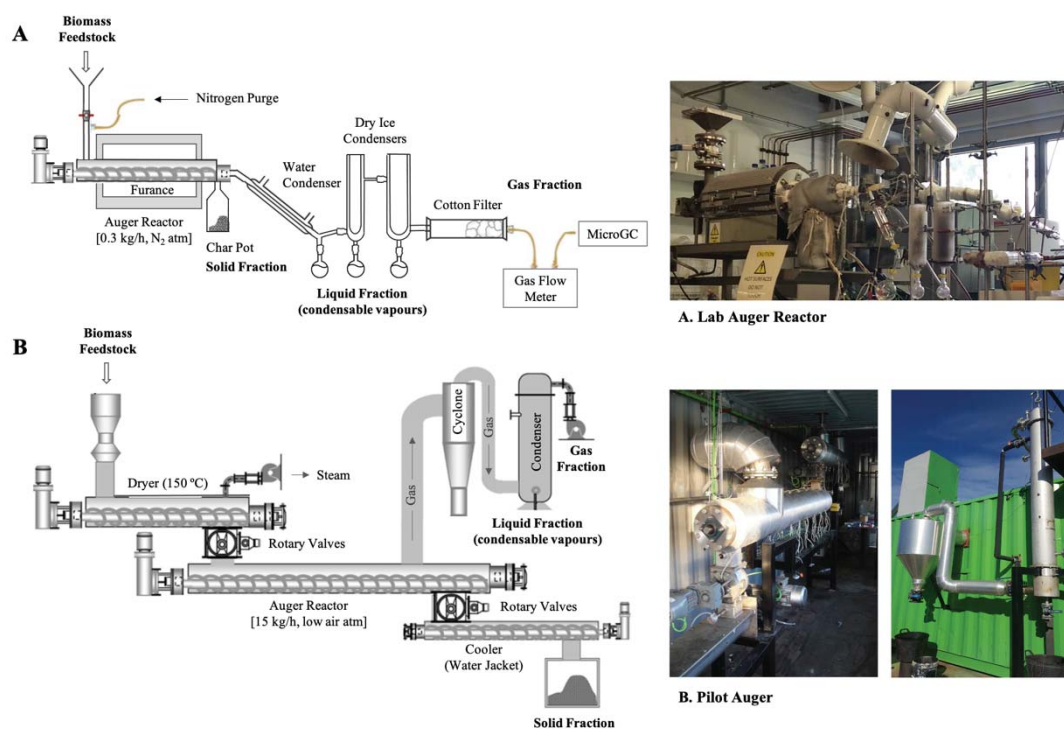


Fig. I. Schematic diagram of the lab auger pyrolysis system (A) at Aston University, and the pilot plant (B) at ENER-G-bas company.

2.3 Product yields

Product yields from the lab auger experiments were the quotient of dividing the mass of the solid, liquid and gas pyrolysis products and the mass of the feedstocks in dry basis. In order to express the data on a dry basis, moisture of CSS, GP and OMW were measured, resulting in 10.05 wt. % (standard deviation (s) = 0.15), 10.86 wt. % (s = 0.13) and 8.89 wt.% (s = 0.13), respectively. The moisture content measurements, performed in triplicate and averaged, were calculated as the lost weight after heating 1.5 g of feedstock at 105 °C overnight. Pyrolysis liquids from up to 400 °C consisted of two phases, an aqueous phase (AP) and a non-aqueous phase (NAP), which were separated (by decantation) and weighed (del Pozo et al., 2021b). Gas product weight was calculated using the following formula, based on the ideal gas law:

$$m \text{ (g)} = \frac{V \cdot MW \cdot P}{R \cdot T} \quad (1)$$

V (L) was the gas volume measured by the gas meter; the pressure (P , atm) and the temperature (T , K) was assumed to be 1 atm and 293.15 K, respectively; R was the ideal gas law constant (0.0821 atm L/ mol K); and MW (g/mol) was the average molecular weight of the gas calculated according to Eq. 2.

$$MW_{\text{gas}} = \sum \frac{\%A_i \cdot MW_i}{100} \quad (2)$$

where %A_i was the area percentage obtained from MicroGC measurement (GC; VARIAN CP-4900, USA), and MW_i was the molecular weight of the gas products. The losses from the experiments were calculated by difference (del Pozo et al., 2021b).

2.4 Analysis of feedstock and biochars

The bulk density, pH, thermogravimetric analysis (TGA), proximate analyses (ash and volatile matter contents), surface functional groups (measured by Fourier-transform infrared spectroscopy, FTIR), elemental composition (CHNS) and higher heating value (HHV) (calculated from Channiwala and Parikh (2002) formula) of CSS, GP, OMW and the resulting biochars were measured as described in del Pozo et al., (2021b).

Before the analyses (pH, TGA, FTIR, elemental), CSS, GP and the derived biochars were ground and sieved to a particle size under 425 µm (del Pozo et al., 2021b). OMW samples were analysed without being ground due to their relatively higher hardness. All feedstocks and biochars were then dried at 105 °C, overnight.

2.5 Analysis of pyrolysis liquids

Pyrolysis liquids were analysed by gas chromatography – mass spectroscopy (GC-MS) as described in del Pozo et al., (2021b). The analyses were carried out in a Shimadzu GCMS QP2010 SE system equipped with a capillary (Rtx-5MS) column (30 m × 0.25 mm inner diameter × 0.25 µm film thickness). Specifically, the analysed samples were the ones collected after the water-cooled condenser (first flask) (see Fig. I, A).

The pyrolysis liquids from the pilot plant, on the other hand, were described in the following publications: del Pozo et al., (2020) for CSS, del Pozo et al., (2021) for GP, and del Pozo et al., (2018) for OMW.

3. Results and discussion

3.1. Pyrolysis process

3.1.1 Thermal degradation of feedstocks and biochars

Thermal degradation of CSS, GP, OMW and the biochars resulting from slow pyrolysis using the lab and pilot auger reactors was studied through TGA analysis (see Fig. II), which shows

how the main polymers of biomass (hemicellulose, cellulose, and lignin) decompose in function of temperature, under nitrogen atmosphere conditions.

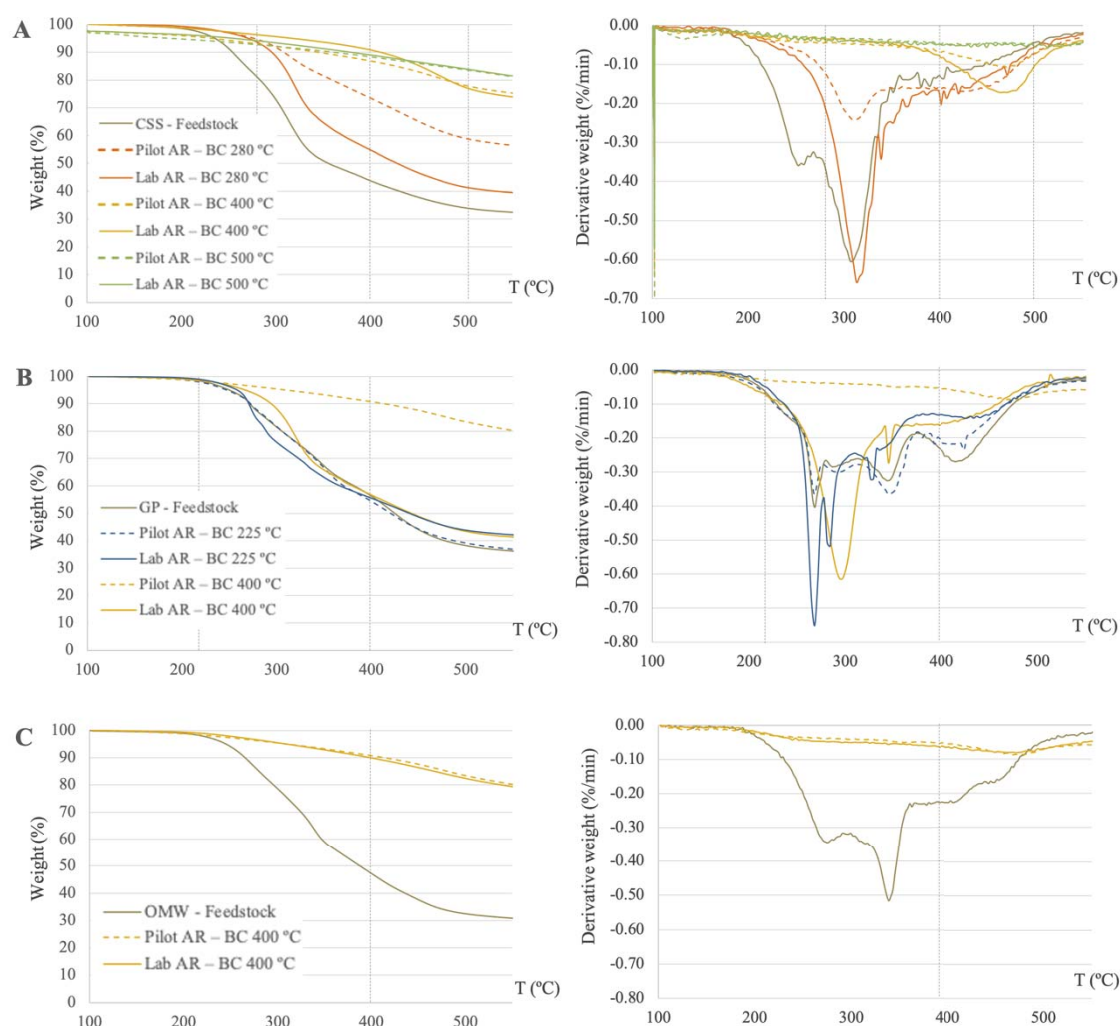


Fig. II. Pyrolysis TGA curves of CSS (A), GP (B), OMW (C) and their respective biochars from the slow pyrolysis at different temperatures, performed at pilot and lab auger reactors. The left graphs show the weight loss of feedstocks and biochars, and the right graphs show their rate of weight loss, on dry basis. (CSS, Coffee Silverskin; GP, Grape Pomace; OMW, Olive Mill Waste; BC, Biochar; AR, Auger Reactor; T, Temperature)

Degradation of hemicelluloses takes place around 220–315 °C (Yang et al., 2007); cellulose, at around 240-350 °C (Mohan et al., 2006), and lignin, which is more difficult to decompose, between 215-585 °C (Zhao et al., 2017). This is reflected on the derivative weight curves of feedstock (see Fig. II), that show three main peaks; the first two correspond to hemicellulose

and cellulose, and the third one, with a wider and flat shape, to lignin. These peaks were reduced in biochars as the temperature of the pyrolysis process increased (see Fig. II), showing how CSS, GP and OMW degraded at the different pyrolysis conditions.

From Fig. II, some differences, although with relatively low significance, were observed between biochars from lab and pilot reactors in terms of the thermal degradation behaviour. CSS graph (see Fig. II, Graph A) presented close values to published data (Polidoro et al., 2018). However, comparing with the previous study of CSS (del Pozo et al., 2020), lignin peak was in that case almost imperceptible. The difference between these data could be related to a different composition of CSS, which consists of a mixture from various roasting processes, performed with different types and proportion of coffees. As shown in Fig. II (Graph A), CSS biochars from pilot and lab reactors presented same peaks, although in lab biochars, the intensity of peaks was higher, mostly in 280 °C case. This could be interpreted as a higher concentration of cellulose in lab CSS samples. Biochars from 280 °C experiments evidenced the decomposition of hemicellulose during the pyrolysis process, since just cellulose and lignin peaks were observed; pyrolysis at 400 °C degraded hemicellulose and cellulose, resulting in lignin-based biochars; at 500 °C, all three polymers were decomposed (see Fig. II, Graph A). It was also observed that in 400 °C biochars, lignin peak changed its maximum to around 470 °C (see Fig. II, Graph A, B, C), fact that could be attributed to structural modifications of lignin at elevated temperatures (Rehrah et al., 2014).

In GP samples (see Fig. II, Graph B), the differences between pilot plant and lab reactor biochars were most notable. Data from pilot plant biochars was as expected; 225 °C biochar was very similar to GP feedstock, since at this temperature almost nothing is degraded. 225 °C lab biochar also showed similar peaks to those of GP, although with different intensity. In reference to 400 °C biochars, pilot plant data was comparable to the ones obtained from the other 400 °C biochars of the study, except for GP lab biochar, which seemed to degrade at a lower temperature, presenting cellulose and lignin peaks in a very similar way as 280 °C CSS biochars did (see Fig. II, Graph A and B).

OMW biochars, on the other hand, did not show significant differences between biochars (see Fig. II, Graph C).

Hence, based on TGA analysis, biochar thermal degradation under inert atmosphere seemed to not be significantly influenced by the reactor scales used (lab and pilot augers) in the slow pyrolysis of CSS, GP, OMW.

3.1.2 Product yields

The product yields from the experiments performed at the lab auger plant (see Table I) showed expected trends: as the temperature of the process increased, solid fraction decreased, and liquid and gas fractions increased. Product yields are therefore indicators of how biomass degrades during the pyrolysis process, thus contributing to determine the best operating temperature in function of the desired pyrolysis products.

Table I

Product yields from the slow pyrolysis of CSS, GP and OMW at the lab auger reactor. Data is expressed as wt. % on dry feedstock basis. (CSS, Coffee Silverskin; GP, Grape Pomace; OMW, Olive Mill Wastes; AP, Aqueous Phase of the pyrolysis liquid; NAP, Non-Aqueous Phase of the pyrolysis liquid)

	CSS			GP		OMW
	280 °C	400 °C	500 °C	225 °C	400 °C	400 °C
Solid residue from TGA¹	80.7	43.6	33.7	97.5	56.3	47.2
Product yields						
Solid	80.5	40.5	31.5	93.5	54.1	38.8
Liquid - AP	4.1	15.4	15.7	-	14.8	40.3
Liquid - NAP	-	18.2	22.6	-	6.3	1.8
Gas	10.5	21.5	24.5	3.4	17.5	19.9
Losses	4.9	4.4	5.7	3.1	7.3	- 0.8

¹ Data obtained from the TGA analysis of CSS, GP and OMW feedstocks.

As shown in Table I, solid fraction (wt.%) was consistent with TGA analysis. Due to the similarity seen in CSS and GP solid yields between lab reactor and TGA data, taking into account the different heating conditions and amounts used, it could be expected that pilot plant experiments had similar values. Concerning OMW, the differences observed between OMW values were probably due to the heterogeneity of the feedstock, which is composed of olive stones (major proportion), pulp, skin and stalks. Hence, in this case, product yields seemed to depend mainly on the biomass feedstocks and the temperature of the process. As shown in Table I, pyrolysis liquids produced at temperatures ≥ 400 °C consisted of an aqueous phase (AP) and a non-aqueous phase (NAP). Slow pyrolysis usually results in two-phase liquid because of the high amount of reaction water produced, separating the hydrophilic and hydrophobic products in AP and NAP (del Pozo et al., 2018; Torri and Fabbri, 2014).

Hydrophilic products are mainly related to hemicellulose and cellulose degradation, while the hydrophobic ones come mostly from lignin decomposition. This resulted in phase separation only occurring for the experiments performed at higher temperatures (400 and 500 °C), where higher amount of lignin was decomposed. Regarding GP 225 °C, the liquid generated came mainly from moisture, not being represented in Table I since data is expressed on dry feedstock basis. Losses, on the other hand, are mainly associated with the fact that mostly CSS and GP could have remained inside the reactor. In the case of OMW, this did not occur to such a significant extent due to the greater density of this feedstock compared to the others.

3.2 Characterisation of feedstocks and biochars

In order to compare the products obtained from the slow pyrolysis of CSS, GP and OMW at the lab and pilot auger reactors, the resulting biochars (and the feedstocks) were analysed through proximate and ultimate analyses, pH value, and density (see Table II and Fig. III and IV). In addition, the characterisation of the resulting biochars also provided information about their potential suitability in different applications.

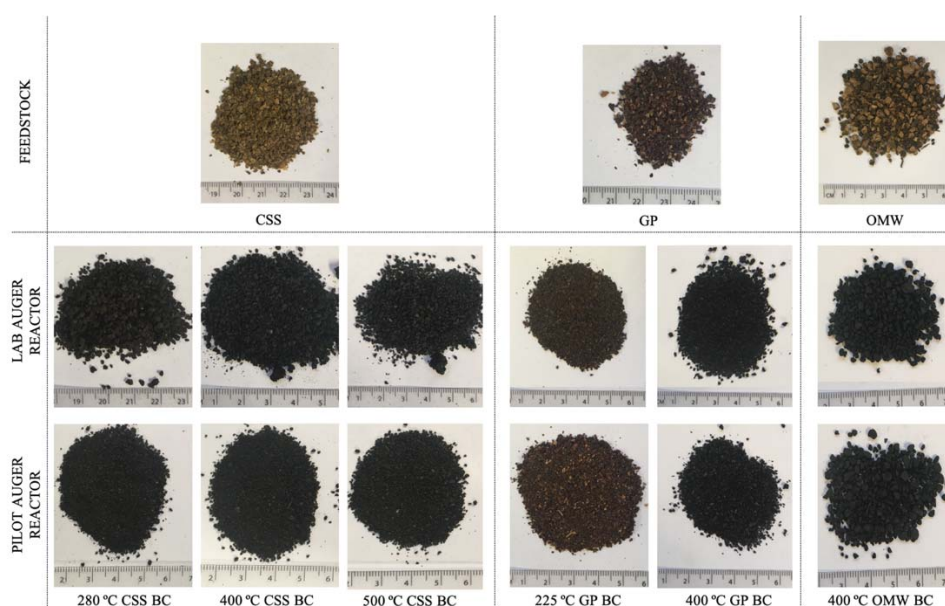


Fig. III. CSS, GP and OMW feedstocks, and biochars from the slow pyrolysis of these compounds, performed at the lab and pilot auger reactors, at different temperatures. The unit of the ruler is in cm. (CSS, Coffee Silverskin; GP, Grape Pomace; OMW, Olive Mill Waste; BC, Biochar)

Table II

Characterisation of CSS, GP, OMW and their respective biochars from slow pyrolysis at different temperatures. Data is expressed as Mean (standard deviation). Ash, proximate and ultimate analysis are expressed as wt. % on dry basis. (CSS, coffee silverskin; GP; Grape Pomace; OMW, Olive Mill Waste; BC, Biochar; AR, Auger Reactor; VM, Volatile Matter; FC, Fixed Carbon; HHV, Higher Heating Value; BET surface area)

	CSS ³	CSS BC 280 °C		CSS BC 400 °C		CSS BC 500 °C	
		Lab AR ³	Pilot AR	Lab AR ³	Pilot AR	Lab AR ³	Pilot AR
Density (g/mL)	0.314 (0.006)	0.256 (0.005)	0.191 (0.002)	0.197 (0.003)	0.194 (0.003)	0.186 (0.010)	0.161 (0.005)
pH	5.358 (0.029)	6.660 (0.035)	7.10 (0.25)	8.900 (0.000)	8.30 (0.19)	10.052 (0.049)	10.112 (0.019)
<u>Proximate Analysis</u>							
VM (%)	65.78 (0.40)	70.43 (0.67)	59.7 (3.5)	41.80 (0.16)	41.235 (0.088)	38.5 (1.7)	37.84 (0.71)
FC (%)¹	26.74 (0.65)	21.0 (1.2)	29.6 (3.1)	41.90 (0.37)	42.17 (0.31)	40.74 (0.66)	38.8 (2.5)
Ash (%)	7.48 (0.25)	8.62 (0.55)	10.75 (0.42)	16.29 (0.53)	16.60 (0.40)	20.7 (1.1)	23.4 (3.2)
<u>Ultimate Analysis</u>							
N (%)	3.504 (0.072)	3.370 (0.090)	3.646 (0.042)	3.099 (0.018)	3.246 (0.033)	2.897 (0.050)	2.80 (0.14)
C (%)	47.685(0.023)	54.23 (0.39)	55.03 (0.27)	60.10 (0.61)	55.71 (0.25)	60.78 (0.72)	56.53 (0.94)
H (%)	5.611 (0.000)	5.868 (0.024)	4.752 (0.072)	4.442 (0.066)	3.33 (0.12)	2.591 (0.047)	2.200 (0.045)
S (%)	0.243 (0.025)	0.110 (0.009)	0.142 (0.013)	0.044 (0.062)	0.139 (0.028)	0.148 (0.022)	0.173 (0.020)
O (%)¹	34.657(0.024)	28.42 (0.49)	21.43 (0.38)	15.92 (0.62)	17.57 (0.19)	11.78 (0.84)	12.6 (1.1)
Molar H/C	1.402 (0.001)	1.289 (0.004)	1.029 (0.010)	0.881 (0.022)	0.713 (0.028)	0.508 (0.003)	0.464 (0.002)
Molar O/C	0.546 (0.000)	0.393 (0.010)	0.292 (0.007)	0.199 (0.010)	0.237 (0.004)	0.146 (0.012)	0.167 (0.017)
Molar (O+N)/C	0.609 (0.001)	0.447 (0.009)	0.349 (0.006)	0.243 (0.010)	0.287 (0.003)	0.186 (0.012)	0.210 (0.016)
HHV (MJ/kg)²	19.471(0.009)	22.70 (0.21)	22.24 (0.22)	24.18 (0.21)	21.102 (0.030)	22.56 (0.39)	20.46 (0.49)

Chapter III

	GP	GP BC 225 °C		GP BC 400 °C		OMW	OMW BC 400 °C	
		Lab AR	Pilot AR	Lab AR	Pilot AR		Lab AR	Pilot AR
Density (g/mL)	0.461 (0.019)	0.484 (0.024)	0.465 (0.011)	0.272 (0.002)	0.245 (0.008)	0.628 (0.024)	0.386 (0.015)	0.364 (0.005)
pH	3.71 (0.10)	3.682 (0.029)	3.394 (0.063)	7.790 (0.019)	8.190 (0.050)	5.328 (0.023)	7.522 (0.024)	8.200 (0.029)
<u>Proximate Analysis</u>								
VM (%)	67.98 (0.29)	70.9 (1.8)	70.3 (1.7)	70.1 (1.1)	35.10 (0.18)	68.8 (1.9)	33.55 (0.60)	35.10 (0.18)
FC (%)¹	24.15 (0.35)	19.7 (3.1)	25.8 (1.6)	22.0 (1.1)	54.9 (2.0)	25.5 (4.0)	61.7 (4.4)	60.9 (2.3)
Ash (%)	7.87 (0.96)	9.4 (1.3)	3.87 (0.10)	7.903 (0.016)	10.0 (1.9)	5.7 (2.1)	4.8 (5.0)	3.9 (2.5)
<u>Ultimate Analysis</u>								
N (%)	2.30 (0.22)	1.8 (1.0)	1.33 (0.66)	2.06 (0.62)	1.341 (0.041)	1.9 (1.2)	1.4 (1.1)	0.87 (0.49)
C (%)	51.91 (0.91)	53.50 (0.49)	52.41 (0.54)	65.68 (0.42)	66.3 (3.0)	51.0 (2.7)	61.3 (7.2)	59 (21)
H (%)	6.271 (0.026)	6.28 (0.42)	5.98 (0.50)	4.92 (0.60)	3.175 (0.019)	6.69 (0.61)	4.33 (0.83)	2.93 (0.28)
S (%)	0.103 (0.003)	0.052 (0.074)	0.035 (0.049)	0.000 (0.000)	0.000 (0.000)	0.114 (0.089)	0.000 (0.000)	0.000 (0.000)
O (%)¹	32.41 (0.66)	31.3 (2.0)	34.2 (1.7)	16.24 (0.79)	17.3 (3.1)	40.3 (3.8)	32.9 (9.2)	37 (21)
Molar H/C	1.440 (0.031)	1.399 (0.081)	1.36 (0.10)	0.89 (0.11)	0.571 (0.023)	1.562 (0.088)	0.837 (0.062)	0.63 (0.18)
Molar O/C	0.469 (0.018)	0.439 (0.032)	0.491 (0.030)	0.186 (0.008)	0.197 (0.044)	0.597 (0.083)	0.41 (0.16)	0.56 (0.33)
Molar (O+N)/C	0.507 (0.022)	0.468 (0.016)	0.512 (0.019)	0.213 (0.000)	0.214 (0.044)	0.629 (0.077)	0.43 (0.15)	0.57 (0.33)
HHV (MJ/kg)²	21.99 (0.36)	22.67 (0.87)	21.66 (0.96)	26.78 (0.63)	24.8 (1.4)	21.4 (2.0)	23.0 (4.4)	20.1 (9.3)

¹ Fixed carbon and oxygen content calculated by difference.

² HHV calculated from Channiwala and Parikh, (2002) formula.

³ Data obtained from del Pozo et al., (2021)

The degradation of biomass is related to the temperature of the pyrolysis process (see Section 3.1.1); as the temperature increases, the biomass decomposes removing the volatile compounds and concentrating the content of fixed carbon and ash (mineral, alkali metals), that remain in the generated biochar (Chen et al., 2016; Wang and Liu, 2018). In the same way, biochar density decreases with the increase of the pyrolysis temperature due to the removal of volatiles (del Pozo et al., 2021b). This trend was reflected in the proximate analysis and density data from Table II. Regarding the biochars from lab and pilot auger reactors, the information obtained from these analyses showed some differences, although with relatively low significance. Specifically, CSS biochars presented similar data in 400 °C and 500 °C lab and pilot reactor experiments, but it was quite different in 280 °C case, being in agreement with TGA analysis (see Section 3.1.1), that showed a higher concentration of cellulose in lab biochar. Concerning GP experiments, it was expected that 225 °C biochars and GP feedstock had similar values, since at this low temperature almost nothing degraded (see Section 3.1.1). Nevertheless, as shown in Table II, ash data presented some differences, which were also translated to fixed carbon data (calculated by difference). 400 °C biochars also showed significant differences, where, in agreement with TGA analysis (see Section 3.1.1) and Table II, lab biochar seemed to be degraded at a lower temperature (proximate analysis showed similar values for 400 °C lab biochar, GP feedstock and 225 °C biochars). In reference to OMW, lab and pilot plant biochars presented similar values. Moreover, Table II also confirmed that the effect of feedstock type on ash content is stronger than the pyrolysis condition (Wang and Liu, 2017), since the higher differences in ash were observed between feedstocks types instead of biochars from different reactors.

On the other hand, the pH of feedstocks and biochars is related to their mineral content, which increases with the increase of the pyrolysis temperature (del Pozo et al., 2021b; Wang and Liu, 2018). In this sense, Wang and Liu (2017) observed that biochars produced beyond 300 °C had a basic pH and that the pH values increased until 600 °C, a fact that was attributed to the separation of alkali salts from the organic matrix of biochar (Novak et al., 2009; Rehrah et al., 2014; Wang and Liu, 2017). Thus, the alkalinity of the biochars justifies their potential use as amendment to neutralize soil acidity (Chen et al., 2016). pH values from Table II also showed to be consistent with the pyrolysis temperature of biochars, which presented similar values, regardless of feedstock type and pyrolysis reactor.

Ultimate analysis (CHNO%) and molar ratios were used to estimate the aromaticity (H:C), polarity (O:C) and oxygen functionality ((O+N):C) of biochars (Lou et al., 2016), providing

information about how CSS, GP and OMW degraded. During the pyrolysis process, biomass undergoes dehydration, decarboxylation and decarbonylation reactions, forming volatile compounds that are released, and graphitic and aromatic structures that condense in the generated biochar (Keiluweit et al., 2010; Liu and Han, 2015; Uchimiya et al., 2011; Wang and Liu, 2018). In this way, with the increasing of pyrolysis temperature, %C increased, and %H and %O decreased, resulting in the decreasing of molar ratios (H/C, O/C, (O+N)/C) (see Table II). On the other hand, it was also observed that lab scale biochars had higher %H and %C than biochars from the pilot reactor. This could be due to the formation of secondary chars in the lab reactor, where volatile organics could condense onto the solid primary char during the thermochemical process (Lucian et al., 2018). The lower vapor retention time of the pilot plant, caused by a fan sucking the product vapours and so, removing them quicker than in the lab scale reactor, makes that, in this case, the secondary reactions took place to a lesser extent. Moreover, Table II showed that N% content was especially high in CSS samples (3%), a fact that promotes its use as compost (del Pozo et al., 2021b).

Regarding the calorific values (HHV) (see Table II), they were calculated from ash and ultimate analysis following Channiwala and Parikh (2002) mathematic formula (see Section 2.4); therefore, the differences observed in these analyses were also reflected in HHV data. Seen from Table II, calorific values increased with the increase of pyrolysis temperature; this is due to HHV data are specially determined by C% content (Chen et al., 2016). Within the different biochars of the study (see Table II), GP 400 °C were the most suitable for combustion, since they not just had the highest calorific values (27 MJ/kg), but also presented low sulphur content (avoiding sulphur oxides emissions) and low ashes (reducing the engine maintenance associated with the combustion process).

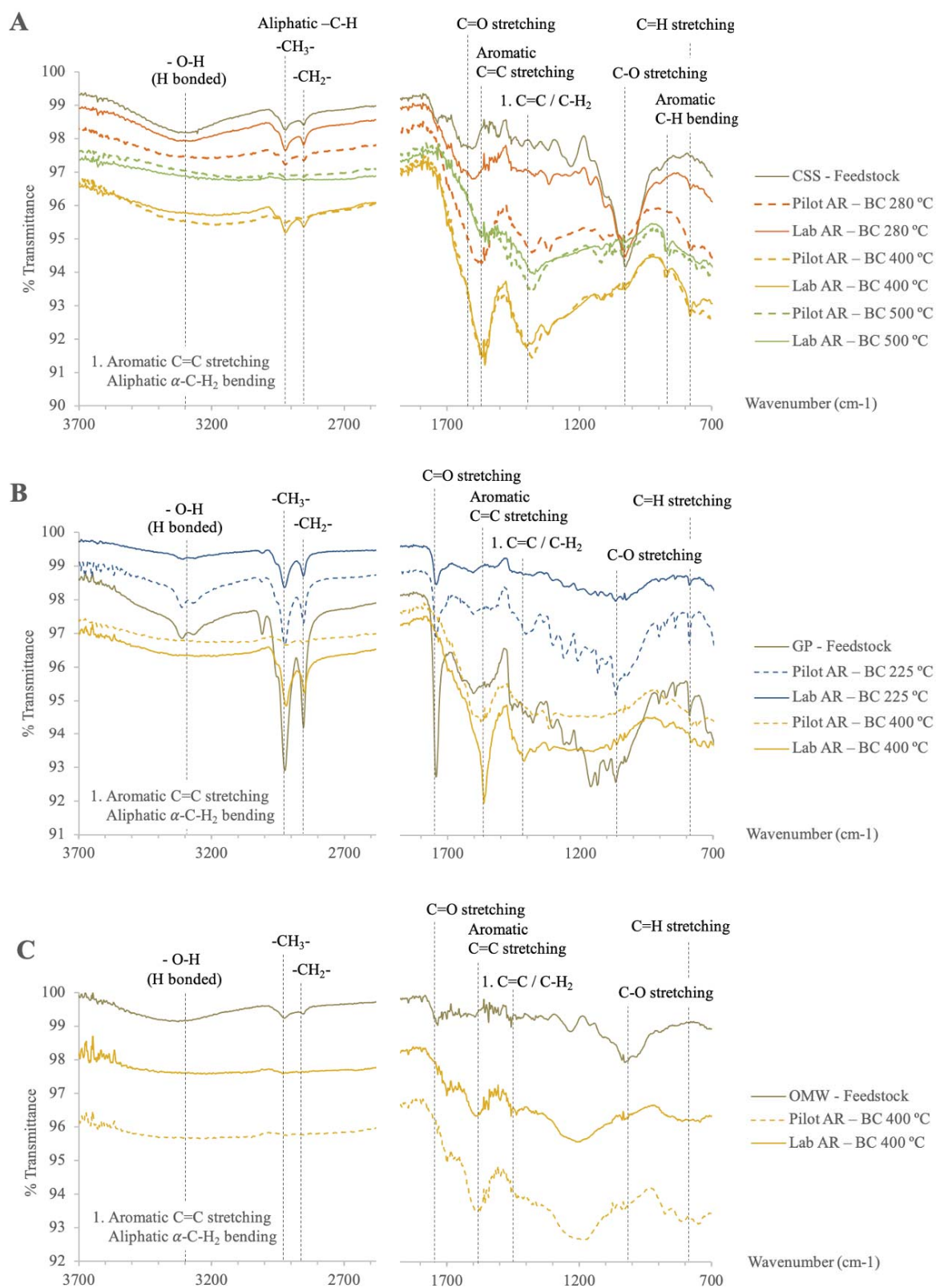


Fig. IV. FTIR spectra for CSS, GP and OMW feedstocks, and biochars from the slow pyrolysis of these compounds, performed at the lab and pilot auger reactors, at different temperatures.

FTIR spectra, on the other hand, informed about the surface functional groups of the feedstocks and biochars, showing the decomposition of CSS, GP and OMW. As shown in Fig. IV, and in agreement with ultimate analysis (see Table II), polar functional groups reduced, and aromatic and graphitic structures increased with the increase of the pyrolysis temperature (del Pozo et al., 2021b). A broad peak around 3300 cm^{-1} , related to O-H stretching vibrations from alcohols, phenols and organic acids, and $2800\text{--}3000\text{ cm}^{-1}$ peaks, corresponding to aliphatic C-H stretching vibration from methyl and methylene groups, decreased with the increase of the temperature, showing the aliphatic loss and the depolymerisation and dehydration reactions that took place during the pyrolysis process (Lou et al., 2016; Uchimiya et al., 2011; Wang and Liu, 2017). Moreover, reduction of C=O ($1630\text{--}1750\text{ cm}^{-1}$), related to carboxylate groups, and C-O ($1000\text{--}1200\text{ cm}^{-1}$) were also observed in biochars from $\geq 400\text{ }^{\circ}\text{C}$ (Uchimiya et al., 2011; Wang and Liu, 2018; Yu et al., 2016). By contrast, aromatic peaks from C=C stretching (1400 and $1620\text{--}1640\text{ cm}^{-1}$), as well as C-H bending (874 cm^{-1}) and C-H stretching ($781\text{--}873\text{ cm}^{-1}$) were enlarged in $400\text{ }^{\circ}\text{C}$ and $500\text{ }^{\circ}\text{C}$ biochars (Lou et al., 2016; Tan et al., 2015; Uchimiya et al., 2011; Wang and Liu, 2018, 2017). Thus, FTIR spectra demonstrated qualitative differences in the surface functional groups of biochars as a result of differences in the original feedstocks as well as pyrolysis temperatures. However, and in line with the observed in TGA (see Section 3.1.1) and in the analyses in Table II, no major differences were observed between biochars from lab and pilot auger reactors. In addition, FTIR analysis justifies the potential use of these biochars as adsorbents (del Pozo et al., 2021b; Hanandeh et al., 2016; Jin et al., 2020), since the surface functional groups play an important role in their adsorption capacity, namely the effectiveness of oxygen-containing functionalities for immobilizing, for instance, heavy metals (Wang and Liu, 2017).

3.3 Pyrolysis liquid

3.3.1 Pyrolysis liquid description

Pyrolysis liquids from lab and pilot auger reactors were also compared, showing similar aspects, except for CSS $400\text{ }^{\circ}\text{C}$ and $500\text{ }^{\circ}\text{C}$ pyrolysis liquids, that were composed of a single phase in pilot plant case, and two phases in lab reactor liquids (see Fig. V). This fact could be related to the different composition of feedstock, being the one from lab reactor richer in lignin (See Section 3.1.1), thus facilitating the phase separation to take place by increasing the number of hydrophobic compounds (resulting from the degradation of lignin) in the lab pyrolysis

liquids. Moreover, the different vapor retention time of the reactors could also affect the composition of the pyrolysis liquids and so, its appearance, being secondary reactions more favoured in the lab auger reactor, due to its longer vapor retention time.

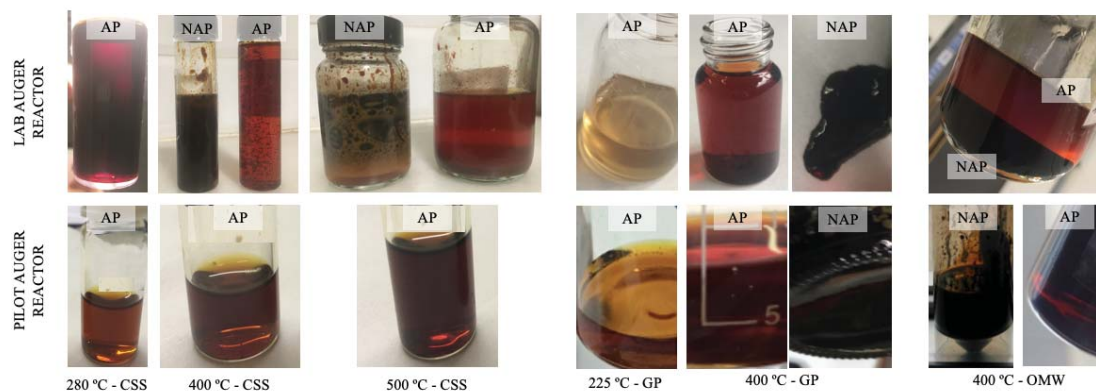


Fig. V. Pyrolysis liquids from the slow pyrolysis of CSS, GP and OMW feedstocks, performed at lab and pilot auger reactors, at different temperatures. (CSS, Coffee Silverskin; GP, Grape Pomace; OMW, Olive Mill Waste; AP, Aqueous Phase of the pyrolysis liquid; NAP, Non-Aqueous Phase of the pyrolysis liquid)

3.3.2 Pyrolysis liquid composition

Pyrolysis liquids were composed of a multitude of low molecular weight oxygenated products from the decomposition of hemicellulose, cellulose and lignin during the thermochemical treatments, that concentrated in the hydrophilic AP fraction (see Table III.I), or in the case of hydrophobic compounds, in NAP fraction (see Table III.II). Chemical composition of AP and NAP from lab and pilot auger reactors was analysed by GC-MS, with products from Table III being a representation of their conformation. AP (see Table III.I) mainly consist of phenolics (compounds 12 - 22) and low molecular weight oxygenated products, such as sugars (3, 4), cyclopentanones (6 - 8) or furans (10, 11); NAP (see Table III.II) mainly contained phenolics (2 - 11). As shown in Table III, and reported in previous work (del Pozo et al., 2021a, 2020, 2018), phenolics were one of the main components of the pyrolysis liquids, and also, one of the most value-added ones, since their antioxidant properties makes them highly appreciated in cosmetic and nutraceuticals industries (del Pozo et al., 2020, 2018). Apart from the above-mentioned products, AP was also composed of small molecular weight carboxylic acids (acetic acid) (del Pozo et al., 2021a, 2018), and in the case of CSS pyrolysis liquids, also of caffeine

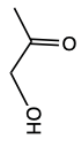
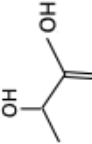

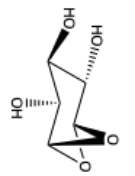
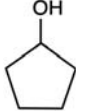
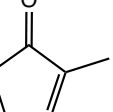
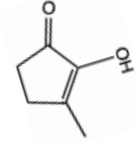
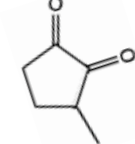
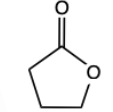
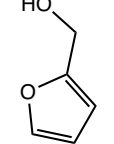
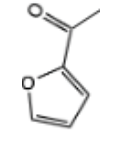
and nitrogenated products (pyridine, pyrrole, 2,4-dimethyl-2-oxazoline-4-methanol, amides and amines) (del Pozo et al., 2020). NAP, on the other hand, also contained fatty acids and esters of fatty acids, hydrocarbon chains, and in CSS case, also caffeine, nitrogenated compounds (pyridine, pyrrole, indoles) and sterols (β -sitosterol) (del Pozo et al., 2021a, 2020, 2018).

GCMS data, together with elemental analysis (see Section 3.2, Table II), indicated that secondary reactions could be mainly produced in the lab auger reactor, where the vapor retention time was longer. This can be observed in Table III, where 2,6-dimethoxy-phenols (compounds 20-22 from Table III.I, and 8-10 from Table III.II) and phenolics para-substituted by carbonyl groups (compounds 19, 22 from Table III.I) were mostly found in the pilot plant samples. The difference between lab and pilot pyrolysis liquids could be then related to the secondary reactions, being the products from lab reactor more degraded.

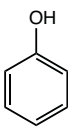
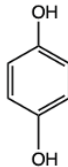
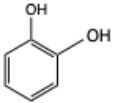
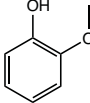
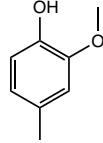
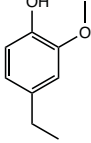
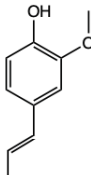
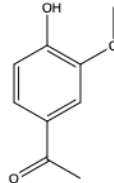
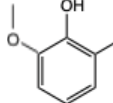
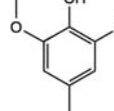
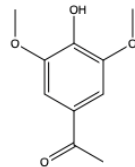
Moreover, it was also observed that OMW and GP pyrolysis liquids showed higher number of phenolic compounds compared to CSS, since part of those phenolics derives from the degradation of lignin, which is lower in CSS feedstock (Murthy and Madhava Naidu, 2012).

Table III. I

Most abundant compounds of the aqueous phase of the pyrolysis liquid obtained from the slow pyrolysis of CSS, GP and OMW at different temperatures, determined by GC–MS analysis. Data is expressed as % Area. 1) 1-Hydroxy-2-propanone; 2) L-Lactic acid; 3) 1,4:3,6-Dianhydro- α -d-glucopyranose; 4) Levoglucosan; 5) Cyclopentanol; 6) 2-Methyl-2-cyclopenten-1-one; 7) 2-hydroxy-3-methyl-2-cyclopenten-1-one; 8) 3-Methyl-1,2-cyclopentanedione; 9) Butyrolactone; 10) 2-Furanmethanol; 11) 1-(2-Furanyl)-ethanone; 12) Phenol; 13) Hydroquinone; 14) Catechol; 15) 2-Methoxyphenol; 16) Creosol; 17) 4-ethyl-2-methoxy-phenol; 18) trans-Isoeugenol; 19) Apocynin; 20) 2,6-Dimethoxy-phenol; 21) 2,6-dimethoxy-4-methylphenol; 22) 1-(4-hydroxy-3,5-dimethoxyphenyl)-ethanone (CCS, coffee silverskin; GP; Grape Pomace; OMW, Olive Mill Waste; AR, Auger Reactor)

Major compounds of the Pyrolysis liquids – Aqueous phase (% Area – GC-MS)											
	1	2	3	4	5	6	7	8	9	10	11
CSS 280 °C - Lab AR	-	-	-	-	-	-	-	0.99	-	6.24	-
CSS 280 °C - Pilot AR¹	8.92	-	1.15	-	2.69	0.11	2.30	-	0.86	0.20	0.20
CSS 400 °C - Lab AR	-	-	1.56	-	-	0.91	-	1.45	-	1.36	-
CSS 400 °C - Pilot AR¹	-	-	1.65	-	1.20	1.12	1.69	-	0.98	0.24	0.18
CSS 500 °C - Lab AR	-	-	1.03	-	-	1.41	-	0.80	-	1.15	0.47
CSS 500 °C - Pilot AR¹	-	-	1.80	-	1.02	0.51	1.62	-	0.92	0.18	-
GP 225 °C - Lab AR	-	29.94	-	-	-	-	-	-	-	2.69	-
GP 225 °C - Pilot AR²	1.55	-	1.34	15.31	6.52	-	-	1.10	0.92	0.25	-
GP 400 °C - Lab AR	-	10.46	4.01	-	-	2.09	1.70	-	-	4.16	-
GP 400 °C - Pilot AR²	3.32	-	1.14	9.76	7.08	0.42	4.93	0.31	1.28	0.73	-
OMW 400 °C - Lab AR	-	-	4.60	-	-	1.34	-	3.43	1.43	3.96	-
OMW 400 °C - Pilot AR³	5.66	-	-	3.27	-	0.48	-	2.32	1.20	0.21	-

Chapter III

Major compounds of the Pyrolysis liquids – Aqueous phase (% Area – GC-MS)											
	12	13	14	15	16	17	18	19	20	21	22
CSS 280 °C - Lab AR	1.56	0.87	1.91	2.40	-	-	-	-	0.75	-	-
CSS 280 °C - Pilot AR ¹	0.33	1.88	1.88	2.38	0.34	0.11	0.12	0.38	1.65	0.25	0.14
CSS 400 °C - Lab AR	1.59	1.33	-	2.15	0.31	1.23	0.38	-	0.25	-	-
CSS 400 °C - Pilot AR ¹	0.96	-	-	1.66	-	-	0.06	0.85	1.24	0.23	0.20
CSS 500 °C - Lab AR	1.84	-	-	0.98	-	0.45	-	-	-	-	-
CSS 500 °C - Pilot AR ¹	0.40	-	-	1.76	-	-	0.10	0.95	1.27	0.14	0.20
GP 225 °C - Lab AR	1.14	-	-	12.23	0.75	2.13	-	-	1.56	-	-
GP 225 °C - Pilot AR ²	0.11	0.68	2.72	0.35	0.50	0.26	-	1.51	6.39	2.33	2.06
GP 400 °C - Lab AR	2.30	-	3.54	13.59	4.98	2.49	-	-	1.49	-	-
GP 400 °C - Pilot AR ²	0.38	0.88	4.23	3.84	1.30	0.87	0.11	0.89	6.97	2.07	1.07
OMW 400 °C - Lab AR	1.90	-	5.98	11.76	3.03	1.57	-	-	11.47	2.26	-
OMW 400 °C - Pilot AR ³	0.32	0.13	1.16	4.29	1.21	0.62	0.41	0.31	5.24	1.46	0.40

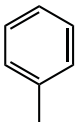
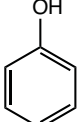
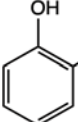
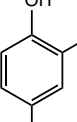
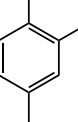
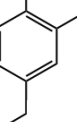
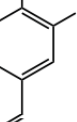
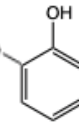
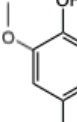
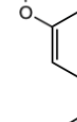
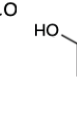
¹Data obtained from del Pozo et al., (2020)

²Data obtained from del Pozo et al., (2021)

³Data obtained from del Pozo et al., (2018)

Table III. II

Most abundant compounds of the non-aqueous phase of the pyrolysis liquid obtained from the slow pyrolysis of CSS, GP and OMW at different temperatures, determined by GC–MS analysis. Data is expressed as % Area. 1) Toluene; 2) Phenol; 3) 2-Methoxyphenol; 4) Creosol; 5) 4-Ethyl-2-methoxy-phenol; 6) 2-Methoxy-4-propyl-phenol; 7) trans-Isoeugenol; 8) 2,6-Dimethoxy-phenol; 9) 2,6-Dimethoxy-4-methylphenol; 10) E)-2,6-dimethoxy-4-(prop-1-en-1-yl)-phenol; 11) 5-tert-Butylpyrogallol (CCS, coffee silverskin; GP; Grape Pomace; OMW, Olive Mill Waste; AR, Auger Reactor).

Major compounds of the Pyrolysis liquids – Non-Aqueous phase (% Area – GC-MS)											
	1	2	3	4	5	6	7	8	9	10	11
CSS 400 °C - Lab AR	3.07	4.65	5.30	0.98	3.19	0.77	1.52	0.48	-	-	-
CSS 500 °C - Lab AR	6.28	4.67	-	-	1.02	-	-	-	-	-	-
GP 400 °C - Lab AR	1.70	3.03	14.99	10.05	11.14	4.65	3.04	2.12	-	-	-
GP 400 °C - Pilot AR ²	0.15	3.63	8.45	5.10	6.23	1.95	7.62	8.62	4.20	6.24	4.91
OMW 400 °C - Lab AR	1.00	2.15	11.56	5.08	5.53	1.99	0.80	10.81	-	1.79	5.11
OMW 400 °C - Pilot AR ³	-	1.07	15.80	8.01	7.78	1.33	7.09	-	5.83	2.81	8.87

¹Data obtained from del Pozo et al., (2020)

²Data obtained from del Pozo et al., (2021)

³Data obtained from del Pozo et al., (2018)

4. Conclusions

This study compared the biochars and pyrolysis liquids from the slow pyrolysis of CSS, GP and OMW, performed using same temperatures and solid retention time (10 min), but different scale reactors (15 kg/h and 0.3 kg/h), with the aim to understand the differences and create correlations on pyrolysis runs at different scale. No major differences were observed between the properties of biochars, meaning they could be used in similar applications, regardless of the auger reactor they have been made. However, in the pyrolysis liquids, there were several differences in their composition, being the ones from the pilot plant richer in 2,6-dimethoxyphenols and phenolics para-substituted by carbonyl groups, than lab reactor liquids. This was related to the longer vapor retention time of the lab reactor, favouring the secondary reactions and so, a higher decomposition of the pyrolysis products. Moreover, comparing the pyrolysis products between them, GP 400 °C biochars showed the best properties as solid fuel; CSS biochars were especially rich in N% content (suitable characteristic for composting), and 400 °C GP and OMW pyrolysis liquids showed the highest number of phenolics (antioxidant compounds highly valued in the nutraceutical industry). Hence, this study has addressed the transferability of CSS, GP and OMW pyrolysis research, performed in auger reactors at different scale, facilitating the biorefinery of these by-products, and thus the way towards a circular bioeconomy.

Acknowledgements

C. del Pozo expresses her gratitude to the Universitat Autònoma de Barcelona for funding her PhD contract through a PIF grant, as well as an Erasmus+ grant to support her exchange stay at Aston University (EBRI).

This research did not receive any specific grant from funding agencies in the public, commercial, or not-for-profit sectors.

References

Brassard, P., Godbout, S., Raghavan, V., 2017. Pyrolysis in auger reactors for biochar and bio-oil production: A review. *Biosyst. Eng.* 161, 80–92. <https://doi.org/10.1016/j.biosystemseng.2017.06.020>

- Brassard, P., Godbout, S., Raghavan, V., 2016. Soil biochar amendment as a climate change mitigation tool: Key parameters and mechanisms involved. *J. Environ. Manage.* 181, 484–497. <https://doi.org/10.1016/j.jenvman.2016.06.063>
- Cabrera, A., Cox, L., Spokas, K., Hermosín, M.C., Cornejo, J., Koskinen, W.C., 2014. Influence of biochar amendments on the sorption-desorption of aminocyclopyrachlor, bentazone and pyraclostrobin pesticides to an agricultural soil. *Sci. Total Environ.* 470–471, 438–443. <https://doi.org/10.1016/j.scitotenv.2013.09.080>
- Channiwala, S.A., Parikh, P.P., 2002. A unified correlation for estimating HHV of solid, liquid and gaseous fuels. *Fuel* 81, 1051–1063. [https://doi.org/10.1016/S0016-2361\(01\)00131-4](https://doi.org/10.1016/S0016-2361(01)00131-4)
- Chen, T., Liu, R., Scott, N.R., 2016. Characterization of energy carriers obtained from the pyrolysis of white ash, switchgrass and corn stover - Biochar, syngas and bio-oil. *Fuel Process. Technol.* 142, 124–134. <https://doi.org/10.1016/j.fuproc.2015.09.034>
- Chertow, M.R., 2007. “Uncovering” industrial symbiosis. *J. Ind. Ecol.* 11, 11–30. <https://doi.org/10.1162/jiec.2007.1110>
- del Pozo, C., Bartrolí, J., Alier, S., Puy, N., Fàbregas, E., 2021a. Production, identification, and quantification of antioxidants from torrefaction and pyrolysis of grape pomace. *Fuel Process. Technol.* 211, 106602. <https://doi.org/10.1016/j.fuproc.2020.106602>
- del Pozo, C., Bartrolí, J., Alier, S., Puy, N., Fàbregas, E., 2020. Production of antioxidants and other value-added compounds from coffee silverskin via pyrolysis under a biorefinery approach. *Waste Manag.* 109, 19–27. <https://doi.org/10.1016/j.wasman.2020.04.044>
- del Pozo, C., Bartrolí, J., Puy, N., Fàbregas, E., 2018. Separation of value-added chemical groups from bio-oil of olive mill waste. *Ind. Crops Prod.* 125. <https://doi.org/10.1016/j.indcrop.2018.08.062>
- del Pozo, C., Rego, F., Yang, Y., Puy, N., Bartrolí, J., Fàbregas, E., Bridgwater, A. V., 2021b. Converting coffee silverskin to value-added products by a slow pyrolysis-based biorefinery process. *Fuel Process. Technol.* 214. <https://doi.org/10.1016/j.fuproc.2020.106708>
- European Commission, 2017. Expert Group Report: Review of the EU Bioeconomy Strategy and its Action Plan, European Commission.
- Hanandeh, A. El, Abu-Zurayk, R.A., Hamadneh, I., Al-Dujaili, A.H., 2016. Characterization of biochar prepared from slow pyrolysis of Jordanian olive oil processing solid waste and

- adsorption efficiency of Hg²⁺ ions in aqueous solutions. *Water Sci. Technol.* 74, 1899–1910. <https://doi.org/10.2166/wst.2016.378>
- Hmid, A., Mondelli, D., Fiore, S., Fanizzi, F.P., Al Chami, Z., Dumontet, S., 2014. Production and characterization of biochar from three-phase olive mill waste through slow pyrolysis. *Biomass and Bioenergy* 71, 330–339. <https://doi.org/10.1016/j.biombioe.2014.09.024>
- Jin, Q., Wang, Z., Feng, Y., Kim, Y.T., Stewart, A.C., O’Keefe, S.F., Neilson, A.P., He, Z., Huang, H., 2020. Grape pomace and its secondary waste management: Biochar production for a broad range of lead (Pb) removal from water. *Environ. Res.* 186, 109442. <https://doi.org/10.1016/j.envres.2020.109442>
- Keiluweit, M., Nico, P.S., Johnson, M.G., KLEBER, M., 2010. Dynamic Molecular Structure of Plant Biomass-derived Black Carbon(Biochar)- Supporting Information -. *Environ. Sci. Technol.* 44, 1247–1253.
- Liu, Z., Han, G., 2015. Production of solid fuel biochar from waste biomass by low temperature pyrolysis. *FUEL* 158, 159–165. <https://doi.org/10.1016/j.fuel.2015.05.032>
- Lou, K., Rajapaksha, A.U., Ok, Y.S., Chang, S.X., 2016. Pyrolysis temperature and steam activation effects on sorption of phosphate on pine sawdust biochars in aqueous solutions. *Chem. Speciat. Bioavailab.* 28, 42–50. <https://doi.org/10.1080/09542299.2016.1165080>
- Lucian, M., Volpe, M., Gao, L., Piro, G., Goldfarb, J.L., Fiori, L., 2018. Impact of hydrothermal carbonization conditions on the formation of hydrochars and secondary chars from the organic fraction of municipal solid waste. *Fuel* 233, 257–268. <https://doi.org/10.1016/j.fuel.2018.06.060>
- Mohan, D., Pittman, C.U., Steele, P.H., 2006. Pyrolysis of wood/biomass for bio-oil: A critical review. *Energy and Fuels* 20, 848–889. <https://doi.org/10.1021/ef0502397>
- Murthy, P.S., Madhava Naidu, M., 2012. Sustainable management of coffee industry by-products and value addition - A review. *Resour. Conserv. Recycl.* 66, 45–58. <https://doi.org/10.1016/j.resconrec.2012.06.005>
- Novak, J.M., Lima, I.M., Xing, B., Gaskin, J.W., Steiner, C., Das, K.C., Ahmedna, M., Rehrh, D., Watts, D.W., Busscher, W.J., Schomberg, H., 2009. Characterization of designer biochar produced at different temperatures and their effects on a loamy sand. *Ann. Environ. Sci.* 5, 195–206.

- Polidoro, A. dos S., Scapin, E., Lazzari, E., Silva, A.N., dos Santos, A.L., Caramao, E.B., Jacques, R.A., 2018. Valorization of coffee silverskin industrial waste by pyrolysis : From optimization of bio-oil production to chemical characterization by GC × GC / qMS. *J. Anal. Appl. Pyrolysis* 129, 43–52. <https://doi.org/10.1016/j.jaap.2017.12.005>
- Recari, J., Berruoco, C., Puy, N., Alier, S., Bartrolí, J., Farriol, X., 2017. Torrefaction of a solid recovered fuel (SRF) to improve the fuel properties for gasification processes. *Appl. Energy* 203, 177–188. <https://doi.org/10.1016/j.apenergy.2017.06.014>
- Rehrah, D., Reddy, M.R., Novak, J.M., Bansode, R.R., Schimmel, K.A., Yu, J., Watts, D.W., Ahmedna, M., 2014. Production and characterization of biochars from agricultural by-products for use in soil quality enhancement. *J. Anal. Appl. Pyrolysis* 108, 301–309. <https://doi.org/10.1016/j.jaap.2014.03.008>
- Ren, S., Ye, X.P., Borole, A.P., 2017. Separation of chemical groups from bio-oil water-extract via sequential organic solvent extraction. *J. Anal. Appl. Pyrolysis* 123, 30–39. <https://doi.org/10.1016/j.jaap.2017.01.004>
- Smith, P., 2016. Soil carbon sequestration and biochar as negative emission technologies. *Glob. Chang. Biol.* 22, 1315–1324. <https://doi.org/10.1111/gcb.13178>
- Tan, X., Liu, Y., Zeng, G., Wang, X., Hu, X., Gu, Y., Yang, Z., 2015. Application of biochar for the removal of pollutants from aqueous solutions. *Chemosphere* 125, 70–85. <https://doi.org/10.1016/j.chemosphere.2014.12.058>
- Torri, C., Fabbri, D., 2014. Biochar enables anaerobic digestion of aqueous phase from intermediate pyrolysis of biomass. *Bioresour. Technol.* 172, 335–341. <https://doi.org/10.1016/j.biortech.2014.09.021>
- Ubando, A.T., Felix, C.B., Chen, W.H., 2020. Biorefineries in circular bioeconomy: A comprehensive review. *Bioresour. Technol.* 299. <https://doi.org/10.1016/j.biortech.2019.122585>
- Uchimiya, M., Wartelle, L.H., Klasson, K.T., Fortier, C.A., Lima, I.M., 2011. Influence of pyrolysis temperature on biochar property and function as a heavy metal sorbent in soil. *J. Agric. Food Chem.* 59, 2501–2510. <https://doi.org/10.1021/jf104206c>
- Wang, Y., Liu, R., 2018. H₂O₂ treatment enhanced the heavy metals removal by manure biochar in aqueous solutions. *Sci. Total Environ.* 628–629, 1139–1148. <https://doi.org/10.1016/j.scitotenv.2018.02.137>

- Wang, Y., Liu, R., 2017. Comparison of characteristics of twenty-one types of biochar and their ability to remove multi-heavy metals and methylene blue in solution. *Fuel Process. Technol.* 160, 55–63. <https://doi.org/10.1016/j.fuproc.2017.02.019>
- Xie, T., Reddy, K.R., Wang, C., Yargicoglu, E., Spokas, K., 2015. Characteristics and applications of biochar for environmental remediation: A review. *Crit. Rev. Environ. Sci. Technol.* 45, 939–969. <https://doi.org/10.1080/10643389.2014.924180>
- Yang, H., Yan, R., Chen, H., Lee, D.H., Chuguang, Z., 2007. Characteristics of hemicellulose, cellulose and lignin pyrolysis. *Fuel* 86, 1781–1788.
- Yu, Y., Yang, Y., Cheng, Z., Blanco, P.H., Liu, R., Bridgwater, A. V., Cai, J., 2016. Pyrolysis of Rice Husk and Corn Stalk in Auger Reactor. 1. Characterization of Char and Gas at Various Temperatures. *Energy and Fuels* 30, 10568–10574. <https://doi.org/10.1021/acs.energyfuels.6b02276>
- Zhao, C., Jiang, E., Chen, A., 2017. Volatile production from pyrolysis of cellulose, hemicellulose and lignin. *J. Energy Inst.* 90, 902–913. <https://doi.org/10.1016/j.joei.2016.08.004>



IV

Discussion

4.1 Discussion of the results

The present thesis is focused on valorising the agricultural wastes from the production of olive oil (OMW), wine (GP) and roasted coffee (CSS) through pyrolysis and torrefaction processes, transforming these wastes into value-added products.

First, it was performed a study to identify and separate interesting compounds from OMW pyrolysis liquid (400 °C), also known as bio-oil (del Pozo et al., 2018); then, a second study was carried out to identify and quantify phenolic compounds in GP pyrolysis (400 °C) and torrefaction (225 °C) liquids (del Pozo et al., 2021a). The thermochemical products of these studies were provided by ENER-G-bas company, which performed the processes in a pilot auger reactor (15 kg/h). The composition of the liquid fraction was analysed by gas chromatography – mass spectrometry (GCMS), showing similar results between OMW and GP pyrolysis liquids, which were composed of two phases: an aqueous phase (AP) that mostly comprised acetic acid, monosaccharides and phenolic derivatives, and a non-aqueous phase (NAP), that mainly contained phenolic derivatives and fatty acids and their methyl esters. In the first study, acid-base extraction, performed with hexane at pH 12 followed by an ethyl acetate extraction at pH 6, was shown to be a successful method to separate value-added chemical groups from pyrolysis liquids: acetic acid, which is a chemical platform, and monosaccharides, that could be potentially used for biogas/bioethanol production, were found in AP aqueous phase; phenolics, which their antioxidant properties makes them highly valued in nutraceutical industries, were identified in AP hexane, and AP and NAP ethyl acetate phases; and methyl esters of fatty acids, that could be directed to produce biodiesel, were located in NAP hexane phase.

From all these compounds, phenolics were the most interesting ones so, in the second study, the suitability of Folin-Ciocalteu (FC) and DPPH methods to quantify them in torrefaction and pyrolysis liquids was studied. FC method is based on the ability of antioxidant molecules to reduce the FC reagent (Magalhães et al., 2008), while DPPH assay evaluates the radical scavenging ability of antioxidant substances toward DPPH• radical (Marina et al., 2008). Both methods measure then two properties that are closely related to antioxidant capacity of the samples, which in this case was mainly attributed to the presence of phenolic compounds. The study showed that both FC and DPPH methods were suitable to quantify phenolics in GP pyrolysis liquids; however, in torrefaction liquids, it is convenient to quantify them by DPPH

assay, since the high content of reducing sugars present in the torrefaction liquids could interfere in the FC measurement (Muñoz-Bernal et al., 2017; Rover and Brown, 2013). This study also showed pyrolysis (400 °C) as a successful method to obtain phenolics, especially when compared to torrefaction (225 °C). Phenolics, which mostly concentrated in NAP, were obtained not only from the composition of GP, but from the degradation of lignin during the thermochemical process. Therefore, pyrolysis process (400 °C) would allow valorising OMW and GP within a waste biorefinery context, turning them into a potential source of mainly phenolic compounds.

The third (del Pozo et al., 2020) and fourth (del Pozo et al., 2021b) studies were focused on the integral valorisation of CSS, the only waste of the coffee roasting process, through pyrolysis. Thus, in this case, it was not just studied the liquid fraction, but also the solid one, getting closer to zero-waste approach. In order to determine which is the best temperature to valorise CSS, pyrolysis was carried out at 280 °C, 400 °C and 500 °C. In the third study, the products were provided by ENERGBAS company (pilot auger reactor, 15 kg/h); in the fourth one, the pyrolysis fractions were obtained from the experiments performed in a lab auger reactor (0.3 kg/h), from EBRI (Aston University, U.K.).

In contrast with OMW and GP, CSS pyrolysis liquids showed low phenolic content, which was associated with its low composition in lignin (1% wt.) (Murthy and Madhava Naidu, 2012). Moreover, the resulting 400 °C and 500 °C CSS pyrolysis liquids from pilot plant presented a single phase, while the ones from lab reactor, had two phases. This could be also related to a different lignin content of feedstocks (which came from different batches), being the one from lab reactor richer in lignin and so, having higher amount of hydrophobic compounds to form the NAP phase. Other difference observed in CSS pyrolysis liquids was their high content in nitrogen compounds, especially caffeine, which resulted in the unusual basic pH of the pyrolysis liquids. Thus, CSS liquid fractions could be a potential source of caffeine, apart from phenolics, among others. In the third study (del Pozo et al., 2020), phenolics were quantified showing 280 °C as the best temperature to obtain them, since in this case, phenolics were the original ones, instead of also coming from the decomposition of lignin. In the fourth study (del Pozo et al., 2021b), CSS pyrolysis liquids has shown as a potential source of caffeine, with 400 °C AP phase presenting the highest concentration (14.3 g caffeine/L AP).

Regarding the solid fraction, the third study (del Pozo et al., 2020) presented them as a source of energy (with up to 21 MJ/kg), showing no many differences between biochars, regardless

the temperature of the process. In order to increase the value of the solid fraction, the fourth study (del Pozo et al., 2021b) was focused on the role of CSS biochars as adsorbent of organic pollutants in water, being potentially useful for cationic and aromatic molecules, and with 400 °C biochar giving the highest removal values.

Concerning the gas fraction, the fourth study (del Pozo et al., 2021b) argued its use as heat source for biomass drying before pyrolysis. Therefore, CSS (the only waste of the coffee roasting process) could be completely valorised through pyrolysis (400 °C), allowing to achieve zero-waste in the coffee roasting industry.

A last study (see Chapter III. Submitted article) was performed to compare the OMW, GP and CSS pyrolysis products from the pilot plant (ENERG-bas company, 15 kg/h) and the lab auger reactor (Aston University, 0.3 kg/h). The study dealt then with the robustness of the pyrolysis process, since using different reactors, especially if they have different capacity, could affect the properties and so, applications, of the resulting products (Brassard et al., 2017). Apart from the reactor type, pyrolysis process is also influenced by the biomass feedstock and the operating parameters, mainly the solid retention time and the temperature (Brassard et al., 2017; Wang and Liu, 2017), which remained constant throughout the study. Besides, the properties of OMW and GP biochars were also analysed, being itself a novelty since there are few studies that compares biochars from common agriculture wastes, performed in different pyrolysis conditions (Wang and Liu, 2017). The results showed no major differences between biochars, regardless the reactor used; however, in pyrolysis liquids, the ones from the pilot plant were richer in 2,6-dimethoxy-phenols and phenolics para-substituted by carbonyl groups, compared to the lab reactor liquids. This was related to a longer vapor retention time in the lab reactor, favouring secondary reactions and so, a higher decomposition of the pyrolysis products. In addition, GP and OMW pyrolysis liquids (400 °C) showed the highest number of phenolics; and GP biochar (400 °C), the best properties for energy purposes. This study addressed then the transferability of CSS, GP and OMW pyrolysis research, using different auger reactors, thus making the biorefinery of the discussed agricultural by-products more feasible.

Therefore, thermochemical treatments in auger reactors can be a good procedure to transform agricultural wastes into value-added products (biochar and pyrolysis liquids) within an integrated biorefinery context, moving towards a circular bioeconomy.

4.2 References of Part IV

- Brassard, P., Godbout, S., Raghavan, V., 2017. Pyrolysis in auger reactors for biochar and bio-oil production: A review. *Biosyst. Eng.* 161, 80–92. <https://doi.org/10.1016/j.biosystemseng.2017.06.020>
- del Pozo, C., Bartrolí, J., Alier, S., Puy, N., Fàbregas, E., 2021a. Production, identification, and quantification of antioxidants from torrefaction and pyrolysis of grape pomace. *Fuel Process. Technol.* 211, 106602. <https://doi.org/10.1016/j.fuproc.2020.106602>
- del Pozo, C., Bartrolí, J., Alier, S., Puy, N., Fàbregas, E., 2020. Production of antioxidants and other value-added compounds from coffee silverskin via pyrolysis under a biorefinery approach. *Waste Manag.* 109, 19–27. <https://doi.org/10.1016/j.wasman.2020.04.044>
- del Pozo, C., Bartrolí, J., Puy, N., Fàbregas, E., 2018. Separation of value-added chemical groups from bio-oil of olive mill waste. *Ind. Crops Prod.* 125. <https://doi.org/10.1016/j.indcrop.2018.08.062>
- del Pozo, C., Rego, F., Yang, Y., Puy, N., Bartrolí, J., Fàbregas, E., Bridgwater, A. V., 2021b. Converting coffee silverskin to value-added products by a slow pyrolysis-based biorefinery process. *Fuel Process. Technol.* 214. <https://doi.org/10.1016/j.fuproc.2020.106708>
- Magalhães, L.M., Segundo, M.A., Reis, S., Lima, J.L.F.C., 2008. Methodological aspects about in vitro evaluation of antioxidant properties. *Anal. Chim. Acta* 613, 1–19. <https://doi.org/10.1016/j.aca.2008.02.047>
- Marina, D., Avella, G., Alberto, C., García, O., Cisneros, A.M., 2008. Medición de Fenoles y Actividad Antioxidante en Malezas Usadas para Alimentación Animal. *Simp. Metrol.* 1–5.
- Muñoz-Bernal, Ó.A., Torres-Aguirre, G.A., Núñez-Gastélum, J.A., de la Rosa, L.A., Rodrigo-García, J., Ayala-Zavala, J.F., Álvarez-Parrilla, E., 2017. Nuevo Acercamiento a La Interacción Del Reactivo De Folin-Ciocalteu Con Azúcares Durante La Cuantificación De Polifenoles Totales. *Tip* 20, 23–28. <https://doi.org/10.1016/j.recqb.2017.04.003>
- Murthy, P.S., Madhava Naidu, M., 2012. Sustainable management of coffee industry by-

products and value addition - A review. *Resour. Conserv. Recycl.* 66, 45–58.
<https://doi.org/10.1016/j.resconrec.2012.06.005>

Rover, M.R., Brown, R.C., 2013. Quantification of total phenols in bio-oil using the Folin-Ciocalteu method. *J. Anal. Appl. Pyrolysis* 104, 366–371.
<https://doi.org/10.1016/j.jaap.2013.06.011>

Wang, Y., Liu, R., 2017. Comparison of characteristics of twenty-one types of biochar and their ability to remove multi-heavy metals and methylene blue in solution. *Fuel Process. Technol.* 160, 55–63. <https://doi.org/10.1016/j.fuproc.2017.02.019>



Conclusions

5.1 Conclusions

The present thesis is focused on the thermochemical treatments (pyrolysis and torrefaction) of OMW, GP and CSS agricultural wastes, performed in auger reactors, as a mean to transform these residues into value-added products, within a waste biorefinery and a circular bioeconomy context. Thus, over this thesis, the resulting liquid and solid pyrolysis and torrefaction products were studied in order to determine their potential applications, the general conclusion being summarised as follows:

- Pyrolysis process has shown to be a suitable procedure to transform OMW, GP and CSS agricultural wastes into value-added products within an integrated biorefinery context. Pyrolysis liquids have shown to be a potential source of chemicals, while biochar can be used as solid biofuel, among other potential high-valued applications.

More specifically,

- OMW and GP pyrolysis liquids (400 °C) presented similar composition, and were composed of the following value-added products:
 - The aqueous phase was composed of acetic acid, which is a chemical platform; sugars, that could be potentially used for biogas/bioethanol production; and phenolic compounds, which their antioxidant properties make them highly valued in nutraceutical industries.
 - On the other hand, the non-aqueous phase mainly comprised phenolics and, to a lesser extent, fatty acids and their methyl esters, the latter being able to be used as biodiesel.
- Intermediate pyrolysis (400 °C) has shown to be a suitable method to obtain phenolics from OMW and GP. Phenolics, which are the highest valued-added products from the pyrolysis liquids, came from OMW and GP composition, aside from lignin devolatilization reactions that take place during the thermochemical process.
- GP biochar (400 °C) showed the best properties for energy purposes (27 MJ/kg, and low ashes and sulphur content), compared to OMW and CSS biochars.
- CSS pyrolysis liquids differed from the OMW and GP pyrolysis liquids.

- CSS pyrolysis liquids had a lower phenolic content, but a rich composition of nitrogen compounds, especially caffeine, which resulted in an unusual basic pH of the liquid fraction.
- Compounds from CSS pyrolysis liquid not always separate in two phases, and so, not always form a non-aqueous phase (NAP).
- CSS could be completely valorised through thermochemical treatments, allowing to achieve the ultimate goal of a zero-waste economy in the coffee roasting industry
 - Biochars could be potentially used to adsorb mainly cationic and aromatic organic pollutants from water, as well as, as solid biofuel (< 21 MJ/kg).
 - Pyrolysis liquids can be considered as a potential source of chemicals, mainly caffeine and phenolics.
 - Gas fraction can be used as a heat source for biomass drying before pyrolysis treatments.

Regarding each particular study, the research findings are addressed at the conclusions section of each article, being the most relevant ones summarised in the following points:

Article I. Separation of value-added chemical groups from bio-oil of olive mill waste

- A procedure to separate compounds of OMW pyrolysis liquid (400 °C) in value-added chemical groups was developed. The procedure consisted of a first extraction with hexane at pH 12, followed by an ethyl acetate extraction at pH 6.
- The resulting value-added chemical groups, after the separation procedure, comprised: acetic acid, monosaccharides and phenolics, concentrated in the AP aqueous phase; phenolics, identified in AP hexane, AP ethyl acetate and NAP ethyl acetate phases; and methyl esters of fatty acids, found in the NAP hexane phase.

Article II. Production, identification, and quantification of antioxidants from torrefaction and pyrolysis of grape pomace

- Folin-Ciocalteu and DPPH methods were suitable to quantify phenolics in GP pyrolysis liquid (400 °C).

- Phenolics from GP torrefaction liquid (225 °C) should be quantified by DPPH assay in order to avoid that the high content of reducing sugars present in the torrefaction liquid interferes in the Folin-Ciocalteu measurement.
- Intermediate pyrolysis (400 °C) has shown to be a suitable method to obtain phenolics from GP, compared to the torrefaction process (225 °C), due to the degradation of lignin, that increase with increasing the temperature of the process.

Article III. Production of antioxidants and other value-added compounds from coffee silverskin via pyrolysis under a biorefinery approach

- CSS can be totally valorised through intermediate pyrolysis.
- CSS pyrolysis liquids were composed of different value-added products, such as acetic acid, nitrogenated compounds (mainly caffeine) and phenolics.
- CSS pyrolysis liquids could be a potential source of phenolics, being 280 °C the best temperature tested to obtain them.
- CSS biochars can be used as a renewable energy source (< 21 MJ/kg), showing no many differences between the studied biochars, regardless the temperature they were produced.

Article IV. Converting coffee silverskin to value-added products by a slow pyrolysis-based biorefinery process

- CSS pyrolysis liquids could be a potential source of caffeine, with 400 °C AP phase having the highest concentration (14.3 g caffeine/L AP).
- CSS biochars could be used as adsorbent of organic pollutants in water, being potentially useful for cationic and aromatic molecules, and with 400 °C biochar giving the highest removal values.
- Gas fraction could be a heat source for biomass drying before pyrolysis.

Submitted article. The effect of reactor scale on biochars and pyrolysis liquids from slow pyrolysis of coffee silverskin, grape pomace and olive mill waste, in auger reactors

- No major differences were observed between biochars obtained at same temperature and solid retention time, but using different auger reactors: a pilot plant (ENERG-bas company, 15 kg/h) and a lab size reactor (Aston University, 0.3 kg/h).
- The pyrolysis liquids from the pilot plant were richer in 2,6-dimethoxy-phenols and phenolics para-substituted by carbonyl groups, than the ones from the lab reactor.
- OMW, GP and CSS biochar existing studies could be replicate, since biochar production has shown to be pretty robust, making the biorefinery of these agricultural wastes more feasible.

5.2 Future Prospects

The research performed within this thesis work opens up some improvements, as well as new research perspective, on this research field. Some of them, which have been divided in future prospects related to this work and new lines of research, are listed as follows:

Future prospects related to this work

- To obtain the product yields of pyrolysis and torrefaction experiments at the pilot plant, and compare them with the product yields from the lab size reactor.
- Further investigation regarding the differences observed between the pyrolysis liquids from the pilot plant and the lab auger reactor.

New lines of research

- To study how using OMW, GP and CSS agricultural wastes from different companies and years affects the pyrolysis products.
- To optimise the pyrolysis operating parameters to valorise OMW, GP and CSS, expanding the research to other temperatures and solid retention times, among others.
- To improve the separation method to be able to separate target compounds from the other chemical species of the bio-oil (pyrolysis liquid), for instance, by distillation or using supercritical CO₂ in the case of phenolics.
- To perform a comprehensive techno-economic and environmental analyses to study the viability of the OMW, GP and CSS biorefineries implementation.
- To extent the study to other organic residues, such as municipal organic wastes or other agricultural residues.
- Further studies regarding the potential uses of the OMW, GP and CSS biochars.



VI

Annex

6.1 Contributions to congresses and seminars

Congresses

- del Pozo, C; Fábregas, E; Puy, N. Characterization and adding value to bio-oil derived from Sansa. Poster. 3rd Scientific Meeting of BCN-b Students. ICMAB, Bellaterra (Spain), 7-8 Nov 2017.
- del Pozo, C; Fábregas, E; Puy, N. Obtention of value-added products from olive oil and wine production wastes through thermochemical treatments. Poster and flash presentation. Jornades Doctorals. Department of Chemistry, Universitat Autònoma de Barcelona (Spain), 22-24 May 2019.
- del Pozo, C; Bartrolí, J; Fábregas, E; Puy, N. Converting coffee silverskin to value-added products under a biorefinery approach. Poster. European Biomass Conference and Exhibition. Lisbon (Portugal), 27-30 May 2019. Organized by ETA-Florence Renewable Energies.

Seminars

- del Pozo, C. Obtaining value-added products from olive oil, wine and coffee roasting production wastes through thermochemical treatments in an intermediate pyrolysis pilot plant. Energy and Bioproducts Research Institute, Aston University (U.K.), 28th Oct 2019.

